UNIVERSIDADE FEDERAL DE MINAS GERAIS

Curso de Pós-Graduação em Engenharia Metalúrgica e de Materiais

Tese de doutorado

"Mecanismo de Biossorção Seletiva de Arsênio (III) em Rejeitos Ricos em Proteínas Fibrosas"

"Mechanism of selective As (III) biosorption onto fibrous protein rich waste material"

Autor: Mônica Cristina Teixeira

Orientador: Profa. Virgínia Sampaio Teixeira Ciminelli

Setembro/2004

Atualizada em junho de 2007

UNIVERSIDADE FEDERAL DE MINAS GERAIS

Curso de Pós-Graduação em Engenharia Metalúrgica e de Materiais

Mônica Cristina Teixeira

Mecanismo de Biossorção Seletiva de Arsênio (III) em Rejeitos Ricos em Proteínas Fibrosas

"Mechanism of elective As (III) biosorption onto fibrous protein rich waste material"

Tese de doutorado apresentada ao Curso de Pós-Graduação em Engenharia Metalúrgica e de Minas da Universidade Federal de Minas Gerais

Área de concentração: Tecnologia Mineral

Orientador: Profa. Virgínia Sampaio Teixeira Ciminelli

Belo Horizonte

Escola de Engenharia da UFMG

2004

AGRADECIMENTOS

Ao dar por encerrado este trabalho, percebo-o, felizmente, ainda não concluído. Finalizou-se uma etapa à qual me dediquei nos últimos anos, mas tratasse apenas disso, uma dentre as muitas etapas de um processo contínuo, duradouro, e talvez perpétuo, da minha busca pelo conhecimento. Costumo dizer que sou movida pela insatisfação e pela curiosidade e gostaria de agradecer a todos que, de alguma maneira, me estimularam com sua inquietação ou me presentearam com seus ensinamentos.

Gostaria de agradecer à minha orientadora, Prof[a] Virgínia Ciminelli pelas discussões estimulantes que tivemos durante todas as fazes deste trabalho e pela sua coragem em assumir comigo os riscos ao enveredarmos por caminhos tão desconhecidos. Gostaria também de agradecer aos grandes professores que conheci ao longo dos anos. Ainda no tempo do colégio, tive o inesquecível prazer de conhecer o mundo através das aulas do Irmão Cristino; só agora percebo o quanto a sua influência foi marcante. Agradeço também aos professores Rogelio L. Brandão, Oswaldo Garcia Jr. e Jacques R. Nicoli que me acompanharam e muito me estimularam durante os primeiros anos de minha vida acadêmica.

Ao grupo de pesquisa do Laboratório de Processamento Aquoso, agradeço muitíssimo pelo fato de terem me recebido tão prontamente, sem nenhum tipo de restrição ou preconceito. Agradeço em particular aos funcionários Ilda e João pela agradável convivência; à primeira, pelo seu bom-humor aparentemente indestrutível, ao segundo, pela disposição em me "socorrer" sempre prontamente. Durante os anos em que estive fazendo parte deste grupo, pude conviver com vários colegas, alunos de graduação e pós-graduação e pesquisadores dos quais me recordarei sempre com carinho. Gostaria de agradecer especialmente ao Ricardo, ao Cláudio e à minha querida Graziele. Com Cláudia e Versiane pude compartilhar de todas as angústias comuns aos alunos de Doutorado visto que estávamos todos na mesma barca. A eles agradeço muito o apoio diário e a troca de opiniões e experiências. Ana Cláudia e Anderson, já mais "evoluídos" foram como irmãos mais velhos, academicamente falando. Procurei aprender com todos eles, calmamente, através da observação diária, da mesma maneira

que se faz na convivência em família. Nos últimos meses recebemos novos membros em nosso grupo e a elas dedico um agradecimento especial. Apesar dos desafios de uma área distinta da sua área de atuação, a professora Maria Sylvia demonstrou uma disposição tão jovial em continuar a aprender e a nos ensinar que me cativou. Christina, muito obrigada pela sua disposição em ajudar sempre, com a maior eficiência.

Aos funcionários do laboratório de Análises Químicas, principalmente ao Sandro e à Olívia peço desculpas pelo volume de análises e pela minha ansiedade em receber os resultados em algumas ocasiões e agradeço muitíssimo, pois, sem sombra de dúvidas, este trabalho não teria sido concluído sem sua ativa e confiável participação. Agradeço a todos os demais professores e funcionários do Departamento de Metalurgia pela acolhida.

Gostaria ainda de agradecer ao Prof. Hélio Anderson e a toda sua equipe pela execução dos cálculos de predição teórica e pelas sugestões interessantes que muito contribuíram para o enriquecimento deste trabalho e ainda à Maria do Carmo Alves pelo auxílio no tratamento dos dados da Espectroscopia de Absorção de Raios-X.

Agradeço à Capes, à Universidade Federal de Ouro Preto, ao Instituto do Milênio-Água uma Visão Mineral e ao CNPq pelo apoio financeiro. Agradeço ainda à Universidade Federal de Minas Gerais e ao Laboratório Nacional de Luz Síncrotron pelo uso de suas instalações.

Agradeço aos meus colegas do Departamento de Farmácia da UFOP pelo apoio. Em particular agradeço a minhas parceiras na BR 040, Andréa, Neila e Dênia, pelo seu companheirismo.

À minha mãe e meu irmão agradeço pelo seu interesse e presença constantes e pelo estímulo nas horas em que mais precisei. Sem eles e sem o apoio, a generosidade e a compreensão de meus filhos, cujas gestações ocorreram por entre salas de aulas e bancadas de laboratórios, e do meu marido, que foi sempre o meu melhor interlocutor, nada disso teria sido possível.

“Não, mil vezes não, não existe uma categoria de ciência à qual alguém possa dar o nome de ciência aplicada. Existem a ciência e as aplicações da ciência, unidas, tal qual a fruta e a árvore que a sustenta”.

Pasteur, 1871.

Dedico este trabalho aos meus filhos e ao meu marido.

SUMÁRIO

LISTA DE FIGURAS

LISTA DE TABELAS

RESUMO

No presente trabalho uma nova abordagem para o tratamento de aguas contaminadas com arsênio é proposta. Tal metodologia se fundamenta nos mecanismos bioquímicos e toxicológicos que explicam a toxicidade do arsênio e envolve a utilização de uma biomassa residual abundante e rica em cisteína para a remoção seletiva de As (III). A esécie trivalente do arsênio é considerada a mais móvel e hidrossolúvel dentre as espécies de As hidrossolúveis.

No estudo em questão, além da seleção do material biosorvente, pó de penas de galinha, a eficiência do material escolhido foi avaliada sob diferentes condições experimentais. Foram avaliados o processamento do biosorvente, a razão sólido/líquido ideal, o pH (2-10) e o efeito da presença de íons competidores (fosfato e As (V)). Os resultados experimentais demonstraram que o material selecionado é altamente seletivo para as espécies trivalentes de As independentemente da presença de íons competidores. A máxima capacidade de remoção observada (170 μmolAs/g biomassa) foi obtida em sistema com pH ácido. Tais dados podem ser explicados por um mecanismo de adsorção muito particular proposto a partir das análises das estruturas dos complexos de adsorção por meio de Espectroscopia de Absorção de Raios-X – XAS (EXAFS e XANES) e Espectroscopia Raman, combinadas ao modelamento teórico estrutural obtido por meio de Cálculos de Densidadade Funcional Teórica (DFT).

Os dados de XAS indicaram que a complexação do As com os resíduos de cisteína do biosorvente se dá por meio de uma interação "*inner sphere*" dos átomos de As (III) com os átomos de S da biomassa. A estrutura do complexo de adsorção apresenta geometria trigonal piramidal com uma proporção As/S de 1:3 e distância interatômica de, aproximadamente, 2.24-2.26 A. Durante a complexação são liberadas três moléculas de água produzidas a partir da reação dos grupamentos OH da espécie arsenical neutra $As(OH)_3$, que predomina em valores de pH inferiores a 9, com o átomo de hidrogênio do grupamento SH do aminoácido. À medida que o pH aumenta para 10,5 a espécie $As(OH)_3$ sofre desprotonação e a capacidade adsortiva da biomassa é reduzida para 30% daquela obtida em sistema com pH ácido. As análises dos complexos de adsorção obtidos em condições de alcalinidade apontaram para a ocorrência oxidação parcial do As (III) associada a formação de um complexo de adsorção mais desordenado. Sob tais

condições, o arsenito é adsorvido como um oxi-ânion sendo que apenas 1 átomo de oxigênio é substituído pelo enxofre gerando um complexo de adorção com proporção As/S de 1:1. Neste caso, a distância interatômica aumenta para 2.31 Å. Por meio da espectroscopia Raman, pode-se obter ainda diuas importantes informações: (i) a estrutura β pregueada da queratina é a principal estrutura secundária da biomassa empregada e (ii) foi comprovada a participação dos átomos de S da cisteína na adsorção de As visto que, durante o processo de adsorção, a intensidade do modos vibracionais atribuídos às ligações As-S aumentava á medida que diminuíam as intensidades daqueles relacionados às ligações S-S. Os dados de modelamento teórico fornecidos pelos cálculos de DFT corroboram estes dados de espectroscopia XAS e Raman.

Os resultados obtidos neste trabalho confirmaram a hipótese inicial de que uma biomassa rica em cisteína poderia ser capaz de adsorver seletivamente as espécies trivalentes de arsênio e fornecendo subsídios para o desenvolvimento de um biosorvente para remoção de As (III) de águas contaminadas.

ABSTRACT

Based on biochemical and toxicological fundamentals that explain arsenic toxicity, a novel approach for the treatment of arsenic-containing waters was developed. The approach involved the use of an abundant cysteine-rich waste biomass for the selective removal of As (III) from waters. The trivalent species is considered the most mobile and toxic hydrosoluble arsenic species.

Following the selection of the waste biomass for the present investigations - chicken feathers - the material was evaluated under different conditions of sorbent preparation and S/L ratio, pH (2-10.5) and the presence of competitor ions (phosphate and As (V)). The experiments demonstrated that the biomass is highly selective for the As (III) species – with no significant effect of the studied competitor ions on adsorption capacity– and the maximum uptake (170 μmolAs/g biomass) is obtained under acidic conditions. These findings were explained by a unique adsorption mechanism based on the results obtained by the combination of two experimental techniques, X- ray Absorption spectroscopy (EXAFS and XANES) and RAMAN spectroscopy, with theoretical modeling by Density Functional Theory - DFT calculations.

XAS measurements indicated inner-sphere complexation of As (III) by the biomass'sulfur atoms. The adsorption structure was represented by a trigonal, pyramidal geometry, with an As/S ratio of 1:3 and an As-S interatomic distance of approximately 2.24-2.26 A. Arsenic uptake leads to the release of 3 water molecules produced by the reaction of the OH groups in the neutral $As(OH)_3$ species, which predominates under pH <9 , with the hydrogen of the biomass' SH group. As pH is increased to 10.5, the $As(OH)_3$ species depronates while uptake is reduced to approximately 30% of that obtained under acid conditions. The analyses of the surface complexes formed at pH 10.5 pointed to a partial oxidation of the monovalent As (III) anion associated with the occurrence of a less ordered surface complex. Under those conditions, arsenite is adsorbed as an oxy-anion, with only one oxygen being replaced by sulfur, i.e. As/S ratio of 1:1. The As-S interatomic distance is increased to 2.31 Å. By using Raman Spectroscopy it was possible to obtain two main informations: (i) the β-sheet structure was identified as the main secondary structure of the keratin biomass and (ii) the involvement of cysteine sulfur atoms during As (III) complexation was clearly indicated

by the vibrational modes of As-S bands combined with the reduction of other bands assigned to S-S bonds. The theoretical modeling provided by DFT calculations has corroborated the conclusions obtained by XAS and RAMAN spectroscopy.

The results obtained in the present work confirmed the initial hypothesis that a cysteine-rich biomass would be capable of adsorb the trivalent arsenic species, and provide the fundamentals for the development of a selective biosorbent for As (III) removal from contaminated waters.

Capítulo 1

Introdução e Objetivos do Trabalho

1.1 INTRODUÇÃO

O arsênio é amplamente distribuído na crosta terrestre, embora quase sempre presente em baixas concentrações. A arsenopirita é o mineral de arsênio mais abundante e ocorre associado a minerais de estanho e tungstênio, bem como à prata, ao cobre e ao ouro. Observam-se ainda associações com sulfetos de chumbo, zinco e ferro: galena-PbS, esfalerita-ZnS e pirita-FeS_2, respectivamente. A concentração de arsênio no solo pode variar na faixa de 0.1 até mais de 1000 ppm. Industrialmente, o As é empregado na manufatura de ligas de zinco, corantes e inseticidas. Combinado ao gálio, na forma de AsGa, é empregado na produção de semi-condutores e componentes de lasers para indústria eletrônica.

A despeito de sua utilidade, o As é extremamente nocivo à saúde, sendo considerados tóxicos quase todos os seus compostos. A inalação de arsênio pode causar principalmente carcinomas de pulmão. Uma vez ingerido, produz sintomas de irritação gastro-intestinal e náuseas. A longo prazo, a ingestão continuada ainda que de pequenas quantidades deste elemento, leva a manifestações crônicas cutâneas, doenças do aparelho respiratório, diabetes, distúrbios vasculares, neurológicos e câncer.

A contaminação ambiental por metais pesados tem sido objeto de diversas discussões, embora, poucas estejam voltadas para o estudo dos mecanismos bioquímicos que lhes conferem importância do ponto de vista toxicológico. As águas residuais das indústrias de mineração e metalurgia são consideradas como as principais fontes de contaminação ambiental por metais pesados como o arsênio. Além destas, níveis de arsênio relativamente altos são encontrados ocasionalmente em fontes de água de abastecimento municipais superficiais e subterrâneas, possivelmente devido à lixiviação de minerais associados aos depósitos minerais. Em vista disso, torna-se necessário o desenvolvimento de metodologias eficientes e economicamente viáveis para a remoção desse elemento. Garantir a qualidade da água de consumo, no que diz respeito aos teores de arsênio e demais metais pesados é, portanto, condição necessária à manutenção da saúde das

populações. Neste contexto, os métodos biológicos surgem como uma alternativa aos métodos convencionais.

Embora já tenham sido desenvolvidos diversos trabalhos de pesquisa abordando a bioacumulação e a oxidação bacteriana do As, com alguns resultados promissores, os relatos científicos a respeito da biossorção desse metal são praticamente inexistentes. Na verdade, observa-se uma lacuna na literatura no que se refere a biossorção de ânions de um modo geral e, em particular, dos ânions arsenicais. Fundamentados nos mecanismos bioquímicos que justificam os efeitos tóxicos das espécies arsenato e arsenito, este projeto vem avaliar a utilização de biomassas animais, ricas em proteínas fibrosas, como biossorventes para espécies hidrossolúveis de arsênio.

1.1.1 O Arsênio e os metais pesados

"Metais pesados" são metais com densidade acima de 5,0 g/cm^3. Dentre os 90 elementos de origem natural, temos 53 metais pesados, incluindo-se o As (Nies, 1999). Segundo o mesmo autor, a maioria dos metais pesados pertence ao grupo dos elementos de transição com orbitais incompletos. Estes orbitais incompletos geram cátions de metais pesados, fortes o suficiente para reagir e formar complexos. Em função disso, quantidades-traço desses elementos são extremamente importantes na manutenção das reações metabólicas de todas as células vivas e são indispensáveis, em baixíssimas concentrações. Em concentrações mais elevadas, entretanto, os metais pesados formam complexos inespecíficos nas células provocando efeitos tóxicos. Assim como outros metais pesados, o arsênio (As) passou recentemente a ser classificado como um dos mais novos elementos essenciais. Uma pequena ingestão de As é necessária à dieta humana. Parece que, de alguma maneira ainda não esclarecida, o As interfere no metabolismo do ferro. A ingestão diária de As na dieta recomendada ainda permanece indeterminada; sabe-se, entretanto, que no corpo humano adulto, existem cerca de 1-2 mg de As (Case *et al.*, 1983)

1.1.2 Farmacologia e Toxicologia do arsênio

A toxicologia reconhece de longa data a influência do estado de valência de um elemento sobre o seu comportamento no corpo humano. A distribuição das espécies arsenicais é essencial para se avaliar corretamente a sua toxicidade. No que diz respeito à especiação do As, a forma trivalente As_2O_3, é tida como altamente tóxica e vem sendo utilizada como veneno desde as eras mais remotas (Gupta *et al.*, 1978; Case *et al.*, 1983; Knowles *et al.*, 1983; Kaur *et al.*, 1992; Wood, 1992; Chiu *et al.*, 1994; Ramaswami *et al.*, 2001; Hughes, 2002). Em regiões da China com alta incidência de uma doença vascular periférica conhecida como "Black Foot Disease", uma manifestação resultante da contaminação por As, a relação As (III)/As (V) é de 9:1. Por outro lado, nos Estados Unidos, a comunidade de Fallon (NV) vem consumindo, desde 1941, água contaminada com níveis de As de 100 μg/L sem que se observem efeitos adversos à saúde da população. Foi confirmado, entretanto, que, nessa região, a forma pentavalente do As é predominante (Chiu *et al.*, 1994).

A forma trivalente do As é dez vezes mais tóxica que sua forma pentavalente e ainda apresenta uma mobilidade no meio ambiente significativamente maior (Rawlins *et al.*, 1997) sendo, portanto, potencialmente mais perigosa.

A ação cancerígena do arsênio é reconhecida desde o século XIX. Já no início do século XX, vários artigos haviam sido publicados relatando casos de neoplasias, dermatoses e irritações das vias aéreas superiores em pacientes trabalhadores de indústrias produtoras de compostos arsenicais ou usuários de medicamentos à base de arsênio (Gontijo, 1980). Na mesma época, sais orgânicos de arsênio trivalente começaram a ser utilizados no tratamento da sífilis na forma do medicamento Salvarsan®. Com o advento da penicilina, os medicamentos arsenicais foram rapidamente abandonados, antes que sua atividade bioquímica fosse completamente elucidada. O arsênio foi e ainda continua sendo utilizado como agente terapêutico, embora seu emprego seja feito hoje com muito mais rigor. Como exemplo da utilização recente de sais deste elemento podemos citar o uso do trióxido de

arsênio (As_2O_3) e do óxido de fenilarsina, que apresentam efeitos comprovados no tratamento da leucemia promielocítica aguda (Estrov *et al.*, 1999).

Tanto a atividade farmacológica quanto a atividade toxicológica do arsênio são baseadas em mecanismos similares. Os cátions de metais pesados, especialmente aqueles com números atômicos elevados, por exemplo, Hg^{2+}, Cd^{2+}, and Ag^{2+} e também o As, tendem a se ligar a grupamentos sulfidrila (SH) dos compostos biológicos (Nies, 1999). Por meio dessas ligações, estes elementos podem causar a inibição da atividade das enzimas sensíveis, cujos grupamentos químicos essenciais presentes nos sítios ativos são exatamente os grupamentos sulfidrila (Knowles *et al.*, 1983; Kaur *et al.*, 1992; Rojas-Chapana *et al.*, 2000). No caso da sífilis, por exemplo, os compostos arsenicais orgânicos trivalentes atuavam bloqueando os grupos sulfidrila (SH), indispensáveis à respiração do treponema (*Treponema palidum*), agente causador da doença, (Gontijo, 1980). O mesmo mecanismo explica o emprego do arsênio com fins toxicológicos, como por exemplo, na fabricação de armas químicas. Durante a Primeira Guerra Mundial uma das armas químicas empregadas foi o Gás Lewisite, um composto orgânico de arsênio trivalente ($C_2H_2AsCl_3$) cuja ação tóxica se devia à inibição da enzima piruvato oxidase. Os efeitos tóxicos desse gás podiam ser revertidos pela administração de antídotos contendo grupamentos SH em sua estrutura. O primeiro antídoto efetivo contra intoxicação por arsênio trivalente sintetizado foi o *British Anti-Lewisite*, mais conhecido como BAL; trata-se do composto 2,3-dimercaptopropanol ($C_3H_8OS_2$) cuja reação com o As (III) produz um composto hidrossolúvel que pode ser excretado pela urina (Jones, 1983).

De maneira geral, cátions de metais pesados interagem com íons ditos fisiológicos, por exemplo, Cd^{2+} com Zn^{2+} ou Ca^{2+}, Ni^{2+} e Co^{2+} com Fe^{2+}, Zn^{2+} com Mg^{2+}, inibindo sua função. Os oxiânions de metais pesados interferem com o metabolismo dos íons não metálicos estruturalmente semelhantes (cromato com sulfato, arsenato com fosfato). O arsenato é, estruturalmente, muito semelhante ao fosfato (PO_4^{3-}) e assim, sua principal toxicidade resulta da interferência com o metabolismo deste maior bio-elemento, que é o fósforo (Nies, 1999). O arsenato compete com fosfato pelos sítios ativos das enzimas fosforilativas, comuns a todos os seres vivos e essenciais ao metabolismo da glicose,

causando bloqueio ou perda de produtividade em diversas rotas metabólicas, através da formação de compostos de carboidrato "arsenilados" ao invés dos intermediários fosfatados esperados. Do ponto de vista funcional, o efeito tóxico do arsenato, equivale à supressão do aporte nutricional de fosfato (Kaur *et al.*, 1992; Hughes, 2002).

Pode-se concluir, portanto, que o arsênio e os compostos arsenicais são tóxicos e carcinogênicos para todos os seres vivos. A dose de As letal para humanos é da ordem de 0,6 mg/kg/dia (http://risk.lsd.ornl.gov/tox/profiles/arsenic.shtml) ou de 1-3 mg/kg, em se tratando exclusivamente de As inorgânico (Hughes, 2002)

O consumo diário de água com concentrações de As superiores a 50 µg/L – menos que 1% da dose letal – pode acarretar problemas de pele, além de distúrbios dos sistemas circulatório e nervoso e da visão e audição. Se as concentrações de As atingirem níveis perigosamente superiores aos recomendados, cânceres, distúrbios nervosos e danos em diversos órgãos podem acontecer, sendo, geralmente, fatais. (Das, 1998; Matschullat *et al.*, 2000).

No que concerne à bioquímica do arsênio, sabe-se que o arsênio inorgânico ingerido é rapidamente absorvido pelo trato gastro-intestinal. O As absorvido é transportado através do sangue, ligado a grupamentos SH das proteínas ou compostos de baixo peso molecular como a glutationa e a cisteína (Figura 1.1) até os órgãos do corpo, principalmente o fígado, onde sofre reações de metilação que diminuem sua toxicidade. A metilação envolve a adição de grupamentos metila doados pela S-adenosilmetionina ao arsênio apenas em seu estado trivalente. A eficiência da metilação depende das taxas de redução do As (V) a As (III). Estudos *in vitro* utilizando hepatócitos isolados de ratos demonstraram que apenas o arsenito é rapidamente captado e metilado pelas células do tecido hepático (Lerman *et al.*, 1983). Tal especificidade pode ser explicada pelo fato de, nas condições de pH fisiológicas, apenas as espécies trivalentes do arsênio se encontrarem não ionizadas.

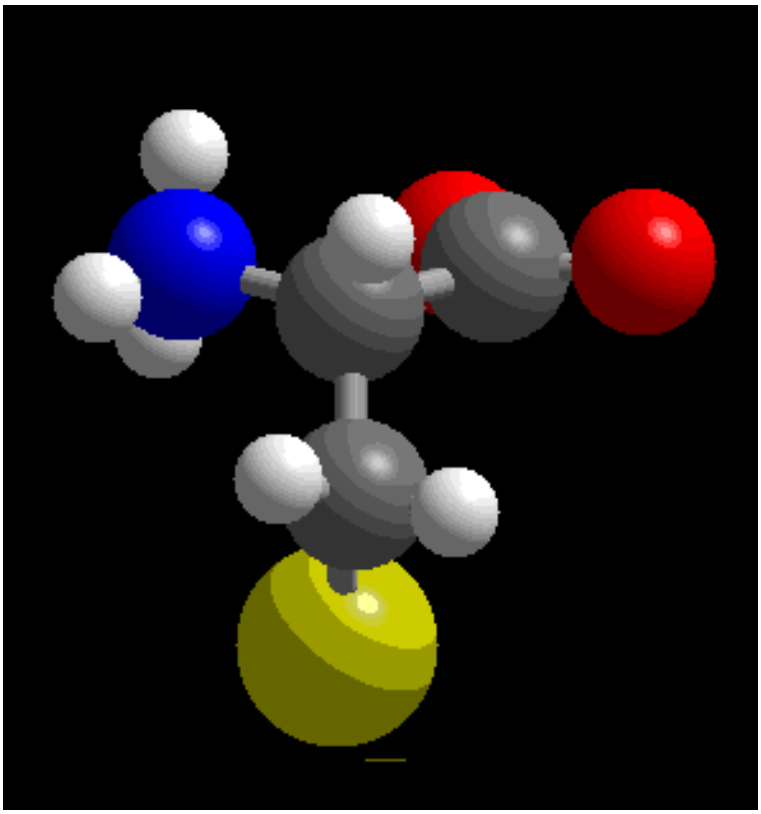

Figura 1.1. Estrutura do aminoácido cisteína (em cinza, C; em azul, N; em vermelho, O; em amarelo, S)

As etapas de redução do As e sua subseqüente metilação, esquematizadas a seguir (Hughes, 2002), produzem um composto final de arsênio oxidado, com toxicidade e mobilidade inferiores ao composto original.

$$As^{V}O(OH)_3 + 2e^- \rightarrow As^{III}(OH)_3 + CH_3^+ \rightarrow CH_3As^{V}O(OH)_2 + 2e^- \rightarrow CH_3As^{III}(OH)_2 + CH_3 \rightarrow (CH_3)_2As^{V}O(OH) + 2e^- \rightarrow (CH_3)_2As^{III}OH + CH_3^+ \rightarrow (CH_3)_3As^{V}O \quad (1.1)$$

A glutationa, bem como o ditiotreitol e a cisteína desempenham papel importante na redução da espécie pentavalente. A redução do As (V) a As (III) resulta no aumento da retenção desse elemento na maioria dos tecidos corporais porque a espécie trivalente é mais reativa com as proteínas dos tecidos corporais do que a espécie pentavalente (Bogdan *et al.*, 1994; Styblo *et al.*, 1995). Estudos experimentais com mamíferos expostos a arsênio inorgânico mostraram que os tecidos com a maior retenção de arsênio são a pele, unhas, os cabelos, o epitélio descamativo do trato gastro-intestinal superior (cavidade oral, língua, esôfago, paredes do estômago), o epidídimo, a tireóide, o esqueleto e as lentes oculares. Com exceção do esqueleto, todos os demais tecidos apresentam maior conteúdo de arsenito do que arsenato, logo após a ingestão simultânea de ambas as formas arsenicais. No caso do tecido ósseo, o arsenato parece substituir o fosfato presente nos cristais de apatita, em função de suas similaridades químicas. A ligação do arsênio trivalente com grupamentos tiólicos funcionais de enzimas pode causar inibição de enzimas importantes em rotas metabólicas essenciais. Entretanto, a mesma interação com sítios secundários de outras proteínas pode resultar na sua detoxificação (Hughes, 2002).

Com base em todas as evidências que relacionam a ocorrência de efeitos toxicológicos crônicos e a ingestão de água contaminada por As, vários órgãos governamentais de controle ambiental recomendaram a redução nos limites máximos admissíveis para As em água potável. A Organização Mundial da Saúde (OMS) recomendou, em 1993, que o limite de 50 μg/L fosse reduzido para 10 μg/L. No caso da Comunidade Européia e do Japão, estes novos valores foram adotados. No Canadá o limite é de 25 μg/L e nos Estados Unidos, após uma resistência inicial em adotar as recomendações da OMS em função dos

custos financeiros envolvidos (Smedley *et al.*, 2002), a legislação foi alterada. A agência de proteção ambiental dos Estados Unidos conseguiu que a recomendação da OMS fosse adotada a partir de outubro de 2001 embora venha a ser completamente implementada apenas a partir de 2006. A legislação ambiental brasileira também adotou a recomendação da OMS e os novos limites passaram a vigorar a partir de dezembro de 2003.

1.1.3 Origem da contaminação por arsênio

O As é encontrado na atmosfera, no solo, nas rochas, em águas naturais e, até mesmo, nos organismos vivos. Sua mobilização se deve a uma combinação de processos naturais, tais como variações climáticas, atividade biológica, atividade vulcânica, bem como atividades antropogênicas (Mandal *et al.*, 2002; Smedley *et al.*, 2002). O As ocorre naturalmente em mais de 200 diferentes formas minerais. Aproximadamente 60% delas são arsenatos, 20% apresentam-se como sulfetos ou sulfo-sais e os outros 20% incluem os arsenitos, arsenetos, óxidos, silicatos e arsênio elementar. O mineral de arsênio mais comum é a arsenopirita, FeAsS (Mandal *et al.*, 2002).

Na crosta terrestre, o As existe em quantidades que variam entre 1 mg /kg (em amostras de apatita, ilmenita, calcita, barita, fluorita) a 77.000-126.000 mg/kg (em amostras de pirita e arsenopirita) e de 0,3 a 8.000 mg /kg em rochas, sedimentos, solos e depósitos superficiais. Em solo não contaminado, a concentração normal de As é de 6 mg/kg (Manning *et al.*, 1997; Mandal *et al.*, 2002). Em ambientes aquáticos as concentrações podem variar de 0,02 (em ambientes marinhos) a mais de 850.000 μg/L (em drenagens ácidas de minas). É grave o fato de que alguns depósitos de água subterrânea de Bangladesh, Argentina, México, China, Índia, Taiwan e Hungria apresentem níveis de contaminação da ordem de 10-5000 μg/L (Smedley *et al.*, 2002). No Brasil, levantamentos recentes feitos por pesquisadores do nosso grupo (Matschullat *et al.*, 2000; Deschamps *et al.*, 2002) indicam a ocorrência de anomalias geológicas em regiões do Quadrilátero Ferrífero, próximas aos

municípios de Santa Bárbara, Barão de Cocais e Nova Lima, com concentrações médias de As da ordem de 100,0 mg/kg no solo e de até 547,0 mg/kg em sedimentos do Ribeirão Cardoso.

Na Índia ou em Bangladesh é relatado um caso de calamidade pública devido à ingestão de água contaminada com arsênio, predominantemente na forma trivalente, devido ao uso de água de poços profundos para consumo humano, com uma significativa porção da população apresentando sinais característicos de intoxicação por compostos arsenicais. No Brasil, dados que apontam indícios de ocorrência de contaminação arsenical em solos e sedimentos, além da água superficial e subterrânea, em algumas regiões do Quadrilátero Ferrífero em Minas Gerais (Rawlins *et al.*, 1997; Matschullat *et al.*, 2000; Deschamps *et al.*, 2002), ainda estão sendo avaliados, e os trabalhos de pesquisa prosseguem de maneira cautelosa. Apesar dos teores de As encontrados no nosso estado não serem tão alarmantes quanto àqueles da Ásia, é preocupante perceber que, em alguns pontos de coleta nas regiões de Nova Lima e Mariana, são encontrados teores de As nas águas superficiais cerca de 10 a 100 vezes superiores aos limites recomendados pela OMS. No caso específico de água subterrânea, na região próxima à mineração de ouro em Passagem de Mariana, o valor encontrado é 170 vezes superior ao recomendado (Rawlins *et al.*, 1997). É, portanto necessária uma avaliação em longo prazo dos efeitos resultantes dessa contaminação sobre as populações dessas regiões que se utilizam, direta ou indiretamente, de água contaminada por arsênio e que estão constantemente submetidas à absorção, por meio da aspiração, de partículas finas de sólidos dispersas na poeira. Do ponto de vista da saúde das populações, em trabalho recente e pioneiro, um consórcio de pesquisadores brasileiros e alemães (Matschullat *et al.*, 2000) realizou um levantamento epidemiológico sobre os índices de contaminação arsenical em material biológico, principalmente urina, de crianças moradoras em distritos dos municípios de Santa Bárbara e Nova Lima. Os resultados obtidos indicavam que aproximadamente 45% das crianças examinadas, com idades ente 7-14 anos apresentavam níveis de arsênio na urina de 15-40 μg/L, enquanto aproximadamente 20% delas apresentavam índices maiores que 40 μg/L podendo, portanto, serem classificadas, respectivamente, dentro dos grupos considerados de médio e alto risco, embora ainda não tenham sido observados os efeitos fisiopatológicos da

intoxicação por esse elemento. Amostragens subseqüentes, entretanto, indicaram uma redução dos valores obtidos na primeira coleta.

A despeito das fontes naturais de contaminação anteriormente citadas, a poluição por metais pesados é causada pelas atividades industriais e da agricultura. As principais atividades responsáveis pela geração de resíduos ricos em arsênio são as indústrias de geração de energia, incluindo a de combustíveis fósseis, a indústria metalúrgica e a agricultura. No Brasil, o arsênio é amplamente encontrado no meio industrial, como resíduo, especialmente das indústrias de processamento metalúrgico de ouro, cobre, prata, zinco e cobalto. Este elemento é empregado ainda como matéria-prima na manufatura de vidros, esmaltes, tintas, tecidos e couros e na produção de insumos agrícolas tais como inseticidas, formicidas, herbicidas e preservativos de madeira. O consumo de arsênio pela indústria é, entretanto, insignificante diante das enormes quantidades desse elemento produzidas como resíduos industriais.

1.1.4 Métodos para remoção de Arsênio

A contaminação por arsênio pode ocorrer tanto nas águas residuais industriais, quanto naquelas destinadas para consumo. A maioria dos relatos de problemas de contaminação por As em fontes de água para consumo humano estão relacionadas a fontes de água subterrâneas, geralmente utilizadas preferencialmente pelas populações de áreas rurais.

A química do arsênio em ambientes aquosos é complexa. No ambiente aquático, o As pode ser encontrado tanto na forma trivalente quanto na forma pentavalente. As espécies de As (III) (H_3AsO_3, $H_2AsO_3^-$ e $HAsO_3^{2-}$) são comumente encontradas em condições anaeróbicas ou redutoras (por exemplo, em águas subterrâneas) enquanto as espécies de As (V) (H_3AsO_4, $H_2AsO_4^-$ e $HAsO_4^{2-}$) prevalecem em condições aeróbicas ou oxidantes (águas superficiais bem oxigenadas) (Gupta *et al.*, 1978; Matschullat *et al.*, 2000; Smedley

et al., 2002). Destacado dentre a maioria dos elementos formadores de oxiânions, o As é singular na sua mobilidade na faixa de pH típico das águas subterrâneas (Smedley *et al.*, 2002). Em valores de pH abaixo de 9,2 (pKa_1=9,23, pKa_2=12,13, pKa_3=13,4 para o H_3AsO_3) predomina a espécie neutra do As (III), que é adsorvida nos oxihidróxidos metálicos presentes em solos típicos de forma bastante reversível. Por outro lado, o As pentavalente se apresenta, predominantemente, nas formas aniônicas (pKa_1=2,22, pKa_2=6,98, pKa_3=11,53 para o H_3AsO_4), que são adsorvidas na forma de estruturas mais estáveis (Ciminelli *et al.*, 2004)

A maioria dos cátions de metais pesados tóxicos (Pb^{2+}, Cu^{2+}, Ni^{2+}, Cd^{2+}, Co^{2+}, Zn^{2+}) tem sua solubilidade diminuída à medida que o pH se eleva, seja por precipitação ou co-precipitação como óxidos, hidróxidos, carbonatos ou fosfatos, ou através da adsorção mais efetiva em óxidos metálicos, argilas ou em matéria orgânica. Por outro lado, a maioria dos oxiânions, tende a se tornar mais fracamente adsorvida à medida que o pH se eleva (Smedley *et al.*, 2002). Existe na literatura um certo consenso de que a remoção efetiva do arsênio da água requer a oxidação completa do As (III) a As (V) (Das, 1998; Roussel *et al.*, 2000; Korngold *et al.*, 2001). Uma vez oxidado, o As é mais eficientemente removido de uma solução, por meio da adsorção ou co-precipitação do As (V) com oxi-hidróxidos de Fe (III) ou Al (Roussel *et al.*, 2000).

Precipitação, troca iônica, processos eletroquímicos ou processos empregando membranas são comumente aplicados no tratamento de efluentes industriais (Wood, 1992; Veglio *et al.*, 1997) mas seus custos operacionais, com exceção da precipitação, são muito elevados (Jansson-Charrier *et al.*, 1995). Os custos de investimento inicial e operacional para instalação de plantas industriais de tratamento de efluentes contaminados com metais pesados são bastante significativos (Eccles, 1999). A Tabela I.1 apresenta os custos envolvidos no emprego de algumas das tecnologias disponíveis (os valores estão expressos em US$ gastos/m^3de efluente tratado).

Algumas das técnicas de remoção de arsênio convencionais disponíveis são descritas a seguir. Os processos podem ser divididos em duas categorias principais: na primeira estão aqueles que envolvem precipitação e na segunda aqueles que envolvem adsorção.

A remoção de arsênio por precipitação com íons metálicos é a técnica melhor conhecida e mais freqüentemente empregada. Os melhores resultados são obtidos na precipitação de As (V) com sais férricos em valores de pH entre 7.2 e 7.5. A remoção de arsênio por precipitação com cal na forma de arsenato de cálcio vem sendo praticada há muito tempo. Todavia, o composto $Ca(AsO_4)_2$ não é considerado apropriado para disposição de longo prazo, devido à possibilidade de redissolução do arsênio nele contido através de reações de carbonatação (Zouboulis *et al.*, 1993). A precipitação do arsênio na forma de sulfeto é uma alternativa: condições ácidas redutoras favorecem a precipitação do ouropigmento (As_2S_3), do realgar (As_4S_4) ou outros sulfetos minerais contendo As co-precipitado. Conseqüentemente, teores elevados de As não são esperados quando se têm altas concentrações de sulfeto livre na água. Entretanto, os sulfetos não são estáveis em condições oxidantes.

Tabela I.1 – Custos iniciais e operacionais envolvidos no tratamento de efluentes líquidos contaminados por metais pesados (Eccles, 1999).

Tecnologia	Custos (US$/m^3)		
	Inicial		Operacional
	Planta 1000 m^3/dia	Planta 10000-20000 m^3/dia	
Precipitação Incluindo:neutralização, coagulação, floculação e separação	12,5	8	0,003-0,013
Adsorção em Carvão Ativado Granulado	500	250	0,020-0,050
Microfiltração em Membranas	12,5	11	0,013-0,050
Troca Iônica	100	75	0,050-0,250

Ao longo dos anos, vários tipos de sorventes vêm sendo testados e utilizados para promover a adsorção do arsênio. Podem ser citados, por exemplo, a alumina ativada, os óxidos de ferro e alumínio hidratados, argilominerais (caulinita, bentonita, goetita), sulfetos como pirita, galena e esfalerita, minerais de manganês ou areia recoberta de óxidos de alumínio. Além desses, há outros sorventes orgânicos ou sintéticos que podem ser empregados com a mesma finalidade. Podem ser citadas as resinas poliméricas de troca iônica, o carvão ativado, a quitina e a quitosana, o carvão de osso, o carvão de casca de coco, casca de laranja, biomassa fúngica e os materiais derivados de celulose (Gupta *et al.*, 1978; Zouboulis *et al.*, 1993; Driehaus *et al.*, 1995; Styles *et al.*, 1996; Ladeira *et al.*, 1997; Manning *et al.*, 1997; Manju *et al.*, 1998; Dambies *et al.*, 1999; Ladeira, 1999; Murcott, 1999; Ramaswami *et al.*, 2001; Dambies *et al.*, 2002; Meng *et al.*, 2002; Bostick *et al.*, 2003; Dixit *et al.*, 2003; Ghimire *et al.*, 2003; Loukidou *et al.*, 2003; Ladeira *et al.*, 2004; Singh *et al.*, 2004; Zhang *et al.*, 2004). Para todas as técnicas citadas anteriormente, sem exceção, a principal limitação da adsorção é a remoção eficiente do As (III).

O arsênio (V) é efetivamente adsorvido pela alumina e pela gibsita ativadas na faixa de pH entre 4,0 e 7,0, entretanto, essas taxas decrescem à medida que o pH se eleva, sendo que a

tendência oposta ocorre com a adsorção do As (III) (Gupta *et al.*, 1978). Diversos autores (Gupta *et al.*, 1978; Driehaus *et al.*, 1995; Ladeira *et al.*, 1997; Manning *et al.*, 1997; Ladeira, 1999) relatam, que o As (III) é menos eficientemente removido do que o As (V) e que, portanto, é necessário promover a oxidação do arsenito a arsenato para se obter uma remoção mais eficiente do ânion.

Além das técnicas previamente discutidas, existem outras opções tecnológicas envolvendo a utilização das membranas semipermeáveis. Tais membranas são seletivamente permeáveis à água e alguns solutos e, em vista disso, se adequam ao emprego na remoção de diversas impurezas da água para consumo, inclusive o arsênio, e se apresentam como alternativas - ainda pouco exploradas, seja devido aos custos envolvidos, seja em decorrência de limitações técnicas. Podemos incluir nessa classe a microfiltração, a osmose reversa, a eletrodiálise, a ultrafiltração e a nanofiltração. Estas técnicas apresentam como inconveniente o custo bastante elevado.

A necessidade de busca de métodos economicamente viáveis e eficientes para remoção de arsênio e outros metais pesados resultou no desenvolvimento de novas tecnologias de separação, dentre as quais aquelas envolvendo biossorção (Schneider *et al.*, 1995). Nesse sentido a biossorção usando biomassa residual, orgânica ou inorgânica, abundante e de baixo custo, surge, recentemente, como método alternativo promissor para remoção de íons metálicos (Volesky *et al.*, 1995), principalmente para operações em pequena escala (Poulin *et al.*, 1996; Cimino *et al.*, 2000). Algas, bactérias, fungos e leveduras já tiveram comprovado seu potencial em atuar como biossorventes de metais.

1.2 RELEVÂNCIA DO PROJETO

O arsênio e seus compostos, apesar de considerados essenciais ao metabolismo, são tóxicos e carcinogênicos a todos os seres vivos. As espécies solúveis de arsênio, tanto as derivadas do ácido arsenioso (H_3AsO_3) quanto àquelas derivadas do ácido arsênico (H_3AsO_4), são capazes de formar complexos inespecíficos com aminoácidos localizados nos sítios ativos de enzimas essenciais à manutenção das funções metabólicas normais dos seres vivos. O arsênio é classificado como um veneno protoplasmático geral que, unindo-se aos grupos SH de certas enzimas, especialmente as piruvatoxidases e as fosfatases, reduz ou abole a respiração celular, denotando claramente a sua especificidade pelos grupamentos sulfidrila.

Sabe-se ainda que as espécies trivalentes apresentam maior toxicidade bem como maior mobilidade, adquirindo, portanto, maior importância tanto do ponto de vista ambiental quanto toxicológico. As metodologias disponíveis para remediação de arsênio, sejam elas convencionais ou alternativas, apresentam uma limitação comum: removem, eficientemente, as espécies pentavalentes do As, mas geralmente falham na remoção/imobilização das espécies trivalentes, o que implica na necessidade de oxidação prévia do arsenito a arsenato como etapa intermediária do processo.

Embora a bioacumulação e a oxidação bacteriana de As sejam processos bastante conhecidos, publicações a respeito da biossorção desse elemento são bastante raras. De fato, existe uma lacuna na literatura no que se refere a biossorção de ânions, de um modo geral e, em particular, dos ânions arsenicais. Percebemos ainda que os trabalhos sobre biossorção são algumas vezes superficiais, restringindo-se apenas à seleção de biossorventes com base nos dados obtidos a partir de isotermas de adsorção. Essa seleção vem em geral acompanhada de pouca ou nenhuma discussão a respeito dos mecanismos físico-químicos que explicam o fenômeno da adsorção em si. Esta superficialidade pode ser conseqüência do fato da biossorção ser uma área do conhecimento que ocupa uma interface entre a biologia, a química e a engenharia e, assim sendo, os pesquisadores,

sentem-se pouco à vontade para "transitar" por áreas aparentemente tão díspares. No nosso grupo de trabalho, buscamos a quebra desses paradigmas através da interação destas diferentes áreas do conhecimento buscando compreender a adsorção, nela incluída a biossorção, ao nível molecular.

Com este objetivo em mente e fundamentados nos mecanismos bioquímicos que justificam os efeitos tóxicos dos oxiânions arsenato e arsenito (Knowles *et al.*, 1983; Kaur *et al.*, 1992) e sua afinidade química por grupamentos SH (Bhattacharjee *et al.*, 1996; Shi *et al.*, 1996; Styles *et al.*, 1996; Farrer *et al.*, 2000; Martin *et al.*, 2001), este trabalho vem propor a utilização de biomassas animais, ricas em proteínas fibrosas, como biossorventes para ânions arsenicais, em particular os íons arsenito, neste caso, sem necessidade de oxidação prévia desse elemento.

Levando-se em consideração (i) o fato de que a cisteína é um aminoácido presente em abundância na estrutura da queratina, constituinte principal das proteínas fibrosas estruturais presentes em estruturas corporais dos animais superiores, tais como, unhas, chifres, cabelos, pêlos, cascos e penas, e (ii) que o grupamento funcional da cisteína é o grupamento sulfidrila, o presente trabalho propõe a utilização de biomassa residual, de baixo custo, para imobilização do arsênio em seu estado reduzido, sem a necessidade de etapas prévias de oxidação. Como material biosorvente foi selecionado um pó obtido pela trituração de penas de galinhas.

1.3 OBJETIVOS E ORGANIZAÇÃO DA TESE

Os principais objetivos deste trabalho de Tese são:

(i) propor, pela primeira vez, a utilização de um biossorvente capaz de adsorver eficientemente, a espécie reduzida do arsênio sem a necessidade de etapas prévias de oxidação;

(ii) contribuir para o entendimento das questões referentes à estabilidade dos compostos arsenicais trivalentes e sua imobilização em presença de matéria orgânica.

Visando atingir aos objetivos gerais propostos, o desenvolvimento deste trabalho de Tese envolveu as seguintes etapas:

- Seleção e preparação de um biossorvente específico para sorção de As (III);
- Avaliação do desempenho do biossorvente selecionado sob diferentes condições de preparação da amostra, pH, concentração de biomassa e presença de íons competidores;
- Identificação dos mecanismos de adsorção através do uso de técnicas de Espectroscopia de absorção de raios-X, *Expanded X-Ray Adsorption Fine Structure* (EXAFS) and *X-Ray Absorption Near Edge Structure* (XANES) e Espectroscopia Vibracional Raman, associadas às predições teóricas baseadas em *Density Functional Theory*-DFT. Proposição, com base nos dados estruturais obtidos, de um modelo estrutural para o complexo de adsorção formado entre o átomo de As (III) e os sítios ativos da biomassa;
- Proposição de um mecanismo de adsorção do arsenito em biomassa animal rica em proteína fibrosa.

Para melhor discussão dos resultados obtidos, esta Tese foi subdividida em 5 capítulos. No Capítulo 1 é apresentada uma introdução ao tema bem como uma sucinta revisão da literatura. São ainda apresentados a relevância e os objetivos do trabalho. Nos três capítulos subseqüentes e nos anexos são apresentados os resultados experimentais obtidos.

No capítulo 2 (aceito para publicação na revista *Environmental Science and Technology*) estão apresentados os resultados referentes à adsorção de arsenito em biomassa animal sob diferentes condições experimentais. São apresentados também os resultados de Espectroscopia de Absorção de Raios X (XANES e EXAFS) que nos levaram à proposição do mecanismo de adsorção.

No capítulo 3 (submetido para publicação na revista *Environmental Science and Technology*) utilizamos novamente da Espectroscopia de Absorção de Raios X para compreender o efeito do pH na formação dos complexos de adsorção entre o arsenito e a biomassa. Confrontamos ainda os dados experimentais obtidos com as predições teóricas baseadas em *Density Functional Theory*-DFT a fim de melhor compreender o modelo de adsorção proposto.

No capítulo 4 (aceito para publicação no *Journal of Colloids and Interface Science*) utilizamos novamente a DFT associada à espectroscopia Raman, para caracterização tanto da biomassa quanto dos complexos de adsorção formados.

No capítulo 5 são apresentadas as considerações finais e conclusões, tentando ressaltar as inter-relações entre os capítulos 2 a 4, além das contribuições específicas deste trabalho, bem como as sugestões de trabalhos futuros e os trabalhos gerados a partir dessa Tese.

1.4 REFERÊNCIAS BIBLIOGRÁFICAS:

Bhattacharjee, H. and Rosen, B. (1996). Spatial Proximity of Cys 113, Cys172, and Cys 422 in the Metalloactivation Domain of the ArsA ATPase. *The Journal of Biological Chemistry*, 271, p. 24465-24470.

Bogdan, G. M.; Sampayo-Reyes, A. and Aposhian, H. V. (1994). Arsenic Binding Proteins of Mammalian Systems: I. Isolation of Three Arsenite-binding Proteins of Rabbit Liver. *Toxicology*, 37, p. 3149-3153.

Bostick, B. C. and Fendorf, S. (2003). Arsenite sorption on troilite (FeS) and pyrite (FeS_2). *Geochimica et Chosmochimica Acta*, 67, p. 909-921.

Case, C. and Robinson, M. F. (1983). Some Aspects in Nutritional Trace Elements. In: H. Siegel. *Methods Involving Metal Ions and Complexes in Clinical Chemistry*. New York, Marcel Dekker, Inc. 16: p. 1-26.

Chiu, K.-H.; Chen, S.-L.; Dzeng, S. R.; Shieh, G.-M.; Yang, M.-H. and Wal, C. M. (1994). Arsenic Species in Groundwaters of the Blackfoot Disease Area, Taiwan. *Environ. Sci. Technol.*, 28, p. 877-881.

Ciminelli, V. S. T.; Ladeira, A. C. Q.; Duarte, H. A. and Oliveira, A. F. (2004). As(III) adsorbed on gibsite: structural model of surface complex based on EXAFS and DFT calculations. *submitted to Geochimica Chosmochimica Acta*.

Cimino, G.; Passerini, A. and Toscano, G. (2000). Removal of Toxic Cations and Cr(VI) from Aqueous Solution by Hazelnut Shell. *Wat. Res.*, 34, p. 2955-2962.

Dambies, L.; Roze, A.; Roussy, J. and Guibal, E. (1999). As (V) removal from dilute solutions using MICB (molybdate-impregnated chitosan beads). International Biohydrometallurgy Symposium - IBS99 Biohydrometallurgy and the environment toward the mining of the 21st century. R. Amils and A. Ballester. Madrid, Elsevier. B**:** 842.

Dambies, L.; Vincent, T. and Guibal, E. (2002). Treatment of Arsenic-Containing Solutions using Chitosan Derivatives: Uptake Mechanism and Sorption Performances. *Water Research*, 36, p. 3699-3710.

Das, H. K. (1998). Alternative Sources of Arsenic-Safe Drinking Water. The Daily Star (http://www.dainichi-consul.co.jp/english/arsenic/removal.htm**:** 6 pages.

Deschamps, E.; Ciminelli, V. S. T.; Lange, F. T.; Matschullat, J.; Raue, B. and Schmidt, H. (2002). Soil and Sediment Geochemistry of the Iron Quadrangle, Brazil. *J Soils & Sediments 2002*, 2, p. 216-222.

Dixit, S. and Hering, J. g. (2003). Comparision of Arsenic(V) and Arsenic(III) Sorption onto Iron Oxide Minerals: Implications for Arsenic Mobility. *Environmental Science and Technology*, 37, p. 4182-4189.

Driehaus, W.; Seith, R. and Jekel, M. (1995). Oxidation of Arsenate(III) with Manganese Oxides in Water Treatment. *Water Research*, 29, p. 297-305.

Eccles, H. (1999). Treatment of Metal-Contaminated Wastes: Why Select a Biological Process? *TIBTECH*, 17, p. 462-464.

Estrov, Z.; Manna, S. K.; Harris, D.; Van, Q.; Estey, E. H.; Kantarjian, H. M.; Talpaz, M. and Aggarwal, B. B. (1999). Phenylarsine oxide blocks interleukin-1 beta-induced activation of the nuclear transcription factor NF-Kappa B, inhibits proliferation and induces apoptosis of acute myelogenous leukemia cells. *Blood*, 94, p. 2844-2853.

Farrer, B. T.; McClure, C. P.; Penner-Hahn, J. E. and Pecoraro, V. L. (2000). Arsenic (III)-Cysteine Interactions Stabilize Three-Helix Bundles in Aqueous Solution. *Inorganic Chemistry*, 39, p. 5422-5423.

Ghimire, K. N.; Inoue, K.; Yamagushi, H.; Makino, K. and Miyajima, T. (2003). Adsorptive separation of arsenate and arsenite anions from aqueous medium by using orange waste. *Water Research*, 37, p. 4945-4953.

Gontijo, B. (1980). *Contribuição ao Estudo do Arsenicismo Cutâneo*. Faculdade de Medicina, UFMG, Belo Horizonte. 48.(M. Sc. Thesis)

Gupta, S. K. and Chen, K. C. (1978). Arsenic removal by adsorption. *Journal of Water Pollution Control Federation*, 50, p. 493-506.

Hughes, M. F. (2002). Arsenic Toxicity and Potential Mechanisms of Action. *Toxicology Letters*, 133, p. 1-16.

Jansson-Charrier, M.; Guibal, E.; Surjous, R. and Cloirec, P. L. (1995). Continuous Removal of Uranium by Biosorption onto Chitosan: Application to an Industrial Effluent. In: International Biohydrometallurgy Symposium /IBS-95, 1995, Vina del Mar, Chile. November, 19-22, 1995. p. 267-276

Jones, M. M. (1983). Therapeutic Chelating Agents. In: H. Siegel. *Methods Involving Metal Ions and Complexes in Clinical Chemistry*. New York, Marcel Dekker, Inc. 16: p. 47-83.

Kaur, P. and Rosen, B. P. (1992). Plasmid-Encoded Resistance to Arsenic and Antimony. *Plasmid*, 27, p. 29-40.

Knowles, F. C. and Benson, A. A. (1983). The biochemistry of arsenic. *TIBS*, 8, p. 178-179.

Korngold, E.; Belayev, N. and Aronov, L. (2001). Removal of Arsenic from Drinking Water by Anion Exchangers. *Desalination*, 141, p. 81-84.

Ladeira, A. C. Q. (1999). *Utilização de Solos e Minerais para Imolização de Arsênio e Mecanismo de Adsoção*. Escola de Engenharia - Departamento de Engenharia Metalúrgica e de Minas, UFMG, Belo Horizonte. 160. (PhD. Thesis)

Ladeira, A. C. Q. and Ciminelli, V. S. T. (2004). Adsorption and desorption of arsenic on an oxisol and its constituents. *Water Research*, 38, p. 2087-2094.

Ladeira, A. C. Q.; Ciminelli, V. S. T. and Fonseca, J. F. M. (1997). Controle da Emissão de Arsênio Através da Imobilização em Argilas. In: 2º Congresso Internacional de Tecnologia Metalúrgica e de Materiais, 1997, São Paulo - SP. CD-ROM

Lerman, S. and Clarkson, T. W. (1983). The Metabolism of Arsenite and Arsenate by the rat. *Fundam. Appl. Toxicol.*, 3, p. 309-314.

Loukidou, M. X.; Matis, K. A.; Zouboulis, A. I. and Liakopoulou-Kyriakidou, M. (2003). Removal of As(V) from wastewaters by chemically modified fungal biomass. *Water Research*, 37, p. 4544-4552.

Mandal, B. K. and Suzuki, K. T. (2002). Arsenic Round the World: a Review. *Talanta*, 58, p. 201-235.

Manju, G. N.; Raji, C. and Anirudhan, T. S. (1998). Evaluation of coconut husk carbon for the removal of arsenic from water. *Water Research*, 32, p. 3062-3070.

Manning, B. A. and Goldberg, S. (1997). Adsorption and Stability of Arsenic(III) at the Clay Mineral-Water Interface. *Environmental Science &Technology*, 31, p. 2005-2011.

Martin, P.; DeMel, S.; Shi, J.; Gladysheva, T.; Gatti, D. L.; Rosen, B. P. and Edwards, B. F. P. (2001). Insights into the structure, solvation and mechanism of ArsC arsenate reductase, a novel arsenic detoxification enzyme. *Structure*, 9, p. 1071-1081.

Matschullat, J.; Borba, R. P.; Deschamps, E.; Figueiredo, B. R.; Gabrio, T. and Schwenk, M. (2000). Human and Environmental Contamination in the Iron quadrangle, Brazil. *Applied Geochemistry*, 15, p. 181-190.

Meng, X.; Korfiatis, G. P.; Bang, S. and Bang, K. W. (2002). Combined Effects of Anions on Arsenic Removal by iron Hydroxides. *Toxicology Letters*, 133, p. 103-111.

Murcott, S. (1999). Appropriate Remediation Technologies for Arsenic - Contaminated Wells in Bangladesh. In: Arsenic in Bangladesh Ground Water, 1999, Wagner College, Staten Island, New York (http:/phys4.harvard.edu/~wilson/murcott.html). February 27 - 28, 1999. p.

Nies, D. H. (1999). Microbial heavy-metal resistance. *Apllied Microbiology Biotechnology*, 51, p. 730-750.

Poulin, R. and Lawrence, R. W. (1996). Economic and Environmental Niches of Biohydrometallurgy. *Minerals Engineering*, 9, p. 799-810.

Ramaswami, A.; Tawachsupa, S. and Isleyen, M. (2001). Batch-Mixed Iron Treatment of High Arsenic Waters. *Wat. Res.*, 35, p. 4474-4479.

Rawlins, B. G.; Williams, T. M.; Breward, N.; Ferpozzi, L.; Figueiredo, B. and Borba, R. (1997). Preliminary Investigation of Mining-related Arsenic Contamination in the Provinces of Mendoza and San Juan (Argentina) and Minas Gerais State (Brazil). Keyworth, Nottingham, British Geological Survey.

Rojas-Chapana, J. A. and Tributsch, H. (2000). Bio-leaching of Pyrite accelerated by Cysteine. *Process Biochemistry*, 35, p. 815-824.

Roussel, C.; Bril, H. and Fernandez, A. (2000). Arsenic Speciation: Involvement in Evaluation of Environmental Impact Caused by Mine Wastes. *J. Environ. Qual.*, 29, p. 182-188.

Schneider, I. A. and Rubio, J. (1995). New Trends in Biosorption of Heavy Metals By Freshwater Macrophytes. In: International Biohydrometallurgy Symposium/IBS-95, 1995, Vina del Mar, Chile. November, 19-22,1995. p. 247-256

Shi, W.; Dong, J.; Scott, R. A.; Kasenzenko, M. Y. and Rosen, B. (1996). The Role of Arsenic-Thiol Interactions in Metalloregulation of the ars Operon. *The Journal of Biological Chemistry*, 271, p. 9291-9297.

Singh, T. S. and Pant, K. K. (2004). Equilibrium, kinetics and thermodynamic studies for adsorption of As(III) on activated alumina. *Separation Purification Technology*, 36, p. 139-1478.

Smedley, P. L. and Kinniburgh, D. G. (2002). A review of the source, behaviour and distribution of arsenic in natural waters. *Apllied Geochemistry*, 17, p. 517-568.

Styblo, M.; Yamauchi, H. and Thomas, D. J. (1995). Comparative in Vitro Methylation of Trivalent and Pentavalent Arsenicals. *Toxicol. Appl. Pharmacol.*, 135, p. 172-178.

Styles, P. M.; Chanda, M. and Rempel, G. L. (1996). Sorption of arsenic anions onto poly(ethylene mercaptoacetimide). *Reactive & Functional Polymers*, 31, p. 89-102.

Veglio, F. and Beolchini, F. (1997). Removal of metals by biosorption: a review. *Hydrometallurgy*, 44, p. 301-316.

Volesky, B. and Holan, Z. R. (1995). Biosorption of heavy metals. *Biotechnology Progress*, 11, p. 235-250.

Wood, A. (1992). Trace metal removal from effluents. Water and Water Treatment**:** 32,36.

Zhang, W.; Singh, P.; Paling, E. and Delides, S. (2004). Arsenic removal from contaminated water by natural iron ores. *Minerals Engineering*, 17, p. 517-524.

Zouboulis, A. I.; Kydros, K. A. and Matis, K. A. (1993). Arsenic(III) and Arsenic(V) Removal from solutions by Pyrite Fines. *Separation Science and Technology*, 28, p. 2449-2463.

Capítulo 2

Development of a Biosorbent for Arsenite: Structural Modeling Based on X-Ray Spectroscopy (XAS)

Environ. Sci. Technol. **2005**, 39, 895-900.

Development of a Biosorbent for Arsenite: Structural Modeling Based on X-Ray Spectroscopy (XAS)

Mônica Cristina Teixeira[1] and Virgínia S. T. Ciminelli[*]

Department of Metallurgical and Materials Engineering – Federal University of Minas Gerais, Brazil

This work describes a biological route for direct sorption of aqueous As (III) species, which are the most toxic and mobile arsenic species found in soils. Based upon the biochemical mechanisms which explain arsenic toxicity, we propose that waste biomass with a high fibrous protein content obtained from chicken feathers can be used for selective As (III) adsorption. Prior to adsorption, the disulfide bridges present in the biomass are reduced by thioglycolate. Our investigations demonstrated that As (III) is specifically adsorbed on the biomass and, contrary to the behavior observed with inorganic sorbents, the lower the pH the more effective the removal. Arsenic uptake reaches values of up to 270 μmol As (III)/g of biomass. Analyses by Synchrotron light techniques, such as XANES, demonstrated that arsenic is adsorbed in its trivalent state, an advantage over conventional techniques for As uptake, which usually require a previous oxidation stage. EXAFS analyses showed that each As atom is directly bound to three S atoms with an estimated distance of 2.26 Å. The uptake mechanism is explained in terms of the structural similarities between the As III-biomass complex structure and that of arsenite ions and Ars-Operon system encoded proteins and phytochelatins. The biological route presented here offers the perspective of a direct removal of arsenic in its reduced form.

Keywords: arsenite, biosorption, bioremediation, EXAFS.

[1]Permanent address: Department of Pharmacy – Federal University of Ouro Preto, Brazil
* Corresponding author - address: Rua Espírito Santo, 35/206. Belo Horizonte-MG. CEP: 30160-030. Brazil. Phone: 55 31 3238-1804; fax: 55 31 3238-1815; e-mail address: ciminelli@demet.ufmg.br

2.1 INTRODUCTION

Arsenic and its compounds are toxic and carcinogenic to all living organisms (Mandal and Suzuki, 2002). Arsenic naturally occurs on the earth's crust in small concentrations, arsenopyrite (FeAsS) being the most common arsenic mineral (Mandal*, et al.*, 2002). In soils, arsenic concentration may vary from 1.0 mg/kg (apatite, fluorite, and calcite samples) to 77,000-126,000 mg/kg (pyrite or arsenopyrite samples) (Smedley and Kinniburgh, 2002). Typical arsenic concentration found in soils is reported at 6 mg/kg (Mandal*, et al.*, 2002). Small amounts of arsenic and its compounds are utilized by the chemical and electronic industries to produce electronic components for laser equipment, wood preservatives, pesticides, and glasses, to name but a few of the numerous applications. Despite its many applications, there is a surplus of arsenic-containing wastes, derived mainly from the mineral and metallurgical industries. The wastewater and solid residues produced by these industries are important potential sources for arsenic contamination of surface and groundwater. Natural leaching of As-enriched soils and rocks has been the main cause for the main arsenic contamination reported worldwide, such as Poland, Canada, New Zealand, Spain, Hungary, Mexico, United States, Chile, Argentina, China, India and Bangladesh.

The toxicity of arsenic and its compounds is well established (Knowles and Benson, 1983; Hughes, 2002). Once ingested, arsenic provokes nausea and gastro-intestinal symptoms. From the toxicological point of view, As (V) causes adverse effects to human and other living organisms due to its chemical similarity with phosphate (Nies, 1999; Hughes, 2002). In this case, arsenic poisoning can be reverted by the administration of an excess of phosphate. On the other hand, the trivalent species As (III) strongly binds to the sulphydril (SH) groups in the active sites of some dehydrogenases enzymes like pyruvate and α-ketoglutarate, or dihydrolipoate, causing irreversible metabolic impairments and, in some cases, cellular mutagenesis (Flessel, et al., 1980; Treagan, 1983), which therefore explains

the higher toxicity of this species. The recognition that even trace amounts of arsenic, after long exposure, may cause severe health problems, such as dermatosis and cancer, have motivated a decrease in international limits for soluble arsenic in drinking water. Following recommendations from the World Health Organization this limit has been reduced from 50 $\mu g.L^{-1}$ to 10 $\mu g.L^{-1}$ in many countries.

Recent disasters involving cases of human poisoning due to arsenic contamination in drinking water, particularly in India and Bangladesh (Nickson, et al., 1998; Acharyya, et al., 1999) have spawned a series of worldwide investigations towards arsenic remediation. The episodes in the Asian countries are considered the most severe in terms of the extent of contamination and the number of persons affected (Nickson*, et al.*, 1998; Acharyya*, et al.*, 1999; Chowdhury, et al., 1999). It has been estimated that more than 25 million people have been exposed to water with arsenic concentration $\geq 50\mu g.L^{-1}$ in West Bengal (India) and Bangladesh (Chakraborti, et al., 2002).

Immobilization and stability of arsenic species in natural environments or under remediation procedures are influenced by its oxidation state. The predominant water-soluble species are the As (III) and As (V) derivatives of the arsenous (H_3AsO_3) and arsenic (H_3AsO_4) acids, respectively. The trivalent species is of great environmental concern not only because of its considerably higher toxicity but also in view of its higher mobility in soils. Even under oxic conditions both arsenic species occur together due to the fact that As (III) oxidation to As (V) is a kinetically slow process (Weerasooriya, et al., 2003). In biological environments, bacterial activity can reduce As (V) species (Knowles*, et al.*, 1983; Ladeira, et al., 2001b; Mukhopadhyay, et al., 2002), thus increasing arsenic toxicity. In the pentavalente state, arsenic acid (H_3AsO_4) species form stable surface complexes with soil constituents containing ferric, manganese or aluminium oxy-hydroxides, such as goethite, alumina, hematite, birnessite and gibbsite (Gupta and Chen, 1978; Driehaus, et al., 1995; Ladeira*, et al.*, 2001b; Smedley*, et al.*, 2002; Deschamps, et al., 2003), which explains its lower environmental mobility. On the other hand, the trivalent arsenous acid (H_3AsO_3) species are weakly bound to inorganic sorbents regardless of the pH. It is

normally assumed that to achieve high efficiency during arsenic remediation processes such as precipitation or co-precipitation with lime as metallic oxides, it is often necessary to promote the oxidation of As (III) ions to As (V). Therefore the conventional techniques used for As immobilisation usually require a previous oxidative stage (Nickson*, et al.*, 1998; Chowdhury*, et al.*, 1999). Those systems could now be classified as As (V) removing systems.

Biosorption has been investigated by many as an alternative to conventional techniques for metal remediation. The predominant uptake mechanism usually involves unspecific ion exchange reactions. For instance, positively charged groups present in the biomass structure, like the amino groups, are potential reactive sites to form adsorptive complexes with negatively charged ions, such as arsenate, arsenite, chromate, sulphate or phosphate (Veglio and Beolchini, 1997). Despite the identification of a number of biosorbents capable of removing a variety of species from aqueous solutions, the process often lacks selectivity in industrial complex, multi-component systems. We believe that the poor selectivity associated with unspecific ion exchange mechanisms has been one of the main limitations hindering biosorption's commercial applications.

The present work aims at designing a specific biosorbent for arsenic, with an approach based on the following premises: (i) the toxicity of As (III) is considerably higher when compared to As (V), (ii) this higher toxicity may be explained in terms of the great chemical affinity that exists between As (III) and the sulphydril groups and (iii) the As (V) affinity for sulphydril groups is lower when compared to As (III).

Based on the previous considerations, a waste biomass with a high fibrous protein content furnished by poultry industry, was selected and tested for As (III) sorption. The biomass is a keratin rich material. Keratin is a fibrous protein, which contains cysteine amino-acid residues in its primary structure; the lateral group of each cysteine molecule is the sulfidryl (SH) group. Two cysteine molecules may react forming a cystine molecule, which is, in fact, a molecule with two cysteine residues bound by a disulfide bridge. Thioglycolate is a

reduction agent that reacts with the disulfide bridge, restoring the SH groups. It is known that arsenite reacts with SH groups from cystein - rich proteins. Our selection of this specific biomass was based on its cysteine content.

Supported by the results shown in the following paragraphs the specificity of the selected biosorbent for As (III) is demonstrated. This feature is explained by the molecular structure of the adsorbed complex determined by Syncrotron light, X-Ray Spectroscopy analyses.

2.2 MATERIALS AND METHODS

2.2.1 Biomass preparation.

White chicken feathers were rinsed thoroughly with warm tap water and dried at 45 ±5°C for 24 hours. The dried material was ground and sieved to obtain a size range below 0.037 mm (400 Mesh Tyler). Biomass activation was accomplished by adding 10 ml of a 7.8 % (w/w) basic ammonium thioglycolate solution. Treatment did not imply any mass loss. After this activation step, the powdered biomass was filtered, washed with 100 mL of Milli-Q water and used in the adsorption tests.

2.2.2 Materials

All solutions were prepared with analytical grade chemicals and Milli-Q water. As (III) stock solutions of 10,000 mg/L were prepared with AsNaO2 (Fluka, 99.0%) salt. The pH values were adjusted with 0.1 N HCl or NaOH solutions; Eh was constantly monitored by means of a platinum Ag/AgCl electrode. Ionic strength (I) was fixed by using 4 mol/L NaCl or 0.01 mol/L Na3PO4 electrolyte solutions.

2.2.3 Adsorption experiments

As (III) batch adsorption experiments were conducted at room temperature (28±3°C), by adding a known amount of biosorbent (1-10 mg/L) to each 250-ml Erlenmeyer flask containing the As solution (100 mL). Flasks were shaken (100 rpm) per 1 hour to achieve equilibrium. As (III) semi-continuous adsorption experiments were undertaken at a constant temperature (25±0.2°C) using an apparatus similar to that described by Pagnanelli and co-workers (Pagnanelli, et al., 2000), and the following procedure “Subsequent Additions Method” - SAM. The liquid volume in the reactor was 1,000 mL, biosorbent concentration was 2 g/L, and agitation and pH values were kept constant. A 10 mL sample was collected

and analysed once an hour after each arsenic addition (equilibrium being achieved). Reaction suspensions were filtered through a 0.45 µm cellulose membrane, and preserved with concentrated nitric acid (5 µL) for chemical analyses by AAS. Experiments were carried out in duplicate and results were averaged.

2.2.4 XANES and EXAFS analyses

X-Ray Absorption Near Edge Structure (XANES) and Extended X-Ray Absorption Fine Structure (EXAFS) analyses of wet biomass samples loaded with As (III) were performed using the synchrotron facilities at the Laboratório Nacional de Luz Synchrotron (LNLS), in Campinas, São Paulo, Brazil. XANES and EXAFS data from the arsenic K edge (11,868 eV) were obtained at XAS workstation, under operation conditions of 1.37 Gev and beam currents of about 200 mA. All spectra were recorded at room temperature using a Si (111) double crystal monochromator with an upstream vertical aperture of 0.6 mm. Arsenic K-edge X-ray absorption spectra were measured by monitoring the transmitted energy using a 15-element Ge detector (Canberra Industries). Solid samples were fixed onto steel holders, sealed with Kapton tape film and placed at an angle of 45° to the incident beam. The energy resolution utilized were 0.8eV at the XANES region (11,855-11,930eV); 2eV between 11,760 and 11,855eV, and 11,930 and 12400eV and 3eV at 12,400-13,000eV region. XANES and EXAFS spectra were obtained simultaneously. Counting times of 3 s were kept constant. XANES spectra were analysed using the Origin 6.0 software and collected data from EXAFS were analysed by using the Winxas 2.0 software. EXAFS data fit was obtained using phase and amplitude parameters calculated with the FEFF 6.01 software.

2.3 RESULTS AND DISCUSSION

There are a limited number of biosorbents specially developed for arsenic. Examples such as MICB (*Molybdate-impregnated chitosan beads*) (Dambies, et al., 2002) are usually more effective in removing the pentavalent species and, as for the inorganic sorbents (i.e. goethite, alumina, gibbsite and ferric oxides), it is often necessary oxidize the trivalent arsenic in order to favor its immobilization. Arsenite uptake by inorganic sorbents is usually favored at high pH, while arsenate uptake is favored at low pH. Besides that, it is necessary to keep in mind the fact that arsenite immobilization by inorganic sorbents is often favored at high pH. Oxyanions usually exhibit adsorption maxima at pH value close to the pK_a of their first dissociation constant (Bostick and Fendorf, 2003). Therefore, for As (III) species this would imply in maximum adsorption at pH close to 9 and for arsenate species at pH close to 2. The development of a specific biosorbent for As (III) removal from dilute aqueous solutions took into account the mechanism that explains the toxicity of arsenic species, i.e. irreversible enzymatic inhibition caused by the reaction of As (III) with cysteine sulphidryl groups. Therefore, the use of a cysteine-rich biomass, as found in animal skin, hair, nails, horns or feathers has been proposed. Chicken feathers were finally selected in view of their abundance as a waste residue from the poultry industry.

Preliminary experimental results related to As (III) adsorption by the selected biomass are shown in Table II. 1 and Figure 2.1. The results shown in Table II. 1 confirm the role of sulphydril reduced groups on arsenic adsorption (tests a and d) and also allow for evaluation of possible loss of arsenic caused by precipitation with thioglycolate or adsorption onto filtration membranes. For those purposes, an excess of thioglycolate (10 times greater than that used in the actual activation procedure) was intentionally used; the results suggest no removal of arsenic by precipitation with the reagent (a and b). Experiments performed with biomass prior to the activation reaction with thioglycolate solution, led to a negligible As uptake. This finding supports the hypothesis that the reduced sulphydril groups are responsible for arsenic adsorption. Arsenite adsorption onto non-

activated biomass is insignificant and similar to that obtained with the cellulose acetate membrane (c). The biomass selectivity towards As (III) is clearly demonstrated.

Table II.1. Pre-treatment influence on As (III) and As (V) removal

Test	Biomass	Thioglycolate solution (%)	Pre-treatment (minutes)	As (III) removal (%)	As (V) removal (%)
A	+	10	60	29.3	6.1
B	+	10	60	29.9	5.5
C	-	-	-	4.0	0
D	+	-	-	3.9	0

Powdered biomass concentration, 1g/L;(I=0,1; Inicial As concentration = 2.67 mmol.L^{-1} (200ppm); pH, 5.0; Equilibrium time, 1hour; Temperature, 25°C; shaker, 150rpm. (a) Biomass pre-treated with thioglycolate solution for one hour; material filtered through a 0.45 μm acetate cellulose membrane; (b) Biomass pre-treated with thioglycolate solution for one hour, material not filtered; (c) Flasks containing only a 0.45 μm acetate cellulose membrane; (d) Flasks containing only natural biomass

Because the experimental conditions were strongly reductive, the formation of volatile arsine (AsH_3) or solid compounds such as realgar (As_2S_2) or orpiment (As_2S_3) were also a matter of concern. According to the Eh vs. pH diagram for the As-S-H_2O system (Johnson and Voegtlin, 1930; Vink, 1996) reduction of As^{3+} to As^{3-} is only achieved at Eh<0 V and therefore at redox potentials considerably lower than the lowest Eh of 297mV determined during the experiments. In a broad pH range (from 2.0 to 10.0) and even with the thioglycolate concentration 10 times greater than that used in the activation protocol no loss of arsenic by volatilisation or precipitation was detected.

The As (III) adsorption on whole and powdered biomass was evaluated by the experiments described in Figure 2.1. The highest As uptake was obtained when waste activated biomass was employed at the concentration of 2.0 g.L^{-1}. The results obtained for powdered biomass were slightly lower than those obtained for whole biomass. Regardless of the biomass concentration, equilibrium was achieved in less than 10 min. The milling process seems to

negatively contribute to As uptake. Nevertheless, all the subsequent experimental tests were performed using ground material for the benefit of sample homogeneity.

The influence of pH on As (III) biosorption can be observed in Figure 2.2. Arsenic uptake at pH values of 2.0, 5.0, 8.0 and 10.0 were compared. During all the adsorption experiments, pH variation was less than 0.2 units. The obtained results showed that the lower the pH, the higher the uptake. This trend is just the opposite of that observed for As (III) adsorption onto inorganic sorbents, for which uptake increases with pH (Gupta*, et al.*, 1978; Goldberg and Johnston, 2001; Bostick*, et al.*, 2003; Dixit and Hering, 2003; Ladeira and Ciminelli, 2004; Singh and Pant, 2004). Taking into account that the pKa_1 for arsenous acid is 9.2, one can see that As (III) neutral species are preferably adsorbed by the biomass instead of the negatively charged ones. Arsine formation during sorption experiments carried out at pH 2.0 was experimentally investigated and also discarded.

In order to obtain the adsorption experimental parameters Q_{max} and k, the experimental data exhibited in Figure 2.2 were adjusted to a linear expression of Langmuir equation:

$$Ceq.q^{-1} = k.Q_{max}^{-1} + Ceq.\ Q_{max}^{-1} \qquad (2.1)$$

where Ceq is the As equilibrium concentration in the aqueous phase.

The obtained Q_{max} values were 173.6 and 135.1 μmol As (III).g^{-1} at pH 2.0 and pH 5.0, respectively. The values for the constant k were 0.06, at pH 2.0 and 0.04 at pH 5.0, the calculated correlations factors were both above 0.996. Those values clearly demonstrated that As adsorption is favoured at pH 2.0.

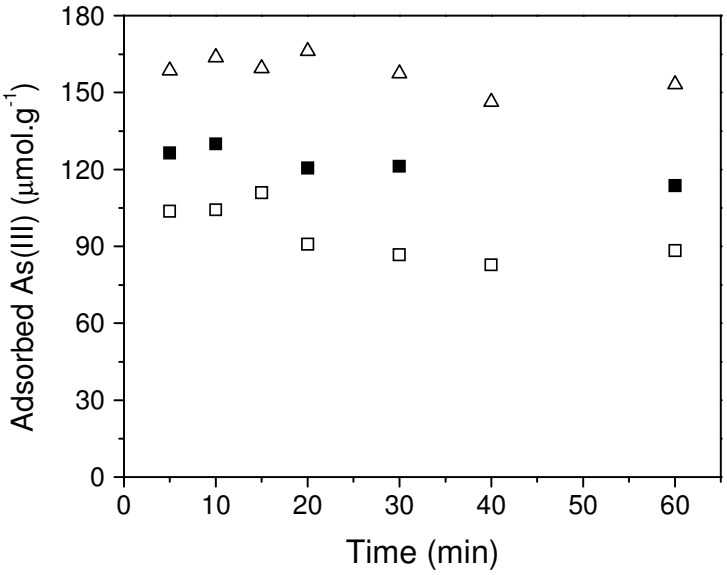

Figure 2.1. As (III) uptake by powdered biomass, $2g.L^{-1}$(open triangle); $1g.L^{-1}$(open square) and whole biomass, $1g.L^{-1}$ (solid square). Flask tests, As (III) initial concentration, 1.34 $mmol.L^{-1}$; initial pH, 9.2; temperature, 28±3°C; pre-treatment, 2h.

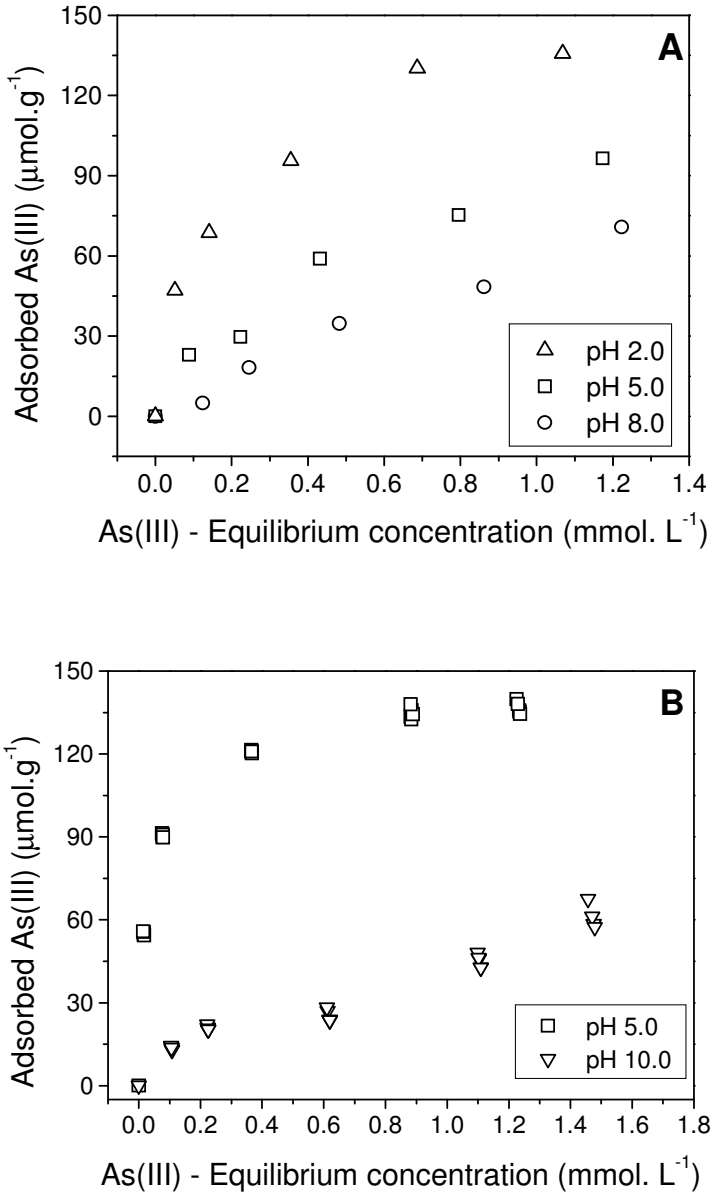

Figure 2.2. Influence of pH on As (III) adsorption, (A) SAM procedure, (B) Flask tests (biomasss, 2g/L; temperature, 25±1°C).

In 1930, Johnson and Voegtlin described As/cysteine ML3 complexes. Their respective stability constants and the As (III)/Cys speciation diagrams were described later by Reyes (Rey, et al., 2004) and showed that at equal arsenic and cysteine concentrations (0.015mol/L) almost 20% of the present As (III) atoms are complexed with almost 60% of the existent cysteine molecules at pH values between 2.5 and 7.0. The other 80% As remained as the neutral arsenic species, $As(OH)_3$. As pH increases and the hydroxyl concentration becomes greater, the negatively charged arsenic species $As(OH)_2O^-$ are formed and stoichiometry of the complexation reaction is changed. Now, hydroxyl groups compete with thiol groups and as a consequence, cysteine molecules are dislocated from the arsenic coordination shell. The resultant complex is the negatively charged $[As(HCys)(OH)O]^-$. At pH 8-9.5 the predominant species is the negatively charged complex with an As/Cys proportion of 1:1. Both As/Cys complexes show trigonal-pyramidal geometry. However, in the negatively charged complex, arsenic inner coordination shell involves two hydroxil groups as ligands, one of them in a non-protonated form (Rey*, et al.*, 2004).

Experimental data obtained for arsenic adsorption at pH values higher than 5.0 corroborate those theoretical considerations (Figure 2.2), Obtained isotherms do not follow the Langmuir adsorption equation and demonstrate that as As uptake is lower when compared to the data obtained under more acid conditions. This behaviour should be explained by the fact that at pH 8 and 10, the neutral arsenic species are replaced by the anionic species producing different adsorption complexes.

Arsenic uptake (Q_{max}) of 173.6 or 135.1 $\mu mol.g^{-1}$ obtained at pH 2.0 and 5.0, respectively, are promising and greater than those values obtained with kaolinite and montmorillonite, 1.33 and 2.66 $\mu mol.g^{-1}$, respectively (Griffin, et al., 1977); alumina, 2.66 $\mu mol.g^{-1}$ (Gupta*, et al.*, 1978); goethite, 39.9 $\mu mol.g^{-1}$ (Deschamps*, et al.*, 2003). Ladeira and co-works in 2001 reported significant uptakes by thermally activated gibbsite, 337.82 $\mu mol.g^{-1}$. Others workers (Driehaus*, et al.*, 1995; and Meng, et al., 2002) also obtained higher arsenic

adsorption capacities (266-532 μmol.g^{-1}) but, in both cases, As (III) was previously oxidized to As (V). The very high value (920.4 μmol of As (III) per gram of Mo reported by Dambies and co-workers in 2002 using a chitosan derivative biosorbent impregnated with molybdenum, can not be compared to other reported results in view of the lack of information with regard to the used quantities (mass) of biosorbent used.

Despite the best adsorption capacity achieved at pH 2.0, a pH of 5.0 was chosen for all the subsequent experiments, as this pH value is more consistent with conditions often found in natural wastewater.

The selectivity towards As (III) shown in Table II. 1, is corroborated by the results shown in Figure 2.3; the good fit of the experimental data to the linear form of Langmuir equation is also depicted (the calculated correlations factors were higher than 0.99). The great majority of As sorbents described in literature are active for both the pentavalent and the trivalent species, the main difference being the relatively higher remobilization of the latter by aqueous solutions.. Under conditions of pH 5.0, I=0.1, biomass concentration of 2.0g.L^{-1}, the Q_{max} obtained in the presence (260.35 μmol.g^{-1}) and absence of phosphate ions (265.35 mol/L) are quite similar (Figure 2.3). Therefore, the well-described competition between arsenic and phosphate during sorptive experiments using biosorbents or resins (Korngold, et al., 2001; Dambies*, et al.*, 2002) is not observed when the fibrous protein rich biomass is utilised for As (III) uptake.

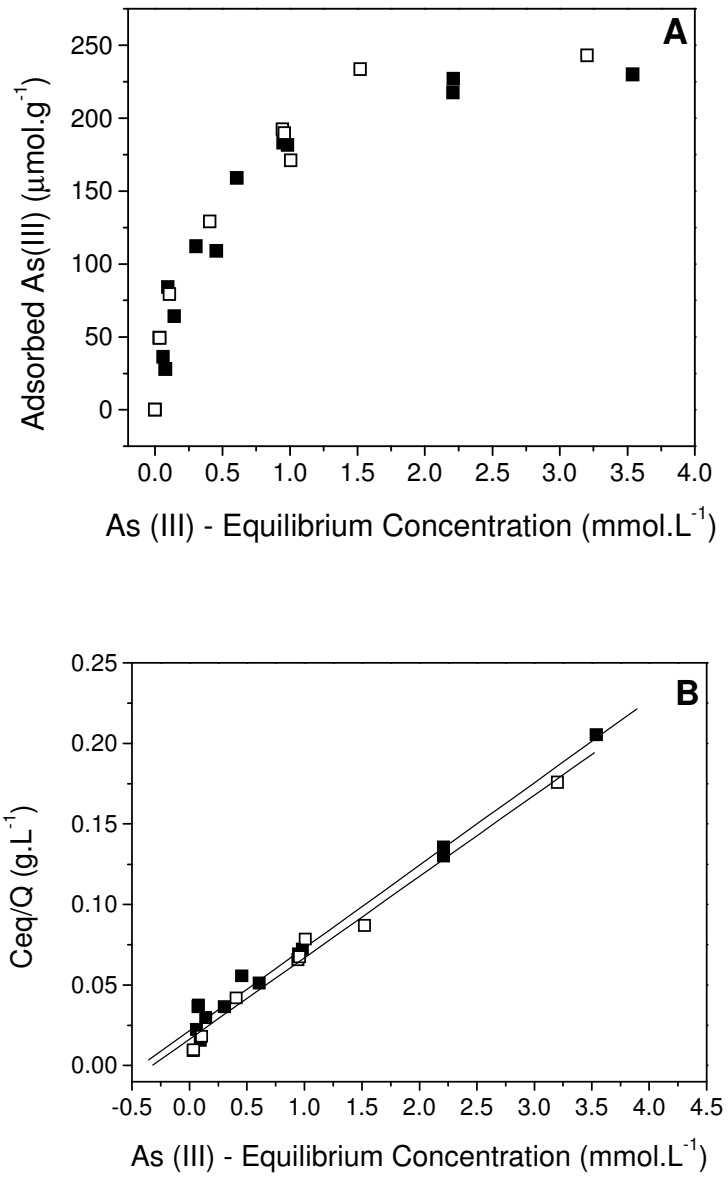

Figure 2.3. Influence of phosphate ions on As (III) adsorption isotherms in the presence (solid squares) or in the absence (open squares) of Phosphate 0.01 mol.L^{-1}. SAM procedure, I = 0.1; pH=5; biomass, 2g/L; temperature, 25±1°C)

Both phosphate and arsenate molecules have the same tetrahedral geometry, which could explain their chemical similarity and their similar affinities for the same chemical ligands. Conversely, arsenite ions possess a trigonal pyramidal geometry. It is possible that a steric hindrance may contribute to the rejection of the tetraedric arsenate and phosphate oxyanions on the biomass adsorptive sites.

X-Ray Absorption Near Edge Structure (XANES) and Extended X-Ray Absorption Fine Structure (EXAFS), provide information that could not be otherwise obtained through the traditional surface analyses techniques. XANES spectra offer electronic and structural information, such as oxidation state, with regard to adsorbed ion (photoabsorbing ion). EXAFS provides information, e.g. the coordination number and interatomic distance, about the nature and position of the neighbour atoms in the coordination shell of the photoabsorbing ion (arsenic, in our case). Thanks to XANES and EXAFS it is now possible to identify the variations inside the arsenic coordination shell caused by adsorption onto cysteine rich biomass. The analysis of the EXAFS data from the arsenite-loaded biomass is illustrated in Figures 4 to 6. The As (III)-biomass EXAFS spectrum is presented in Figure 2.4. The averaged data from seven different spectra were converted to an eV energy unit and then had its background line extracted. The experimentally obtained K edge value (E_0) was found as 11,868 eV, the same obtained for the arsenite standard sample, confirming that arsenite was not oxidized by the biomass. XANES spectra (data not shown) validated this value and the trivalent state of arsenic atoms. The spectrum oscillations caused by all the atoms in the neighbouring coordination shells are also presented. This spectrum was submitted to Fourier Transform, thus allowing the identification of one amplified peak that corresponds to the first Arsenic coordination shell (Figure 2.5).

The signal obtained after submitting this data to another Fourier Transform treatment results in one spectrum that represents only the oscillations caused by the atoms in the As first coordination shell. At this point, it is possible to calculate the structural parameters such as interatomic distance between As and atoms in the first coordination shell,

coordination number as well as to identify the "first neighbour" ligand. By adjusting the experimental data with the theoretical model provided by the FEFF program (Figure 2.6) it was possible to confirm that sulphur is the retro-scattering atom. It was also possible to determine that each arsenic atom is bound to three sulphur atoms. The final structural parameters obtained in the analyses were coordination number (n) = 2.52±0.4 and interatomic distance (R) = 2.26±0.01 Å.

The structural parameters obtained during this work are quite different from those obtained by arsenic adsorption on inorganic matrices. As arsenic is adsorbed as an oxyanion, often as a bidentate binuclear complex, the element found in the first coordination shell is always oxygen, in coordination numbers (n) varying from 3.6-4 and interatomic (R) distances in a range of 1.72 to 1.78 Å. The metal ligands (Fe or Al) are found in the second coordination shell with R values often greater than 3.0 Å (Farquhar, et al., 2002).

The coordination number and interatomic distance obtained in the present study are, as expected, very similar to those reported in EXAFS analyses of biological As (III)/protein complexes, showing As atoms directly bound to S atoms in the first coordination shell. Each As atom is bound to the sulphur atoms coming from three different cysteine residues, R values vary from 2.20-2.25 Å (Bhattacharjee and Rosen, 1996; Shi, et al., 1996; Farrer, et al., 2000; Pickering, et al., 2000; Bennett, et al., 2001). The information provided by XAS analyses is consistent with the strong arsenic uptake reported here. The results explain that rather than adsorbed as a counter ion, or specifically adsorbed as arsenous species in the inner Helmoltz plane, As (III) undergoes a chemical reaction leading to dehydration of H_3AsO_3 molecule.

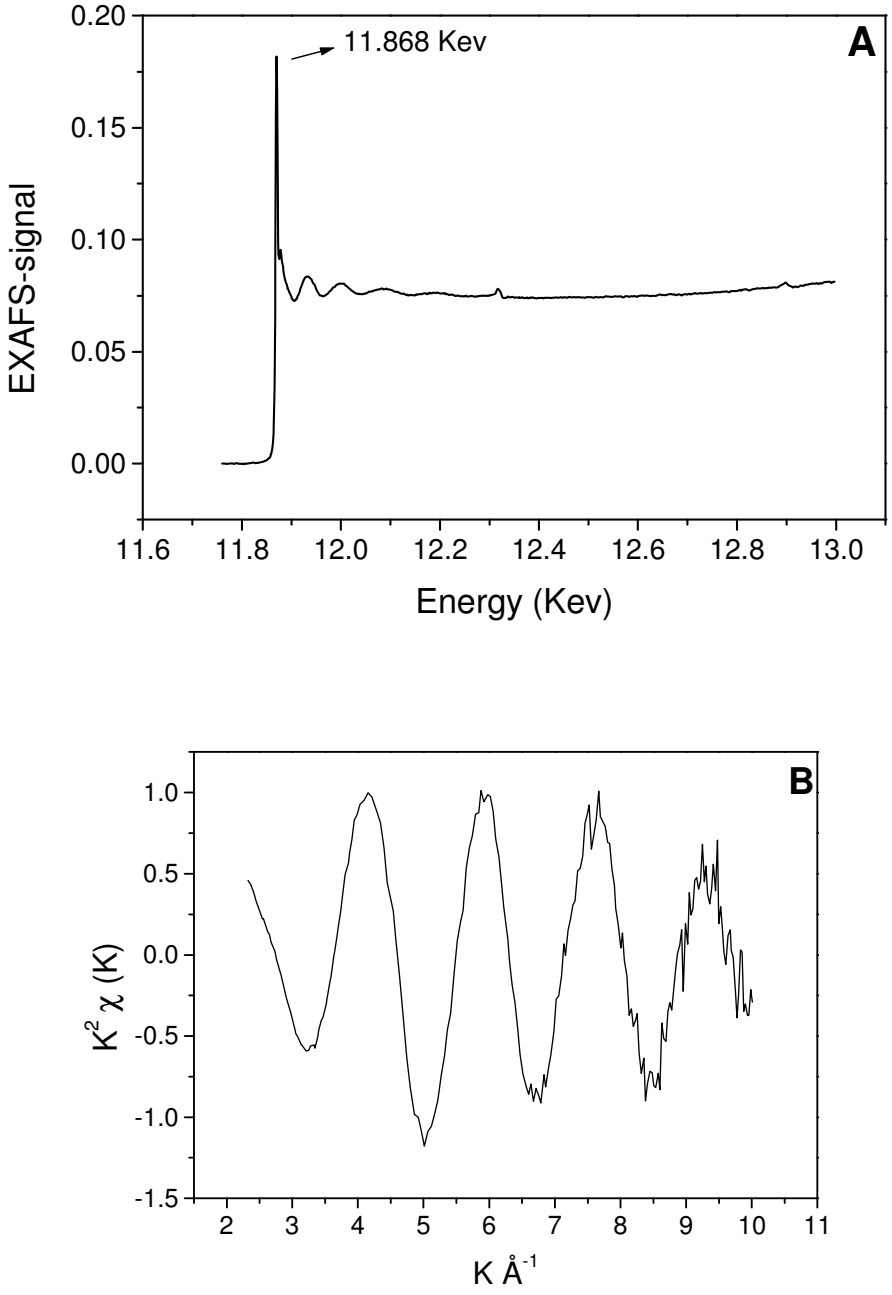

Figure 2.4. EXAFS signal of As (III) ($AsNaO_2$) adsorbed onto biomass, after background correction.

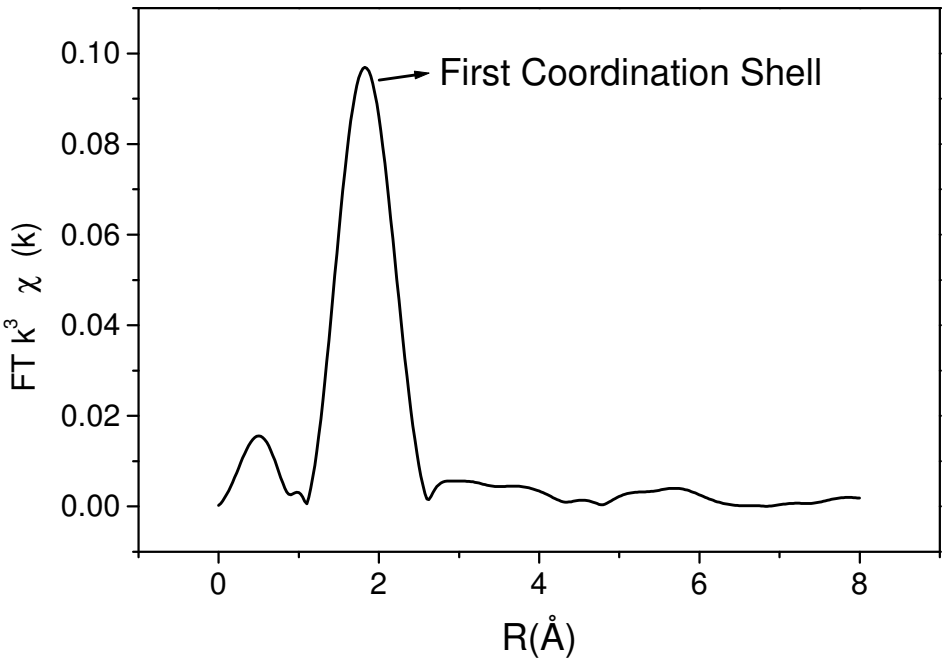

Figure 2.5. Fourier Transform amplitude (K=3). Radial distribution functions for As(III) adsorbed onto biomass.

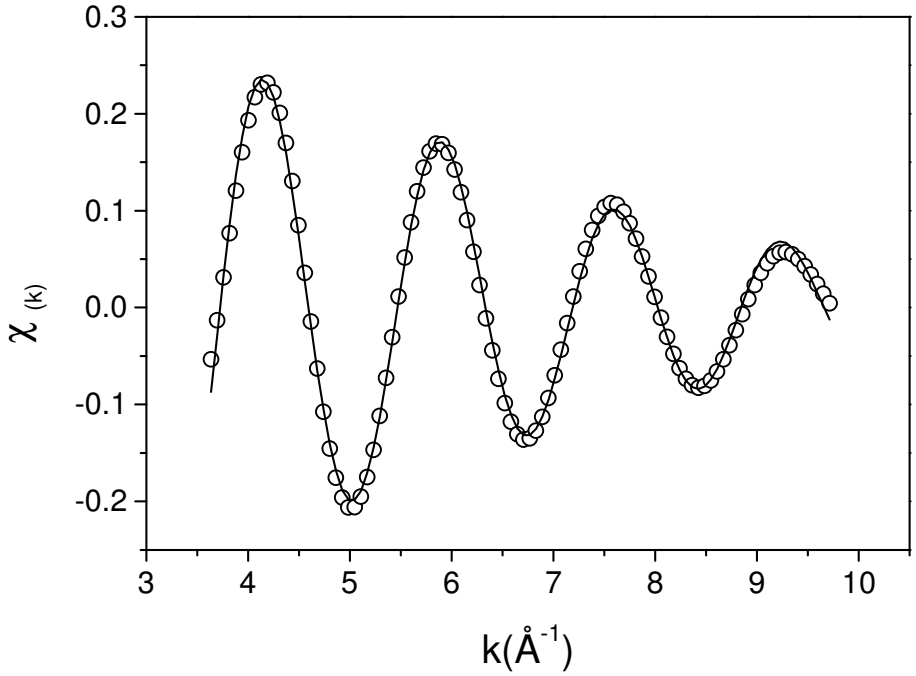

Figure 2.6. Back Fourier Transform (K-space), first coordination shell. Best fit of EXAFS data to As (III) adsorbed on biomass. Experimental data were fitted to hypothetical As/S complex using FEFF 6.0. Scatter and line curves represent experimental and theoretical data, respectively. Structural parameters obtained are R=2.26±0.01Å, n=2.5±0.4, E_0=6.87 and σ^2=0.002.

Based on these findings, the following equation is proposed to describe arsenite adsorption by fibrous protein biomass:

$$H_3AsO_3 + 3B\text{-}CysSH \rightarrow As(B\text{-}CysS\text{-})_3 + 3H_2O \qquad (2.2)$$

where *B* represents the biomass matrix.

This adsorption mechanism is supported by the structural similarities between As (III)/biomass complex and those natural complexes formed between Arsenic atoms and Ars Operon proteins (Kaur and Rosen, 1992; Bhattacharjee*, et al.*, 1996; Shi*, et al.*, 1996; Farrer*, et al.*, 2000; Bennett*, et al.*, 2001), phytochelatins (Pickering*, et al.*, 2000; Schmoger, et al., 2000) or cysteine and glutathione (Knowles*, et al.*, 1983; Farrer*, et al.*, 2000; Hughes, 2002; Mukhopadhyay*, et al.*, 2002), previously identified. Finally, it may be stressed that the adsorption phenomenon studied here involves a chemical reaction between the dissolved arsenite ions and the sulphydril groups of biomass, strong enough to dislocate oxygen atoms from the arsenic atom first coordination shell in arsenous acid molecules. These facts explain the specificity of this tested biosorbent with respect to the trivalent species of arsenic as well as its minor affinity for phosphate and arsenate ions. Our findings are consistent with the statements of Farrer (Farrer*, et al.*, 2000): "As (III) is able to distort polypeptide structure in order to satisfy its desire to form trigonal-pyramidal thiolate coordination" and "Arsenic causes structural distortion and aggregation in biopolymers, an action which may be involved in the mechanism of arsenic toxicity".

2.4 CONCLUSIONS

The features of the model proposed to explain As (III) adsorption onto the selected fibrous, protein-rich biomass can be summarized as follows. Sulphydril reduced groups are the active groups involved in arsenic biosorption. Uptake increases as pH decreases; phosphate ions do not compete with arsenite ions for the biomass' active sites. Arsenic (III) uptake involves an inner sphere complexation phenomenon that takes place within the As first coordination shell. Three water molecules are released while the arsenic atom directly binds to the sulphydril groups. XAS analyses indicated that each arsenic atom is bound directly to three sulphur atoms from the reduced cysteine aminoacids. The arsenic/sulphur interatomic distance was found to be 2.26 ± 0.01 Å. Finally, the specificity of the biosorbent dispenses the need for previous As (III) oxidation.

2.5 REFERENCES

Acharyya, S. K.;Chakraborty, P.;Lahiri, S.;Raymahashay, B. C.;Guha, S. and Bhowmik, A. (1999). Arsenic poisoning in the Ganges delta. *Nature*, 401, p. 545.

Bennett, M. S.;Guan, Z.;Laurberg, M. and Su, X.-D. (2001). *Bacillus subtilis* arsenate reductase is structurally and functionally similar to low molecular weight protein tyrosine phosphatases. *PNAS*, 98, p. 13577-13582.

Bhattacharjee, H. and Rosen, B. (1996). Spatial Proximity of Cys 113, Cys172, and Cys 422 in the Metalloactivation Domain of the ArsA ATPase. *The Journal of Biological Chemistry*, 271, p. 24465-24470.

Bostick, B. C. and Fendorf, S. (2003). Arsenite sorption on troilite (FeS) and pyrite (FeS_2). *Geochimica et Chosmochimica Acta*, 67, p. 909-921.

Chakraborti, D.;Rahman, M. M.;Paul, K.;Chowdhury, U. K.;Sengupta, M. K.;Lodh, D.;Chanda, C. R.;Saha, K. C. and Mukherjee, S. C. (2002). Arsenic calamity in the Indian subcontinent. What lessons have been learned? *Talanta*, 58, p. 3-22.

Chowdhury, T. R.;Basu, G. K.;Mandal, B. K.;Biswas, B. K.;Samanta, G.;Chowdhury, U. K.;Chanda, C. R.;Lodh, D.;Roy, S. L.;Saha, K. C.;Roy, S.;Kabir, S.;Quamruzzaman, Q. and Chakraborti, D. (1999). Arsenic poisoning in the Ganges delta. *Nature*, 401, p. 545-546.

Dambies, L.;Vincent, T. and Guibal, E. (2002). Treatment of Arsenic-Containing Solutions using Chitosan Derivatives: Uptake Mechanism and Sorption Performances. *Water Research*, 36, p. 3699-3710.

Deschamps, E.;Ciminelli, V.;Weidler, P. G. and Ramos, A. Y. (2003). Arsenic sorption onto soils enriched with manganese and iron minerals. *Clays and Clay Minerals*, 51, p. 198-205.

Dixit, S. and Hering, J. g. (2003). Comparision of Arsenic(V) and Arsenic(III) Sorption onto Iron Oxide Minerals: Implications for Arsenic Mobility. *Environmental Science and Technology*, 37, p. 4182-4189.

Driehaus, W.;Seith, R. and Jekel, M. (1995). Oxidation of Arsenate(III) with Manganese Oxides in Water Treatment. *Water Research*, 29, p. 297-305.

Farquhar, M. L.;Charnock, J. M.;Livens, F. R. and Vaughan, D. J. (2002). Mechanisms of Arsenic Uptake from Aqueous Solution by Interaction with Goethite, Lepidocrocite, Mackinawite and Pyrite: An X-ray Absorption Spectroscopy Study. *Environmental Science &Technology*, 36, p. 1757-1762.

Farrer, B. T.;McClure, C. P.;Penner-Hahn, J. E. and Pecoraro, V. L. (2000). Arsenic (III)-Cysteine Interactions Stabilize Three-Helix Bundles in Aqueous Solution. *Inorganic Chemistry*, 39, p. 5422-5423.

Flessel, P.;Furst, A. and Radding, S. B. (1980). A comparison of carcinogenic metals. In: Siegel, H. *Carcinogenicity and metal ions*. New York, Marcel Dekker, Inc. 10: p. 22-54.

Goldberg, S. and Johnston, C. T. (2001). Mechanisms of arsenic adsorption on amorphous oxides evaluated using macroscopic measurements, vibrational spectroscopy and surface complexation modeling. *Journal of Colloid and Interface Science*, 234, p. 204-216.

Griffin, R. A.;Frost, R. R.;Au, A. K.;Robinson, G. D. and Shimp, N. F. (1977). Attenuation of pollutants in municipal landfill leachate by clay minerals. *Environmental Geology Notes*, 79, p. 1-47.

Gupta, S. K. and Chen, K. C. (1978). Arsenic removal by adsorption. *Journal of Water Pollution Control Federation*, 50, p. 493-506.

Hughes, M. F. (2002). Arsenic Toxicity and Potential Mechanisms of Action. *Toxicology Letters*, 133, p. 1-16.

Johnson, J. M. and Voegtlin, C. (1930). Arsenic derivatives of cysteine. *Journal of Biological Chemistry*, 89, p. 27.

Kaur, P. and Rosen, B. P. (1992). Plasmid-Encoded Resistance to Arsenic and Antimony. *Plasmid*, 27, p. 29-40.

Knowles, F. C. and Benson, A. A. (1983). The biochemistry of arsenic. *TIBS*, 8, p. 178-179.

Korngold, E.;Belayev, N. and Aronov, L. (2001). Removal of Arsenic from Drinking Water by Anion Exchangers. *Desalination*, 141, p. 81-84.

Ladeira, A. C. Q.;Ciminelli, V. and Paniago, E. B. (2001b). The use of Al-based adsorbents for mitigation of arsenic contamination. In: VI Southern Hemisphere Meeting on Mineral Technology, 2001b, Rio de Janeiro. CETEM/MCT, Maio 2001. p. 549-554

Ladeira, A. C. Q. and Ciminelli, V. S. T. (2004). Adsorption and desorption of arsenic on an oxisol and its constituents. *Water Research*, 38, p. 2087-2094.

Mandal, B. K. and Suzuki, K. T. (2002). Arsenic Round the World: a Review. *Talanta*, 58, p. 201-235.

Meng, X.;Korfiatis, G. P.;Bang, S. and Bang, K. W. (2002). Combined Effects of Anions on Arsenic Removal by iron Hydroxides. *Toxicology Letters*, 133, p. 103-111.

Mukhopadhyay, R.;Rosen, B. P.;Phung, L. T. and Silver, S. (2002). Microbial Arsenic: from Geocycles to Genes and Enzymes. *FEMS Microbiology*, 26, p. 311-325.

Nickson, R.;McArthur, J.;Burgess, W.;Ahmed, K. M.;Ravenscroft, P. and Rahman, M. (1998). Arsenic poisoning of Bangladesh groundwater. *Nature*, 395, p. 338.

Nies, D. H. (1999). Microbial heavy-metal resistance. *Apllied Microbiology Biotechnology*, 51, p. 730-750.

Pagnanelli, F.;Papini, M. P.;Trifoni, M.;Toro, L. and Veglio, F. (2000). Biosorption of metals ions on Arthrobacter sp.: biomass characterization and biosorption modeling. *Environmental Science Technology*, 34, p. 301-316.

Pickering, I. J.;Price, R. C.;George, M. J.;Smith, R. D.;George, G. N. and Salt, D. E. (2000). Reduction and Coordination of Arsenic in Indian Mustard. *Plant Physiology*, 122, p. 1171-1177.

Rey, N. A.;Howarth, O. W. and Maia, E. C. P. (2004). Equilibrium characterization of the As(III)-cysteine and the As(III)-glutathione systems in aqueous solution. *Journal of Inorganic Biochemistry*, 98, p. 1151-1159.

Schmoger, M. E. V.;Oven, M. and Grill, E. (2000). Detoxification of Arsenic by Phytochelatins in Plants. *Plant Physiology*, 122, p. 793-801.

Shi, W.;Dong, J.;Scott, R. A.;Kasenzenko, M. Y. and Rosen, B. (1996). The Role of Arsenic-Thiol Interactions in Metalloregulation of the ars Operon. *The Journal of Biological Chemistry*, 271, p. 9291-9297.

Singh, T. S. and Pant, K. K. (2004). Equilibrium, kinetics and thermodynamic studies for adsorption of As(III) on activated alumina. *Separation Purification Technology*, 36, p. 139-1478.

Smedley, P. L. and Kinniburgh, D. G. (2002). A review of the source, behaviour and distribution of arsenic in natural waters. *Apllied Geochemistry*, 17, p. 517-568.

Treagan, L. (1983). Metals and Immunity. In: Siegel, H. *Methods Involving Metal Ions and Complexes in Clinical Chemistry*. New York, Marcel Dekker, Inc. 16: p. 47-83.

Veglio, F. and Beolchini, F. (1997). Removal of metals by biosorption: a review. *Hydrometallurgy*, 44, p. 301-316.

Vink, B. W. (1996). Stability relations of antimony and arsenic compounds in the light of revised and extended Eh-pH diagrams. *Chemical Geology*, 130, p. 21-30.

Weerasooriya, R.;Tobschall, H. J.;Wijesekara, H. K. D. K.;Arachchige, E. K. I. A. U. K. and Pathirathne, K. A. S. (2003). On the mechanistic modeling of As(III) adsorption on gibbsite. *Chemosphere*, 51, p. 1001-1013.

Capítulo 3

Effect of pH on Arsenite Adsorption onto Cysteine-rich Biomass: X-ray Absorption Studies and Density Functional Calculations

3.1 INTRODUCTION

Arsenic (As) is a heavy metal largely disseminated on the earth crust and the 20th mostly abundant element (Mandal and Suzuki, 2002). At normal conditions, arsenic concentrations in surface or ground waters are very low; eventually this naturally occurred arsenic might be dissolved and contaminates water deposits. Depending on the pH and redox potential conditions in the environment, arsenic ions will be oxidized (arsenate) or reduced (arsenite). The mobility of arsenic species in natural environments or under remediation conditions is influenced by its oxidation state. The predominant water-soluble species are the As (III) and As (V) derivatives of the arsenous (H_3AsO_3) and arsenic (H_3AsO_4) acids, respectively. The trivalent species is of great environmental concern not only due to its considerably higher toxicity but also in view of its higher mobility in soils. Even under oxic conditions, both arsenic species occur together due to the fact that As (III) oxidation to As (V) is a kinetically slow process (Weerasooriya, et al., 2003). Thus, chemical speciation of the arsenic has to be taken into account in order to understand its impact in the environment.

In Chapter 2 we discussed the adsorption of arsenite species onto cysteine rich biomass obtained as a waste material from the poultry industry. During the process, arsenic is directly bound to three sulfur atoms available in the cysteine-reduced residues present in the keratin protein of the biomass. It was therefore demonstrated that arsenic (III) uptake involves an inner sphere complexation phenomenon that takes place within the arsenic first coordination shell. Arsenic complexation with cysteine amino acid forming As/cysteine ML3 complexes is well established (Johnson and Voegtlin, 1930). Nevertheless, to our knowledge the application of that concept to arsenic remediation has not been previously reported.

It has been demonstrated that lower the pH, higher the arsenite ions uptake. Therefore, neutral arsenic species (H_3AsO_3) were preferably adsorbed instead of the negatively charged ones. In this case, electrostatic attraction does not explain adsorption. In addition, no pH alteration was observed within the system in view of the fact that the

model assumes that for each arsenite molecule adsorbed onto the biomass three water molecules are released (Teixeira and Ciminelli, 2005). It has been shown in Chapter 2 that arsenic adsorption on the protein-rich biomass is favored at low pH. The results achieved under acid conditions were: 173.6 and 135.1 μmol As (III)/g of biomass at pH 2.0 and pH 5.0, respectively. At pH 10.5 the biomass loading is reduced to approximately 30% of the uptake at pH 2.0.

It is an interesting feature in view of the fact that oxyanions usually exhibit adsorption maxima near the pK_a for the first dissociation (Bostick and Fendorf, 2003). In the case of As (III) species this would imply in maximum adsorption at pH close to 9. The analysis of recently published data for arsenic adsorption on different inorganic materials corroborates the previous statement. Arsenate adsorption on inorganic materials such as soils containing Al or Fe oxides is favored at acid pH while arsenite is preferably adsorbed at pH close to the neutrality or higher than 8.0 (Goldberg and Johnston, 2001; Dixit and Hering, 2003; Ciminelli, et al., 2004; Singh and Pant, 2004). Arsenic acid (H_3AsO_4) pKa values are 2.19, 6.94 and 11.5. Arsenite adsorption onto zinc or lead sulfides also increases with pH (Bostick*, et al.*, 2003).

Concerning arsenic adsorption on organic materials there are few examples of biosorbents reported for adsorption of arsenate and arsenite ions. Some rechearches (Manju, et al., 1998) related the use of "*copper impregnated coconut husk carbon (CICHC)*" for adsorption of arsenite ions; maximum uptake was achieved at pH 12.0 or higher. Another interesting experience was described by Dambies and coworkers in 2002, they succeed in adsorbing trivalent and pentavalent arsenic species using "*molybdate coagulated chitosan beads (MCCB)*". However, comparing arsenate and arsenite uptake one concludes that the highest uptake obtained for the adsorption of the trivalent species at pH values between 3.0 and 5.0 is one third of the maximum uptake of the pentavalent ion obtained at pH 5.5. In both cases, the uptake mechanisms involve the participation of metal ions. Cu or Mo were the binding atoms for arsenic; and the positive charges on the biomass surface provided by the adsorbed copper hydroxide (*CICHC*) or by the protonated amino groups (*MCCB*) stabilized the adsorptive complex

with the negatively charged arsenic species. A "*phosphorylated cross linked orange waste (POW)*" loaded with Fe (III) was recently tested for arsenic adsorption (Ghimire, et al., 2003). Arsenate adsorption was favored at pH 3.0 while arsenite was better adsorbed at pH 10.0 and, once more, with the need of a metal binding atom. Loukidou and coworkers (Loukidou, et al., 2003) suggested the utilization of a chemically modified non-living fungal biomass of *P. chrysogenum* for As (V) adsorption. The proposed adsorption mechanism involved electrostatic interactions; the biomass presented a positive surface charge and arsenic adsorption was more effective at pH 3.0.

In this present work, XANES and EXAFS techniques together with Density Functional Calculations are been used to study the As (III) adsorption on treated chicken feathers at a molecular level. XANES spectra were collected and analyzed in order to confirm the oxidation state of arsenic while EXAFS analysis were performed to provide detailed information about the neighborhood of the arsenite adsorbed ion. By fitting the experimental spectra to the theoretical data it is possible to identify the elements, the coordination number (CN), the interatomic distances (R), and the Debye-Waller factor (σ^2) for the first coordination shell of the As atom.

The interaction of As (III) and cysteine in a homogenous solution has been studied by means of potentiometric and spectrophotometric techniques, showing that species 1:3 metal/ligand are the most prevalent species (Rey, et al., 2004) in the usual pH range. The association of some classic statements (Johnson*, et al.*, 1930) with the recent data provided by Rey and coworkers led us to postulate the formation of similar As (III)/Cys complexes during arsenite adsorption on cysteine-rich biomass. In our laboratory, the interatomic distance between sulfur and arsenic centers was investigated by Expanded X-Ray Absorption Fine Structure (EXAFS) analysis and the obtained result (Teixeira*, et al.*, 2005) are in agreement with the As $(Cys)_3$ species on the surface and with the studies in solution performed by Rey and coworkers. At the same time some theoretical predictions of As (III)/Cys complexes structure were performed using Density Functional Method (DFT). DFT studies allow us to explore the potential energy surface where the atoms move. The minima on the surface correspond to the equilibrium geometry. The interaction of arsenious acid (H_3AsO_3) with cysteine has been studied

using the LCGTO-KS-DF (Linear Combination of Gaussian Type Orbital-Kohn Sham-Density Functional) method implemented in deMon-2002 program (Koester, et al., 2002).

Combining all those techniques, the initial study described in Chapter 2 is now expanded with the aim to investigate the effect of pH on the mechanism of As (III) uptake.

3.2 MATERIALS AND METHODS

3.2.1. Materials

White chicken feathers were rinsed thoroughly with warm tap water and dried at 45 ±5°C for 24 hours. The dried material was ground and sieved to obtain a size range below 0.037 mm (400 Mesh Tyler). Biomass activation was accomplished by adding 10 ml of a 7.8 % (w/w) basic ammonium thioglycolate solution. This treatment did not imply any mass loss. After this activation step, the powdered biomass was filtered in a 45μm cellulose membrane, washed with 100 mL of Milli-Q water and used for the adsorption tests and for the spectroscopic analyses as well.

All solutions were prepared with analytical grade chemicals and Milli-Q water. As (III) stock solutions of 10,000 mg/L were prepared with a sodium meta-arsenite salt ($AsNaO_2$) (Fluka, 99.0%). The pH values were adjusted with 0.1 or 0.01 N HCl or NaOH solutions. Arsenic adsorption experiments were carried out according to the conditions described previously (Teixeira*, et al.*, 2005).

3.2.2 X-Ray Absorption Experiments

X-Ray absorption Near Edge Structure (XANES) and Extended X-Ray Absorption Fine Structure (EXAFS) analyses of wet biomass loaded with As (III) were performed. XANES and EXAFS data from the arsenic K-edge (11,868 eV) were obtained at XAS workstation, under operation conditions of 1.37 GeV and beam currents of about 200 mA. All spectra were recorded at room temperature using a Si (111) double crystal monochromator with an upstream vertical aperture of 0.4 mm. Arsenic K-edge X-Ray absorption spectra were measured by monitoring the transmitted energy using a 15-element Ge detector (Canberra Industries). Wet solid samples were fixed onto steel holders, sealed with Kapton tape film and placed at an angle of 45° to the incident beam. The energy resolution utilized was 0.7 eV at the XANES region (11,855-11,900 eV); 2 eV between 11,820 and 11,855 eV and 1 eV between 11,900 and 12,020 eV. Therefore XANES and EXAFS spectra were simultaneously obtained. Counting times of 4 s were kept constant. At least five spectra were collected and averaged for XANES and EXAFS analysis.

After background correction, the spectra have been normalized using the Origin 6.0 software and analyzed by Winxas 2.0 software. Experimental As (III) adsorbed spectra obtained at different adsorption pH were compared to the spectra of arsenate (Na_2HAsO_4) and arsenite ($AsNaO_2$) standards. Experimental spectra were fitted to different combinations of reduced (arsenite) or oxidized (arsenite) spectra and the proportions of both curves were determined.

After averaging, spectra were submitted to a background correction using a Victorian function and then normalized to unity. To isolate the EXAFS signal a 4-point cubic spline function was used. The energy (KeV) was transformed to k-range ($Å^{-1}$) using the arsenic K edge value (E_0) graphically determined. All the χ k spectra were weighted by k^3 to amplify the upper k-range and Fourier-Transformed to produce a Radial Structure

Functions using a Δk of approximately 7.0 Å (from ~2.8-9.8 Å). After that, the first coordination shell of each Radial Structure Function (RSF) was back-transformed to isolate the spectral contributions of As neighbor atoms in this shell. The Winxas software package was used for EXAFS data analysis. Final data fit was obtained using phase and amplitude functions derived from FEFF 6.01 software simulating the occurrence of the pair As-S at the adsorption site. Biomass samples analyzed by XAS were loaded with approximately 14 mg of arsenite for each gram of biomass at pH 4.5; at pH 10.5 the biomass loading is reduced to approximately 30% of the uptake at acid pH.

3.2.3 Computational Approach

The generalized exchange correlation (XC) functional has been used with the Becke expression (Becke, 1988) for exchange and that of Perdew (Perdew, 1986) for correlation (GGA-BP). For the arsenic atoms the basis set have the contraction pattern (63321/5321/41*). For oxygen atoms, the basis sets have the contraction pattern (621/41/1*) and hydrogen atoms the contraction pattern (41*/1). Auxiliary basis sets have been used for fitting the density and XC potential. The auxiliary basis sets (3,5) have been used for arsenic center, (4,3) for oxygen atoms and (3,1) for hydrogen atoms. The orbital and auxiliary basis sets have been optimized explicitly for DFT calculations by Godbout *et al.* (Godbout, et al., 1992). The calculation of the expansion coefficients of the approximated density is described in detail elsewhere (Koester*, et al.*, 2002). The numerical integration is based on the partition scheme of Becke (Becke, 1987) in an adaptive grid. All structures have been fully optimized using the BFGS (Schlegel, 1987) method.

3.3 RESULTS

It has been shown in Chapter 2 that arsenic adsorption on the protein-rich biomass is favored at low pH. The results achieved under acid conditions were: 173.6 and 135.1 μmol As (III)/g of biomass at pH 2.0 and pH 5.0, respectively. At pH 10.5 the biomass loading is reduced to approximately 30% of the uptake at pH 2.0.

The $As(OH)_3$ molecule is protonated up to the pH 9.0 (pK_{a1} = 9.2). Cysteine pKs are approximately 1.67, 8.17 and 10.30 for RCOOH, RSH and RNH_3^+ groups (Bhattacharjee, et al., 2004). Therefore, the biomass' SH groups will deprotonate at pH lower than 9.2, which may become an obstacle for the sulfur atom to act as a ligand for arsenite. The main point is that pH variation may influence both, the adsorbate and the adsorbent and therefore, to fully understand arsenic adsorption onto cysteine rich biomass, the effect of this variable should be taken into account.

The alterations on arsenic first coordination shell during adsorption of arsenite onto cysteine-rich biomass under different pH conditions, are investigated by means of X-Ray absorption Near Edge Structure (XANES) and Extended X-Ray Absorption Fine Structure (EXAFS).

3.3.1. X-Ray spectroscopy

Figure 3.1 shows the XANES spectra of the As (III) loaded biomass at pH 4.5, 7.0 and 10.5. One could observe that the As k-edge energy threshold for As (III) standard sample was almost 4 eV lower than the value obtained for the As (V) standard. No oxidation of arsenite was observed during arsenic adsorption under neutral or acid pH conditions. One may also observe that the energy threshold for the adsorbed arsenite (11,861.2; 11,862.8 and 11,863.5 eV at pH 4.5; 7 and 10.5, respectively) at acid pH, was lower than the value obtained for the As (III) standard sample (11862.9 eV). This

behavior is explained by the fact that in the adsorbed complex, arsenic atoms will be directly bound to sulfur atoms. As oxygen is replaced by sulfur, a decrease in the ligand electronegativity takes place, thus inducing a shift on the As k-edge energy to lower values. This effect was also reported by others (Bostick*, et al.*, 2003) for the arsenic adsorption on PbS and ZnS.

Conversely, the arsenic adsorption at pH 10.5 shows a shift towards to the As (V) standard energy threshold of 11,666.7 eV, thus suggesting the oxidation of arsenite species. A more detailed comparison of the XANES spectra of the adsorptive complex obtained at pH 10.5 with those of the arsenate and arsenite standards confirmed that almost 37% of the initially added As (III) ions are oxidized to As (V). In fact, the kinetics of arsenite oxidation is favored by moderately alkaline conditions.

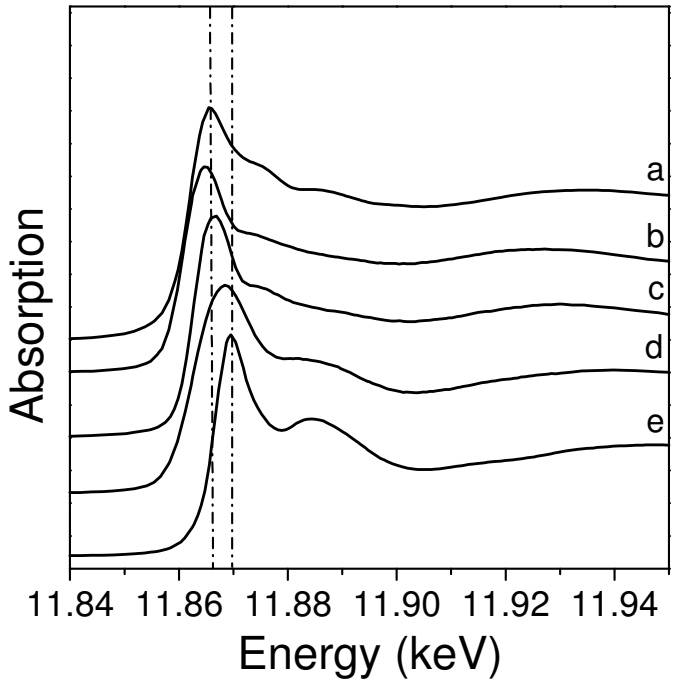

Figure 3.1. XANES spectra of As (III) loaded biomass:(a) arsenite standard; (b) (c) and (d) are relative to arsenite loaded biomass at pH 4.5, 7.0 and 10.5, respectively and (e) arsenate standard.

EXAFS analyses are shown in Figures 3.2 and 3.3 and in Table III.1. Figure 3.2 depicts the three Fourier Transformed (FT) spectra at the arsenic K-edge obtained at adsorption pH of 4.5, 7.0 and 10.5. Analyses were carried out with the original EXAFS data without any previous treatment. Figure 3.2 indicates that the adsorption spectrum under neutral conditions is quite similar to that obtained at acid pH. The lower intensity of the peak corresponding to the arsenic first coordination shell at neutral pH is ascribed to the lower As uptake at this pH. The FT was back transformed and fitted to phase and amplitude parameters for the hypothetical pair As-S. The structural parameters and respective standard deviations are shown in Table III.1. Arsenic adsorbs directly to sulfur atoms on the cysteine molecules, with the lost of three water molecules and no pH variation (Rey*, et al.*, 2004; Teixeira*, et al.*, 2005).Arsenic is adsorbed by the biomass as an inner-sphere complex. Structural parameters obtained experimentally in the present work - coordination number (CN) 2.5-2.7 and interatomic distance of approximately 2.25Å at neutral or acid pH - are in accordance with the results described in Chapter 2 for pH 5.0 and to the theoretical predictions described later in this chapter.

The adsorptive complexes obtained at acid or neutral pH are similar to those pyramidal As/S structures described for As interaction with biological material such as those bonds to the active sites of some enzymes responsible for arsenic resistance and detoxification (Kaur and Rosen, 1992; Bhattacharjee and Rosen, 1996; Farrer, et al., 2000; Bennett, et al., 2001; Messens, et al., 2002); phytochelatins (Pickering, et al., 2000; Schmoger, et al., 2000) or cysteine and gluthathione molecules (Knowles and Benson, 1983; Farrer*, et al.*, 2000; Hughes, 2002; Mukhopadhyay, et al., 2002; Bhattacharjee*, et al.*, 2004). They are also in accordance with inorganic As/S complex obtained by Helz (Helz, et al., 1995), who proposes that in As (III) sulfide solutions arsenite forms oligomers, such as As_3S_6 rings.

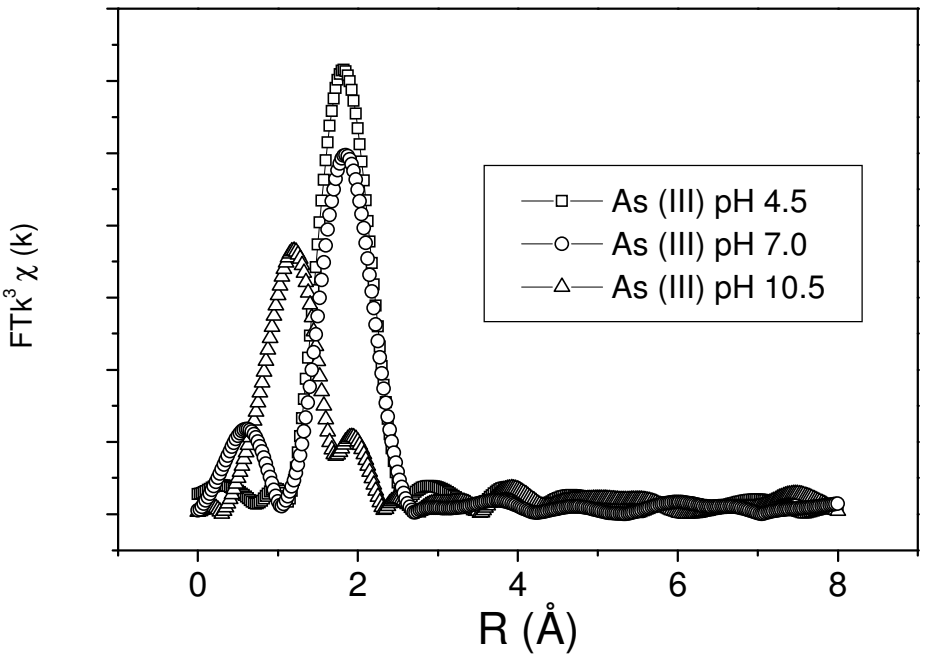

Figure 3.2. Fourier Transform amplitude (K=3). Radial distribution functions for As (III) adsorbed onto biomass at pH 4.5, 7.0 and 10.5. Uncorrected for phase shift.

In fact, each one of those rings consists of three AsS_3 pyramids, joined by two S corners to the other two pyramids. In these oligomers, the experimentally determined As-S and As-As distances are 2.21-2.23 and 3.4-3.5Å. Adsorption of arsenite on PbS and ZnS (Bostick*, et al.*, 2003) produced As-S distances of 2.23-2.52Å. By comparing the As-S distance in realgar, 2.15-2.18Å (Helz*, et al.*, 1995) with the As-S distances shown in Table III.1 it is possible to rule out the precipitation of that sulfide. The As-S interatomic distances in the mineral structure (Helz*, et al.*, 1995; Bostick*, et al.*, 2003) are significantly shorter than the values obtained here assuming adsorption.

Figure 3.2 shows also the FT spectrum produced by the adsorption of arsenite at pH 10.5. By comparing the three spectra, the differences between the results obtained in alkaline with those obtained at neutral and acid pH become evident. The differences are not restricted to the intensity of the peak, that may be explained by the relatively low adsorption observed at basic pH, but also by the occurrence of two "shoulders", one at R value lower than 2.0 Å and a very small one close to R=2.0 Å. This feature is an indication of the co-existence of two different elements in the arsenic first coordination shell when arsenite adsorption is carried out at pH 10.5. It is important to observe that the distance assigned to this second "shoulder" is not big enough to characterize a second coordination shell.

Figure 3.3 shows the EXAFS data fitting using phase and amplitude functions derived from FEFF 6.01 software. The approach simulated the occurrence of two distinct pairs As-S and As-O at the arsenic (arsenite) first coordination shell environment during adsorption at pH 10.5. Under those conditions the structural parameters experimentally obtained for the pairs As-S and As-O are respectively: interatomic distance (R) of 2.31 and 1.626 Å and coordination number (CN) of 0.9 and 2.1 for sulfur and oxygen atoms. The occurrence of only oxygen atoms in the arsenic first coordination shell was also simulated but the fitting was not satisfactory (E_0=12.81).

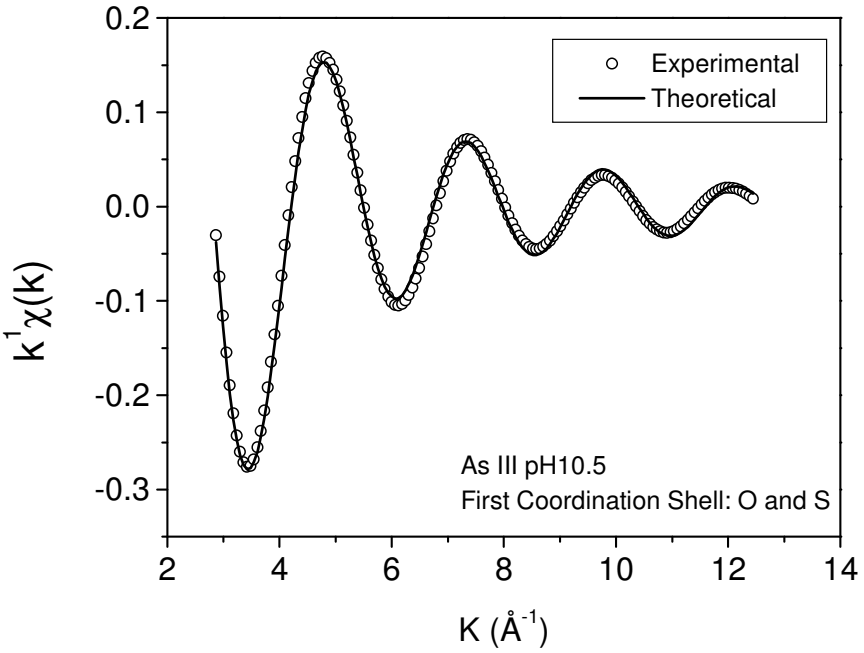

Figure 3.3. Second Fourier Transform (K-space), first coordination shell. Best fit of EXAFS data to As (III) adsorbed on biomass. Experimental data were fitted to hypothetical As-S and As-O pairs using FEFF 6.0. Scatter and line curves represent experimental and theoretical data, respectively. Structural parameters obtained are: R=2.31±0.02 Å, CN=0.92±0.02, E_0=-7±1 and σ^2=0.055±0.005 for As-S and R=1.63±0.0 Å, CN=2.08±0.0, E_0=1.4±0.1 and σ^2=0.00379±0.00015 for As-O.

Table III.1 summarizes the data obtained at various pH values. One may observe that as pH increases, the CN for the As-S pair decreases with the pH while the Debye-Waller factor (σ^2) increases. This parameter has not one absolute value; it offers rather an estimation of the bond length deviation compared to the data adopted for phase and amplitude calculations. As σ^2 is inversely related to the order of the system it is possible to conclude that as pH increases, the degree of order of the adsorptive complex decreases (once more compared to the hypothetical model). The σ^2 obtained at pH 10.5 is 40 times greater than that obtained at acid pH. Hence it means that at basic pH the presence of oxygen atom in the adsorptive complex causes a decrease in the order degree of the system. Farrer and coworkers (Farrer*, et al.*, 2000) stated that As (III) is always able to distort polypeptide structure in order to satisfy its desire to form trigonal-pyramidal thiolate coordination with a 1:3 As/S ratio, justifying in that way the mechanism of arsenic toxicity. However, in that study the authors only considered the physiological pH. Helz (1995) (Helz*, et al.*, 1995) analyzed the molecular structure of an amorphous orpiment ($AsS_{2.86}$) and concluded that its first shell geometry was affected by the sulfur deficiency, i.e. by the increase in the As/S molar ratio. The observed twisting in the orpiment molecular structure was attributed to the occasional replacement of As-S-As by As-As bonds or by As-O-As bridges, causing distortion in the structural sheets.

A similar approach may explain the results obtained at pH 10.5. The high disorder degree detected by σ^2 and the variation on As-S and As-O interatomic distances compared to the experiments done at acid or neutral pH may have been caused by a distortion on the trigonal pyramidal As/S complex structure. The As-S distance increased from 2.25 to 2.31 Å while the arsenic coordination number decreased from ~2.6 to 0.9. We propose that the complexation of arsenite at pH 10.5 will involve the replacement of only one oxygen atom from the negatively charged arsenic species ($H_2AsO_3^-$) by one sulfur atom from the biomass (Table III.1). The loose structure produced by the different interatomic distances of the pairs As-O^-, As-OH and As-S (see Table III.2) and also different bond angles, 92.7° for S-As-S (Bhattacharjee*, et al.*, 1996) and 109.33° for O-As-O bonds (Ferraris and Chiari, 1970), justifies the

occurrence of a twisted less ordered structure, in which two oxygen atoms together with one sulfur atom fulfills the structure of the pyramid.

Table III.1 indicates an As-O interatomic distance of 1.63 Å for the experiments at pH10.5. The As-O distances within the arsenic first coordination shell are typically of 1.8Å for As (III) and 1.68 Å for As (V). According to the literature (Table III.2), these values may vary between 1.67-1.85 Å for arsenite and from 1.62 to 1.88 Å for arsenate. Compared to the typical As (III)-O distances, a shorter distance reported here may be partially explained by the presence of As(V) at pH 10.5, as indicated by XANES measurements. As the EXAFS analyses do not distinguish between the different possible As-O bonds, the obtained result would be an average of the different distances corresponding to the arsenite and arsenate species but, the main responsible for the decrease in the As-O distance is proposed to be the depronation of the hydroxyl groups.

Table III.1 – EXAFS structural parameters obtained for arsenite adsorption onto cysteine rich biomass at different pH values.

		As-S	
	pH 4.5	**pH 7.0**	**pH 10.5**
CN	2.669±0.003	2.516±0.003	0.92±0.02
R	2.2460±0.0001	2.251±0.001	2.31±0.02
σ^2	0.00126±0.00002	0.00276±0.00002	0.055±0.005
E_0	7.016±0.006	7.498±0.007	-7±1
		As-O	
CN	-	-	2.08±0.0
R	-	-	1.6264±0.0007
σ^2	-	-	0.003793±0.00015
E0	-	-	1.4±0.1

Coordination Number (CN) typical error is approximately 30%, while interatomic distance (R) varies within 0.02 Å. Debye Waller (σ^2) represents the variance in R and is correlated with the disorder of the system.

Table III.2 – Interatomic distances between Arsenic and Sulfur or Oxygen atoms. Theoretical and experimental data.

Molecule	Bond Distance (Å)	Bond Angle (degrees)	Observation
	As-S		
$As(SH)_3$	2.236[a]; 2.23[b]	97.3	Calc.
$AsS(OH)(SH)^-$	2.11-2.26[b]		Calc.
$As(OH)(SH)_2$	2.25 [b]		Calc.
$AsS(SH)_2^-$	1x2.119; 2x2.314 2.249(average)		Calc.[a]
$AsS(SH)_2^-$	2.08-2.32		Exp.[a]
$AsS_2(SH)^{2-}$	2x2.176; 1x2.532 2.295(average)		Calc.[a]
AsS_3^{3-}	2.289[a]	107.3	Calc.
AsS_3^{3-}	2.27[a]		Exp.
$As_3S_6^{3-}$ (ring)	2.21-2.314 (As-S) int 2.153-2.159 (As-S)ext	95.8-98.6 ($As\text{-}S_{int}\text{-}As$) 99.6-100.1 ($As\text{-}S_{ext}\text{-}As$)	Exp.[a]
AsIII on PbS	2.48		Exp.[b]
$As(Cys)_3$	2.23[c] 2.24[d,e] 3.2 (S-S)[c]	92.7 (S-As-S)[c]	Biological system Exp.[c,d,e]
	As-O		
As (V)	1.68-1.69[f] 1.661-1.742[g]	109.33 (O-As-O, average) [g]	
	1.62-1.66 [h] 1.75-1.88 (As-OH) [h]		In metal complexes Calc.
As (III)	1.70[b]; 1.83[d]; 1.78[f] 1.67[d] (As=O)		Exp.
$AsS(OH)(SH)^-$	1.81[b]		Calc.
$As(OH)(SH)_2$	1.82[b]		Calc.

[a] (Helz, *et al.*, 1995); [b] (Bostick, *et al.*, 2003); [c](Bhattacharjee, *et al.*, 1996); [d] (Bennett, *et al.*, 2001); [e] (Farrer, *et al.*, 2000); [f] (Arai, et al., 2001); [g] (Ferraris, *et al.*, 1970); [h] (Myneni, et al., 1998).

The data listed in Table III.2, corroborated by the detailed work of Myneni (1998) show clearly that the As-O distance may varies significantly with arsenic speciation, and therefore with pH. Different As-O distances are found for solvated, protonated or metal complexed arsenate molecules (Myneni*, et al.*, 1998).Those experimental and theoretical As-O and As-OH distances point to the fact that regardless of the As oxidation state, As-O distances are always shorter than As-OH distances. Therefore, the As-O distance of 1.63 Å would represent an average of the contributions of the As (III)-O distance on the adsorptive complex $[As(Cys)(OH)O]^-$ and the As (V)-O distance in adsorption complexes, such as $[As(Cys)(OH)O_2]^-$ or $[As(Cys)O_3]^{2-}$. In the latter, arsenic is bound to oxygen by single or double bonds. According to the optimized DFT calculations the As-O distance for the deprotoned species were 1.688 Å for As (III) ($H_2AsO_3^-$) and 1.679 Å for As (V) ($H_2AsO_4^-$). Therefore, both species showed As-O bond distances of the same order magnitude of the EXAFS measurements.

3.3.2 Density Functional Calculations

The interaction of cysteine with As (III) has been studied using Density Functional (DFT) calculations. Cysteine is the amino acid residue available to adsorb As (III) in the treated biomass. However, due to the lack of detailed structural information, it was considered the interaction of the free, gas phase cysteine molecule with As (III) as a model for the adsorption process. Different possible structures for the 1:3, 1:2 and 1:1 As/cysteine complexes have been fully optimized and vibrational analysis performed. All frequencies are real values assuring that a minimum in the potential energy surface has been achieved. Calculated geometrical properties of the most stable structures are shown in Table III.3.

The optimized 1:3 ($As(HL)_3$), 1:2 ($AsOH(HL)_2$) and 1:1 ($As(OH)_2HL$) metal/ligand species are shown in Figure 3.4. Rey *et al.* (2004) had studied the coordination of As (III) by cysteine and estimated the respective stability constants. However, the formation of 1:2 metal/ligand species was not observed in the pH range studied. According to these authors, the species 1:1 is an anion. Considering the pKa's of the

$As(OH)_3$ it is expected that the oxo group from the $As(OH)_2HL$ complex will deprotonate, thus forming the $As(OH)OHL^-$ species in pH above 9.0. In the present work this species was also calculated, since the deprotonation can lead to significant geometry changes. The As-S bond distances increase with the number of cysteine molecules and it is estimated to be about 2.28 Å. The As-OH distance in the H_3AsO_3 is estimated to be about 1.801 Å, and this increases to 1.830 Å in the $As(OH)(HL)_2$. However, the deprotonation of the $As(OH)_2(HL)$, leads to a decrease of the As-O and an increase of the As-S bond distances. The As-O distance is estimated to be 1.688 Å and the As-S distance of 2.450 Å for the deprotonated species. The As-O bond becomes stronger, which increases the charge density on the As center and, in turn, decreases the strength of the As-S bond. A detailed analysis of the bonding mechanism in this species is presently being undertaken in our laboratory.

Table III.3: Geometrical properties of the As/cysteine species. DFT and experimental bond distances in the As(III)/cysteine species.

Species	As-O (Å)	As-S (Å)
H_3AsO_3	1.801	—
$As(OH)OHL^-$	1.688/1.852	2.450
$As(OH)_2(HL)^-$	1.812	2.276
$As(OH)(HL)_2^-$	1.830	2.283
$As(HL)_3$	—	2.287
$As(HL)_3$ experimental[a]	—	2.25

[a] Ref.(Teixeira, *et al.*, 2005).

The coordination ability of the cysteine residues may not be affected by the protein structure surrounding it, in that sense; one could argue that the system might behavior similarly to the interaction of cysteine molecules with As (III) in aqueous solution. Based on this assumption, at pH < 8 the predominant species is expected to be $As(HL)_3$ (Rey *et al.*, 2004). In fact, the EXAFS data at pH 4.5 and 7 do not present the As-O bond. According to our results, the As-S bond distance is approximately 2.287 Å, i.e. 0.041 and 0.036 Å larger than the experimental values obtained at the pH 4.5 and 7.0. The DFT results are in very good agreement with the EXAFS experiments and support

the model in which the sulfydryl groups at the cysteine solid residues are available to coordinate metals, similarly to the reactions in solution. The increase of pH increases the hydroxyl concentration in solution, leading to a competition that favors the 1:1 species. This was discussed by Rey (2002) for complexation in aqueous phase. The presence of an As-O distance in the EXAFS data for the system at pH 10.5 is a strong evidence that the As/biomass behaves similarly. An EXAFS distance of 1.63Å for As-O is typical for the oxo groups, i.e., the deprotonated species. Since that pH is about 10.5 (pKa_1 = 9.2 for the arsenous acid) it is expected that in fact the species will be at least partially deprotonated. DFT calculations for the $As(OH)O(HL)^-$ species estimates the As-O and As-OH bond distances of 1.688 and 1.852 Å A, respectively. The first value is in good agreement with the experimental value of 1.63A. The presence of a As-OH bond distance of 1.852 Å, would cause a broadening in the EXAFS spectra, as observed by the larger value of σ^2. On the other hand, the estimated As-S bond distance of 2.450 Å is about 0.15 Å larger than the expected EXAFS value. This is much larger than the usually error bars of theoretical estimates at the level of theory used. We do not have an explanation for this discrepancy at this moment. However, it is important to observe that the calculation was done for the gas phase and considering the adsorption sites as cysteine molecules while in the biomass, the cysteine residues are immobilized. In addition, pH variation can modify the chemical adsorption sites and their rigidity significantly, thus preventing that the As (III) and sulfydryl groups find their best geometrical arrange.

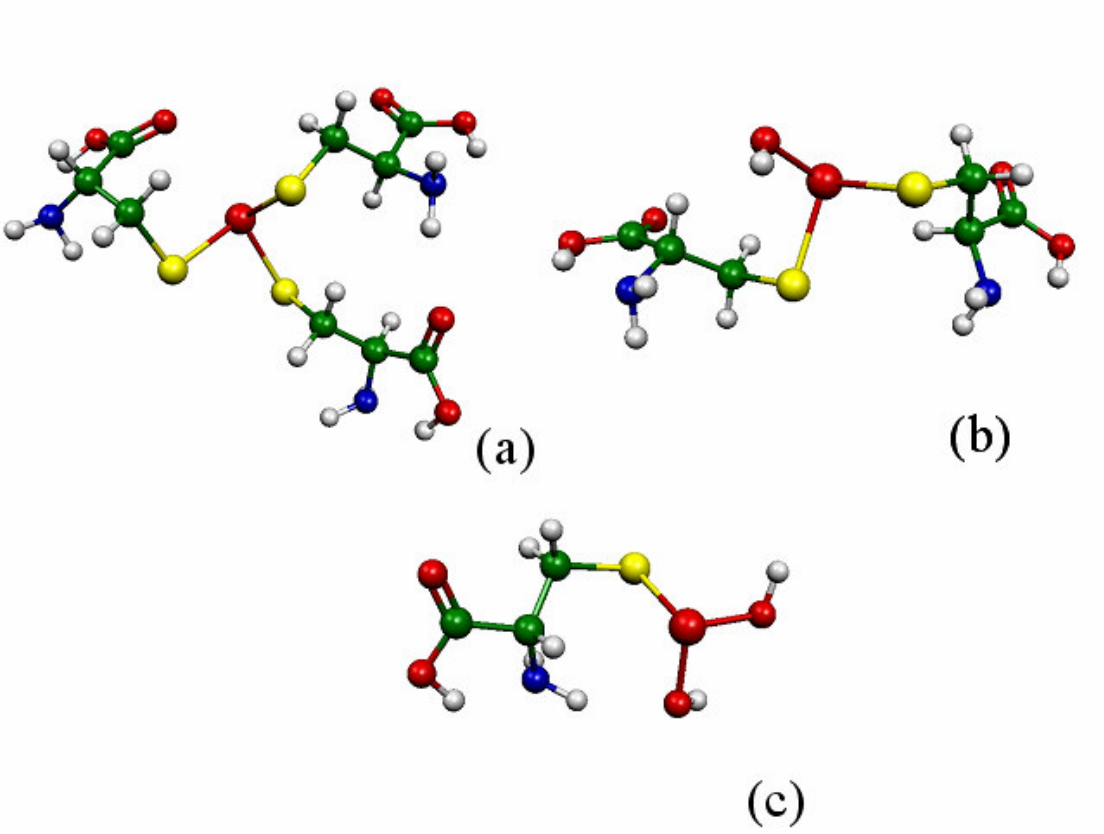

Figure 3.4. DFT optimized structures of the cystein/As (III) system.(a) 1:3 ($As(HL)_3$), (b) 1:2 ($AsOH(HL)_2$) and (c) 1:1 ($As(OH)_2HL$) metal/ligand species.

Colors legend: white, H; green, C; blue, N; red (small) O; yellow, S and red (big), As.

3.4 CONCLUSIONS

The adsorptive complexes formed during arsenite adsorption on protein rich biomass, at different pH, have been determined by a combination of macroscopic measurements with the analysis of structural data provided by X-Ray Absorption Spectroscopy (XANES and EXAFS) and with the theoretical predictions provided by Density Functional Calculations. Under acid or neutral conditions, arsenic atoms are directly bound to sulfur atoms; as pH increases, the sulfur groups may be replaced by the oxo-hydroxyl groups. This mechanism is consistent with the highest As (III) uptake observed under neutral and acid conditions. XAS analyses indicated that the stoichiometry of the As/Cys complex will depend on pH and, in turn, on the arsenous acid speciation. At acid or neutral pH, each arsenic atom is bound directly to three sulphur atoms at the reduced cysteine aminoacids, with the release of three water molecules. The As-S interatomic distance was found to be approximately 2.25 Å. At pH 10.5 a partial oxidation of arsenite to arsenate is observed. In addition, arsenic species become deprotonated. EXAFS and DFT data point to the existence of oxygen and sulfur atoms within the As first coordination shell. At pH 10.5, the As-S and As-O interatomic distances are respectively, 2.3 and 1.63 Å, for the experimental data, and 2.45 and 1.69 Å, for the calculated data. The presence of oxygen causes a distortion in the original trigonal-pyramidal structure of the arsenite adsorption complex, which is corroborated by the increase of the Debye Waller factor.

3.5. REFERENCES

Arai, Y.;Elzinga, E. J. and Sparks, D. (2001). X-ray absorption spectroscopy investigation of arsenite and arsenate adsorption at the aluminum oxide-water interface. *Journal of Colloid and Interface Science*, 235, p. 80-88.

Becke, A. D. (1987). A multicenter numerical integration scheme for polyatomic molecules. *J. Chem. Phys*, 88, p. 2547-2553.

Becke, A. D. (1988). Density-functional exchange-energy approximation with correct asymptotic-behavior. *Phys. Rev. A*, 38, p. 3098-3100.

Bennett, M. S.;Guan, Z.;Laurberg, M. and Su, X.-D. (2001). *Bacillus subtilis* arsenate reductasse is structurally and functionally similar to low molecular weight protein tyrosine phosphatases. *PNAS*, 98, p. 13577-13582.

Bhattacharjee, H.;Carbrey, J.;Rosen, B. P. and Mukhopadhyay, R. (2004). Drug uptake and pharmacological modulation of drug sensitivity

in leukemia by AQP9. *Biochemical and Biophysical Research Communications*, 322, p. 836–841.

Bhattacharjee, H. and Rosen, B. (1996). Spatial Proximity of Cys 113, Cys172, and Cys 422 in the Metalloactivation Domain of the ArsA ATPase. *The Journal of Biological Chemistry*, 271, p. 24465-24470.

Bostick, B. C. and Fendorf, S. (2003). Arsenite sorption on troilite (FeS) and pyrite (FeS_2). *Geochimica et Chosmochimica Acta*, 67, p. 909-921.

Ciminelli, V. S. T.;Ladeira, A. C. Q.;Duarte, H. A. and Oliveira, A. F. (2004). As(III) adsorbed on gibsite: structural model of surface complex based on EXAFS and DFT calculations. *submitted to Geochimica Chosmochimica Acta.*

Dambies, L.;Vincent, T. and Guibal, E. (2002). Treatment of Arsenic-Containing Solutions using Chitosan Derivatives: Uptake Mechanism and Sorption Performances. *Water Research*, 36, p. 3699-3710.

Dixit, S. and Hering, J. g. (2003). Comparision of Arsenic(V) and Arsenic(III) Sorption onto Iron Oxide Minerals: Implications for Arsenic Mobility. *Environmental Science and Technology*, 37, p. 4182-4189.

Farrer, B. T.;McClure, C. P.;Penner-Hahn, J. E. and Pecoraro, V. L. (2000). Arsenic (III)-Cysteine Interactions Stabilize Three-Helix Bundles in Aqueous Solution. *Inorganic Chemistry*, 39, p. 5422-5423.

Ferraris, G. and Chiari, G. (1970). The crystal structure of $Na_2HAsO_4.7H_2O$. *Acta Cryst.*, B26, p. 1574-1583.

Ghimire, K. N.;Inoue, K.;Yamagushi, H.;Makino, K. and Miyajima, T. (2003). Adsorptive separation of arsenate and arsenite anions from aqueous medium by using orange waste. *Water Research*, 37, p. 4945-4953.

Godbout, N.;Salahub, D. R.;Andzelm, J. and Wimmer, E. (1992). Optimization of gaussian-type basis-sets for local spin-density functional calculations 1. Boron through neon, optimization technique and validation. *Can.J. Chem.*, 70, p. 560-571.

Goldberg, S. and Johnston, C. T. (2001). Mechanisms of arsenic adsorption on amorphous oxides evaluated using macroscopic measurements, vibrational spectroscopy and surface complexation modeling. *Journal of Colloid and Interface Science*, 234, p. 204-216.

Helz, G. R.;Tossel, J. A.;Charnock, J. M.;Pattrick, R. A. D.;Vaughan, D. J. and Garner, C. D. (1995). Oligomerization in As(III) sulfide solutions: Theoretical constraints and spectroscopy evidence. *Geochimica et Cosmochimica Acta*, 59, p. 4591-4604.

Hughes, M. F. (2002). Arsenic Toxicity and Potential Mechanisms of Action. *Toxicology Letters*, 133, p. 1-16.

Johnson, J. M. and Voegtlin, C. (1930). Arsenic derivatives of cysteine. *Journal of Biological Chemistry*, 89, p. 27.

Kaur, P. and Rosen, B. P. (1992). Plasmid-Encoded Resistance to Arsenic and Antimony. *Plasmid*, 27, p. 29-40.

Knowles, F. C. and Benson, A. A. (1983). The biochemistry of arsenic. *TIBS*, 8, p. 178-179.

Koester, A. M.;Calaminici, P.;Gómez, Z. and Reveles, U. (2002). Density Functional Theory Calculation of Transition Metal Clusters. In: Sen, K. *"Reviews of Modern Quantum Chemistry, A Celebration of the Contribution of Robert G. Parr"*. World Scientific Publishing Co: p.

Loukidou, M. X.;Matis, K. A.;Zouboulis, A. I. and Liakopoulou-Kyriakidou, M. (2003). Removal of As(V) from wastewaters by chemically modified fungal biomass. *Water Research*, 37, p. 4544-4552.

Mandal, B. K. and Suzuki, K. T. (2002). Arsenic Round the World: a Review. *Talanta*, 58, p. 201-235.

Manju, G. N.;Raji, C. and Anirudhan, T. S. (1998). Evaluation of coconut husk carbon for the removal of arsenic from water. *Water Research*, 32, p. 3062-3070.

Messens, J.;Martins, J. C.;Belle, K. V.;Brossens, E.;Desmyter, A.;Gieter, M. D.;Wieruszeski, J.-M.;Willem, R.;Wyns, L. and Zegers, I. (2002). All intermediates of the arsenate reductase mechanism, including an intramolecular dynamic disulfide cascade. *PNAS*, 99, p. 8506-8511.

Mukhopadhyay, R.;Rosen, B. P.;Phung, L. T. and Silver, S. (2002). Microbial Arsenic: from Geocycles to Genes and Enzymes. *FEMS Microbiology*, 26, p. 311-325.

Myneni, S. C. B.;Traina, S. J.;Waychunas, G. A. and Logan, T. J. (1998). Experimental and theoretical vibrational spectroscopic evaluation of arsenate coordination in aqueous solutions, solids and at mineral-water interfaces. *Geochimica et Cosmochimica Acta*, 62, p. 3285-3300.

Perdew, J. P. (1986). Density-functional approximation for the correlation-energy of the inhomogeneous electron-gas. *Phys. Rev. B*, 33, p. 8822-8824.

Pickering, I. J.;Price, R. C.;George, M. J.;Smith, R. D.;George, G. N. and Salt, D. E. (2000). Reduction and Coordination of Arsenic in Indian Mustard. *Plant Physiology*, 122, p. 1171-1177.

Rey, N. A.;Howarth, O. W. and Maia, E. C. P. (2004). Equilibrium characterization of the As(III)-cysteine and the As(III)-glutathione systems in aqueous solution. *Journal of Inorganic Biochemistry*, 98, p. 1151-1159.

Schlegel, H. B. (1987). Optimization of equilibrium geometries and transition structures. In: Lawley, K. P. *Ab-Initio Methods in Quantum Chemistry-I*. Wiley & Sons: p. 249-286.

Schmoger, M. E. V.;Oven, M. and Grill, E. (2000). Detoxification of Arsenic by Phytochelatins in Plants. *Plant Physiology*, 122, p. 793-801.

Singh, T. S. and Pant, K. K. (2004). Equilibrium, kinetics and thermodynamic studies for adsorption of As(III) on activated alumina. *Separation Purification Technology*, 36, p. 139-1478.

Teixeira, M. C. and Ciminelli, V. S. T. (2005). Development of a Biosorbent for Arsenite: Structural Modelling Based on X-Ray Spectroscopy (XAS). *Environmental Science and Technology*, 39, p. 895-900.

Weerasooriya, R.;Tobschall, H. J.;Wijesekara, H. K. D. K.;Arachchige, E. K. I. A. U. K. and Pathirathne, K. A. S. (2003). On the mechanistic modeling of As(III) adsorption on gibbsite. *Chemosphere*, 51, p. 1001-1013.

Capítulo 4

Raman Spectroscopy Analyses and Theoretical Studies of Arsenite Complexes with Avian Keratin and Cysteine

Aceito para publicação no Journal of Colloid and Interface Science

Autores: *Mônica C. Teixeira, Virgínia S.T. Ciminelli, Maria Sylvia S. Dantas, Sirlaine F. Diniz e Hélio A. Duarte*

Raman Spectroscopy and DFT calculations of As (III) Complexation with a Cysteine-rich biomaterial

Mônica C. Teixeira[1], Virgínia S.T. Ciminelli[2a], Maria Sylvia Silva Dantas[2]; Sirlaine F. Diniz[3], Hélio A. Duarte[3].

[1] Permanent Address: Department of Pharmacy – Federal University of Ouro Preto (UFOP), 35400-000 – Ouro Preto, MG, Brazil. teixeira@ef.ufop.br
[2] Department of Metallurgical and Materials Engineering – Federal University of Minas Gerais (UFMG). 30 030 160 – Belo Horizonte – MG, Brazil. ciminelli@demet.ufmg.br
[3] Chemistry Department – Federal University of Minas Gerais (UFMG), 31270-901 – Belo Horizonte – MG, Brazil. duarteh@ufmg.br

[a] Corresponding Author

Abstract

Arsenite adsorption onto a protein-rich biomass and, more specifically, the chemical groups involved in the uptake were investigated using Raman Spectroscopy and DFT calculations. The study was based on spectroscopic analyses of raw and arsenic loaded biomass as well as standard samples of amino acids and arsenic salts. The predominant secondary structure of the protein was identified as the β-sheet type, with some contribution from α-helix structures. The participation of sulfidryl groups from cystine/cysteine molecules during the adsorption of arsenite was demonstrated. Only the *gauche-gauche-gauche* (g-g-g) conformation type of the disulfide bonds was involved in arsenic complexation. The formation of a pyramidal trigonal As $(HCys)_3$ complex was modeled according to the Density Functional Theory - DFT. The agreement of the DFT harmonic frequencies with the RAMAN spectra of the As $(HCys)_3$ complex demonstrated the relevant features of the cysteine-rich biomaterial regarding arsenic uptake as well as of the mechanism involved in the As (III)/biomass interaction at a molecular level. The results also illustrate that Raman spectroscopy can be successfully applied to investigate the mechanism of metal adsorption onto amorphous biomaterials.

Keywords: Arsenite sorption, arsenite complexes, cysteine, Raman Spectroscopy, sulphidryl, DFT calculations.

4.1 INTRODUCTION

Arsenic is a ubiquitous toxic metalloid. A worldwide concern about human contamination with arsenic from superficial and ground waters has resulted in a vast number of reports covering the various aspects related to this issue. The significance of this contamination, as well as the efficiency of the remediation techniques, is very much dependent on arsenic speciation. The predominant water-soluble species are the inorganic As (III) and As (V) derivatives of the arsenous (H_3AsO_3) and arsenic (H_3AsO_4) acids, respectively. Under conditions of moderate or high redox potential, such as those found in well-oxygenated surface waters, As (V) (arsenate) species predominate. Under reducing conditions, as usually observed in ground waters, As (III) (arsenite) species prevail. (Gupta and Chen, 1978; Case and Robinson, 1983; Knowles and Benson, 1983; Kaur and Rosen, 1992; Chiu, et al., 1994; Ramaswami, et al., 2001).

Arsenite species are considered 10 times more toxic than arsenate species and 70 times more toxic than organic species - dimethylarsinate ($(CH_3)_2AsOH$ and $(CH_3)_2OAsOH$) and monomethylarsonate ($CH_3AsO_2H_2$, and $CH_3AsO_3H_2$) (Kumaresan and Riyazuddin, 2001). The toxicity of As (III) species can mostly be explained by its irreversible complexation with sulphydril groups present in active biomolecules, such as enzymes. (Kumaresan*, et al.*, 2001). Sulphydril groups are usually found in the structure of some aminoacids, mainly cysteine. Therefore, enzymes whose activity sites depend on the sulphydril groups may have their metabolic activities totally or partially impaired by complexation with As (III). As (III) reacts when in contact with sulphur and sulphydryl groups such as cysteine, organic dithiols, proteins and enzymes, but it does not react when in contact with amine groups or organics with reduced nitrogen constituents. On the other hand, As (V) reacts when in contact with reduced nitrogen groups such as amines, but not when in contact with sulphydryl groups. The toxicity of arsenate species is mainly related to its competition with phosphate groups. Pentavalent arsenic can disrupt the oxidative phosphorylation - the process by which ATP is formed - by the production of an arsenate ester of ADP. This process is known as arsenolysis (Kumaresan*, et al.*, 2001; Mandal and Suzuki, 2002).

In addition to its toxicity, arsenite is the most mobile species in the environment due to its weaker, reversible adsorption on soil constituents, such as iron and aluminum oxyhydroxides (Ladeira and Ciminelli, 2004). This reversible, weaker adsorption of As (III) on soil constituents, and apparently inconsistent formation of inner-sphere adsorption complexes, was discussed by before (Oliveira, et al., 2006). Based on density functional methods and cluster models, it was shown that in contrast to the As (V) species, As (III) is not adsorbed via an acid/base, but rather by a non-dissociative mechanism in which O–H bonds are not broken. The complexation of As (III and V) in natural environments by dissolved organic matter, thus preventing sorption and co-precipitation, may also increase arsenic mobility (Kumaresan*, et al.*, 2001)

Various potential applications can be envisaged for materials capable of a direct As (III) removal and immobilization. Arsenic speciation in natural waters and effluents is increasingly important for the assessment of toxicity and bioavailability of arsenic species in an aqueous environment. Therefore, the possibility of an efficient separation of As (III) and As (V) species in the field, during sampling, minimizes the errors resulting from sample alteration prior to the analyses. In another context – treatment of water and aqueous effluents - a direct removal of As (III) would eliminate the need of previous oxidation of arsenite to arsenate by solid-phase or liquid-phase oxidants. The oxidation of As (III) is an obligatory and expensive stage of the usual schemes for water and effluent treatment by co-precipitation or adsorption on iron oxy-hydroxides (Deschamps, et al., 2005)

The understanding of the interaction mechanism of arsenite with biological molecules, and more specifically the biochemical fundamentals that explain arsenic toxicity, was applied to the development of a biomaterial capable to selectively remove As (III) from aqueous environments (Teixeira and Ciminelli, 2005). The results of this original approach for the treatment of arsenic-containing solutions demonstrated that a cysteine-rich biomass – a residue from the poultry industry - was highly selective for arsenic removal in its trivalent form, without important effects of the studied competitor ions on the solid's adsorption capacity. X-Ray Absorption Analysis (XAS) indicated that each arsenic atom is bound directly to three sulphur atoms from the reduced cysteine

aminoacids present in biomass. Arsenic is adsorbed as As (III) thus avoiding the need for previous arsenite oxidation.

In a further development of this project, the aim was to obtain detailed structural information about the protein-rich biomaterial as well as the changes taking place during arsenite complexation. The present work shows the results obtained by Raman Vibrational Spectroscopy of the raw and arsenic loaded biomass, as well as of selected amino acids and standard As (III) salts. Density functional calculations were also performed and the results were compared with the Raman frequencies observed experimentally. The obtained results provide a better understanding of the relevant features of the cysteine-rich biomaterial regarding arsenic uptake as well as of the mechanism involved in the As (III)/biomass interaction at a molecular level. It was demonstrated that only the *gauche-gauche-gauche* (g-g-g) conformation type of the disulfide bonds is involved in arsenic complexation.

4.2 MATERIALS AND METHODS

4.2.1 Materials

Residues from the poultry industry - white chicken feathers - were rinsed thoroughly with warm tap water and dried at 45 ±5°C for 24 hours. The dried material was ground and sieved to obtain a size range below 0.037 mm (400 Mesh Tyler). Biomass activation was accomplished by adding 10 ml of a 7.8 % (w/w) basic ammonium thioglycolate solution. The treatment did not imply any loss of mass. Following this activation step, the powdered biomaterial was filtered and washed with 100 mL of Milli-Q water. The adsorption experiments were carried out according to the previously described protocol (Teixeira*, et al.*, 2005). Arsenic uptake at pH 5 was 20 mg As (III)/g of biomass.

An As (III)-cysteine precipitate was prepared by the reaction created upon mixing As (III) (13.4 mmol.L^{-1}) with Cysteine (3.0 mmol.L^{-1}) at pH 5.0. The reaction was

carried out in an aqueous solution, degassed with N_2 at pH 5.0, with an excess of sodium meta-arsenite. Cystine and cysteine amino acids (Merck, 99.0%), sodium arsenite and arsenate aqueous solutions (13.4 mmol.L^{-1}, pH 4.5 and 10.5), and an $AsNaO_2$ salt (Fluka, 99.0%) were also used in the present investigation.

4.2.2 Raman Spectroscopy

Raman spectra were obtained through a Labran HR 800 (Jobin Yvon/Horiba). A He-Ne laser with a 632.8 nm wavelength and a 20 mW power output measured at the laser head was used as the excitation source. The Raman signal was collected by Olympus microscope objectives (50 X 0.75 and 100 X 0.90) in back scattering configuration. The entrance slits to the spectrograph were 100 µm with a correspondent resolution of 2.0 cm^{-1}. The utilized holographic grating was of 600 or 1800 g/mm for inorganic or biological material. Liquid nitrogen cooled CCD was used as a detector.

Depending on the sample background fluorescence, the acquisition time ranged from 10 to 120s. To reduce the signal/noise ratio, spectra were acquired 100-300 times after a photobleaching of 5-30 minutes. Collected Raman spectra were analyzed and optimized with Labspec 1.1 and Origin 5.0. Spectra collected were averaged, the background was corrected and, if necessary, normalized, and the peak was deconvoluted.

4.2.3 Computational aspects

The interactions of $As(OH)_3$ with Cysteine (HCys) leading to different metal/ligand proportion complexes have been studied using the LCGTO-KS-DF (Linear Combination of Gaussian Type Orbital-Kohn Sham-Density Functional) method implemented in deMon-2002 program (Koester, et al., 2002b). The generalized exchange correlation (XC) functional has been used with the Becke expression (Becke, 1988) for exchange and with that of Perdew (Perdew, 1986a; Perdew, 1986b) for correlation (GGA-BP). The one-electron orbitals are expanded in triple-zeta orbital basis sets explicitly optimized by Godbout (Godbout, et al., 1992). Auxiliary basis sets (A2) have been used for fitting the density charge. Adaptive grid (Krack and Koster, 1998; Koster, et al., 2004) with a tolerance of 10^{-6} for the numerical integration of the

exchange-correlation energy and potential was used. The numerical integration is based on Becke's partition scheme (Becke, 1987) in an adaptive grid. The calculation of the expansion coefficients of the approximated density is described in detail elsewhere (Koester, et al., 2002a). All structures have been fully optimized using the BFGS (Schlegel, 1987) method. Vibrational analysis was performed for the most stable species using the harmonic approximation. The Hessian matrix was evaluated numerically from the analytical gradients of the potential energy surface. Positive frequencies assure that true minima on the potential energy surface have been found.

4.3 Results and Discussion

4.3.1 Raman Spectroscopy

Over the past two decades, Raman spectroscopy has been successfully applied to the area of biopolymer research. It has also helped to elucidate the structure of amorphous, biological materials, such as proteins, enzyme lipids, or nucleic acids (Fabian and Anzenbacher, 1993), which show short range ordering for distances up to three or four bond lengths (Brodsky, 1983). Therefore, despite the amorphous nature of the sorbent, Raman spectroscopy can provide information about the intrinsic structure of the avian biomass prepared for As (III) uptake in addition to the molecular level modification following the reaction.

Figure 4.1 shows the Raman vibrational spectrum obtained with the raw biomass sample. The main band observed at 510 cm^{-1} is assigned to the (S-S) symmetric stretching vibrational mode (Yu, et al., 1985; Akhtar, et al., 1997b). It is also possible to observe two weak bands at 622 and 644 cm^{-1} attributed to the stretching of the gauche C-S bonds, much like those described by previously (Akhtar and Edwards, 1997a) at 621 and 643 cm^{-1}. The intensity of C-S band is usually related to the sulfur content in amino acids, such as methionine, cysteine, and cystine. The methionine contribution to the C-S vibrational modes is expected to be negligible since its content in avian keratin

is lower than 0.4% as compared to 7.8% from cysteine (Akhtar*, et al.*, 1997a; Akhtar*, et al.*, 1997b).

Other relatively intense bands are observed at 827, 855 (highlighted) and 1205 cm^{-1} (not shown) and may be attributed to the vibrational modes of the C-OH stretching of the phenolic OH groups from the amino acids tyrosine and phenylalanine. The first two bands are exclusive from tyrosine (Fabian*, et al.*, 1993). A relatively low intensity 1603 cm^{-1} band may also be attributed to the vibrational mode ν(C=C) of olefinic carbon bonds (Akhtar*, et al.*, 1997a).

At the region near 1000-1100 cm^{-1}, the observed bands were correlated with the C-C stretching vibrational modes (Fabian*, et al.*, 1993; Akhtar*, et al.*, 1997a; Akhtar*, et al.*, 1997b). The sharp band observed at 1003 cm^{-1} is attributed to the C-C stretching vibration mode of aromatic carbon rings in the phenylalanine side chain (Akhtar*, et al.*, 1997a). This assigning is consistent with the fact that phenylalanine is the major aromatic side chain amino acid detected in the composition of avian keratin (3.1%) Some other less intense bands (not highlighted in Figure 4.1) were observed at 1031, 1088, 1124, 1156, and 1171 cm^{-1}. The bands located at 1031 and 1124 cm^{-1} are assigned to the *cis* and *trans* (C-C) stretching, respectively, while the band at 1088 is characteristic of a randomic (C-C) skeletal conformation.

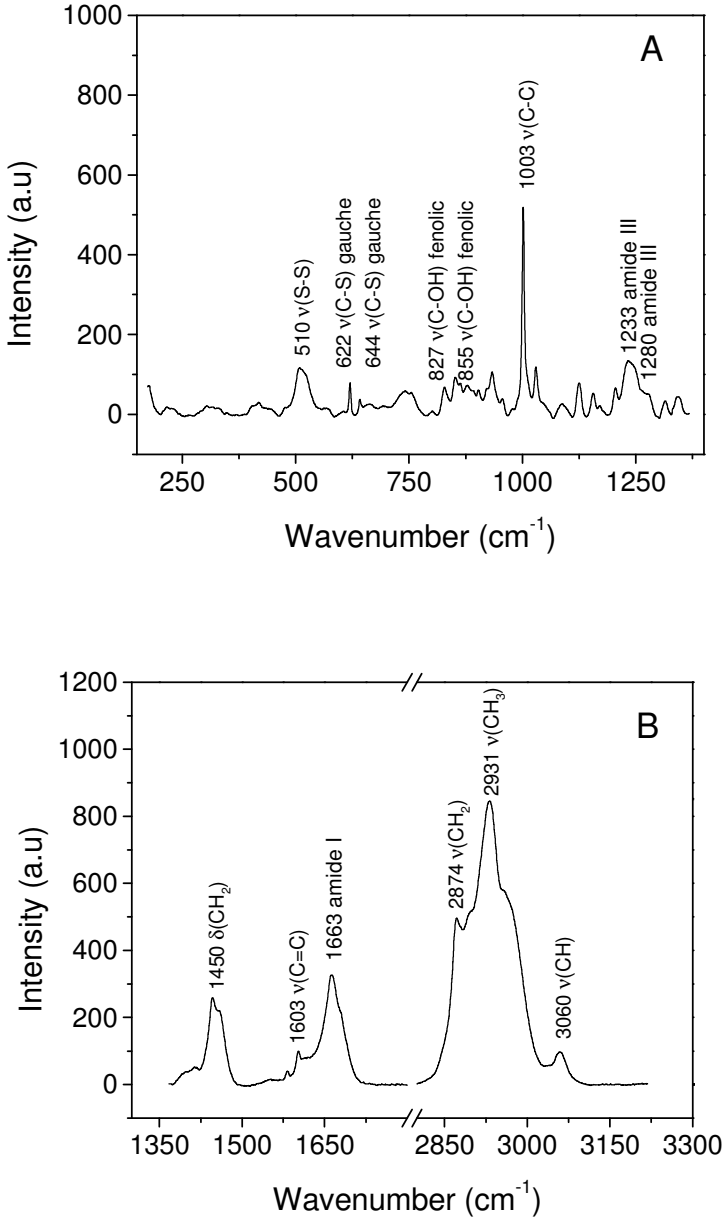

Figure 4.1 Raman spectroscopy of natural biomass (Baseline corrected for fluorescence)

Raman spectra of proteins contain the contributions from the vibrational groups of peptide backbones and those related to the amino acids themselves. There are some characteristic bands frequently detected in Raman spectra of all proteins. These include the amide I vibrational modes, with the contribution of C=O stretching, and the amide III band, resulting of C-N stretching coupled with N-H bending. Depending on the secondary structure (which include the bidimensional structures stabilized by hydrogen bonds) of the protein, the hydrogen atom from the amino group will be bound to the nitrogen in a different manner (in or out of the plane) and amide I and III vibrational modes will show different absorption wavenumbers. At 1233 cm^{-1} (Figure 4.1) one may observe a relatively intense and broad band, which, together with a small band at 1280 cm^{-1}, is related to the amide III vibrational modes. At 1663 cm^{-1}, another intense broad band with other contributions at 1680 cm^{-1} attributed to amide I vibrational mode, was observed. For β-sheet proteins, like avian keratins, the amide I and III bands are detected between 1665 and 1680 and between 1230 and 1240 cm^{-1}, while for α-helix proteins the expected wavenumbers were between 1645 and 1657 and between 1260 and 1300 cm^{-1} (Akhtar*, et al.*, 1997a; Akhtar*, et al.*, 1997b; Edwards, et al., 1998). The presence of a broad amide III band, resulting from the overlapping of bands located at 1233 and 1280 cm^{-1}, is suggestive of the existence of a less ordered protein secondary structure comprised mainly of β-sheet, with a possible minor contribution of α-helix structures.

The vibrational modes of CH_3, CH_2, and CH groups were also detected but only the most intense bands were highlighted in Figure 4.1. The CH_3 deformation modes were observed at 932 and 956 cm^{-1}, which is characteristic of $\rho(CH_3)$ and at 1415 cm^{-1} for $\delta(CH_3)$. The $\nu(CH_3)$ symmetric stretching produced a band with the wavenumber of 2931 cm^{-1}. Two bands located at 744 and 754 cm^{-1} may be attributed to the deformation ρCH_2) in phase. The vibrational modes of the deformation (δ) and the stretching (ν_3) of CH_2 were observed at 1317 and 2874 cm^{-1}. Another two bands located near 1450 cm^{-1} (1447 and 1460) may also be assigned to methylene (CH_2) scissoring deformation, which is a characteristic band of keratins. For the CH group, the observed vibrational modes were one relative to the C-H bending at 1345 cm^{-1} and

other two at 2721 and 3060 cm^{-1} related to the stretching of the aliphatic and olefinic ν(CH) vibrational modes, respectively (Fabian*, et al.*, 1993; Akhtar*, et al.*, 1997b). The sum of the contribution of CH, CH_2, and CH_3 stretching vibrational modes results in a broad intense band observed at the region between 2800 and 3100 cm^{-1}.

In this section, the features of the biomass prior to and after adsorption of As (III) will be discussed. Prior to adsorption, the predominant arsenic species in the aqueous phase at pH 5 is the neutral H_3AsO_3. XAS measurements indicated that As (III) adsorption involves an inner sphere complexation with the sulphydril groups available in the biomass upon the release of three water molecules. Figure 4.2 illustrates the normalized spectra of the natural powdered biomass and arsenite-loaded powdered biomass. The spectra are similar in the regions between 600 and 3200 cm^{-1}. It is important to emphasize that the reduction with thioglycolate caused no detected modification in the characteristic spectra of the natural sample (data not shown).

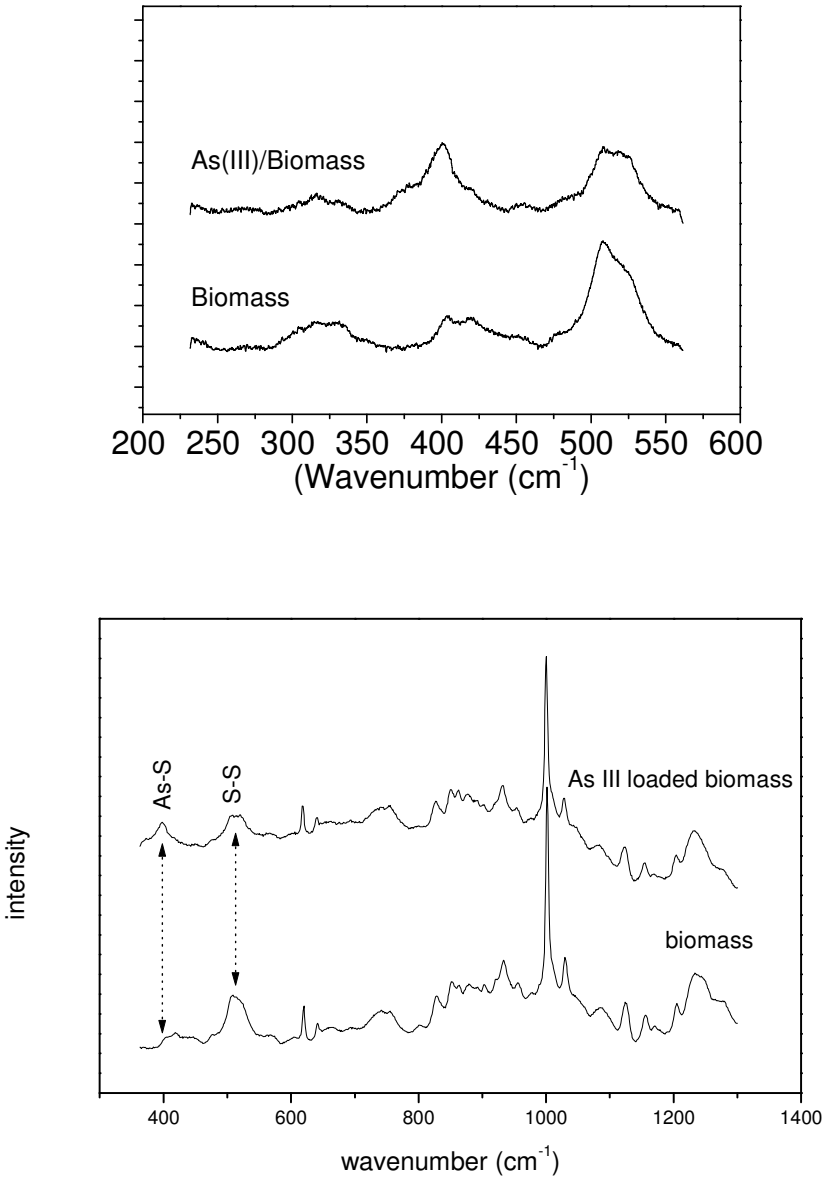

Figure 4.2 Raman spectra for natural powdered biomass and arsenite-loaded powdered biomass at pH 5.0. Detailed spectra (top) were obtained with an 1800 g/mm holographic grating.

The major differences between the natural and the arsenite loaded biomass spectra were observed in the region below 600 cm^{-1}, which is highlighted in the upper part of Figure 4.2. The first represents the decrease in the intensity of the band located between 500 and 550 cm^{-1} following As (III) uptake. The second interesting aspect is the appearance of one broad band between 340 and 420 cm^{-1} after arsenic uptake. Both phenomena took place within the regions where the main expected features were the S-S symmetric stretching and the As-S symmetric stretching (for arsenite loaded biomass), respectively.

Figure 4.3 (a and b) explores the characteristic region of S-S stretching vibrational modes, which were fitted and deconvoluted using a Lorentz function. It was possible to observe that the broad band at 500-550 cm^{-1} is the result of the overlapping of two bands - one centered at 507 cm^{-1} and the second at 524 or 522 cm^{-1} for the biomass samples prior to and after arsenic adsorption, respectively. It was also possible to notice that while the intensity of the second band is maintained after adsorption, the first had its intensity diminished by more than 50%. The S-S symmetric stretching mode, frequently detected at frequencies around 510 cm^{-1} (Yu*, et al.*, 1985; Fabian*, et al.*, 1993; Akhtar*, et al.*, 1997b), is caused exclusively by cystine. Each cystine molecule is comprised of two cysteine residues that bind to each other by one disulfide bridge (S-S) in a strong chemical binding characteristic of keratins produced after the oxidation of two sulfydryl groups. All the analyzed samples provide broad bands centered at 507 cm^{-1}. It was also observed that the S-S vibrational mode amplitude was slightly diminished for the sample treated with thioglycolate (data not shown), confirming the reduction of the S-S bridge.

Figure 4.3c shows the spectrum produced after the subtraction of the spectra obtained prior to and after arsenic uptake. The resulting spectrum indicates that the amplitudes of the vibrational modes located at the region around 500 cm^{-1} have decreased (negative). The negative values observed at Figure 4.3c around 500 cm^{-1} indicate the utilization of sulfur containing groups during arsenite adsorption according Figure 4.4. Based on the results shown above, it is possible to conclude that only a special type of S-S bonds is involved in arsenite complexation. In fact, the atoms involved in the disulfide bonds (C-

C-S-S-C-C) of keratin structure may assume different spatial orientations, causing three different conformations for the chemical bonds: *trans-gauche-trans*, *gauche-gauche-trans* and *gauche-gauche-gauche.* The latter is the characteristic conformation of the avian β-keratin. For the *trans-gauche-trans* and *gauche-gauche-trans* conformations, the expected wavenumbers for the S-S stretching vibration are 540 and 525 cm^{-1} respectively, while for the *gauche-gauche-gauche* it is 510 cm^{-1} (Yu*, et al.*, 1985; Fabian*, et al.*, 1993; Akhtar*, et al.*, 1997b). The results shown in Figure 4.3 indicate that the *gauche-gauche-gauche* disulfide bridges prevail in the keratin-rich biomass utilized in the present work and was preferably consumed during arsenite adsorption. The involvement of the other type of disulfide bridge, *gauche-gauche-trans* and *trans-gauche-trans*, in arsenic complexation may be disregarded.

Figure 4.3c also depicted an evident alteration on the spectral features at 340 and 420 cm^{-1} after arsenite adsorption. The S-S bridges are disrupted by reduction, thus producing two SH groups, which are involved in arsenic adsorption. The region between 350 and 450 cm^{-1} is usually assigned to the vibrational modes of the As-S group (Brodsky, 1983; Bell, et al., 1997). For the arsenic containing pigments, the vibrational modes of the As-S stretching produced bands are 292, 309, 353, and 381 cm^{-1} for orpiment (As_2S_3), 330 and 360-376 cm^{-1} for realgar (As_4S_4), and a broad band composed of four different peaks centered in 330 cm^{-1} produced by pararealgar (As_4S_4) (Trentelman, et al., 1996). The As-S stretching vibrational mode frequencies calculated for synthetic arsenite sulfide solutions were found at 286 and 430 cm^{-1} depending on the oligomerization of arsenic complexes in the solution (Helz, et al., 1995).

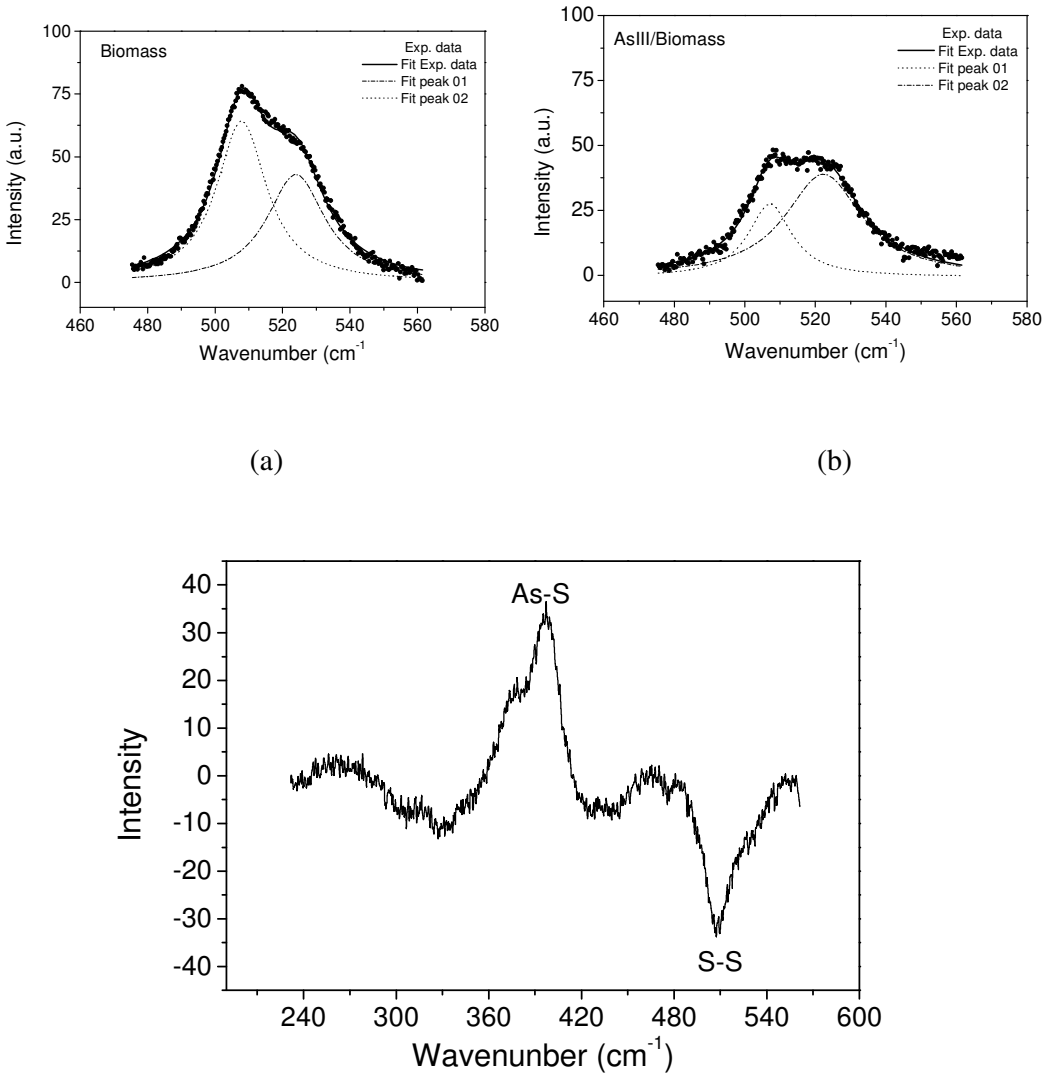

Figure 4.3 - Differences between natural and arsenite loaded biomass. Fitting of S-S stretching band for the (a) biomass, (b) As (III)/Biomass, and (c) Difference spectrum As (III)/Biomass-Natural Biomass (lower)

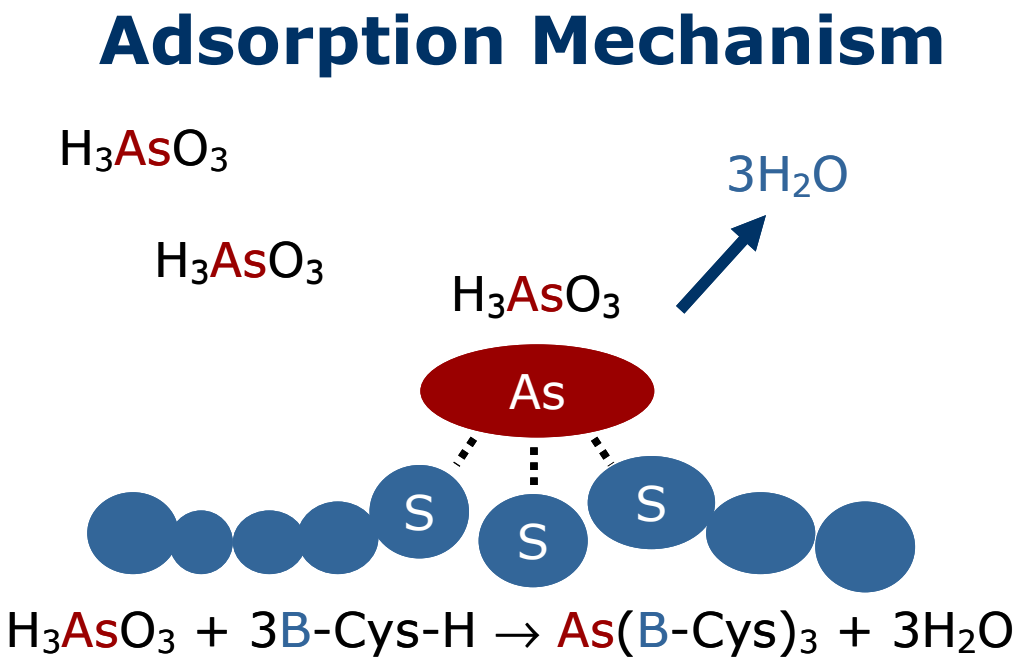

Figure 4.4 – Schematic picture of As (III) adsorption onto a protein-rich biomass. Each arsenic atom reacts with three sulfur atoms from cysteine aminoacids. Three water molecules are released and a pyramidal As-S complex is formed. Biomass structure is represented by B.

4.3.2 Cysteine/As (III) complexes

In order to maximize the signal amplitude of the As-S vibrational modes, the arsenic complexation with pure cysteine amino acid was investigated. The As (III)-cysteine precipitate was prepared by reacting pure cysteine with an excess of sodium meta-arsenite. Raman analyses of the precipitate produced a spectrum with well-defined bands, which is compared to the cysteine standard spectrum in Figure 4.5.

Figure 4.5 clearly demonstrates that the sharp band at 2556 cm^{-1} (ν(S-H) vibrational mode) shown in the cysteine spectrum disappears after reaction with arsenite. In the precipitate spectrum, one may notice the appearance of four intense bands near to 400 cm^{-1} (358.5; 384, 401.5, and 427.8 cm -1). These frequency values coincide with the frequency range of the broad band described earlier in Figure 4.3. The vibrational frequency calculated for the As-S symmetrical stretching was 390-403 cm^{-1} for the internal or the externally located As-S bonds, respectively, in the $As_3S_3(SH)_6$ complex (Helz*, et al.*, 1995). The intense band observed at 401.5 cm^{-1} (Figure 4.5) indicates the formation of an As-S band (symmetric stretching) after cysteine reaction with sodium arsenite.

It can also be observed that the intense and sharp band at 684 cm^{-1}assigned to the C-S stretching (Susi, et al., 1983) in the cysteine spectrum is preserved as a broad band after reaction with arsenite. The C-H symmetric stretching vibrational mode, observed for the cysteine molecule at 2996 cm^{-1} and the NH_3^+ stretching mode at 3000 cm^{-1}, seems to have been shifted to the lower frequencies of 2924 and 2960 cm^{-1}, respectively, in the precipitate sample. There is also an apparent splitting in the precipitate in the NH_3^+ band. Due to the complexity of the keratin structure, or perhaps because of the low arsenite content, the signal was not strong to indicate the participation of C-H and NH_3^+ groups during arsenic adsorption

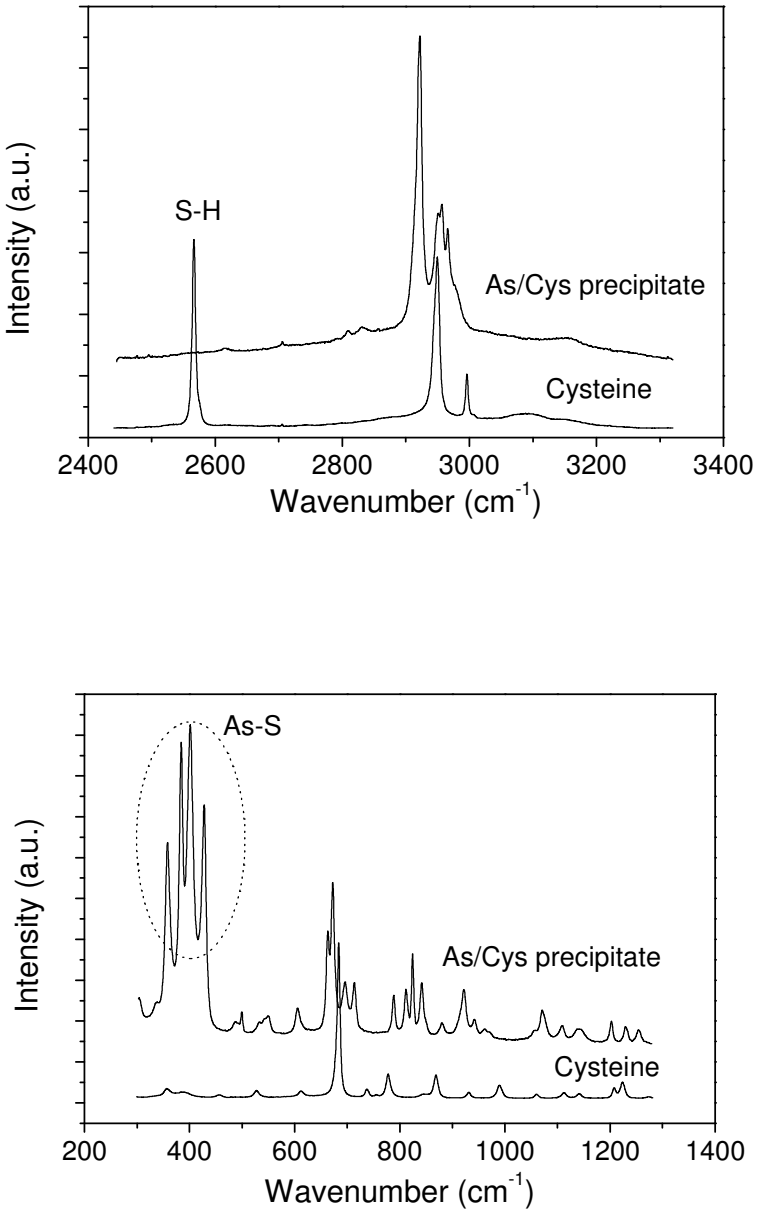

Figure 4.5 - Raman spectra of Cysteine and As/Cysteine complex (centered at 800 and 2900 cm $^{-1}$)

4.3.3 DFT calculations

Recent XANES and EXAFS studies of the As (III) with the cysteine rich biomass showed that As (III) is adsorbed in its trivalent form (Teixeira*, et al.*, 2005). Therefore, the theoretical model for the adsorption was based on the 1:3 As:HCys complex, shown in Figure 4.6. The optimized structure presents the As center with a pyramid trigonal as expected and the As-S bond distance at approximately 2.287Å. This value may be compared to the EXAFS value of 2.26 Å. Table IV. 1 shows the DFT harmonic frequencies for different complexes with respect to the As-O, As-S, and S-C strengths. At the level of theory used, the calculated frequencies are commonly overestimated and the error bars are normally up to 50 cm^{-1} (Frisch, et al., 1998). The calculated C-S frequencies are about 657-685 cm^{-1}, in reasonable agreement with the experimental range of around 622-644 cm^{-1}. The C-S frequency for the cysteine is predicted to be 684 cm^{-1}, slightly shifted for larger wavenumbers. The As-O frequency for the $As(OH)_3$ is in the range of 600-634 cm^{-1}, approximately 60 cm^{-1} smaller than the respective experimental value. The As-S frequency is the most important feature of the Raman spectra, since this bond strength is not present in the original biomass. However, it lies in the range of low frequencies and its precise peak is difficult to be determined experimentally. The $As(SH)_3$ complex has been calculated for comparison. The As-S frequency is about 372-382 cm^{-1}, in the same range as the predicted values for the As/cysteine complexes. Vibrational frequencies reflect the nature of the bond and, therefore, provide information about the adsorption site. However, it is reasonable to observe that the As-S frequency is probably modified due to the extended solid (biomass) that can perturb the As-S strength through the steric hindrance of the system or through an inductive chemical mechanism. To answer those questions, more detailed calculations with larger models that can take into account part of the molecular structure of the β-keratin would be required. The DFT results show that the $As(HCys)_3$ is a satisfactory model to describe the interaction of the As (III) with the cysteine rich biomass with a pyramid trigonal geometry.

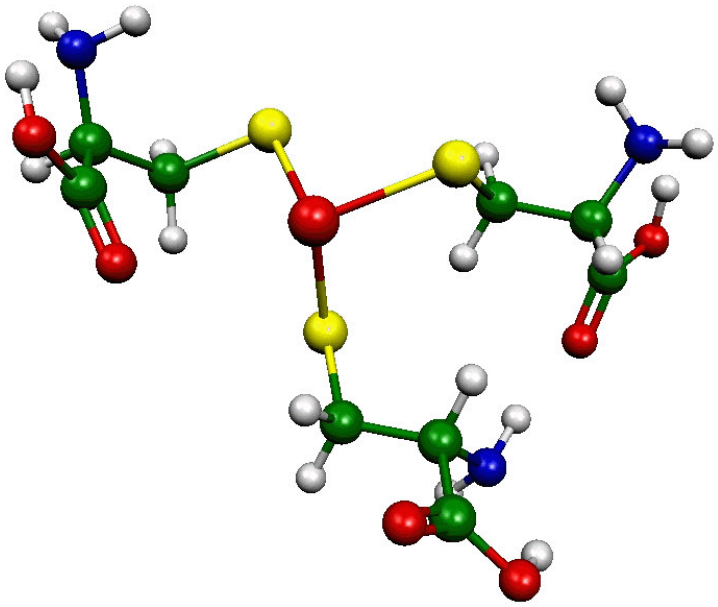

Figure 4.6 - Optimized structure of As $(HCys)_3$. Arsenic atoms are represented by the central sphere in red surrounded by three yellow spheres representing sulfur atoms from three different cysteine molecules.

Table IV. 1 - DFT harmonic frequencies (in cm^{-1}) for As-O, As-S and C-S bond strength.

Complexes	**As-O**	**As-S**	**C-S**
As $(HCys)_3$		368.7 372.2 401.1	657.8 681.7 684.5
H_2Cys			684
As $(OH)_3$	600.1(669)[a] 609.6(709)[a] 633.2		
As $(SH)_3$		372.5 372.5 381.2	
Raman[b]		350-460	622/644 (684)[c]

[a] Value in parentheses are from Refs. (Tossel, 1997; Goldberg and Johnston, 2001).
[b]Values in parentheses are for cysteine/As (III) system at pH 5.0.
[c] Value in parentheses for the cysteine.

4.4 Conclusions

The secondary structure of the proteins contained in the biomass utilized during this work was investigated by Raman spectroscopy. The predominant secondary structure of the protein was shown to be the β-sheet, as expected for avian keratins, with minor contribution from the α-helix structures. The adsorption of arsenite on the sulfidryl groups from cystine/cysteine molecules present in the biomass was investigated. The disulfide bond in the biomass protein structure is spatially ordered, predominantly in a *gauche-gauche-gauche* (g-g-g) conformation. Part of the disulfide bonds assumes the *gauche-gauche-trans* (g-g-t) conformation. The results showed that only the g-g-g type disulfide bonds are involved in arsenic adsorption. The adsorption site is correctly modeled by the interaction of cysteine molecules with the As (III) forming a pyramid trigonal As $(HCys)_3$ complex as was evidenced by the RAMAN and DFT calculations.

4.5 References

Akhtar, W. and Edwards, H. G. M. (1997a). Fourier-transform Raman spectroscopy of mammalian and avian keratotic biopolymers. *Spectrochimica Acta Part A*, 53, p. 81-90.

Akhtar, W.;Edwards, H. G. M.;Farwell, D. W. and M.Nutbrown (1997b). Fourier-transform Raman spectroscopic study of human hair. *Spectrochimica Acta Part A*, 53, p. 1021-1031.

Becke, A. D. (1987). A multicenter numerical integration scheme for polyatomic molecules. *J. Chem. Phys*, 88, p. 2547-2553.

Becke, A. D. (1988). Density-functional exchange-energy approximation with correct asymptotic-behavior. *Phys. Rev. A*, 38, p. 3098-3100.

Bell, I. M.;Clark, R. J. H. and Gibbs, P. J. (1997). Raman spectroscopy library of natural and synthetic pigments (pre 1850 AD). *Spectrochimica Acta Part A*, 53, p. 2159-2179.

Brodsky, M. H. (1983). Raman scattering in amorphous semiconductors. In: Cardona, M. *Light Scattering in solids I*. Second. Berlin, Heidelberg, New York, Springer-Verlag. 8: p. 205-251.

Case, C. and Robinson, M. F. (1983). Some Aspects in Nutritional Trace Elements. In: Siegel, H. *Methods Involving Metal Ions and Complexes in Clinical Chemistry*. New York, Marcel Dekker, Inc. 16: p. 1-26.

Chiu, K.-H.;Chen, S.-L.;Dzeng, S. R.;Shieh, G.-M.;Yang, M.-H. and Wal, C. M. (1994). Arsenic Species in Groundwaters of the Blackfoot Disease Area, Taiwan. *Environ. Sci. Technol.*, 28, p. 877-881.

Deschamps, E.;Ciminelli, V. S. T. and Holl, W. H. (2005). Removal of As(III) and As(V) from water using a natural Fe and Mn enriched sample. *Water Research*, 39, p. 5212-5220.

Edwards, H. G. M.;Hunt, D. E. and Sibley, M. G. (1998). FT-Raman spectroscopic study of keratotic materials: horn, hoof and tortoiseshell. *Spectrochimica Acta Part A*, 54, p. 745-757.

Fabian, H. and Anzenbacher, P. (1993). New developments in Raman spectroscopy of biological systems. *Vibrational Spectroscopy*, 4, p. 125-148.

Frisch, M. J.;Trucks, G. W.;Schlegel, H. B.;Scuseria, G. E.;Robb, M. A.;Cheeseman, J. R.;Zakrzewski, V. G.;J. A. Montgomery, J.;Stratmann, R. E.;Burant, J. C.;Dapprich, S.;Millam, J. M.;Daniels, A. D.;Kudin, K. N.;Strain, M. C.;Farkas, O.;Tomasi, J.;Barone, V.;Cossi, M.;Cammi, R.;Mennucci, B.;Pomelli, C.;Adamo, C.;Clifford, S.;Ochterski, J.;Petersson, G. A.;Ayala, P. Y.;Q. Cui;Morokuma, K.;Malick, D. K.;Rabuck, A. D.;Raghavachari, K.;Foresman, J. B.;Cioslowski, J.;Ortiz, J. V.;A. G. Baboul;Stefanov, B. B.;Liu, G.;Liashenko, A.;Piskorz, P.;Komaromi, I.;Gomperts, R.;Martin, R. L.;Fox, D. J.;Keith, T.;Al-Laham, M. A.;Peng, C. Y.;Nanayakkara, A.;Gonzalez, C.;Challacombe, M.;Gill, P. M. W.;Johnson, B.;Chen, W.;Wong, M. W.;Andres, J. L.;Gonzalez, C.;Head-Gordon, M.;Replogle, E. S. and Pople, J. A. (1998). Gaussian 98-Revision A.7. Pittsburgh PA, Gaussian, Inc.

Godbout, N.;Salahub, D. R.;Andzelm, J. and Wimmer, E. (1992). Optimization of gaussian-type basis-sets for local spin-density functional calculations 1. Boron through neon, optimization technique and validation. *Can.J. Chem.*, 70, p. 560-571.

Goldberg, S. and Johnston, C. T. (2001). Mechanisms of arsenic adsorption on amorphous oxides evaluated using macroscopic measurements, vibrational spectroscopy and surface complexation modeling. *Journal of Colloid and Interface Science*, 234, p. 204-216.

Gupta, S. K. and Chen, K. C. (1978). Arsenic removal by adsorption. *Journal of Water Pollution Control Federation*, 50, p. 493-506.

Helz, G. R.;Tossel, J. A.;Charnock, J. M.;Pattrick, R. A. D.;Vaughan, D. J. and Garner, C. D. (1995). Oligomerization in As(III) sulfide solutions: Theoretical constraints and spectroscopy evidence. *Geochimica et Cosmochimica Acta*, 59, p. 4591-4604.

Kaur, P. and Rosen, B. P. (1992). Plasmid-Encoded Resistance to Arsenic and Antimony. *Plasmid*, 27, p. 29-40.

Knowles, F. C. and Benson, A. A. (1983). The biochemistry of arsenic. *TIBS*, 8, p. 178-179.

Koester, A. M.;Calaminici, P.;Gómez, Z. and Reveles, U. (2002a). Density Functional Theory Calculation of Transition Metal Clusters. In: Sen, K. *"Reviews of Modern Quantum Chemistry, A Celebration of the Contribution of Robert G. Parr"*. World Scientific Publishing Co: p.

Koester, A. M.;Flores, R.;Geudtner, G.;Goursot, A.;Heine, T.;Patchkovskii, S.;Reveles, U.;Vela, A. and Salahub, D. (2002b). deMon Software.

Koster, A. M.;Reveles, J. U. and del Campo, J. M. (2004). Calculation of exchange-correlation potentials with auxiliary function densities. *Journal of Chemical Physics*, 121, p. 3417-3424.

Krack, M. and Koster, A. M. (1998). An adaptive numerical integrator for molecular integrals. *Journal of Chemical Physics*, 108, p. 3226-3234.

Kumaresan, M. and Riyazuddin, P. (2001). Overview of speciation chemistry of arsenic. *Current Science*, 80, p. 837-846.

Ladeira, A. C. Q. and Ciminelli, V. S. T. (2004). Adsorption and desorption of arsenic on an oxisol and its constituents. *Water Research*, 38, p. 2087-2094.

Mandal, B. K. and Suzuki, K. T. (2002). Arsenic Round the World: a Review. *Talanta*, 58, p. 201-235.

Oliveira, A. F.;Ladeira, A. C. Q.;Ciminelli, V. S. T.;Heine, T. and Duarte, H. A. (2006). Structural model of arsenic(III) adsorbed on gibbsite based on DFT calculations. *Journal of Molecular Structure-Theochem*, 762, p. 17-23.

Perdew, J. P. (1986a). Density-functional approximation for the correlation-energy of the inhomogeneous electron-gas. *Phys. Rev. B*, 33, p. 8822-8824.

Perdew, J. P. (1986b). Erratum: Density-functional approximation for the correlation-energy of the inhomogeneous electron-gas. *Phys. Rev. B*, 34, p. 7404E.

Ramaswami, A.;Tawachsupa, S. and Isleyen, M. (2001). Batch-Mixed Iron Treatment of High Arsenic Waters. *Wat. Res.*, 35, p. 4474-4479.

Schlegel, H. B. (1987). Optimization of equilibrium geometries and transition structures. In: Lawley, K. P. *Ab-Initio Methods in Quantum Chemistry-I*. Wiley & Sons: p. 249-286.

Susi, H.;Byler, D. M. and Gerasimowiscz, W. V. (1983). Vibrational analisis of aminoacids: cysteine, serine, β-chloroalanine. *Journal of molecular structure*, 102, p. 63-79.

Teixeira, M. C. and Ciminelli, V. S. T. (2005). Development of a Biosorbent for Arsenite: Structural Modelling Based on X-Ray Spectroscopy (XAS). *Environmental Science and Technology*, 39, p. 895-900.

Tossel, J. A. (1997). Theoretical studies on arsenic oxide and hydroxide species in minerals and in aqueous solution. *Geochimica et Cosmochimica Acta*, 61, p. 1613-1623.

Trentelman, K.;Stodulski, L. and Pavlosky, M. (1996). Characterization of pararealgar and other light-induced transformation products from realgar by Raman microspectroscopy. *Analytical Chemistry*, 68, p. 1755-1761.

Yu, N. T.;DeNagel, D. C.;Pruett, P. L. and J.F. Kuck, J. (1985). Disulfide bond formation in the eye lens. *Proc. Natl. Acad. Sci USA Biochemistry*, 82, p. 7965-7968.

Capítulo 5

Considerações Finais

5.1 CONCLUSÕES

Foi demonstrado que biomassa obtida a partir da trituração de penas de galinha é eficiente e seletiva na remoção do arsênio em sua forma trivalente. A adsorção do As (III) ocorre de maneira quase imediata, sem alteração de pH, sendo necessários menos de 10 minutos para que o sistema atinja o equilíbrio.

A capacidade de adsorção da biomassa é inversamente proporcional ao pH da solução. A biomassa adsorve mais eficientemente as espécies neutras do arsenito, corroborando a hipótese de que o mecanismo de adsorção de arsênio por biomassa rica em proteínas fibrosas não pode ser creditado à ocorrência de interações eletrostáticas entre as espécies arsenicais e a superfície da biomassa.

Ainda no capítulo 2, os resultados da Espectroscopia de Absorção de Raios X (XANES e EXAFS) do complexo de adsorção obtido em pH 5,0 confirmaram que o As é adsorvido em seu estado trivalente e que são necessários aproximadamente três átomos de enxofre para promover a adsorção de cada átomo de arsênio trivalente. Foi observado ainda que a distância interatômica As-S é de aproximadamente 2,26 Å para os complexos de adsorção obtidos em pH ácido.

Foi observado que a estrutura molecular do complexo de adsorção As (III)/Biomassa varia em função do pH. Em pH ácido ou neutro o As (III) complexa diretamente com os átomos de enxofre da biomassa. A primeira camada de coordenação do As sofre uma alteração estrutural confirmada pelos valores de distância interatômica observados experimentalmente. Os grupamentos hidroxila da estrutura do arsenito são substituídos pelos átomos de enxofre da biomassa, com a liberação simultânea de três moléculas de água. Em pH básico, a espécie de As (III) negativamente carregada conserva parcialmente a estrutura da sua primeira esfera de coordenação e é adsorvida como um oxi-ânion. A estrutura molecular do complexo de adsorção formado em pH 10,5 é completamente diferente e apresenta-se desordenada. Na primeira esfera de coordenação do As tem-se a substituição de um único átomo de O. A proporção As (III)/S é de 1:1, e a distância entre eles é aumentada, passando a aproximadamente 2,3 Å. Além disso, parte do arsênio presente no sistema sofre oxidação. O fato de que em pH 10,5 as espécies arsenicais apresentam-se negativamente carregadas e

parcialmente oxidadas explica a diminuição na eficiência da adsorção observada anteriormente para valores de pH elevados.

Os cálculos baseados na Teoria DFT confirmaram os dados experimentais discutidos nos Capítulos 2 e 3. Os valores calculados para as distâncias interatômicas As (III)/S nos complexos de adsorção obtidos simulando-se diferentes condições de pH são bastante próximos daqueles obtidos experimentalmente. As diferenças são creditadas às limitações do modelo teórico.

Os dados de Espectroscopia Vibracional Raman e das predições teóricas baseadas em DFT, obtidos até o momento, possibilitaram a caracterização estrutural tanto da biomassa quanto dos complexos de adsorção obtidos em pH ácido. Os grupos vibracionais característicos das proteínas estruturais foram identificados nas amostras analisadas. Além disso, foi possível também observar os modos de vibração dos grupamentos químicos característicos das estruturas das queratinas e em particular, das β-queratinas das aves.

As pontes dissulfeto (S-S) presentes na estrutura da biomassa em seu estado natural assumem duas conformações estruturais distintas, *gauche-gauche-trans (g-g-t-)* e *gauche-gauche-gauche* (*g-g-g*), sendo esta segunda, a conformação predominante. Após os processos de pré-tratamento da biomassa e adsorção de arsênio, observou-se um consumo das pontes dissulfeto, evidenciado pela diminuição da intensidade do sinal correspondente ao modo vibracional da ligação S-S do tipo *g-g-g*. Considerando-se esse dado e os resultados das análises de EXAFS discutidas anteriormente pode-se concluir que os átomos de enxofre presentes na estrutura da biomassa rica em queratina participam ativamente da reação de complexação do arsênio trivalente. Além disso, pode-se perceber também que apenas um tipo específico de ponte dissulfeto (*g-g-g*) é consumido durante o processo. Simultaneamente à diminuição da intensidade do sinal das bandas Raman referentes aos modos vibracionais de estiramento da ligação S-S observou-se o surgimento de outras bandas cujas freqüências estavam localizadas na região onde são observados os modos vibracionais do estiramento das ligações entre o arsênio e o enxofre. Os cálculos de predição teórica DFT foram empregados no sentido de validar os dados experimentais obtidos e os resultados foram coincidentes.

O mecanismo de adsorção de arsenito em biomassa animal rica em queratina em pH neutro ou ácido pode ser resumido da seguinte maneira: a molécula neutra do arsenito interage com três átomos de enxofre de três resíduos de cisteína, após a redução das pontes dissulfeto do tipo *g-g-g* presentes na estrutura da queratina. Durante a interação os três grupamentos hidroxila da molécula do oxi-ânion arsenito são substituídos por três átomos de enxofre. Simultaneamente, os três prótons H^+ liberados dos grupamentos sulfidrila da biomassa reagem com as três hidroxilas liberadas do oxi-ânion, formando três moléculas de água, evitando alterações de pH do sistema. Os três átomos de enxofre se organizam em torno do átomo de arsênio formando uma estrutura trigonal piramidal regular, na qual a distância entre os átomos de As e S é de aproximadamente 2,3 Å.

5.2 CONTRIBUIÇÕES ESPECÍFICAS DESTE TRABALHO

Este trabalho de Tese apresenta a particularidade de ter sido embasado nos conhecimentos clássicos de Bioquímica, Química, Física e Metalurgia bem como em dados recentemente publicados sobre a toxicologia dos compostos arsenicais e a remediação de problemas ambientais causados por este elemento. Durante a realização desta Tese a adsorção de arsenito na biomassa selecionada foi avaliada experimentalmente tanto do ponto de vista macro quanto microscópico. Aos resultados experimentais somaram-se os resultados dos cálculos de predição teórica das estruturas dos complexos de adsorção. A estrutura molecular dos complexos As/S foi elucidada com o emprego de técnicas espectroscópicas clássicas e modernas, bastante sensíveis e precisas. Como contribuições específicas deste trabalho podem ser consideradas:

- O uso de material biológico de origem animal como suporte para a adsorção dos ânions arsenicais. Geralmente os materiais utilizados como biossorventes têm origem vegetal ou microbiana.

- O desenvolvimento de um biossorvente específico para os íons de arsênio trivalente capaz de removê-los mais eficientemente em pH neutro ou ácido. Esse fato é interessante, visto que o pH natural dos efluentes contaminados com arsênio é, em geral, ácido.

- Até onde se tem conhecimento, essa é a primeira vez que se propõe o emprego de um biossorvente efetivo na remoção do As (III) que ao mesmo tempo rejeita os ânions arsenato e os tradicionais íons competidores, como o fosfato. Além disso, o processo de adsorção de arsênio aqui proposto dispensa a etapa de oxidação do arsenito a arsenato usualmente necessária para garantir a eficiência de sua remoção.

- A elucidação da estrutura molecular do complexo formado entre o As e o S, por meio do emprego das técnicas de Espectroscopia de Absorção de Raios-X e de Espectroscopia Vibracional, nos permitiu identificar os grupamentos ativos do adsorvente e propor um mecanismo de adsorção de arsênio muito particular, no qual o arsenito é adsorvido como o íon As^{3+} e não como o oxi-ânion $As(OH)_3$.

5.3 PERSPECTIVAS DE TRABALHOS FUTUROS

- Avançar na utilização dos conhecimentos adquiridos para a produção de um biossorvente ou biosensor.

- Avaliar mais detalhadamente a adsorção de arsenito em meio básico e a sua complexação com cisteína por intermédio de Espectroscopia de Absorção de Raios-X (XAS) e Espectroscopia Raman.

- Avaliar a capacidade de adsorção de arsênio de outros materiais biológicos ricos em queratina e compará-las aos dados aqui obtidos.

- Comparar a toxicidade e a bioacumulação dos sais de arsênio trivalente e dos complexos de As (III)/cysteína através de estudos biológicos *in vivo*. Avaliar a distribuição dos compostos resultantes das reações de detoxificação do arsênio nos diferentes órgãos e tecidos corporais por meio de XAS e espectroscopia Raman.

- Avaliar a possibilidade de emprego dos sais de arsênio trivalente e dos complexos de As (III)/cysteína no tratamento da Tripanossomíase e da Leishmaniose experimentais usando como modelo o cão.

5.4 PRODUÇÃO CIENTÍFICA GERADA A PARTIR DO PRESENTE TRABALHO DE TESE

Trabalhos publicados em periódicos internacionais:

Teixeira, M.C. and Ciminelli, V.S.T. Development of a Biosorbent for Arsenite: Structural Modeling Based on X-Ray Spectroscopy (XAS). Environ. Sci. Technol. 2005, 39, 895-900

Teixeira, M.C.; Ciminelli, V.S.T.; Dantas, M.S.S.; Diniz, S. F.; Duarte, H. A. Raman Spectroscopy and DFT calculations of As (III) Complexation with a Cysteine-rich biomaterial. Aceito para publicação: Journal of Colloid Interface Science em junho de 2007.

Trabalhos publicados em periódicos nacionais:

TEIXEIRA, Mônica Cristina; DUARTE, Graziele; CIMINELLI, Virgínia Sampaio Teixeira. Arsenic Biosorption Mechanism - A X-Ray Spectroscopy Study. Activity Report 2002 Brazillian Synchrotron Light Laboratory, Campinas - SP, p. 115-116, 2003.

Trabalhos apresentados em eventos internacionais

TEIXEIRA, Mônica Cristina; DUARTE, Graziele; CIMINELLI, Virgínia Sampaio Teixeira. Structural modelling of arsenic biosorption using X-ray spectroscopy (XAS). In: 15TH INTERNATIONAL BIOHYDROMETALLURGY SYMPOSIUM, 2003, Atenas. 15th International Biohydrometallurgy Symposium - Symposium Proceedings. 2003.

Trabalhos apresentados em eventos nacionais

TEIXEIRA, Mônica Cristina; DUARTE, Graziele; CIMINELLI, Virgínia Sampaio Teixeira. Uso de biomassa animal rica em proteínas fibrosas como biossorvente para remoção de arsênio trivalente. In: ENCONTRO NACIONAL DE TRATAMENTO DE MINÉRIOS E METALURGIA EXTRATIVA XX ENTMME, 2004, Florianópolis. Encontro Nacional de Tratamento de Minérios e Metalurgia Extrativa XX ENTMME. 2004. p. 451-458.

TEIXEIRA, Mônica Cristina; DUARTE, Graziele; CIMINELLI, Virgínia Sampaio Teixeira. Arsenic sorption onto proteic biomass - a X-Ray approach. In: XIV REUNIÃO ANUAL DE USUÁRIOS DO LNLS, 2004, Campinas. XIV Reunião Anual de Usuários do LNLS. 2004. v. 1, p. 93-93.

ANEXOS

ANEXO 1

Balanço de massa do íon metálico no sistema SAM (Pagnaneli *et al*., 2000).

$$v_1 C_0 + q_{i-1} X_{i-1} (V_{i-1} - u) + (V_{i-1} - u) C_{i-1} = C_i V_i + q_i X_i V_i$$

(*i*) e (*i-1*) – referentes à etapa de adição do metal

(C_0) – concentração da solução de metal adicionada

(*v*) – volume de solução de metal adicionada

(*V*) – volume total da suspensão

(*u*) – Volume de alíquota retirada para análise

(*X*) – concentração de biomassa

(*q*) – carregamento específico para o metal

ANEXO 2

Ajuste dos dados da Figura 4.4 – Modelo Lorentz, Programa Origin 5.0

Pena Natural		Pico 1	Pico 2
	Centro	507.8±0.1	524.0±0.2
	Largura	18.0±0.3	21.0±0.4
	Intensidade	1821±42	1419±44
χ^2	3.13177		
Pena + As (III)		Pico 1	Pico2
	Centro	507.1±0.2	522±0.4
	Largura	14.9±0.7	27±1
	Intensidade	658±54	1648±89
χ^2	3.66355		

ANEXO 3

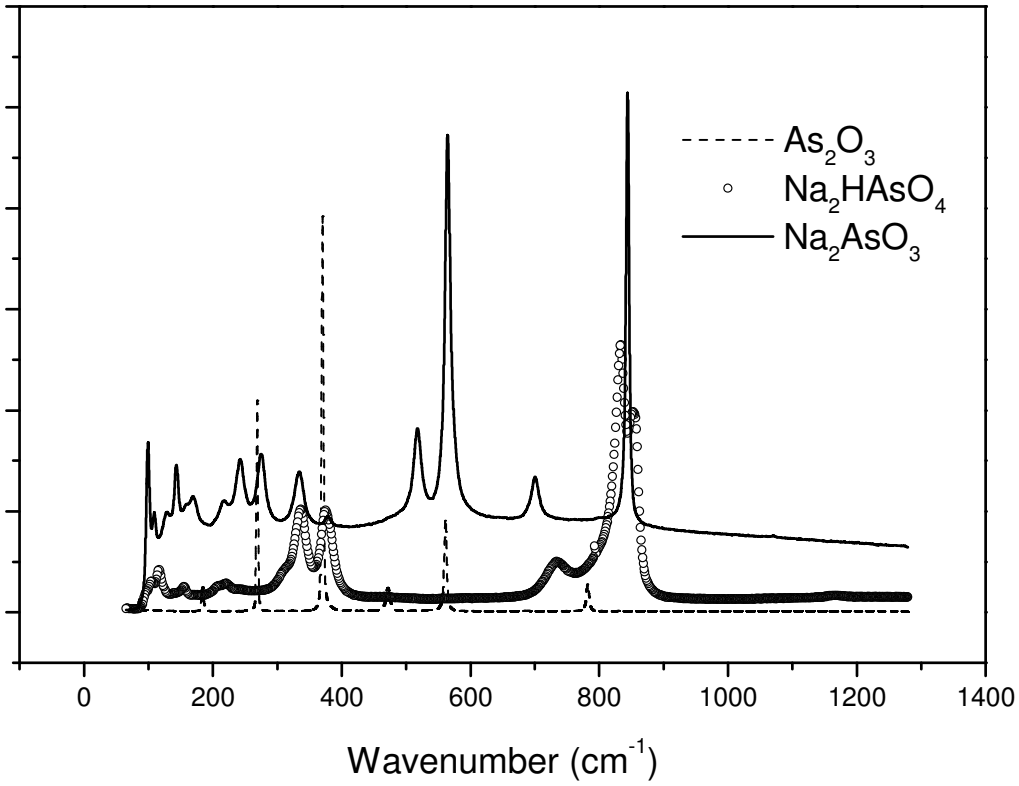

Espectros Raman dos padrões de Arsênio

UNIVERSIDADE FEDERAL DE MINAS GERAIS

Curso de Pós-Graduação em Engenharia Metalúrgica e de Materiais

Tese de doutorado

"Mecanismo de Biossorção Seletiva de Arsênio (III) em Rejeitos Ricos em Proteínas Fibrosas"

"Mechanism of selective As (III) biosorption onto fibrous protein rich waste material"

Autor: Mônica Cristina Teixeira

Orientador: Profa. Virgínia Sampaio Teixeira Ciminelli

Setembro/2004

Atualizada em junho de 2007

UNIVERSIDADE FEDERAL DE MINAS GERAIS

Curso de Pós-Graduação em Engenharia Metalúrgica e de Materiais

Mônica Cristina Teixeira

Mecanismo de Biossorção Seletiva de Arsênio (III) em Rejeitos Ricos em Proteínas Fibrosas

"Mechanism of selective As (III) biosorption onto fibrous protein rich waste material"

Tese de doutorado apresentada ao Curso de Pós-Graduação em Engenharia Metalúrgica e de Minas da Universidade Federal de Minas Gerais

Área de concentração: Tecnologia Mineral

Orientador: Profa. Virgínia Sampaio Teixeira Ciminelli

Belo Horizonte

Escola de Engenharia da UFMG

2004

AGRADECIMENTOS

Ao dar por encerrado este trabalho, percebo-o, felizmente, ainda não concluído. Finalizou-se uma etapa à qual me dediquei nos últimos anos, mas tratasse apenas disso, uma dentre as muitas etapas de um processo contínuo, duradouro, e talvez perpétuo, da minha busca pelo conhecimento. Costumo dizer que sou movida pela insatisfação e pela curiosidade e gostaria de agradecer a todos que, de alguma maneira, me estimularam com sua inquietação ou me presentearam com seus ensinamentos.

Gostaria de agradecer à minha orientadora, Prof[a] Virgínia Ciminelli pelas discussões estimulantes que tivemos durante todas as fazes deste trabalho e pela sua coragem em assumir comigo os riscos ao enveredarmos por caminhos tão desconhecidos. Gostaria também de agradecer aos grandes professores que conheci ao longo dos anos. Ainda no tempo do colégio, tive o inesquecível prazer de conhecer o mundo através das aulas do Irmão Cristino; só agora percebo o quanto a sua influência foi marcante. Agradeço também aos professores Rogelio L. Brandão, Oswaldo Garcia Jr. e Jacques R. Nicoli que me acompanharam e muito me estimularam durante os primeiros anos de minha vida acadêmica.

Ao grupo de pesquisa do Laboratório de Processamento Aquoso, agradeço muitíssimo pelo fato de terem me recebido tão prontamente, sem nenhum tipo de restrição ou preconceito. Agradeço em particular aos funcionários Ilda e João pela agradável convivência; à primeira, pelo seu bom-humor aparentemente indestrutível, ao segundo, pela disposição em me "socorrer" sempre prontamente. Durante os anos em que estive fazendo parte deste grupo, pude conviver com vários colegas, alunos de graduação e pós-graduação e pesquisadores dos quais me recordarei sempre com carinho. Gostaria de agradecer especialmente ao Ricardo, ao Cláudio e à minha querida Graziele. Com Cláudia e Versiane pude compartilhar de todas as angústias comuns aos alunos de Doutorado visto que estávamos todos na mesma barca. A eles agradeço muito o apoio diário e a troca de opiniões e experiências. Ana Cláudia e Anderson, já mais "evoluídos" foram como irmãos mais velhos, academicamente falando. Procurei aprender com todos eles, calmamente, através da observação diária, da mesma maneira

que se faz na convivência em família. Nos últimos meses recebemos novos membros em nosso grupo e a elas dedico um agradecimento especial. Apesar dos desafios de uma área distinta da sua área de atuação, a professora Maria Sylvia demonstrou uma disposição tão jovial em continuar a aprender e a nos ensinar que me cativou. Christina, muito obrigada pela sua disposição em ajudar sempre, com a maior eficiência.

Aos funcionários do laboratório de Análises Químicas, principalmente ao Sandro e à Olívia peço desculpas pelo volume de análises e pela minha ansiedade em receber os resultados em algumas ocasiões e agradeço muitíssimo, pois, sem sombra de dúvidas, este trabalho não teria sido concluído sem sua ativa e confiável participação. Agradeço a todos os demais professores e funcionários do Departamento de Metalurgia pela acolhida.

Gostaria ainda de agradecer ao Prof. Hélio Anderson e a toda sua equipe pela execução dos cálculos de predição teórica e pelas sugestões interessantes que muito contribuíram para o enriquecimento deste trabalho e ainda à Maria do Carmo Alves pelo auxílio no tratamento dos dados da Espectroscopia de Absorção de Raios-X.

Agradeço à Capes, à Universidade Federal de Ouro Preto, ao Instituto do Milênio-Água uma Visão Mineral e ao CNPq pelo apoio financeiro. Agradeço ainda à Universidade Federal de Minas Gerais e ao Laboratório Nacional de Luz Síncrotron pelo uso de suas instalações.

Agradeço aos meus colegas do Departamento de Farmácia da UFOP pelo apoio. Em particular agradeço a minhas parceiras na BR 040, Andréa, Neila e Dênia, pelo seu companheirismo.

À minha mãe e meu irmão agradeço pelo seu interesse e presença constantes e pelo estímulo nas horas em que mais precisei. Sem eles e sem o apoio, a generosidade e a compreensão de meus filhos, cujas gestações ocorreram por entre salas de aulas e bancadas de laboratórios, e do meu marido, que foi sempre o meu melhor interlocutor, nada disso teria sido possível.

“Não, mil vezes não, não existe uma categoria de ciência à qual alguém possa dar o nome de ciência aplicada. Existem a ciência e as aplicações da ciência, unidas, tal qual a fruta e a árvore que a sustenta”.

Pasteur, 1871.

Dedico este trabalho aos meus filhos e ao meu marido.

SUMÁRIO

LISTA DE FIGURAS

LISTA DE TABELAS

RESUMO

No presente trabalho uma nova abordagem para o tratamento de aguas contaminadas com arsênio é proposta. Tal metodologia se fundamenta nos mecanismos bioquímicos e toxicológicos que explicam a toxicidade do arsênio e envolve a utilização de uma biomassa residual abundante e rica em cisteína para a remoção seletiva de As (III). A esécie trivalente do arsênio é considerada a mais móvel e hidrossolúvel dentre as espécies de As hidrossolúveis.

No estudo em questão, além da seleção do material biosorvente, pó de penas de galinha, a eficiência do material escolhido foi avaliada sob diferentes condições experimentais. Foram avaliados o processamento do biosorvente, a razão sólido/líquido ideal, o pH (2-10) e o efeito da presença de íons competidores (fosfato e As (V)). Os resultados experimentais demonstraram que o material selecionado é altamente seletivo para as espécies trivalentes de As independentemente da presença de íons competidores. A máxima capacidade de remoção observada (170 μmolAs/g biomassa) foi obtida em sistema com pH ácido. Tais dados podem ser explicados por um mecanismo de adsorção muito particular proposto a partir das análises das estruturas dos complexos de adsorção por meio de Espectroscopia de Absorção de Raios-X – XAS (EXAFS e XANES) e Espectroscopia Raman, combinadas ao modelamento teórico estrutural obtido por meio de Cálculos de Densidadade Funcional Teórica (DFT).

Os dados de XAS indicaram que a complexação do As com os resíduos de cisteína do biosorvente se dá por meio de uma interação "*inner sphere*" dos átomos de As (III) com os átomos de S da biomassa. A estrutura do complexo de adsorção apresenta geometria trigonal piramidal com uma proporção As/S de 1:3 e distância interatômica de, aproximadamente, 2.24-2.26 A. Durante a complexação são liberadas três moléculas de água produzidas a partir da reação dos grupamentos OH da espécie arsenical neutra $As(OH)_3$, que predomina em valores de pH inferiores a 9, com o átomo de hidrogênio do grupamento SH do aminoácido. À medida que o pH aumenta para 10,5 a espécie $As(OH)_3$ sofre desprotonação e a capacidade adsortiva da biomassa é reduzida para 30% daquela obtida em sistema com pH ácido. As análises dos complexos de adsorção obtidos em condições de alcalinidade apontaram para a ocorrência oxidação parcial do As (III) associada a formação de um complexo de adsorção mais desordenado. Sob tais

condições, o arsenito é adsorvido como um oxi-ânion sendo que apenas 1 átomo de oxigênio é substituído pelo enxofre gerando um complexo de adorção com proporção As/S de 1:1. Neste caso, a distância interatômica aumenta para 2.31 Å. Por meio da espectroscopia Raman, pode-se obter ainda diuas importantes informações: (i) a estrutura β pregueada da queratina é a principal estrutura secundária da biomassa empregada e (ii) foi comprovada a participação dos átomos de S da cisteína na adsorção de As visto que, durante o processo de adsorção, a intensidade do modos vibracionais atribuídos às ligações As-S aumentava á medida que diminuíam as intensidades daqueles relacionados às ligações S-S. Os dados de modelamento teórico fornecidos pelos cálculos de DFT corroboram estes dados de espectroscopia XAS e Raman.

Os resultados obtidos neste trabalho confirmaram a hipótese inicial de que uma biomassa rica em cisteína poderia ser capaz de adsorver seletivamente as espécies trivalentes de arsênio e fornecendo subsídios para o desenvolvimento de um biosorvente para remoção de As (III) de águas contaminadas.

ABSTRACT

Based on biochemical and toxicological fundamentals that explain arsenic toxicity, a novel approach for the treatment of arsenic-containing waters was developed. The approach involved the use of an abundant cysteine-rich waste biomass for the selective removal of As (III) from waters. The trivalent species is considered the most mobile and toxic hydrosoluble arsenic species.

Following the selection of the waste biomass for the present investigations - chicken feathers - the material was evaluated under different conditions of sorbent preparation and S/L ratio, pH (2-10.5) and the presence of competitor ions (phosphate and As (V)). The experiments demonstrated that the biomass is highly selective for the As (III) species – with no significant effect of the studied competitor ions on adsorption capacity– and the maximum uptake (170 μmolAs/g biomass) is obtained under acidic conditions. These findings were explained by a unique adsorption mechanism based on the results obtained by the combination of two experimental techniques, X- ray Absorption spectroscopy (EXAFS and XANES) and RAMAN spectroscopy, with theoretical modeling by Density Functional Theory - DFT calculations.

XAS measurements indicated inner-sphere complexation of As (III) by the biomass'sulfur atoms. The adsorption structure was represented by a trigonal, pyramidal geometry, with an As/S ratio of 1:3 and an As-S interatomic distance of approximately 2.24-2.26 A. Arsenic uptake leads to the release of 3 water molecules produced by the reaction of the OH groups in the neutral $As(OH)_3$ species, which predominates under pH <9 , with the hydrogen of the biomass' SH group. As pH is increased to 10.5, the $As(OH)_3$ species depronates while uptake is reduced to approximately 30% of that obtained under acid conditions. The analyses of the surface complexes formed at pH 10.5 pointed to a partial oxidation of the monovalent As (III) anion associated with the occurrence of a less ordered surface complex. Under those conditions, arsenite is adsorbed as an oxy-anion, with only one oxygen being replaced by sulfur, i.e. As/S ratio of 1:1. The As-S interatomic distance is increased to 2.31 Å. By using Raman Spectroscopy it was possible to obtain two main informations: (i) the β-sheet structure was identified as the main secondary structure of the keratin biomass and (ii) the involvement of cysteine sulfur atoms during As (III) complexation was clearly indicated

by the vibrational modes of As-S bands combined with the reduction of other bands assigned to S-S bonds. The theoretical modeling provided by DFT calculations has corroborated the conclusions obtained by XAS and RAMAN spectroscopy.

The results obtained in the present work confirmed the initial hypothesis that a cysteine-rich biomass would be capable of adsorb the trivalent arsenic species, and provide the fundamentals for the development of a selective biosorbent for As (III) removal from contaminated waters.

Capítulo 1

Introdução e Objetivos do Trabalho

1.1 INTRODUÇÃO

O arsênio é amplamente distribuído na crosta terrestre, embora quase sempre presente em baixas concentrações. A arsenopirita é o mineral de arsênio mais abundante e ocorre associado a minerais de estanho e tungstênio, bem como à prata, ao cobre e ao ouro. Observam-se ainda associações com sulfetos de chumbo, zinco e ferro: galena-PbS, esfalerita-ZnS e pirita-FeS_2, respectivamente. A concentração de arsênio no solo pode variar na faixa de 0.1 até mais de 1000 ppm. Industrialmente, o As é empregado na manufatura de ligas de zinco, corantes e inseticidas. Combinado ao gálio, na forma de AsGa, é empregado na produção de semi-condutores e componentes de lasers para indústria eletrônica.

A despeito de sua utilidade, o As é extremamente nocivo à saúde, sendo considerados tóxicos quase todos os seus compostos. A inalação de arsênio pode causar principalmente carcinomas de pulmão. Uma vez ingerido, produz sintomas de irritação gastro-intestinal e náuseas. A longo prazo, a ingestão continuada ainda que de pequenas quantidades deste elemento, leva a manifestações crônicas cutâneas, doenças do aparelho respiratório, diabetes, distúrbios vasculares, neurológicos e câncer.

A contaminação ambiental por metais pesados tem sido objeto de diversas discussões, embora, poucas estejam voltadas para o estudo dos mecanismos bioquímicos que lhes conferem importância do ponto de vista toxicológico. As águas residuais das indústrias de mineração e metalurgia são consideradas como as principais fontes de contaminação ambiental por metais pesados como o arsênio. Além destas, níveis de arsênio relativamente altos são encontrados ocasionalmente em fontes de água de abastecimento municipais superficiais e subterrâneas, possivelmente devido à lixiviação de minerais associados aos depósitos minerais. Em vista disso, torna-se necessário o desenvolvimento de metodologias eficientes e economicamente viáveis para a remoção desse elemento. Garantir a qualidade da água de consumo, no que diz respeito aos teores de arsênio e demais metais pesados é, portanto, condição necessária à manutenção da saúde das

populações. Neste contexto, os métodos biológicos surgem como uma alternativa aos métodos convencionais.

Embora já tenham sido desenvolvidos diversos trabalhos de pesquisa abordando a bioacumulação e a oxidação bacteriana do As, com alguns resultados promissores, os relatos científicos a respeito da biossorção desse metal são praticamente inexistentes. Na verdade, observa-se uma lacuna na literatura no que se refere a biossorção de ânions de um modo geral e, em particular, dos ânions arsenicais. Fundamentados nos mecanismos bioquímicos que justificam os efeitos tóxicos das espécies arsenato e arsenito, este projeto vem avaliar a utilização de biomassas animais, ricas em proteínas fibrosas, como biossorventes para espécies hidrossolúveis de arsênio.

1.1.1 O Arsênio e os metais pesados

"Metais pesados" são metais com densidade acima de 5,0 g/cm^3. Dentre os 90 elementos de origem natural, temos 53 metais pesados, incluindo-se o As (Nies, 1999). Segundo o mesmo autor, a maioria dos metais pesados pertence ao grupo dos elementos de transição com orbitais incompletos. Estes orbitais incompletos geram cátions de metais pesados, fortes o suficiente para reagir e formar complexos. Em função disso, quantidades-traço desses elementos são extremamente importantes na manutenção das reações metabólicas de todas as células vivas e são indispensáveis, em baixíssimas concentrações. Em concentrações mais elevadas, entretanto, os metais pesados formam complexos inespecíficos nas células provocando efeitos tóxicos. Assim como outros metais pesados, o arsênio (As) passou recentemente a ser classificado como um dos mais novos elementos essenciais. Uma pequena ingestão de As é necessária à dieta humana. Parece que, de alguma maneira ainda não esclarecida, o As interfere no metabolismo do ferro. A ingestão diária de As na dieta recomendada ainda permanece indeterminada; sabe-se, entretanto, que no corpo humano adulto, existem cerca de 1-2 mg de As (Case *et al.*, 1983)

1.1.2 Farmacologia e Toxicologia do arsênio

A toxicologia reconhece de longa data a influência do estado de valência de um elemento sobre o seu comportamento no corpo humano. A distribuição das espécies arsenicais é essencial para se avaliar corretamente a sua toxicidade. No que diz respeito à especiação do As, a forma trivalente As_2O_3, é tida como altamente tóxica e vem sendo utilizada como veneno desde as eras mais remotas (Gupta *et al.*, 1978; Case *et al.*, 1983; Knowles *et al.*, 1983; Kaur *et al.*, 1992; Wood, 1992; Chiu *et al.*, 1994; Ramaswami *et al.*, 2001; Hughes, 2002). Em regiões da China com alta incidência de uma doença vascular periférica conhecida como "Black Foot Disease", uma manifestação resultante da contaminação por As, a relação As (III)/As (V) é de 9:1. Por outro lado, nos Estados Unidos, a comunidade de Fallon (NV) vem consumindo, desde 1941, água contaminada com níveis de As de 100 μg/L sem que se observem efeitos adversos à saúde da população. Foi confirmado, entretanto, que, nessa região, a forma pentavalente do As é predominante (Chiu *et al.*, 1994).

A forma trivalente do As é dez vezes mais tóxica que sua forma pentavalente e ainda apresenta uma mobilidade no meio ambiente significativamente maior (Rawlins *et al.*, 1997) sendo, portanto, potencialmente mais perigosa.

A ação cancerígena do arsênio é reconhecida desde o século XIX. Já no início do século XX, vários artigos haviam sido publicados relatando casos de neoplasias, dermatoses e irritações das vias aéreas superiores em pacientes trabalhadores de indústrias produtoras de compostos arsenicais ou usuários de medicamentos à base de arsênio (Gontijo, 1980). Na mesma época, sais orgânicos de arsênio trivalente começaram a ser utilizados no tratamento da sífilis na forma do medicamento Salvarsan®. Com o advento da penicilina, os medicamentos arsenicais foram rapidamente abandonados, antes que sua atividade bioquímica fosse completamente elucidada. O arsênio foi e ainda continua sendo utilizado como agente terapêutico, embora seu emprego seja feito hoje com muito mais rigor. Como exemplo da utilização recente de sais deste elemento podemos citar o uso do trióxido de

arsênio (As_2O_3) e do óxido de fenilarsina, que apresentam efeitos comprovados no tratamento da leucemia promielocítica aguda (Estrov *et al.*, 1999).

Tanto a atividade farmacológica quanto a atividade toxicológica do arsênio são baseadas em mecanismos similares. Os cátions de metais pesados, especialmente aqueles com números atômicos elevados, por exemplo, Hg^{2+}, Cd^{2+}, and Ag^{2+} e também o As, tendem a se ligar a grupamentos sulfidrila (SH) dos compostos biológicos (Nies, 1999). Por meio dessas ligações, estes elementos podem causar a inibição da atividade das enzimas sensíveis, cujos grupamentos químicos essenciais presentes nos sítios ativos são exatamente os grupamentos sulfidrila (Knowles *et al.*, 1983; Kaur *et al.*, 1992; Rojas-Chapana *et al.*, 2000). No caso da sífilis, por exemplo, os compostos arsenicais orgânicos trivalentes atuavam bloqueando os grupos sulfidrila (SH), indispensáveis à respiração do treponema (*Treponema palidum*), agente causador da doença, (Gontijo, 1980). O mesmo mecanismo explica o emprego do arsênio com fins toxicológicos, como por exemplo, na fabricação de armas químicas. Durante a Primeira Guerra Mundial uma das armas químicas empregadas foi o Gás Lewisite, um composto orgânico de arsênio trivalente ($C_2H_2AsCl_3$) cuja ação tóxica se devia à inibição da enzima piruvato oxidase. Os efeitos tóxicos desse gás podiam ser revertidos pela administração de antídotos contendo grupamentos SH em sua estrutura. O primeiro antídoto efetivo contra intoxicação por arsênio trivalente sintetizado foi o *British Anti-Lewisite*, mais conhecido como BAL; trata-se do composto 2,3-dimercaptopropanol ($C_3H_8OS_2$) cuja reação com o As (III) produz um composto hidrossolúvel que pode ser excretado pela urina (Jones, 1983).

De maneira geral, cátions de metais pesados interagem com íons ditos fisiológicos, por exemplo, Cd^{2+} com Zn^{2+} ou Ca^{2+}, Ni^{2+} e Co^{2+} com Fe^{2+}, Zn^{2+} com Mg^{2+}, inibindo sua função. Os oxiânions de metais pesados interferem com o metabolismo dos íons não metálicos estruturalmente semelhantes (cromato com sulfato, arsenato com fosfato). O arsenato é, estruturalmente, muito semelhante ao fosfato (PO_4^{3-}) e assim, sua principal toxicidade resulta da interferência com o metabolismo deste maior bio-elemento, que é o fósforo (Nies, 1999). O arsenato compete com fosfato pelos sítios ativos das enzimas fosforilativas, comuns a todos os seres vivos e essenciais ao metabolismo da glicose,

causando bloqueio ou perda de produtividade em diversas rotas metabólicas, através da formação de compostos de carboidrato "arsenilados" ao invés dos intermediários fosfatados esperados. Do ponto de vista funcional, o efeito tóxico do arsenato, equivale à supressão do aporte nutricional de fosfato (Kaur *et al.*, 1992; Hughes, 2002).

Pode-se concluir, portanto, que o arsênio e os compostos arsenicais são tóxicos e carcinogênicos para todos os seres vivos. A dose de As letal para humanos é da ordem de 0,6 mg/kg/dia (http://risk.lsd.ornl.gov/tox/profiles/arsenic.shtml) ou de 1-3 mg/kg, em se tratando exclusivamente de As inorgânico (Hughes, 2002)

O consumo diário de água com concentrações de As superiores a 50 µg/L – menos que 1% da dose letal – pode acarretar problemas de pele, além de distúrbios dos sistemas circulatório e nervoso e da visão e audição. Se as concentrações de As atingirem níveis perigosamente superiores aos recomendados, cânceres, distúrbios nervosos e danos em diversos órgãos podem acontecer, sendo, geralmente, fatais. (Das, 1998; Matschullat *et al.*, 2000).

No que concerne à bioquímica do arsênio, sabe-se que o arsênio inorgânico ingerido é rapidamente absorvido pelo trato gastro-intestinal. O As absorvido é transportado através do sangue, ligado a grupamentos SH das proteínas ou compostos de baixo peso molecular como a glutationa e a cisteína (Figura 1.1) até os órgãos do corpo, principalmente o fígado, onde sofre reações de metilação que diminuem sua toxicidade. A metilação envolve a adição de grupamentos metila doados pela S-adenosilmetionina ao arsênio apenas em seu estado trivalente. A eficiência da metilação depende das taxas de redução do As (V) a As (III). Estudos *in vitro* utilizando hepatócitos isolados de ratos demonstraram que apenas o arsenito é rapidamente captado e metilado pelas células do tecido hepático (Lerman *et al.*, 1983). Tal especificidade pode ser explicada pelo fato de, nas condições de pH fisiológicas, apenas as espécies trivalentes do arsênio se encontrarem não ionizadas.

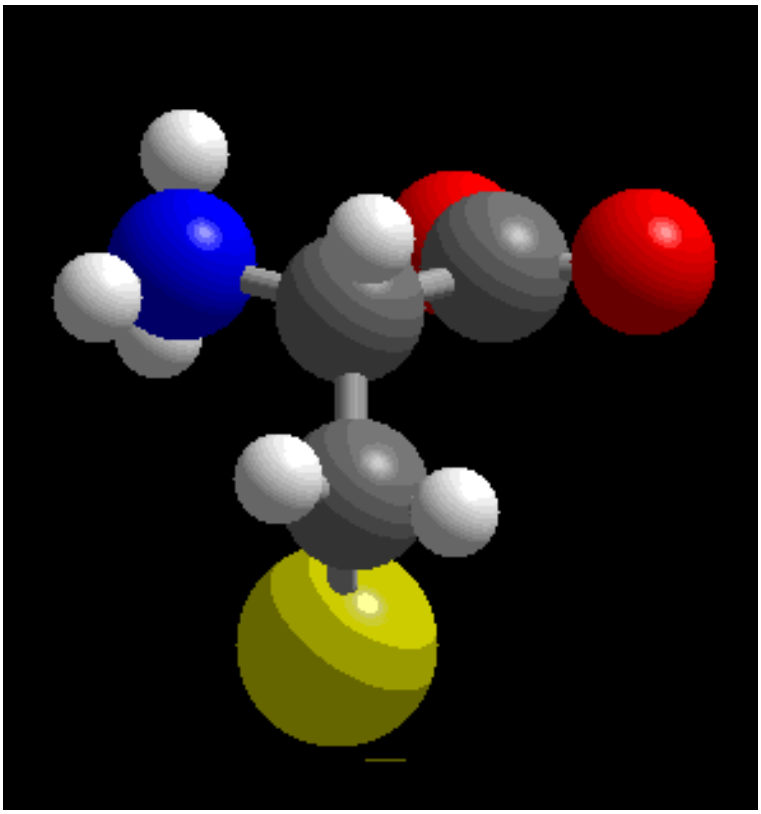

Figura 1.1. Estrutura do aminoácido cisteína (em cinza, C; em azul, N; em vermelho, O; em amarelo, S)

As etapas de redução do As e sua subseqüente metilação, esquematizadas a seguir (Hughes, 2002), produzem um composto final de arsênio oxidado, com toxicidade e mobilidade inferiores ao composto original.

$$As^{V}O(OH)_3 + 2e^- \rightarrow As^{III}(OH)_3 + CH_3^+ \rightarrow CH_3As^{V}O(OH)_2 + 2e^- \rightarrow CH_3As^{III}(OH)_2 + CH_3 \rightarrow (CH_3)_2As^{V}O(OH) + 2e^- \rightarrow (CH_3)_2As^{III}OH + CH_3^+ \rightarrow (CH_3)_3As^{V}O \quad (1.1)$$

A glutationa, bem como o ditiotreitol e a cisteína desempenham papel importante na redução da espécie pentavalente. A redução do As (V) a As (III) resulta no aumento da retenção desse elemento na maioria dos tecidos corporais porque a espécie trivalente é mais reativa com as proteínas dos tecidos corporais do que a espécie pentavalente (Bogdan *et al.*, 1994; Styblo *et al.*, 1995). Estudos experimentais com mamíferos expostos a arsênio inorgânico mostraram que os tecidos com a maior retenção de arsênio são a pele, unhas, os cabelos, o epitélio descamativo do trato gastro-intestinal superior (cavidade oral, língua, esôfago, paredes do estômago), o epidídimo, a tireóide, o esqueleto e as lentes oculares. Com exceção do esqueleto, todos os demais tecidos apresentam maior conteúdo de arsenito do que arsenato, logo após a ingestão simultânea de ambas as formas arsenicais. No caso do tecido ósseo, o arsenato parece substituir o fosfato presente nos cristais de apatita, em função de suas similaridades químicas. A ligação do arsênio trivalente com grupamentos tiólicos funcionais de enzimas pode causar inibição de enzimas importantes em rotas metabólicas essenciais. Entretanto, a mesma interação com sítios secundários de outras proteínas pode resultar na sua detoxificação (Hughes, 2002).

Com base em todas as evidências que relacionam a ocorrência de efeitos toxicológicos crônicos e a ingestão de água contaminada por As, vários órgãos governamentais de controle ambiental recomendaram a redução nos limites máximos admissíveis para As em água potável. A Organização Mundial da Saúde (OMS) recomendou, em 1993, que o limite de 50 μg/L fosse reduzido para 10 μg/L. No caso da Comunidade Européia e do Japão, estes novos valores foram adotados. No Canadá o limite é de 25 μg/L e nos Estados Unidos, após uma resistência inicial em adotar as recomendações da OMS em função dos

custos financeiros envolvidos (Smedley *et al.*, 2002), a legislação foi alterada. A agência de proteção ambiental dos Estados Unidos conseguiu que a recomendação da OMS fosse adotada a partir de outubro de 2001 embora venha a ser completamente implementada apenas a partir de 2006. A legislação ambiental brasileira também adotou a recomendação da OMS e os novos limites passaram a vigorar a partir de dezembro de 2003.

1.1.3 Origem da contaminação por arsênio

O As é encontrado na atmosfera, no solo, nas rochas, em águas naturais e, até mesmo, nos organismos vivos. Sua mobilização se deve a uma combinação de processos naturais, tais como variações climáticas, atividade biológica, atividade vulcânica, bem como atividades antropogênicas (Mandal *et al.*, 2002; Smedley *et al.*, 2002). O As ocorre naturalmente em mais de 200 diferentes formas minerais. Aproximadamente 60% delas são arsenatos, 20% apresentam-se como sulfetos ou sulfo-sais e os outros 20% incluem os arsenitos, arsenetos, óxidos, silicatos e arsênio elementar. O mineral de arsênio mais comum é a arsenopirita, FeAsS (Mandal *et al.*, 2002).

Na crosta terrestre, o As existe em quantidades que variam entre 1 mg /kg (em amostras de apatita, ilmenita, calcita, barita, fluorita) a 77.000-126.000 mg/kg (em amostras de pirita e arsenopirita) e de 0,3 a 8.000 mg /kg em rochas, sedimentos, solos e depósitos superficiais. Em solo não contaminado, a concentração normal de As é de 6 mg/kg (Manning *et al.*, 1997; Mandal *et al.*, 2002). Em ambientes aquáticos as concentrações podem variar de 0,02 (em ambientes marinhos) a mais de 850.000 μg/L (em drenagens ácidas de minas). É grave o fato de que alguns depósitos de água subterrânea de Bangladesh, Argentina, México, China, Índia, Taiwan e Hungria apresentem níveis de contaminação da ordem de 10-5000 μg/L (Smedley *et al.*, 2002). No Brasil, levantamentos recentes feitos por pesquisadores do nosso grupo (Matschullat *et al.*, 2000; Deschamps *et al.*, 2002) indicam a ocorrência de anomalias geológicas em regiões do Quadrilátero Ferrífero, próximas aos

municípios de Santa Bárbara, Barão de Cocais e Nova Lima, com concentrações médias de As da ordem de 100,0 mg/kg no solo e de até 547,0 mg/kg em sedimentos do Ribeirão Cardoso.

Na Índia ou em Bangladesh é relatado um caso de calamidade pública devido à ingestão de água contaminada com arsênio, predominantemente na forma trivalente, devido ao uso de água de poços profundos para consumo humano, com uma significativa porção da população apresentando sinais característicos de intoxicação por compostos arsenicais. No Brasil, dados que apontam indícios de ocorrência de contaminação arsenical em solos e sedimentos, além da água superficial e subterrânea, em algumas regiões do Quadrilátero Ferrífero em Minas Gerais (Rawlins *et al.*, 1997; Matschullat *et al.*, 2000; Deschamps *et al.*, 2002), ainda estão sendo avaliados, e os trabalhos de pesquisa prosseguem de maneira cautelosa. Apesar dos teores de As encontrados no nosso estado não serem tão alarmantes quanto àqueles da Ásia, é preocupante perceber que, em alguns pontos de coleta nas regiões de Nova Lima e Mariana, são encontrados teores de As nas águas superficiais cerca de 10 a 100 vezes superiores aos limites recomendados pela OMS. No caso específico de água subterrânea, na região próxima à mineração de ouro em Passagem de Mariana, o valor encontrado é 170 vezes superior ao recomendado (Rawlins *et al.*, 1997). É, portanto necessária uma avaliação em longo prazo dos efeitos resultantes dessa contaminação sobre as populações dessas regiões que se utilizam, direta ou indiretamente, de água contaminada por arsênio e que estão constantemente submetidas à absorção, por meio da aspiração, de partículas finas de sólidos dispersas na poeira. Do ponto de vista da saúde das populações, em trabalho recente e pioneiro, um consórcio de pesquisadores brasileiros e alemães (Matschullat *et al.*, 2000) realizou um levantamento epidemiológico sobre os índices de contaminação arsenical em material biológico, principalmente urina, de crianças moradoras em distritos dos municípios de Santa Bárbara e Nova Lima. Os resultados obtidos indicavam que aproximadamente 45% das crianças examinadas, com idades ente 7-14 anos apresentavam níveis de arsênio na urina de 15-40 μg/L, enquanto aproximadamente 20% delas apresentavam índices maiores que 40 μg/L podendo, portanto, serem classificadas, respectivamente, dentro dos grupos considerados de médio e alto risco, embora ainda não tenham sido observados os efeitos fisiopatológicos da

intoxicação por esse elemento. Amostragens subseqüentes, entretanto, indicaram uma redução dos valores obtidos na primeira coleta.

A despeito das fontes naturais de contaminação anteriormente citadas, a poluição por metais pesados é causada pelas atividades industriais e da agricultura. As principais atividades responsáveis pela geração de resíduos ricos em arsênio são as indústrias de geração de energia, incluindo a de combustíveis fósseis, a indústria metalúrgica e a agricultura. No Brasil, o arsênio é amplamente encontrado no meio industrial, como resíduo, especialmente das indústrias de processamento metalúrgico de ouro, cobre, prata, zinco e cobalto. Este elemento é empregado ainda como matéria-prima na manufatura de vidros, esmaltes, tintas, tecidos e couros e na produção de insumos agrícolas tais como inseticidas, formicidas, herbicidas e preservativos de madeira. O consumo de arsênio pela indústria é, entretanto, insignificante diante das enormes quantidades desse elemento produzidas como resíduos industriais.

1.1.4 Métodos para remoção de Arsênio

A contaminação por arsênio pode ocorrer tanto nas águas residuais industriais, quanto naquelas destinadas para consumo. A maioria dos relatos de problemas de contaminação por As em fontes de água para consumo humano estão relacionadas a fontes de água subterrâneas, geralmente utilizadas preferencialmente pelas populações de áreas rurais.

A química do arsênio em ambientes aquosos é complexa. No ambiente aquático, o As pode ser encontrado tanto na forma trivalente quanto na forma pentavalente. As espécies de As (III) (H_3AsO_3, $H_2AsO_3^-$ e $HAsO_3^{2-}$) são comumente encontradas em condições anaeróbicas ou redutoras (por exemplo, em águas subterrâneas) enquanto as espécies de As (V) (H_3AsO_4, $H_2AsO_4^-$ e $HAsO_4^{2-}$) prevalecem em condições aeróbicas ou oxidantes (águas superficiais bem oxigenadas) (Gupta *et al.*, 1978; Matschullat *et al.*, 2000; Smedley

et al., 2002). Destacado dentre a maioria dos elementos formadores de oxiânions, o As é singular na sua mobilidade na faixa de pH típico das águas subterrâneas (Smedley *et al.*, 2002). Em valores de pH abaixo de 9,2 (pKa_1=9,23, pKa_2=12,13, pKa_3=13,4 para o H_3AsO_3) predomina a espécie neutra do As (III), que é adsorvida nos oxihidróxidos metálicos presentes em solos típicos de forma bastante reversível. Por outro lado, o As pentavalente se apresenta, predominantemente, nas formas aniônicas (pKa_1=2,22, pKa_2=6,98, pKa_3=11,53 para o H_3AsO_4), que são adsorvidas na forma de estruturas mais estáveis (Ciminelli *et al.*, 2004)

A maioria dos cátions de metais pesados tóxicos (Pb^{2+}, Cu^{2+}, Ni^{2+}, Cd^{2+}, Co^{2+}, Zn^{2+}) tem sua solubilidade diminuída à medida que o pH se eleva, seja por precipitação ou co-precipitação como óxidos, hidróxidos, carbonatos ou fosfatos, ou através da adsorção mais efetiva em óxidos metálicos, argilas ou em matéria orgânica. Por outro lado, a maioria dos oxiânions, tende a se tornar mais fracamente adsorvida à medida que o pH se eleva (Smedley *et al.*, 2002). Existe na literatura um certo consenso de que a remoção efetiva do arsênio da água requer a oxidação completa do As (III) a As (V) (Das, 1998; Roussel *et al.*, 2000; Korngold *et al.*, 2001). Uma vez oxidado, o As é mais eficientemente removido de uma solução, por meio da adsorção ou co-precipitação do As (V) com oxi-hidróxidos de Fe (III) ou Al (Roussel *et al.*, 2000).

Precipitação, troca iônica, processos eletroquímicos ou processos empregando membranas são comumente aplicados no tratamento de efluentes industriais (Wood, 1992; Veglio *et al.*, 1997) mas seus custos operacionais, com exceção da precipitação, são muito elevados (Jansson-Charrier *et al.*, 1995). Os custos de investimento inicial e operacional para instalação de plantas industriais de tratamento de efluentes contaminados com metais pesados são bastante significativos (Eccles, 1999). A Tabela I.1 apresenta os custos envolvidos no emprego de algumas das tecnologias disponíveis (os valores estão expressos em US$ gastos/m^3de efluente tratado).

Algumas das técnicas de remoção de arsênio convencionais disponíveis são descritas a seguir. Os processos podem ser divididos em duas categorias principais: na primeira estão aqueles que envolvem precipitação e na segunda aqueles que envolvem adsorção.

A remoção de arsênio por precipitação com íons metálicos é a técnica melhor conhecida e mais freqüentemente empregada. Os melhores resultados são obtidos na precipitação de As (V) com sais férricos em valores de pH entre 7.2 e 7.5. A remoção de arsênio por precipitação com cal na forma de arsenato de cálcio vem sendo praticada há muito tempo. Todavia, o composto $Ca(AsO_4)_2$ não é considerado apropriado para disposição de longo prazo, devido à possibilidade de redissolução do arsênio nele contido através de reações de carbonatação (Zouboulis *et al.*, 1993). A precipitação do arsênio na forma de sulfeto é uma alternativa: condições ácidas redutoras favorecem a precipitação do ouropigmento (As_2S_3), do realgar (As_4S_4) ou outros sulfetos minerais contendo As co-precipitado. Conseqüentemente, teores elevados de As não são esperados quando se têm altas concentrações de sulfeto livre na água. Entretanto, os sulfetos não são estáveis em condições oxidantes.

Tabela I.1 – Custos iniciais e operacionais envolvidos no tratamento de efluentes líquidos contaminados por metais pesados (Eccles, 1999).

Tecnologia	Custos (US$/m^3)		
	Inicial		Operacional
	Planta 1000 m^3/dia	Planta 10000-20000 m^3/dia	
Precipitação Incluindo:neutralização, coagulação, floculação e separação	12,5	8	0,003-0,013
Adsorção em Carvão Ativado Granulado	500	250	0,020-0,050
Microfiltração em Membranas	12,5	11	0,013-0,050
Troca Iônica	100	75	0,050-0,250

Ao longo dos anos, vários tipos de sorventes vêm sendo testados e utilizados para promover a adsorção do arsênio. Podem ser citados, por exemplo, a alumina ativada, os óxidos de ferro e alumínio hidratados, argilominerais (caulinita, bentonita, goetita), sulfetos como pirita, galena e esfalerita, minerais de manganês ou areia recoberta de óxidos de alumínio. Além desses, há outros sorventes orgânicos ou sintéticos que podem ser empregados com a mesma finalidade. Podem ser citadas as resinas poliméricas de troca iônica, o carvão ativado, a quitina e a quitosana, o carvão de osso, o carvão de casca de coco, casca de laranja, biomassa fúngica e os materiais derivados de celulose (Gupta *et al.*, 1978; Zouboulis *et al.*, 1993; Driehaus *et al.*, 1995; Styles *et al.*, 1996; Ladeira *et al.*, 1997; Manning *et al.*, 1997; Manju *et al.*, 1998; Dambies *et al.*, 1999; Ladeira, 1999; Murcott, 1999; Ramaswami *et al.*, 2001; Dambies *et al.*, 2002; Meng *et al.*, 2002; Bostick *et al.*, 2003; Dixit *et al.*, 2003; Ghimire *et al.*, 2003; Loukidou *et al.*, 2003; Ladeira *et al.*, 2004; Singh *et al.*, 2004; Zhang *et al.*, 2004). Para todas as técnicas citadas anteriormente, sem exceção, a principal limitação da adsorção é a remoção eficiente do As (III).

O arsênio (V) é efetivamente adsorvido pela alumina e pela gibsita ativadas na faixa de pH entre 4,0 e 7,0, entretanto, essas taxas decrescem à medida que o pH se eleva, sendo que a

tendência oposta ocorre com a adsorção do As (III) (Gupta *et al.*, 1978). Diversos autores (Gupta *et al.*, 1978; Driehaus *et al.*, 1995; Ladeira *et al.*, 1997; Manning *et al.*, 1997; Ladeira, 1999) relatam, que o As (III) é menos eficientemente removido do que o As (V) e que, portanto, é necessário promover a oxidação do arsenito a arsenato para se obter uma remoção mais eficiente do ânion.

Além das técnicas previamente discutidas, existem outras opções tecnológicas envolvendo a utilização das membranas semipermeáveis. Tais membranas são seletivamente permeáveis à água e alguns solutos e, em vista disso, se adequam ao emprego na remoção de diversas impurezas da água para consumo, inclusive o arsênio, e se apresentam como alternativas - ainda pouco exploradas, seja devido aos custos envolvidos, seja em decorrência de limitações técnicas. Podemos incluir nessa classe a microfiltração, a osmose reversa, a eletrodiálise, a ultrafiltração e a nanofiltração. Estas técnicas apresentam como inconveniente o custo bastante elevado.

A necessidade de busca de métodos economicamente viáveis e eficientes para remoção de arsênio e outros metais pesados resultou no desenvolvimento de novas tecnologias de separação, dentre as quais aquelas envolvendo biossorção (Schneider *et al.*, 1995). Nesse sentido a biossorção usando biomassa residual, orgânica ou inorgânica, abundante e de baixo custo, surge, recentemente, como método alternativo promissor para remoção de íons metálicos (Volesky *et al.*, 1995), principalmente para operações em pequena escala (Poulin *et al.*, 1996; Cimino *et al.*, 2000). Algas, bactérias, fungos e leveduras já tiveram comprovado seu potencial em atuar como biossorventes de metais.

1.2 RELEVÂNCIA DO PROJETO

O arsênio e seus compostos, apesar de considerados essenciais ao metabolismo, são tóxicos e carcinogênicos a todos os seres vivos. As espécies solúveis de arsênio, tanto as derivadas do ácido arsenioso (H_3AsO_3) quanto àquelas derivadas do ácido arsênico (H_3AsO_4), são capazes de formar complexos inespecíficos com aminoácidos localizados nos sítios ativos de enzimas essenciais à manutenção das funções metabólicas normais dos seres vivos. O arsênio é classificado como um veneno protoplasmático geral que, unindo-se aos grupos SH de certas enzimas, especialmente as piruvatoxidases e as fosfatases, reduz ou abole a respiração celular, denotando claramente a sua especificidade pelos grupamentos sulfidrila.

Sabe-se ainda que as espécies trivalentes apresentam maior toxicidade bem como maior mobilidade, adquirindo, portanto, maior importância tanto do ponto de vista ambiental quanto toxicológico. As metodologias disponíveis para remediação de arsênio, sejam elas convencionais ou alternativas, apresentam uma limitação comum: removem, eficientemente, as espécies pentavalentes do As, mas geralmente falham na remoção/imobilização das espécies trivalentes, o que implica na necessidade de oxidação prévia do arsenito a arsenato como etapa intermediária do processo.

Embora a bioacumulação e a oxidação bacteriana de As sejam processos bastante conhecidos, publicações a respeito da biossorção desse elemento são bastante raras. De fato, existe uma lacuna na literatura no que se refere a biossorção de ânions, de um modo geral e, em particular, dos ânions arsenicais. Percebemos ainda que os trabalhos sobre biossorção são algumas vezes superficiais, restringindo-se apenas à seleção de biossorventes com base nos dados obtidos a partir de isotermas de adsorção. Essa seleção vem em geral acompanhada de pouca ou nenhuma discussão a respeito dos mecanismos físico-químicos que explicam o fenômeno da adsorção em si. Esta superficialidade pode ser conseqüência do fato da biossorção ser uma área do conhecimento que ocupa uma interface entre a biologia, a química e a engenharia e, assim sendo, os pesquisadores,

sentem-se pouco à vontade para "transitar" por áreas aparentemente tão díspares. No nosso grupo de trabalho, buscamos a quebra desses paradigmas através da interação destas diferentes áreas do conhecimento buscando compreender a adsorção, nela incluída a biossorção, ao nível molecular.

Com este objetivo em mente e fundamentados nos mecanismos bioquímicos que justificam os efeitos tóxicos dos oxiânions arsenato e arsenito (Knowles *et al.*, 1983; Kaur *et al.*, 1992) e sua afinidade química por grupamentos SH (Bhattacharjee *et al.*, 1996; Shi *et al.*, 1996; Styles *et al.*, 1996; Farrer *et al.*, 2000; Martin *et al.*, 2001), este trabalho vem propor a utilização de biomassas animais, ricas em proteínas fibrosas, como biossorventes para ânions arsenicais, em particular os íons arsenito, neste caso, sem necessidade de oxidação prévia desse elemento.

Levando-se em consideração (i) o fato de que a cisteína é um aminoácido presente em abundância na estrutura da queratina, constituinte principal das proteínas fibrosas estruturais presentes em estruturas corporais dos animais superiores, tais como, unhas, chifres, cabelos, pêlos, cascos e penas, e (ii) que o grupamento funcional da cisteína é o grupamento sulfidrila, o presente trabalho propõe a utilização de biomassa residual, de baixo custo, para imobilização do arsênio em seu estado reduzido, sem a necessidade de etapas prévias de oxidação. Como material biosorvente foi selecionado um pó obtido pela trituração de penas de galinhas.

1.3 OBJETIVOS E ORGANIZAÇÃO DA TESE

Os principais objetivos deste trabalho de Tese são:

(i) propor, pela primeira vez, a utilização de um biossorvente capaz de adsorver eficientemente, a espécie reduzida do arsênio sem a necessidade de etapas prévias de oxidação;

(ii) contribuir para o entendimento das questões referentes à estabilidade dos compostos arsenicais trivalentes e sua imobilização em presença de matéria orgânica.

Visando atingir aos objetivos gerais propostos, o desenvolvimento deste trabalho de Tese envolveu as seguintes etapas:

- Seleção e preparação de um biossorvente específico para sorção de As (III);
- Avaliação do desempenho do biossorvente selecionado sob diferentes condições de preparação da amostra, pH, concentração de biomassa e presença de íons competidores;
- Identificação dos mecanismos de adsorção através do uso de técnicas de Espectroscopia de absorção de raios-X, *Expanded X-Ray Adsorption Fine Structure* (EXAFS) and *X-Ray Absorption Near Edge Structure* (XANES) e Espectroscopia Vibracional Raman, associadas às predições teóricas baseadas em *Density Functional Theory*-DFT. Proposição, com base nos dados estruturais obtidos, de um modelo estrutural para o complexo de adsorção formado entre o átomo de As (III) e os sítios ativos da biomassa;
- Proposição de um mecanismo de adsorção do arsenito em biomassa animal rica em proteína fibrosa.

Para melhor discussão dos resultados obtidos, esta Tese foi subdividida em 5 capítulos. No Capítulo 1 é apresentada uma introdução ao tema bem como uma sucinta revisão da literatura. São ainda apresentados a relevância e os objetivos do trabalho. Nos três capítulos subseqüentes e nos anexos são apresentados os resultados experimentais obtidos.

No capítulo 2 (aceito para publicação na revista *Environmental Science and Technology*) estão apresentados os resultados referentes à adsorção de arsenito em biomassa animal sob diferentes condições experimentais. São apresentados também os resultados de Espectroscopia de Absorção de Raios X (XANES e EXAFS) que nos levaram à proposição do mecanismo de adsorção.

No capítulo 3 (submetido para publicação na revista *Environmental Science and Technology*) utilizamos novamente da Espectroscopia de Absorção de Raios X para compreender o efeito do pH na formação dos complexos de adsorção entre o arsenito e a biomassa. Confrontamos ainda os dados experimentais obtidos com as predições teóricas baseadas em *Density Functional Theory*-DFT a fim de melhor compreender o modelo de adsorção proposto.

No capítulo 4 (aceito para publicação no *Journal of Colloids and Interface Science*) utilizamos novamente a DFT associada à espectroscopia Raman, para caracterização tanto da biomassa quanto dos complexos de adsorção formados.

No capítulo 5 são apresentadas as considerações finais e conclusões, tentando ressaltar as inter-relações entre os capítulos 2 a 4, além das contribuições específicas deste trabalho, bem como as sugestões de trabalhos futuros e os trabalhos gerados a partir dessa Tese.

1.4 REFERÊNCIAS BIBLIOGRÁFICAS:

Bhattacharjee, H. and Rosen, B. (1996). Spatial Proximity of Cys 113, Cys172, and Cys 422 in the Metalloactivation Domain of the ArsA ATPase. *The Journal of Biological Chemistry*, 271, p. 24465-24470.

Bogdan, G. M.; Sampayo-Reyes, A. and Aposhian, H. V. (1994). Arsenic Binding Proteins of Mammalian Systems: I. Isolation of Three Arsenite-binding Proteins of Rabbit Liver. *Toxicology*, 37, p. 3149-3153.

Bostick, B. C. and Fendorf, S. (2003). Arsenite sorption on troilite (FeS) and pyrite (FeS_2). *Geochimica et Chosmochimica Acta*, 67, p. 909-921.

Case, C. and Robinson, M. F. (1983). Some Aspects in Nutritional Trace Elements. In: H. Siegel. *Methods Involving Metal Ions and Complexes in Clinical Chemistry*. New York, Marcel Dekker, Inc. 16: p. 1-26.

Chiu, K.-H.; Chen, S.-L.; Dzeng, S. R.; Shieh, G.-M.; Yang, M.-H. and Wal, C. M. (1994). Arsenic Species in Groundwaters of the Blackfoot Disease Area, Taiwan. *Environ. Sci. Technol.*, 28, p. 877-881.

Ciminelli, V. S. T.; Ladeira, A. C. Q.; Duarte, H. A. and Oliveira, A. F. (2004). As(III) adsorbed on gibsite: structural model of surface complex based on EXAFS and DFT calculations. *submitted to Geochimica Chosmochimica Acta*.

Cimino, G.; Passerini, A. and Toscano, G. (2000). Removal of Toxic Cations and Cr(VI) from Aqueous Solution by Hazelnut Shell. *Wat. Res.*, 34, p. 2955-2962.

Dambies, L.; Roze, A.; Roussy, J. and Guibal, E. (1999). As (V) removal from dilute solutions using MICB (molybdate-impregnated chitosan beads). International Biohydrometallurgy Symposium - IBS99 Biohydrometallurgy and the environment toward the mining of the 21st century. R. Amils and A. Ballester. Madrid, Elsevier. B**:** 842.

Dambies, L.; Vincent, T. and Guibal, E. (2002). Treatment of Arsenic-Containing Solutions using Chitosan Derivatives: Uptake Mechanism and Sorption Performances. *Water Research*, 36, p. 3699-3710.

Das, H. K. (1998). Alternative Sources of Arsenic-Safe Drinking Water. The Daily Star (http://www.dainichi-consul.co.jp/english/arsenic/removal.htm**:** 6 pages.

Deschamps, E.; Ciminelli, V. S. T.; Lange, F. T.; Matschullat, J.; Raue, B. and Schmidt, H. (2002). Soil and Sediment Geochemistry of the Iron Quadrangle, Brazil. *J Soils & Sediments 2002*, 2, p. 216-222.

Dixit, S. and Hering, J. g. (2003). Comparision of Arsenic(V) and Arsenic(III) Sorption onto Iron Oxide Minerals: Implications for Arsenic Mobility. *Environmental Science and Technology*, 37, p. 4182-4189.

Driehaus, W.; Seith, R. and Jekel, M. (1995). Oxidation of Arsenate(III) with Manganese Oxides in Water Treatment. *Water Research*, 29, p. 297-305.

Eccles, H. (1999). Treatment of Metal-Contaminated Wastes: Why Select a Biological Process? *TIBTECH*, 17, p. 462-464.

Estrov, Z.; Manna, S. K.; Harris, D.; Van, Q.; Estey, E. H.; Kantarjian, H. M.; Talpaz, M. and Aggarwal, B. B. (1999). Phenylarsine oxide blocks interleukin-1 beta-induced activation of the nuclear transcription factor NF-Kappa B, inhibits proliferation and induces apoptosis of acute myelogenous leukemia cells. *Blood*, 94, p. 2844-2853.

Farrer, B. T.; McClure, C. P.; Penner-Hahn, J. E. and Pecoraro, V. L. (2000). Arsenic (III)-Cysteine Interactions Stabilize Three-Helix Bundles in Aqueous Solution. *Inorganic Chemistry*, 39, p. 5422-5423.

Ghimire, K. N.; Inoue, K.; Yamagushi, H.; Makino, K. and Miyajima, T. (2003). Adsorptive separation of arsenate and arsenite anions from aqueous medium by using orange waste. *Water Research*, 37, p. 4945-4953.

Gontijo, B. (1980). *Contribuição ao Estudo do Arsenicismo Cutâneo*. Faculdade de Medicina, UFMG, Belo Horizonte. 48.(M. Sc. Thesis)

Gupta, S. K. and Chen, K. C. (1978). Arsenic removal by adsorption. *Journal of Water Pollution Control Federation*, 50, p. 493-506.

Hughes, M. F. (2002). Arsenic Toxicity and Potential Mechanisms of Action. *Toxicology Letters*, 133, p. 1-16.

Jansson-Charrier, M.; Guibal, E.; Surjous, R. and Cloirec, P. L. (1995). Continuous Removal of Uranium by Biosorption onto Chitosan: Application to an Industrial Effluent. In: International Biohydrometallurgy Symposium /IBS-95, 1995, Vina del Mar, Chile. November, 19-22, 1995. p. 267-276

Jones, M. M. (1983). Therapeutic Chelating Agents. In: H. Siegel. *Methods Involving Metal Ions and Complexes in Clinical Chemistry*. New York, Marcel Dekker, Inc. 16: p. 47-83.

Kaur, P. and Rosen, B. P. (1992). Plasmid-Encoded Resistance to Arsenic and Antimony. *Plasmid*, 27, p. 29-40.

Knowles, F. C. and Benson, A. A. (1983). The biochemistry of arsenic. *TIBS*, 8, p. 178-179.

Korngold, E.; Belayev, N. and Aronov, L. (2001). Removal of Arsenic from Drinking Water by Anion Exchangers. *Desalination*, 141, p. 81-84.

Ladeira, A. C. Q. (1999). *Utilização de Solos e Minerais para Imolização de Arsênio e Mecanismo de Adsoção*. Escola de Engenharia - Departamento de Engenharia Metalúrgica e de Minas, UFMG, Belo Horizonte. 160. (PhD. Thesis)

Ladeira, A. C. Q. and Ciminelli, V. S. T. (2004). Adsorption and desorption of arsenic on an oxisol and its constituents. *Water Research*, 38, p. 2087-2094.

Ladeira, A. C. Q.; Ciminelli, V. S. T. and Fonseca, J. F. M. (1997). Controle da Emissão de Arsênio Através da Imobilização em Argilas. In: 2º Congresso Internacional de Tecnologia Metalúrgica e de Materiais, 1997, São Paulo - SP. CD-ROM

Lerman, S. and Clarkson, T. W. (1983). The Metabolism of Arsenite and Arsenate by the rat. *Fundam. Appl. Toxicol.*, 3, p. 309-314.

Loukidou, M. X.; Matis, K. A.; Zouboulis, A. I. and Liakopoulou-Kyriakidou, M. (2003). Removal of As(V) from wastewaters by chemically modified fungal biomass. *Water Research*, 37, p. 4544-4552.

Mandal, B. K. and Suzuki, K. T. (2002). Arsenic Round the World: a Review. *Talanta*, 58, p. 201-235.

Manju, G. N.; Raji, C. and Anirudhan, T. S. (1998). Evaluation of coconut husk carbon for the removal of arsenic from water. *Water Research*, 32, p. 3062-3070.

Manning, B. A. and Goldberg, S. (1997). Adsorption and Stability of Arsenic(III) at the Clay Mineral-Water Interface. *Environmental Science &Technology*, 31, p. 2005-2011.

Martin, P.; DeMel, S.; Shi, J.; Gladysheva, T.; Gatti, D. L.; Rosen, B. P. and Edwards, B. F. P. (2001). Insights into the structure, solvation and mechanism of ArsC arsenate reductase, a novel arsenic detoxification enzyme. *Structure*, 9, p. 1071-1081.

Matschullat, J.; Borba, R. P.; Deschamps, E.; Figueiredo, B. R.; Gabrio, T. and Schwenk, M. (2000). Human and Environmental Contamination in the Iron quadrangle, Brazil. *Applied Geochemistry*, 15, p. 181-190.

Meng, X.; Korfiatis, G. P.; Bang, S. and Bang, K. W. (2002). Combined Effects of Anions on Arsenic Removal by iron Hydroxides. *Toxicology Letters*, 133, p. 103-111.

Murcott, S. (1999). Appropriate Remediation Technologies for Arsenic - Contaminated Wells in Bangladesh. In: Arsenic in Bangladesh Ground Water, 1999, Wagner College, Staten Island, New York (http:/phys4.harvard.edu/~wilson/murcott.html). February 27 - 28, 1999. p.

Nies, D. H. (1999). Microbial heavy-metal resistance. *Apllied Microbiology Biotechnology*, 51, p. 730-750.

Poulin, R. and Lawrence, R. W. (1996). Economic and Environmental Niches of Biohydrometallurgy. *Minerals Engineering*, 9, p. 799-810.

Ramaswami, A.; Tawachsupa, S. and Isleyen, M. (2001). Batch-Mixed Iron Treatment of High Arsenic Waters. *Wat. Res.*, 35, p. 4474-4479.

Rawlins, B. G.; Williams, T. M.; Breward, N.; Ferpozzi, L.; Figueiredo, B. and Borba, R. (1997). Preliminary Investigation of Mining-related Arsenic Contamination in the Provinces of Mendoza and San Juan (Argentina) and Minas Gerais State (Brazil). Keyworth, Nottingham, British Geological Survey.

Rojas-Chapana, J. A. and Tributsch, H. (2000). Bio-leaching of Pyrite accelerated by Cysteine. *Process Biochemistry*, 35, p. 815-824.

Roussel, C.; Bril, H. and Fernandez, A. (2000). Arsenic Speciation: Involvement in Evaluation of Environmental Impact Caused by Mine Wastes. *J. Environ. Qual.*, 29, p. 182-188.

Schneider, I. A. and Rubio, J. (1995). New Trends in Biosorption of Heavy Metals By Freshwater Macrophytes. In: International Biohydrometallurgy Symposium/IBS-95, 1995, Vina del Mar, Chile. November, 19-22,1995. p. 247-256

Shi, W.; Dong, J.; Scott, R. A.; Kasenzenko, M. Y. and Rosen, B. (1996). The Role of Arsenic-Thiol Interactions in Metalloregulation of the ars Operon. *The Journal of Biological Chemistry*, 271, p. 9291-9297.

Singh, T. S. and Pant, K. K. (2004). Equilibrium, kinetics and thermodynamic studies for adsorption of As(III) on activated alumina. *Separation Purification Technology*, 36, p. 139-1478.

Smedley, P. L. and Kinniburgh, D. G. (2002). A review of the source, behaviour and distribution of arsenic in natural waters. *Apllied Geochemistry*, 17, p. 517-568.

Styblo, M.; Yamauchi, H. and Thomas, D. J. (1995). Comparative in Vitro Methylation of Trivalent and Pentavalent Arsenicals. *Toxicol. Appl. Pharmacol.*, 135, p. 172-178.

Styles, P. M.; Chanda, M. and Rempel, G. L. (1996). Sorption of arsenic anions onto poly(ethylene mercaptoacetimide). *Reactive & Functional Polymers*, 31, p. 89-102.

Veglio, F. and Beolchini, F. (1997). Removal of metals by biosorption: a review. *Hydrometallurgy*, 44, p. 301-316.

Volesky, B. and Holan, Z. R. (1995). Biosorption of heavy metals. *Biotechnology Progress*, 11, p. 235-250.

Wood, A. (1992). Trace metal removal from effluents. Water and Water Treatment**:** 32,36.

Zhang, W.; Singh, P.; Paling, E. and Delides, S. (2004). Arsenic removal from contaminated water by natural iron ores. *Minerals Engineering*, 17, p. 517-524.

Zouboulis, A. I.; Kydros, K. A. and Matis, K. A. (1993). Arsenic(III) and Arsenic(V) Removal from solutions by Pyrite Fines. *Separation Science and Technology*, 28, p. 2449-2463.

Capítulo 2

Development of a Biosorbent for Arsenite: Structural Modeling Based on X-Ray Spectroscopy (XAS)

Environ. Sci. Technol. **2005**, 39, 895-900.

Development of a Biosorbent for Arsenite: Structural Modeling Based on X-Ray Spectroscopy (XAS)

Mônica Cristina Teixeira[1] and Virgínia S. T. Ciminelli[*]

Department of Metallurgical and Materials Engineering – Federal University of Minas Gerais, Brazil

This work describes a biological route for direct sorption of aqueous As (III) species, which are the most toxic and mobile arsenic species found in soils. Based upon the biochemical mechanisms which explain arsenic toxicity, we propose that waste biomass with a high fibrous protein content obtained from chicken feathers can be used for selective As (III) adsorption. Prior to adsorption, the disulfide bridges present in the biomass are reduced by thioglycolate. Our investigations demonstrated that As (III) is specifically adsorbed on the biomass and, contrary to the behavior observed with inorganic sorbents, the lower the pH the more effective the removal. Arsenic uptake reaches values of up to 270 μmol As (III)/g of biomass. Analyses by Synchrotron light techniques, such as XANES, demonstrated that arsenic is adsorbed in its trivalent state, an advantage over conventional techniques for As uptake, which usually require a previous oxidation stage. EXAFS analyses showed that each As atom is directly bound to three S atoms with an estimated distance of 2.26 Å. The uptake mechanism is explained in terms of the structural similarities between the As III-biomass complex structure and that of arsenite ions and Ars-Operon system encoded proteins and phytochelatins. The biological route presented here offers the perspective of a direct removal of arsenic in its reduced form.

Keywords: arsenite, biosorption, bioremediation, EXAFS.

[1]Permanent address: Department of Pharmacy – Federal University of Ouro Preto, Brazil
* Corresponding author - address: Rua Espírito Santo, 35/206. Belo Horizonte-MG. CEP: 30160-030. Brazil. Phone: 55 31 3238-1804; fax: 55 31 3238-1815; e-mail address: ciminelli@demet.ufmg.br

2.1 INTRODUCTION

Arsenic and its compounds are toxic and carcinogenic to all living organisms (Mandal and Suzuki, 2002). Arsenic naturally occurs on the earth's crust in small concentrations, arsenopyrite (FeAsS) being the most common arsenic mineral (Mandal*, et al.*, 2002). In soils, arsenic concentration may vary from 1.0 mg/kg (apatite, fluorite, and calcite samples) to 77,000-126,000 mg/kg (pyrite or arsenopyrite samples) (Smedley and Kinniburgh, 2002). Typical arsenic concentration found in soils is reported at 6 mg/kg (Mandal*, et al.*, 2002). Small amounts of arsenic and its compounds are utilized by the chemical and electronic industries to produce electronic components for laser equipment, wood preservatives, pesticides, and glasses, to name but a few of the numerous applications. Despite its many applications, there is a surplus of arsenic-containing wastes, derived mainly from the mineral and metallurgical industries. The wastewater and solid residues produced by these industries are important potential sources for arsenic contamination of surface and groundwater. Natural leaching of As-enriched soils and rocks has been the main cause for the main arsenic contamination reported worldwide, such as Poland, Canada, New Zealand, Spain, Hungary, Mexico, United States, Chile, Argentina, China, India and Bangladesh.

The toxicity of arsenic and its compounds is well established (Knowles and Benson, 1983; Hughes, 2002). Once ingested, arsenic provokes nausea and gastro-intestinal symptoms. From the toxicological point of view, As (V) causes adverse effects to human and other living organisms due to its chemical similarity with phosphate (Nies, 1999; Hughes, 2002). In this case, arsenic poisoning can be reverted by the administration of an excess of phosphate. On the other hand, the trivalent species As (III) strongly binds to the sulphydril (SH) groups in the active sites of some dehydrogenases enzymes like pyruvate and α-ketoglutarate, or dihydrolipoate, causing irreversible metabolic impairments and, in some cases, cellular mutagenesis (Flessel, et al., 1980; Treagan, 1983), which therefore explains

the higher toxicity of this species. The recognition that even trace amounts of arsenic, after long exposure, may cause severe health problems, such as dermatosis and cancer, have motivated a decrease in international limits for soluble arsenic in drinking water. Following recommendations from the World Health Organization this limit has been reduced from 50 $\mu g.L^{-1}$ to 10 $\mu g.L^{-1}$ in many countries.

Recent disasters involving cases of human poisoning due to arsenic contamination in drinking water, particularly in India and Bangladesh (Nickson, et al., 1998; Acharyya, et al., 1999) have spawned a series of worldwide investigations towards arsenic remediation. The episodes in the Asian countries are considered the most severe in terms of the extent of contamination and the number of persons affected (Nickson*, et al.*, 1998; Acharyya*, et al.*, 1999; Chowdhury, et al., 1999). It has been estimated that more than 25 million people have been exposed to water with arsenic concentration $\geq 50\mu g.L^{-1}$ in West Bengal (India) and Bangladesh (Chakraborti, et al., 2002).

Immobilization and stability of arsenic species in natural environments or under remediation procedures are influenced by its oxidation state. The predominant water-soluble species are the As (III) and As (V) derivatives of the arsenous (H_3AsO_3) and arsenic (H_3AsO_4) acids, respectively. The trivalent species is of great environmental concern not only because of its considerably higher toxicity but also in view of its higher mobility in soils. Even under oxic conditions both arsenic species occur together due to the fact that As (III) oxidation to As (V) is a kinetically slow process (Weerasooriya, et al., 2003). In biological environments, bacterial activity can reduce As (V) species (Knowles*, et al.*, 1983; Ladeira, et al., 2001b; Mukhopadhyay, et al., 2002), thus increasing arsenic toxicity. In the pentavalente state, arsenic acid (H_3AsO_4) species form stable surface complexes with soil constituents containing ferric, manganese or aluminium oxy-hydroxides, such as goethite, alumina, hematite, birnessite and gibbsite (Gupta and Chen, 1978; Driehaus, et al., 1995; Ladeira*, et al.*, 2001b; Smedley*, et al.*, 2002; Deschamps, et al., 2003), which explains its lower environmental mobility. On the other hand, the trivalent arsenous acid (H_3AsO_3) species are weakly bound to inorganic sorbents regardless of the pH. It is

normally assumed that to achieve high efficiency during arsenic remediation processes such as precipitation or co-precipitation with lime as metallic oxides, it is often necessary to promote the oxidation of As (III) ions to As (V). Therefore the conventional techniques used for As immobilisation usually require a previous oxidative stage (Nickson*, et al.*, 1998; Chowdhury*, et al.*, 1999). Those systems could now be classified as As (V) removing systems.

Biosorption has been investigated by many as an alternative to conventional techniques for metal remediation. The predominant uptake mechanism usually involves unspecific ion exchange reactions. For instance, positively charged groups present in the biomass structure, like the amino groups, are potential reactive sites to form adsorptive complexes with negatively charged ions, such as arsenate, arsenite, chromate, sulphate or phosphate (Veglio and Beolchini, 1997). Despite the identification of a number of biosorbents capable of removing a variety of species from aqueous solutions, the process often lacks selectivity in industrial complex, multi-component systems. We believe that the poor selectivity associated with unspecific ion exchange mechanisms has been one of the main limitations hindering biosorption's commercial applications.

The present work aims at designing a specific biosorbent for arsenic, with an approach based on the following premises: (i) the toxicity of As (III) is considerably higher when compared to As (V), (ii) this higher toxicity may be explained in terms of the great chemical affinity that exists between As (III) and the sulphydril groups and (iii) the As (V) affinity for sulphydril groups is lower when compared to As (III).

Based on the previous considerations, a waste biomass with a high fibrous protein content furnished by poultry industry, was selected and tested for As (III) sorption. The biomass is a keratin rich material. Keratin is a fibrous protein, which contains cysteine amino-acid residues in its primary structure; the lateral group of each cysteine molecule is the sulfidryl (SH) group. Two cysteine molecules may react forming a cystine molecule, which is, in fact, a molecule with two cysteine residues bound by a disulfide bridge. Thioglycolate is a

reduction agent that reacts with the disulfide bridge, restoring the SH groups. It is known that arsenite reacts with SH groups from cystein - rich proteins. Our selection of this specific biomass was based on its cysteine content.

Supported by the results shown in the following paragraphs the specificity of the selected biosorbent for As (III) is demonstrated. This feature is explained by the molecular structure of the adsorbed complex determined by Syncrotron light, X-Ray Spectroscopy analyses.

2.2 MATERIALS AND METHODS

2.2.1 Biomass preparation.

White chicken feathers were rinsed thoroughly with warm tap water and dried at 45 ±5°C for 24 hours. The dried material was ground and sieved to obtain a size range below 0.037 mm (400 Mesh Tyler). Biomass activation was accomplished by adding 10 ml of a 7.8 % (w/w) basic ammonium thioglycolate solution. Treatment did not imply any mass loss. After this activation step, the powdered biomass was filtered, washed with 100 mL of Milli-Q water and used in the adsorption tests.

2.2.2 Materials

All solutions were prepared with analytical grade chemicals and Milli-Q water. As (III) stock solutions of 10,000 mg/L were prepared with AsNaO2 (Fluka, 99.0%) salt. The pH values were adjusted with 0.1 N HCl or NaOH solutions; Eh was constantly monitored by means of a platinum Ag/AgCl electrode. Ionic strength (I) was fixed by using 4 mol/L NaCl or 0.01 mol/L Na3PO4 electrolyte solutions.

2.2.3 Adsorption experiments

As (III) batch adsorption experiments were conducted at room temperature (28±3°C), by adding a known amount of biosorbent (1-10 mg/L) to each 250-ml Erlenmeyer flask containing the As solution (100 mL). Flasks were shaken (100 rpm) per 1 hour to achieve equilibrium. As (III) semi-continuous adsorption experiments were undertaken at a constant temperature (25±0.2°C) using an apparatus similar to that described by Pagnanelli and co-workers (Pagnanelli, et al., 2000), and the following procedure “Subsequent Additions Method” - SAM. The liquid volume in the reactor was 1,000 mL, biosorbent concentration was 2 g/L, and agitation and pH values were kept constant. A 10 mL sample was collected

and analysed once an hour after each arsenic addition (equilibrium being achieved). Reaction suspensions were filtered through a 0.45 µm cellulose membrane, and preserved with concentrated nitric acid (5 µL) for chemical analyses by AAS. Experiments were carried out in duplicate and results were averaged.

2.2.4 XANES and EXAFS analyses

X-Ray Absorption Near Edge Structure (XANES) and Extended X-Ray Absorption Fine Structure (EXAFS) analyses of wet biomass samples loaded with As (III) were performed using the synchrotron facilities at the Laboratório Nacional de Luz Synchrotron (LNLS), in Campinas, São Paulo, Brazil. XANES and EXAFS data from the arsenic K edge (11,868 eV) were obtained at XAS workstation, under operation conditions of 1.37 Gev and beam currents of about 200 mA. All spectra were recorded at room temperature using a Si (111) double crystal monochromator with an upstream vertical aperture of 0.6 mm. Arsenic K-edge X-ray absorption spectra were measured by monitoring the transmitted energy using a 15-element Ge detector (Canberra Industries). Solid samples were fixed onto steel holders, sealed with Kapton tape film and placed at an angle of 45° to the incident beam. The energy resolution utilized were 0.8eV at the XANES region (11,855-11,930eV); 2eV between 11,760 and 11,855eV, and 11,930 and 12400eV and 3eV at 12,400-13,000eV region. XANES and EXAFS spectra were obtained simultaneously. Counting times of 3 s were kept constant. XANES spectra were analysed using the Origin 6.0 software and collected data from EXAFS were analysed by using the Winxas 2.0 software. EXAFS data fit was obtained using phase and amplitude parameters calculated with the FEFF 6.01 software.

2.3 RESULTS AND DISCUSSION

There are a limited number of biosorbents specially developed for arsenic. Examples such as MICB (*Molybdate-impregnated chitosan beads*) (Dambies, et al., 2002) are usually more effective in removing the pentavalent species and, as for the inorganic sorbents (i.e. goethite, alumina, gibbsite and ferric oxides), it is often necessary oxidize the trivalent arsenic in order to favor its immobilization. Arsenite uptake by inorganic sorbents is usually favored at high pH, while arsenate uptake is favored at low pH. Besides that, it is necessary to keep in mind the fact that arsenite immobilization by inorganic sorbents is often favored at high pH. Oxyanions usually exhibit adsorption maxima at pH value close to the pK_a of their first dissociation constant (Bostick and Fendorf, 2003). Therefore, for As (III) species this would imply in maximum adsorption at pH close to 9 and for arsenate species at pH close to 2. The development of a specific biosorbent for As (III) removal from dilute aqueous solutions took into account the mechanism that explains the toxicity of arsenic species, i.e. irreversible enzymatic inhibition caused by the reaction of As (III) with cysteine sulphidryl groups. Therefore, the use of a cysteine-rich biomass, as found in animal skin, hair, nails, horns or feathers has been proposed. Chicken feathers were finally selected in view of their abundance as a waste residue from the poultry industry.

Preliminary experimental results related to As (III) adsorption by the selected biomass are shown in Table II. 1 and Figure 2.1. The results shown in Table II. 1 confirm the role of sulphydril reduced groups on arsenic adsorption (tests a and d) and also allow for evaluation of possible loss of arsenic caused by precipitation with thioglycolate or adsorption onto filtration membranes. For those purposes, an excess of thioglycolate (10 times greater than that used in the actual activation procedure) was intentionally used; the results suggest no removal of arsenic by precipitation with the reagent (a and b). Experiments performed with biomass prior to the activation reaction with thioglycolate solution, led to a negligible As uptake. This finding supports the hypothesis that the reduced sulphydril groups are responsible for arsenic adsorption. Arsenite adsorption onto non-

activated biomass is insignificant and similar to that obtained with the cellulose acetate membrane (c). The biomass selectivity towards As (III) is clearly demonstrated.

Table II.1. Pre-treatment influence on As (III) and As (V) removal

Test	Biomass	Thioglycolate solution (%)	Pre-treatment (minutes)	As (III) removal (%)	As (V) removal (%)
A	+	10	60	29.3	6.1
B	+	10	60	29.9	5.5
C	-	-	-	4.0	0
D	+	-	-	3.9	0

Powdered biomass concentration, 1g/L;(I=0,1; Inicial As concentration = 2.67 mmol.L^{-1} (200ppm); pH, 5.0; Equilibrium time, 1hour; Temperature, 25°C; shaker, 150rpm. (a) Biomass pre-treated with thioglycolate solution for one hour; material filtered through a 0.45 μm acetate cellulose membrane; (b) Biomass pre-treated with thioglycolate solution for one hour, material not filtered; (c) Flasks containing only a 0.45 μm acetate cellulose membrane; (d) Flasks containing only natural biomass

Because the experimental conditions were strongly reductive, the formation of volatile arsine (AsH_3) or solid compounds such as realgar (As_2S_2) or orpiment (As_2S_3) were also a matter of concern. According to the Eh vs. pH diagram for the As-S-H_2O system (Johnson and Voegtlin, 1930; Vink, 1996) reduction of As^{3+} to As^{3-} is only achieved at Eh<0 V and therefore at redox potentials considerably lower than the lowest Eh of 297mV determined during the experiments. In a broad pH range (from 2.0 to 10.0) and even with the thioglycolate concentration 10 times greater than that used in the activation protocol no loss of arsenic by volatilisation or precipitation was detected.

The As (III) adsorption on whole and powdered biomass was evaluated by the experiments described in Figure 2.1. The highest As uptake was obtained when waste activated biomass was employed at the concentration of 2.0 g.L^{-1}. The results obtained for powdered biomass were slightly lower than those obtained for whole biomass. Regardless of the biomass concentration, equilibrium was achieved in less than 10 min. The milling process seems to

negatively contribute to As uptake. Nevertheless, all the subsequent experimental tests were performed using ground material for the benefit of sample homogeneity.

The influence of pH on As (III) biosorption can be observed in Figure 2.2. Arsenic uptake at pH values of 2.0, 5.0, 8.0 and 10.0 were compared. During all the adsorption experiments, pH variation was less than 0.2 units. The obtained results showed that the lower the pH, the higher the uptake. This trend is just the opposite of that observed for As (III) adsorption onto inorganic sorbents, for which uptake increases with pH (Gupta*, et al.*, 1978; Goldberg and Johnston, 2001; Bostick*, et al.*, 2003; Dixit and Hering, 2003; Ladeira and Ciminelli, 2004; Singh and Pant, 2004). Taking into account that the pKa_1 for arsenous acid is 9.2, one can see that As (III) neutral species are preferably adsorbed by the biomass instead of the negatively charged ones. Arsine formation during sorption experiments carried out at pH 2.0 was experimentally investigated and also discarded.

In order to obtain the adsorption experimental parameters Q_{max} and k, the experimental data exhibited in Figure 2.2 were adjusted to a linear expression of Langmuir equation:

$$Ceq.q^{-1} = k.Q_{max}^{-1} + Ceq.\ Q_{max}^{-1} \qquad (2.1)$$

where Ceq is the As equilibrium concentration in the aqueous phase.

The obtained Q_{max} values were 173.6 and 135.1 μmol As (III).g^{-1} at pH 2.0 and pH 5.0, respectively. The values for the constant k were 0.06, at pH 2.0 and 0.04 at pH 5.0, the calculated correlations factors were both above 0.996. Those values clearly demonstrated that As adsorption is favoured at pH 2.0.

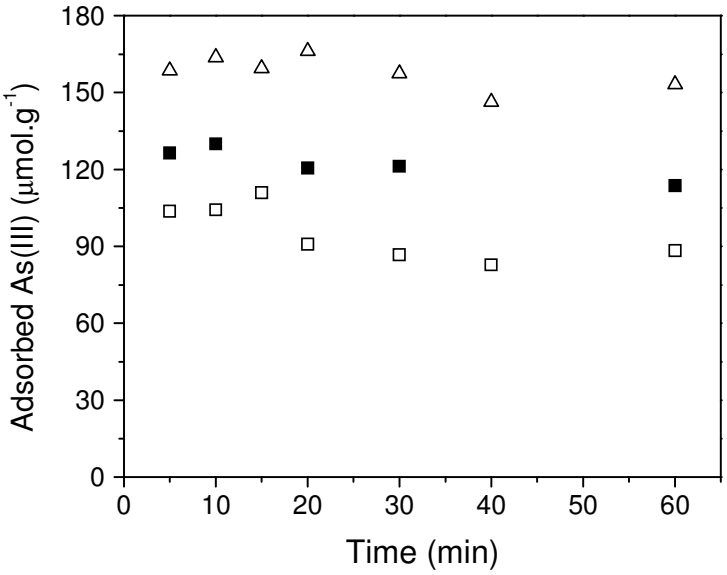

Figure 2.1. As (III) uptake by powdered biomass, $2g.L^{-1}$(open triangle); $1g.L^{-1}$(open square) and whole biomass, $1g.L^{-1}$ (solid square). Flask tests, As (III) initial concentration, 1.34 $mmol.L^{-1}$; initial pH, 9.2; temperature, 28±3°C; pre-treatment, 2h.

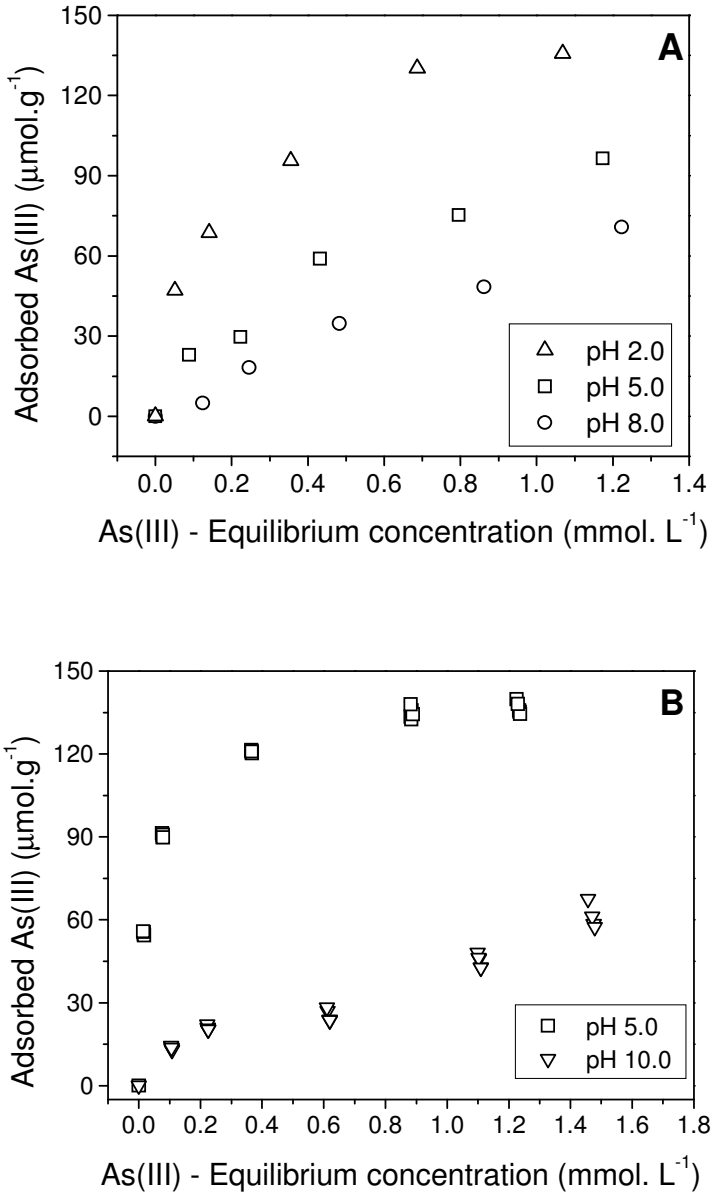

Figure 2.2. Influence of pH on As (III) adsorption, (A) SAM procedure, (B) Flask tests (biomasss, 2g/L; temperature, 25±1°C).

In 1930, Johnson and Voegtlin described As/cysteine ML3 complexes. Their respective stability constants and the As (III)/Cys speciation diagrams were described later by Reyes (Rey, et al., 2004) and showed that at equal arsenic and cysteine concentrations (0.015mol/L) almost 20% of the present As (III) atoms are complexed with almost 60% of the existent cysteine molecules at pH values between 2.5 and 7.0. The other 80% As remained as the neutral arsenic species, $As(OH)_3$. As pH increases and the hydroxyl concentration becomes greater, the negatively charged arsenic species $As(OH)_2O^-$ are formed and stoichiometry of the complexation reaction is changed. Now, hydroxyl groups compete with thiol groups and as a consequence, cysteine molecules are dislocated from the arsenic coordination shell. The resultant complex is the negatively charged $[As(HCys)(OH)O]^-$. At pH 8-9.5 the predominant species is the negatively charged complex with an As/Cys proportion of 1:1. Both As/Cys complexes show trigonal-pyramidal geometry. However, in the negatively charged complex, arsenic inner coordination shell involves two hydroxil groups as ligands, one of them in a non-protonated form (Rey*, et al.*, 2004).

Experimental data obtained for arsenic adsorption at pH values higher than 5.0 corroborate those theoretical considerations (Figure 2.2), Obtained isotherms do not follow the Langmuir adsorption equation and demonstrate that as As uptake is lower when compared to the data obtained under more acid conditions. This behaviour should be explained by the fact that at pH 8 and 10, the neutral arsenic species are replaced by the anionic species producing different adsorption complexes.

Arsenic uptake (Q_{max}) of 173.6 or 135.1 $\mu mol.g^{-1}$ obtained at pH 2.0 and 5.0, respectively, are promising and greater than those values obtained with kaolinite and montmorillonite, 1.33 and 2.66 $\mu mol.g^{-1}$, respectively (Griffin, et al., 1977); alumina, 2.66 $\mu mol.g^{-1}$ (Gupta*, et al.*, 1978); goethite, 39.9 $\mu mol.g^{-1}$ (Deschamps*, et al.*, 2003). Ladeira and co-works in 2001 reported significant uptakes by thermally activated gibbsite, 337.82 $\mu mol.g^{-1}$. Others workers (Driehaus*, et al.*, 1995; and Meng, et al., 2002) also obtained higher arsenic

adsorption capacities (266-532 μmol.g^{-1}) but, in both cases, As (III) was previously oxidized to As (V). The very high value (920.4 μmol of As (III) per gram of Mo reported by Dambies and co-workers in 2002 using a chitosan derivative biosorbent impregnated with molybdenum, can not be compared to other reported results in view of the lack of information with regard to the used quantities (mass) of biosorbent used.

Despite the best adsorption capacity achieved at pH 2.0, a pH of 5.0 was chosen for all the subsequent experiments, as this pH value is more consistent with conditions often found in natural wastewater.

The selectivity towards As (III) shown in Table II. 1, is corroborated by the results shown in Figure 2.3; the good fit of the experimental data to the linear form of Langmuir equation is also depicted (the calculated correlations factors were higher than 0.99). The great majority of As sorbents described in literature are active for both the pentavalent and the trivalent species, the main difference being the relatively higher remobilization of the latter by aqueous solutions.. Under conditions of pH 5.0, I=0.1, biomass concentration of 2.0g.L^{-1}, the Q_{max} obtained in the presence (260.35 μmol.g^{-1}) and absence of phosphate ions (265.35 mol/L) are quite similar (Figure 2.3). Therefore, the well-described competition between arsenic and phosphate during sorptive experiments using biosorbents or resins (Korngold, et al., 2001; Dambies*, et al.*, 2002) is not observed when the fibrous protein rich biomass is utilised for As (III) uptake.

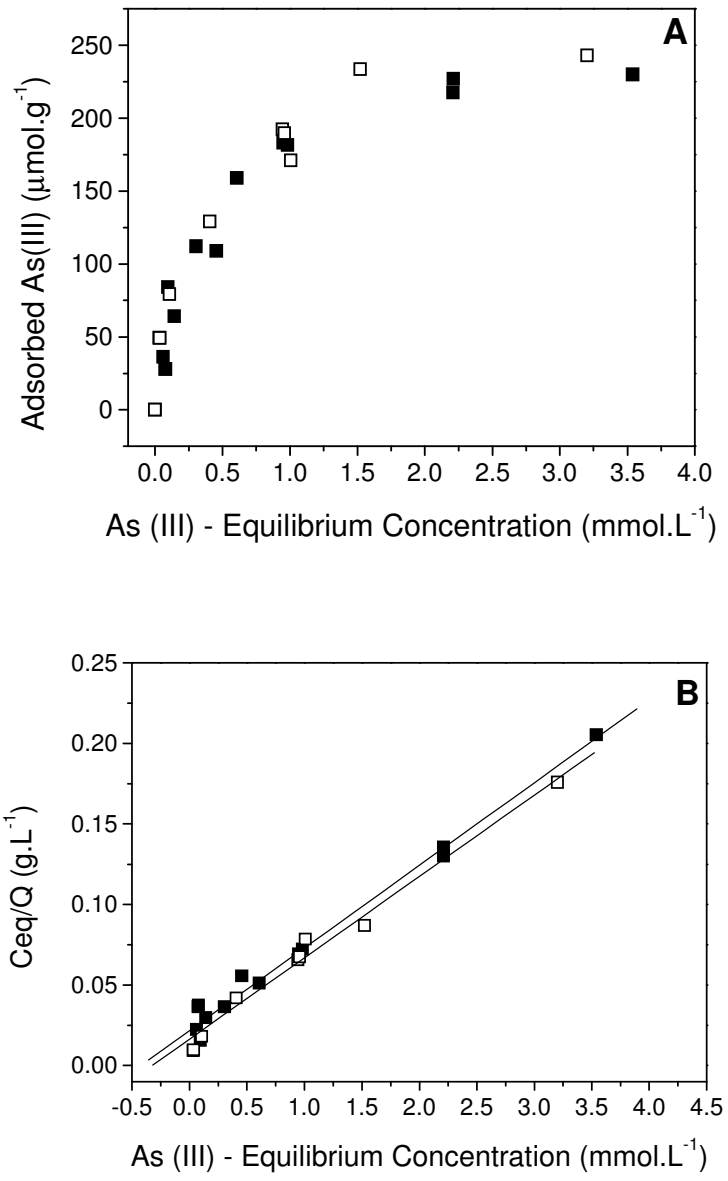

Figure 2.3. Influence of phosphate ions on As (III) adsorption isotherms in the presence (solid squares) or in the absence (open squares) of Phosphate 0.01 mol.L^{-1}. SAM procedure, I = 0.1; pH=5; biomass, 2g/L; temperature, 25±1°C)

Both phosphate and arsenate molecules have the same tetrahedral geometry, which could explain their chemical similarity and their similar affinities for the same chemical ligands. Conversely, arsenite ions possess a trigonal pyramidal geometry. It is possible that a steric hindrance may contribute to the rejection of the tetraedric arsenate and phosphate oxyanions on the biomass adsorptive sites.

X-Ray Absorption Near Edge Structure (XANES) and Extended X-Ray Absorption Fine Structure (EXAFS), provide information that could not be otherwise obtained through the traditional surface analyses techniques. XANES spectra offer electronic and structural information, such as oxidation state, with regard to adsorbed ion (photoabsorbing ion). EXAFS provides information, e.g. the coordination number and interatomic distance, about the nature and position of the neighbour atoms in the coordination shell of the photoabsorbing ion (arsenic, in our case). Thanks to XANES and EXAFS it is now possible to identify the variations inside the arsenic coordination shell caused by adsorption onto cysteine rich biomass. The analysis of the EXAFS data from the arsenite-loaded biomass is illustrated in Figures 4 to 6. The As (III)-biomass EXAFS spectrum is presented in Figure 2.4. The averaged data from seven different spectra were converted to an eV energy unit and then had its background line extracted. The experimentally obtained K edge value (E_0) was found as 11,868 eV, the same obtained for the arsenite standard sample, confirming that arsenite was not oxidized by the biomass. XANES spectra (data not shown) validated this value and the trivalent state of arsenic atoms. The spectrum oscillations caused by all the atoms in the neighbouring coordination shells are also presented. This spectrum was submitted to Fourier Transform, thus allowing the identification of one amplified peak that corresponds to the first Arsenic coordination shell (Figure 2.5).

The signal obtained after submitting this data to another Fourier Transform treatment results in one spectrum that represents only the oscillations caused by the atoms in the As first coordination shell. At this point, it is possible to calculate the structural parameters such as interatomic distance between As and atoms in the first coordination shell,

coordination number as well as to identify the "first neighbour" ligand. By adjusting the experimental data with the theoretical model provided by the FEFF program (Figure 2.6) it was possible to confirm that sulphur is the retro-scattering atom. It was also possible to determine that each arsenic atom is bound to three sulphur atoms. The final structural parameters obtained in the analyses were coordination number (n) = 2.52±0.4 and interatomic distance (R) = 2.26±0.01 Å.

The structural parameters obtained during this work are quite different from those obtained by arsenic adsorption on inorganic matrices. As arsenic is adsorbed as an oxyanion, often as a bidentate binuclear complex, the element found in the first coordination shell is always oxygen, in coordination numbers (n) varying from 3.6-4 and interatomic (R) distances in a range of 1.72 to 1.78 Å. The metal ligands (Fe or Al) are found in the second coordination shell with R values often greater than 3.0 Å (Farquhar, et al., 2002).

The coordination number and interatomic distance obtained in the present study are, as expected, very similar to those reported in EXAFS analyses of biological As (III)/protein complexes, showing As atoms directly bound to S atoms in the first coordination shell. Each As atom is bound to the sulphur atoms coming from three different cysteine residues, R values vary from 2.20-2.25 Å (Bhattacharjee and Rosen, 1996; Shi, et al., 1996; Farrer, et al., 2000; Pickering, et al., 2000; Bennett, et al., 2001). The information provided by XAS analyses is consistent with the strong arsenic uptake reported here. The results explain that rather than adsorbed as a counter ion, or specifically adsorbed as arsenous species in the inner Helmoltz plane, As (III) undergoes a chemical reaction leading to dehydration of H_3AsO_3 molecule.

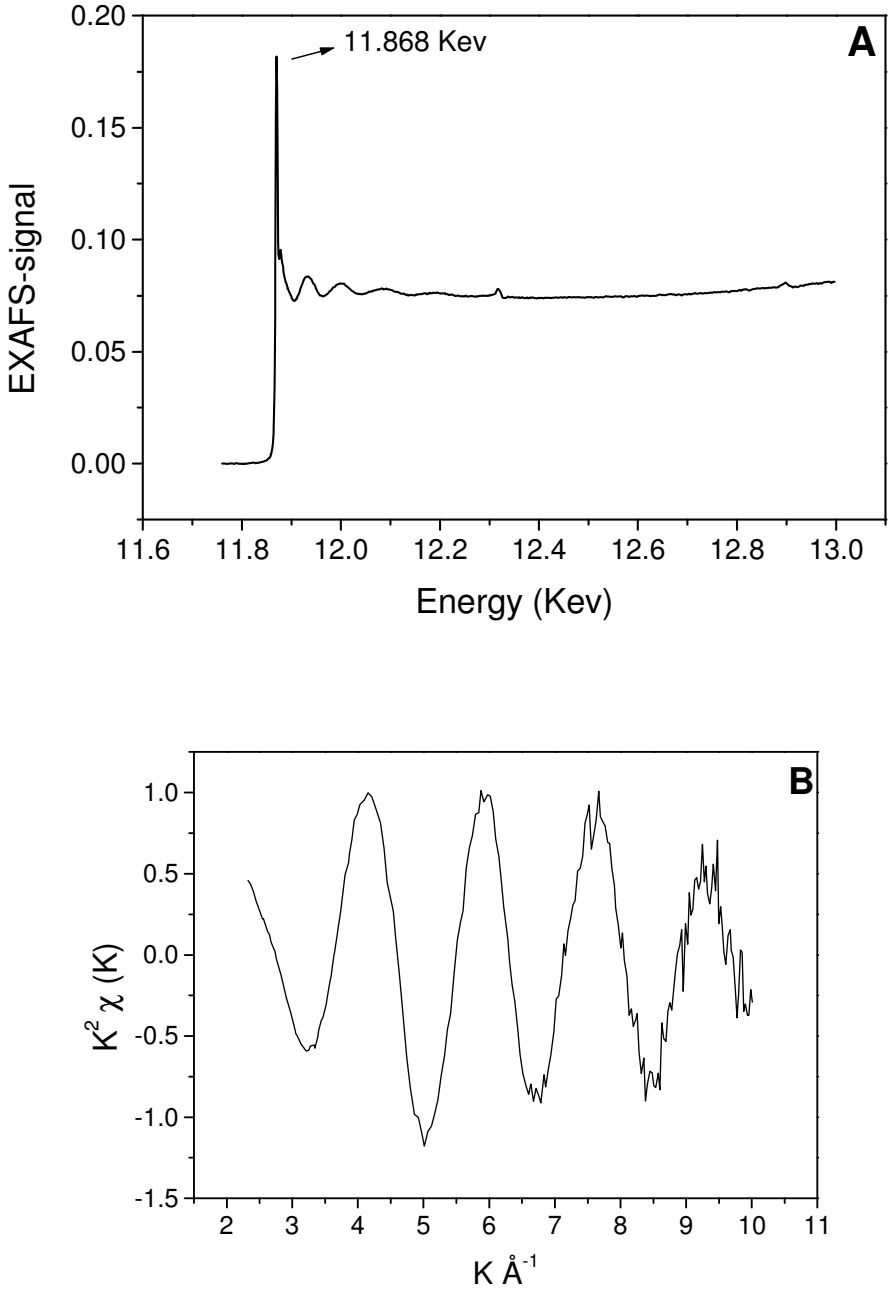

Figure 2.4. EXAFS signal of As (III) ($AsNaO_2$) adsorbed onto biomass, after background correction.

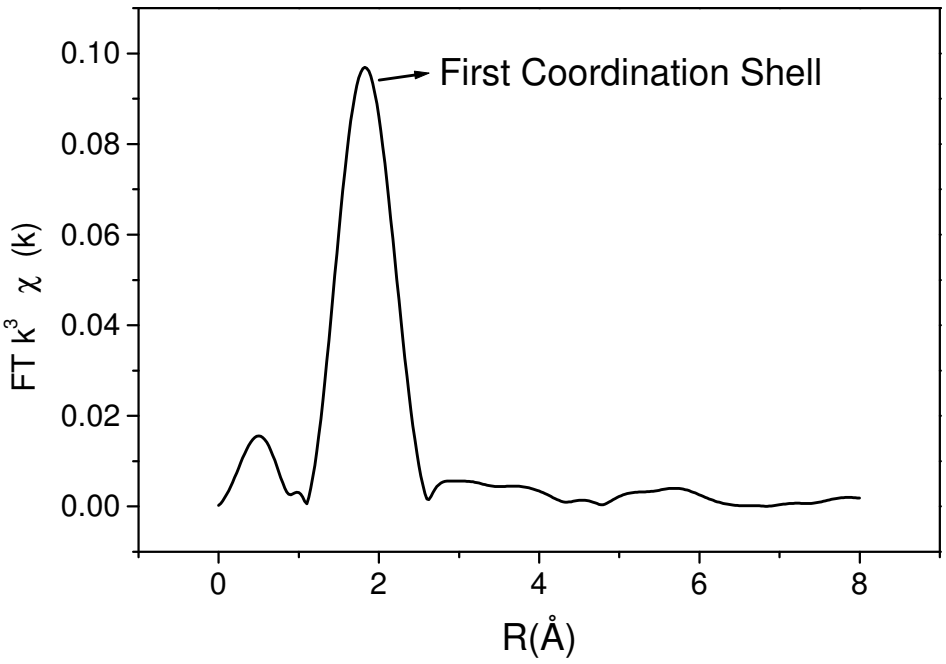

Figure 2.5. Fourier Transform amplitude (K=3). Radial distribution functions for As(III) adsorbed onto biomass.

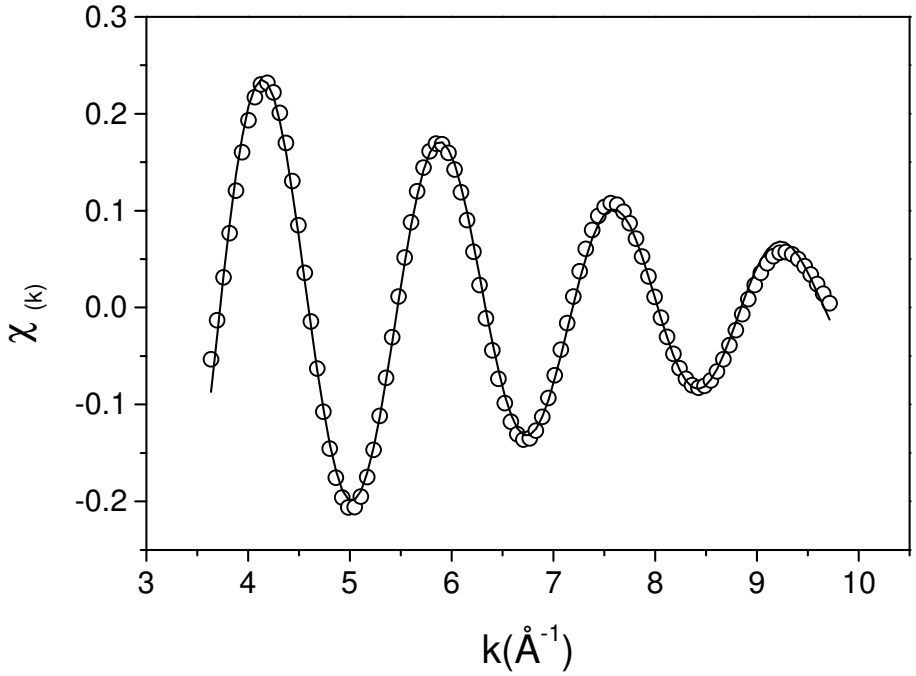

Figure 2.6. Back Fourier Transform (K-space), first coordination shell. Best fit of EXAFS data to As (III) adsorbed on biomass. Experimental data were fitted to hypothetical As/S complex using FEFF 6.0. Scatter and line curves represent experimental and theoretical data, respectively. Structural parameters obtained are R=2.26±0.01Å, n=2.5±0.4, E_0=6.87 and σ^2=0.002.

Based on these findings, the following equation is proposed to describe arsenite adsorption by fibrous protein biomass:

$$H_3AsO_3 + 3B\text{-}CysSH \rightarrow As(B\text{-}CysS\text{-})_3 + 3H_2O \qquad (2.2)$$

where *B* represents the biomass matrix.

This adsorption mechanism is supported by the structural similarities between As (III)/biomass complex and those natural complexes formed between Arsenic atoms and Ars Operon proteins (Kaur and Rosen, 1992; Bhattacharjee*, et al.*, 1996; Shi*, et al.*, 1996; Farrer*, et al.*, 2000; Bennett*, et al.*, 2001), phytochelatins (Pickering*, et al.*, 2000; Schmoger, et al., 2000) or cysteine and glutathione (Knowles*, et al.*, 1983; Farrer*, et al.*, 2000; Hughes, 2002; Mukhopadhyay*, et al.*, 2002), previously identified. Finally, it may be stressed that the adsorption phenomenon studied here involves a chemical reaction between the dissolved arsenite ions and the sulphydril groups of biomass, strong enough to dislocate oxygen atoms from the arsenic atom first coordination shell in arsenous acid molecules. These facts explain the specificity of this tested biosorbent with respect to the trivalent species of arsenic as well as its minor affinity for phosphate and arsenate ions. Our findings are consistent with the statements of Farrer (Farrer*, et al.*, 2000): "As (III) is able to distort polypeptide structure in order to satisfy its desire to form trigonal-pyramidal thiolate coordination" and "Arsenic causes structural distortion and aggregation in biopolymers, an action which may be involved in the mechanism of arsenic toxicity".

2.4 CONCLUSIONS

The features of the model proposed to explain As (III) adsorption onto the selected fibrous, protein-rich biomass can be summarized as follows. Sulphydril reduced groups are the active groups involved in arsenic biosorption. Uptake increases as pH decreases; phosphate ions do not compete with arsenite ions for the biomass' active sites. Arsenic (III) uptake involves an inner sphere complexation phenomenon that takes place within the As first coordination shell. Three water molecules are released while the arsenic atom directly binds to the sulphydril groups. XAS analyses indicated that each arsenic atom is bound directly to three sulphur atoms from the reduced cysteine aminoacids. The arsenic/sulphur interatomic distance was found to be 2.26 ± 0.01 Å. Finally, the specificity of the biosorbent dispenses the need for previous As (III) oxidation.

2.5 REFERENCES

Acharyya, S. K.;Chakraborty, P.;Lahiri, S.;Raymahashay, B. C.;Guha, S. and Bhowmik, A. (1999). Arsenic poisoning in the Ganges delta. *Nature*, 401, p. 545.

Bennett, M. S.;Guan, Z.;Laurberg, M. and Su, X.-D. (2001). *Bacillus subtilis* arsenate reductase is structurally and functionally similar to low molecular weight protein tyrosine phosphatases. *PNAS*, 98, p. 13577-13582.

Bhattacharjee, H. and Rosen, B. (1996). Spatial Proximity of Cys 113, Cys172, and Cys 422 in the Metalloactivation Domain of the ArsA ATPase. *The Journal of Biological Chemistry*, 271, p. 24465-24470.

Bostick, B. C. and Fendorf, S. (2003). Arsenite sorption on troilite (FeS) and pyrite (FeS_2). *Geochimica et Chosmochimica Acta*, 67, p. 909-921.

Chakraborti, D.;Rahman, M. M.;Paul, K.;Chowdhury, U. K.;Sengupta, M. K.;Lodh, D.;Chanda, C. R.;Saha, K. C. and Mukherjee, S. C. (2002). Arsenic calamity in the Indian subcontinent. What lessons have been learned? *Talanta*, 58, p. 3-22.

Chowdhury, T. R.;Basu, G. K.;Mandal, B. K.;Biswas, B. K.;Samanta, G.;Chowdhury, U. K.;Chanda, C. R.;Lodh, D.;Roy, S. L.;Saha, K. C.;Roy, S.;Kabir, S.;Quamruzzaman, Q. and Chakraborti, D. (1999). Arsenic poisoning in the Ganges delta. *Nature*, 401, p. 545-546.

Dambies, L.;Vincent, T. and Guibal, E. (2002). Treatment of Arsenic-Containing Solutions using Chitosan Derivatives: Uptake Mechanism and Sorption Performances. *Water Research*, 36, p. 3699-3710.

Deschamps, E.;Ciminelli, V.;Weidler, P. G. and Ramos, A. Y. (2003). Arsenic sorption onto soils enriched with manganese and iron minerals. *Clays and Clay Minerals*, 51, p. 198-205.

Dixit, S. and Hering, J. g. (2003). Comparision of Arsenic(V) and Arsenic(III) Sorption onto Iron Oxide Minerals: Implications for Arsenic Mobility. *Environmental Science and Technology*, 37, p. 4182-4189.

Driehaus, W.;Seith, R. and Jekel, M. (1995). Oxidation of Arsenate(III) with Manganese Oxides in Water Treatment. *Water Research*, 29, p. 297-305.

Farquhar, M. L.;Charnock, J. M.;Livens, F. R. and Vaughan, D. J. (2002). Mechanisms of Arsenic Uptake from Aqueous Solution by Interaction with Goethite, Lepidocrocite, Mackinawite and Pyrite: An X-ray Absorption Spectroscopy Study. *Environmental Science &Technology*, 36, p. 1757-1762.

Farrer, B. T.;McClure, C. P.;Penner-Hahn, J. E. and Pecoraro, V. L. (2000). Arsenic (III)-Cysteine Interactions Stabilize Three-Helix Bundles in Aqueous Solution. *Inorganic Chemistry*, 39, p. 5422-5423.

Flessel, P.;Furst, A. and Radding, S. B. (1980). A comparison of carcinogenic metals. In: Siegel, H. *Carcinogenicity and metal ions*. New York, Marcel Dekker, Inc. 10: p. 22-54.

Goldberg, S. and Johnston, C. T. (2001). Mechanisms of arsenic adsorption on amorphous oxides evaluated using macroscopic measurements, vibrational spectroscopy and surface complexation modeling. *Journal of Colloid and Interface Science*, 234, p. 204-216.

Griffin, R. A.;Frost, R. R.;Au, A. K.;Robinson, G. D. and Shimp, N. F. (1977). Attenuation of pollutants in municipal landfill leachate by clay minerals. *Environmental Geology Notes*, 79, p. 1-47.

Gupta, S. K. and Chen, K. C. (1978). Arsenic removal by adsorption. *Journal of Water Pollution Control Federation*, 50, p. 493-506.

Hughes, M. F. (2002). Arsenic Toxicity and Potential Mechanisms of Action. *Toxicology Letters*, 133, p. 1-16.

Johnson, J. M. and Voegtlin, C. (1930). Arsenic derivatives of cysteine. *Journal of Biological Chemistry*, 89, p. 27.

Kaur, P. and Rosen, B. P. (1992). Plasmid-Encoded Resistance to Arsenic and Antimony. *Plasmid*, 27, p. 29-40.

Knowles, F. C. and Benson, A. A. (1983). The biochemistry of arsenic. *TIBS*, 8, p. 178-179.

Korngold, E.;Belayev, N. and Aronov, L. (2001). Removal of Arsenic from Drinking Water by Anion Exchangers. *Desalination*, 141, p. 81-84.

Ladeira, A. C. Q.;Ciminelli, V. and Paniago, E. B. (2001b). The use of Al-based adsorbents for mitigation of arsenic contamination. In: VI Southern Hemisphere Meeting on Mineral Technology, 2001b, Rio de Janeiro. CETEM/MCT, Maio 2001. p. 549-554

Ladeira, A. C. Q. and Ciminelli, V. S. T. (2004). Adsorption and desorption of arsenic on an oxisol and its constituents. *Water Research*, 38, p. 2087-2094.

Mandal, B. K. and Suzuki, K. T. (2002). Arsenic Round the World: a Review. *Talanta*, 58, p. 201-235.

Meng, X.;Korfiatis, G. P.;Bang, S. and Bang, K. W. (2002). Combined Effects of Anions on Arsenic Removal by iron Hydroxides. *Toxicology Letters*, 133, p. 103-111.

Mukhopadhyay, R.;Rosen, B. P.;Phung, L. T. and Silver, S. (2002). Microbial Arsenic: from Geocycles to Genes and Enzymes. *FEMS Microbiology*, 26, p. 311-325.

Nickson, R.;McArthur, J.;Burgess, W.;Ahmed, K. M.;Ravenscroft, P. and Rahman, M. (1998). Arsenic poisoning of Bangladesh groundwater. *Nature*, 395, p. 338.

Nies, D. H. (1999). Microbial heavy-metal resistance. *Apllied Microbiology Biotechnology*, 51, p. 730-750.

Pagnanelli, F.;Papini, M. P.;Trifoni, M.;Toro, L. and Veglio, F. (2000). Biosorption of metals ions on Arthrobacter sp.: biomass characterization and biosorption modeling. *Environmental Science Technology*, 34, p. 301-316.

Pickering, I. J.;Price, R. C.;George, M. J.;Smith, R. D.;George, G. N. and Salt, D. E. (2000). Reduction and Coordination of Arsenic in Indian Mustard. *Plant Physiology*, 122, p. 1171-1177.

Rey, N. A.;Howarth, O. W. and Maia, E. C. P. (2004). Equilibrium characterization of the As(III)-cysteine and the As(III)-glutathione systems in aqueous solution. *Journal of Inorganic Biochemistry*, 98, p. 1151-1159.

Schmoger, M. E. V.;Oven, M. and Grill, E. (2000). Detoxification of Arsenic by Phytochelatins in Plants. *Plant Physiology*, 122, p. 793-801.

Shi, W.;Dong, J.;Scott, R. A.;Kasenzenko, M. Y. and Rosen, B. (1996). The Role of Arsenic-Thiol Interactions in Metalloregulation of the ars Operon. *The Journal of Biological Chemistry*, 271, p. 9291-9297.

Singh, T. S. and Pant, K. K. (2004). Equilibrium, kinetics and thermodynamic studies for adsorption of As(III) on activated alumina. *Separation Purification Technology*, 36, p. 139-1478.

Smedley, P. L. and Kinniburgh, D. G. (2002). A review of the source, behaviour and distribution of arsenic in natural waters. *Apllied Geochemistry*, 17, p. 517-568.

Treagan, L. (1983). Metals and Immunity. In: Siegel, H. *Methods Involving Metal Ions and Complexes in Clinical Chemistry*. New York, Marcel Dekker, Inc. 16: p. 47-83.

Veglio, F. and Beolchini, F. (1997). Removal of metals by biosorption: a review. *Hydrometallurgy*, 44, p. 301-316.

Vink, B. W. (1996). Stability relations of antimony and arsenic compounds in the light of revised and extended Eh-pH diagrams. *Chemical Geology*, 130, p. 21-30.

Weerasooriya, R.;Tobschall, H. J.;Wijesekara, H. K. D. K.;Arachchige, E. K. I. A. U. K. and Pathirathne, K. A. S. (2003). On the mechanistic modeling of As(III) adsorption on gibbsite. *Chemosphere*, 51, p. 1001-1013.

Capítulo 3

Effect of pH on Arsenite Adsorption onto Cysteine-rich Biomass: X-ray Absorption Studies and Density Functional Calculations

3.1 INTRODUCTION

Arsenic (As) is a heavy metal largely disseminated on the earth crust and the 20th mostly abundant element (Mandal and Suzuki, 2002). At normal conditions, arsenic concentrations in surface or ground waters are very low; eventually this naturally occurred arsenic might be dissolved and contaminates water deposits. Depending on the pH and redox potential conditions in the environment, arsenic ions will be oxidized (arsenate) or reduced (arsenite). The mobility of arsenic species in natural environments or under remediation conditions is influenced by its oxidation state. The predominant water-soluble species are the As (III) and As (V) derivatives of the arsenous (H_3AsO_3) and arsenic (H_3AsO_4) acids, respectively. The trivalent species is of great environmental concern not only due to its considerably higher toxicity but also in view of its higher mobility in soils. Even under oxic conditions, both arsenic species occur together due to the fact that As (III) oxidation to As (V) is a kinetically slow process (Weerasooriya, et al., 2003). Thus, chemical speciation of the arsenic has to be taken into account in order to understand its impact in the environment.

In Chapter 2 we discussed the adsorption of arsenite species onto cysteine rich biomass obtained as a waste material from the poultry industry. During the process, arsenic is directly bound to three sulfur atoms available in the cysteine-reduced residues present in the keratin protein of the biomass. It was therefore demonstrated that arsenic (III) uptake involves an inner sphere complexation phenomenon that takes place within the arsenic first coordination shell. Arsenic complexation with cysteine amino acid forming As/cysteine ML3 complexes is well established (Johnson and Voegtlin, 1930). Nevertheless, to our knowledge the application of that concept to arsenic remediation has not been previously reported.

It has been demonstrated that lower the pH, higher the arsenite ions uptake. Therefore, neutral arsenic species (H_3AsO_3) were preferably adsorbed instead of the negatively charged ones. In this case, electrostatic attraction does not explain adsorption. In addition, no pH alteration was observed within the system in view of the fact that the

model assumes that for each arsenite molecule adsorbed onto the biomass three water molecules are released (Teixeira and Ciminelli, 2005). It has been shown in Chapter 2 that arsenic adsorption on the protein-rich biomass is favored at low pH. The results achieved under acid conditions were: 173.6 and 135.1 μmol As (III)/g of biomass at pH 2.0 and pH 5.0, respectively. At pH 10.5 the biomass loading is reduced to approximately 30% of the uptake at pH 2.0.

It is an interesting feature in view of the fact that oxyanions usually exhibit adsorption maxima near the pK_a for the first dissociation (Bostick and Fendorf, 2003). In the case of As (III) species this would imply in maximum adsorption at pH close to 9. The analysis of recently published data for arsenic adsorption on different inorganic materials corroborates the previous statement. Arsenate adsorption on inorganic materials such as soils containing Al or Fe oxides is favored at acid pH while arsenite is preferably adsorbed at pH close to the neutrality or higher than 8.0 (Goldberg and Johnston, 2001; Dixit and Hering, 2003; Ciminelli, et al., 2004; Singh and Pant, 2004). Arsenic acid (H_3AsO_4) pKa values are 2.19, 6.94 and 11.5. Arsenite adsorption onto zinc or lead sulfides also increases with pH (Bostick*, et al.*, 2003).

Concerning arsenic adsorption on organic materials there are few examples of biosorbents reported for adsorption of arsenate and arsenite ions. Some rechearches (Manju, et al., 1998) related the use of "*copper impregnated coconut husk carbon (CICHC)*" for adsorption of arsenite ions; maximum uptake was achieved at pH 12.0 or higher. Another interesting experience was described by Dambies and coworkers in 2002, they succeed in adsorbing trivalent and pentavalent arsenic species using "*molybdate coagulated chitosan beads (MCCB)*". However, comparing arsenate and arsenite uptake one concludes that the highest uptake obtained for the adsorption of the trivalent species at pH values between 3.0 and 5.0 is one third of the maximum uptake of the pentavalent ion obtained at pH 5.5. In both cases, the uptake mechanisms involve the participation of metal ions. Cu or Mo were the binding atoms for arsenic; and the positive charges on the biomass surface provided by the adsorbed copper hydroxide (*CICHC*) or by the protonated amino groups (*MCCB*) stabilized the adsorptive complex

with the negatively charged arsenic species. A "*phosphorylated cross linked orange waste (POW)*" loaded with Fe (III) was recently tested for arsenic adsorption (Ghimire, et al., 2003). Arsenate adsorption was favored at pH 3.0 while arsenite was better adsorbed at pH 10.0 and, once more, with the need of a metal binding atom. Loukidou and coworkers (Loukidou, et al., 2003) suggested the utilization of a chemically modified non-living fungal biomass of *P. chrysogenum* for As (V) adsorption. The proposed adsorption mechanism involved electrostatic interactions; the biomass presented a positive surface charge and arsenic adsorption was more effective at pH 3.0.

In this present work, XANES and EXAFS techniques together with Density Functional Calculations are been used to study the As (III) adsorption on treated chicken feathers at a molecular level. XANES spectra were collected and analyzed in order to confirm the oxidation state of arsenic while EXAFS analysis were performed to provide detailed information about the neighborhood of the arsenite adsorbed ion. By fitting the experimental spectra to the theoretical data it is possible to identify the elements, the coordination number (CN), the interatomic distances (R), and the Debye-Waller factor (σ^2) for the first coordination shell of the As atom.

The interaction of As (III) and cysteine in a homogenous solution has been studied by means of potentiometric and spectrophotometric techniques, showing that species 1:3 metal/ligand are the most prevalent species (Rey, et al., 2004) in the usual pH range. The association of some classic statements (Johnson*, et al.*, 1930) with the recent data provided by Rey and coworkers led us to postulate the formation of similar As (III)/Cys complexes during arsenite adsorption on cysteine-rich biomass. In our laboratory, the interatomic distance between sulfur and arsenic centers was investigated by Expanded X-Ray Absorption Fine Structure (EXAFS) analysis and the obtained result (Teixeira*, et al.*, 2005) are in agreement with the As $(Cys)_3$ species on the surface and with the studies in solution performed by Rey and coworkers. At the same time some theoretical predictions of As (III)/Cys complexes structure were performed using Density Functional Method (DFT). DFT studies allow us to explore the potential energy surface where the atoms move. The minima on the surface correspond to the equilibrium geometry. The interaction of arsenious acid (H_3AsO_3) with cysteine has been studied

using the LCGTO-KS-DF (Linear Combination of Gaussian Type Orbital-Kohn Sham-Density Functional) method implemented in deMon-2002 program (Koester, et al., 2002).

Combining all those techniques, the initial study described in Chapter 2 is now expanded with the aim to investigate the effect of pH on the mechanism of As (III) uptake.

3.2 MATERIALS AND METHODS

3.2.1. Materials

White chicken feathers were rinsed thoroughly with warm tap water and dried at 45 ±5°C for 24 hours. The dried material was ground and sieved to obtain a size range below 0.037 mm (400 Mesh Tyler). Biomass activation was accomplished by adding 10 ml of a 7.8 % (w/w) basic ammonium thioglycolate solution. This treatment did not imply any mass loss. After this activation step, the powdered biomass was filtered in a 45μm cellulose membrane, washed with 100 mL of Milli-Q water and used for the adsorption tests and for the spectroscopic analyses as well.

All solutions were prepared with analytical grade chemicals and Milli-Q water. As (III) stock solutions of 10,000 mg/L were prepared with a sodium meta-arsenite salt ($AsNaO_2$) (Fluka, 99.0%). The pH values were adjusted with 0.1 or 0.01 N HCl or NaOH solutions. Arsenic adsorption experiments were carried out according to the conditions described previously (Teixeira*, et al.*, 2005).

3.2.2 X-Ray Absorption Experiments

X-Ray absorption Near Edge Structure (XANES) and Extended X-Ray Absorption Fine Structure (EXAFS) analyses of wet biomass loaded with As (III) were performed. XANES and EXAFS data from the arsenic K-edge (11,868 eV) were obtained at XAS workstation, under operation conditions of 1.37 GeV and beam currents of about 200 mA. All spectra were recorded at room temperature using a Si (111) double crystal monochromator with an upstream vertical aperture of 0.4 mm. Arsenic K-edge X-Ray absorption spectra were measured by monitoring the transmitted energy using a 15-element Ge detector (Canberra Industries). Wet solid samples were fixed onto steel holders, sealed with Kapton tape film and placed at an angle of 45° to the incident beam. The energy resolution utilized was 0.7 eV at the XANES region (11,855-11,900 eV); 2 eV between 11,820 and 11,855 eV and 1 eV between 11,900 and 12,020 eV. Therefore XANES and EXAFS spectra were simultaneously obtained. Counting times of 4 s were kept constant. At least five spectra were collected and averaged for XANES and EXAFS analysis.

After background correction, the spectra have been normalized using the Origin 6.0 software and analyzed by Winxas 2.0 software. Experimental As (III) adsorbed spectra obtained at different adsorption pH were compared to the spectra of arsenate (Na_2HAsO_4) and arsenite ($AsNaO_2$) standards. Experimental spectra were fitted to different combinations of reduced (arsenite) or oxidized (arsenite) spectra and the proportions of both curves were determined.

After averaging, spectra were submitted to a background correction using a Victorian function and then normalized to unity. To isolate the EXAFS signal a 4-point cubic spline function was used. The energy (KeV) was transformed to k-range ($Å^{-1}$) using the arsenic K edge value (E_0) graphically determined. All the χ k spectra were weighted by k^3 to amplify the upper k-range and Fourier-Transformed to produce a Radial Structure

Functions using a Δk of approximately 7.0 Å (from ~2.8-9.8 Å). After that, the first coordination shell of each Radial Structure Function (RSF) was back-transformed to isolate the spectral contributions of As neighbor atoms in this shell. The Winxas software package was used for EXAFS data analysis. Final data fit was obtained using phase and amplitude functions derived from FEFF 6.01 software simulating the occurrence of the pair As-S at the adsorption site. Biomass samples analyzed by XAS were loaded with approximately 14 mg of arsenite for each gram of biomass at pH 4.5; at pH 10.5 the biomass loading is reduced to approximately 30% of the uptake at acid pH.

3.2.3 Computational Approach

The generalized exchange correlation (XC) functional has been used with the Becke expression (Becke, 1988) for exchange and that of Perdew (Perdew, 1986) for correlation (GGA-BP). For the arsenic atoms the basis set have the contraction pattern (63321/5321/41*). For oxygen atoms, the basis sets have the contraction pattern (621/41/1*) and hydrogen atoms the contraction pattern (41*/1). Auxiliary basis sets have been used for fitting the density and XC potential. The auxiliary basis sets (3,5) have been used for arsenic center, (4,3) for oxygen atoms and (3,1) for hydrogen atoms. The orbital and auxiliary basis sets have been optimized explicitly for DFT calculations by Godbout *et al.* (Godbout, et al., 1992). The calculation of the expansion coefficients of the approximated density is described in detail elsewhere (Koester*, et al.*, 2002). The numerical integration is based on the partition scheme of Becke (Becke, 1987) in an adaptive grid. All structures have been fully optimized using the BFGS (Schlegel, 1987) method.

3.3 RESULTS

It has been shown in Chapter 2 that arsenic adsorption on the protein-rich biomass is favored at low pH. The results achieved under acid conditions were: 173.6 and 135.1 μmol As (III)/g of biomass at pH 2.0 and pH 5.0, respectively. At pH 10.5 the biomass loading is reduced to approximately 30% of the uptake at pH 2.0.

The $As(OH)_3$ molecule is protonated up to the pH 9.0 (pK_{a1} = 9.2). Cysteine pKs are approximately 1.67, 8.17 and 10.30 for RCOOH, RSH and RNH_3^+ groups (Bhattacharjee, et al., 2004). Therefore, the biomass' SH groups will deprotonate at pH lower than 9.2, which may become an obstacle for the sulfur atom to act as a ligand for arsenite. The main point is that pH variation may influence both, the adsorbate and the adsorbent and therefore, to fully understand arsenic adsorption onto cysteine rich biomass, the effect of this variable should be taken into account.

The alterations on arsenic first coordination shell during adsorption of arsenite onto cysteine-rich biomass under different pH conditions, are investigated by means of X-Ray absorption Near Edge Structure (XANES) and Extended X-Ray Absorption Fine Structure (EXAFS).

3.3.1. X-Ray spectroscopy

Figure 3.1 shows the XANES spectra of the As (III) loaded biomass at pH 4.5, 7.0 and 10.5. One could observe that the As k-edge energy threshold for As (III) standard sample was almost 4 eV lower than the value obtained for the As (V) standard. No oxidation of arsenite was observed during arsenic adsorption under neutral or acid pH conditions. One may also observe that the energy threshold for the adsorbed arsenite (11,861.2; 11,862.8 and 11,863.5 eV at pH 4.5; 7 and 10.5, respectively) at acid pH, was lower than the value obtained for the As (III) standard sample (11862.9 eV). This

behavior is explained by the fact that in the adsorbed complex, arsenic atoms will be directly bound to sulfur atoms. As oxygen is replaced by sulfur, a decrease in the ligand electronegativity takes place, thus inducing a shift on the As k-edge energy to lower values. This effect was also reported by others (Bostick*, et al.*, 2003) for the arsenic adsorption on PbS and ZnS.

Conversely, the arsenic adsorption at pH 10.5 shows a shift towards to the As (V) standard energy threshold of 11,666.7 eV, thus suggesting the oxidation of arsenite species. A more detailed comparison of the XANES spectra of the adsorptive complex obtained at pH 10.5 with those of the arsenate and arsenite standards confirmed that almost 37% of the initially added As (III) ions are oxidized to As (V). In fact, the kinetics of arsenite oxidation is favored by moderately alkaline conditions.

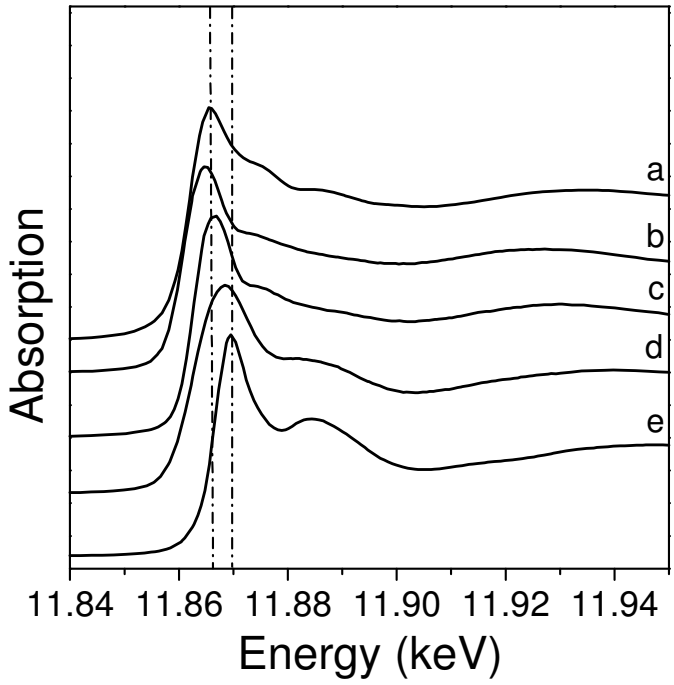

Figure 3.1. XANES spectra of As (III) loaded biomass:(a) arsenite standard; (b) (c) and (d) are relative to arsenite loaded biomass at pH 4.5, 7.0 and 10.5, respectively and (e) arsenate standard.

EXAFS analyses are shown in Figures 3.2 and 3.3 and in Table III.1. Figure 3.2 depicts the three Fourier Transformed (FT) spectra at the arsenic K-edge obtained at adsorption pH of 4.5, 7.0 and 10.5. Analyses were carried out with the original EXAFS data without any previous treatment. Figure 3.2 indicates that the adsorption spectrum under neutral conditions is quite similar to that obtained at acid pH. The lower intensity of the peak corresponding to the arsenic first coordination shell at neutral pH is ascribed to the lower As uptake at this pH. The FT was back transformed and fitted to phase and amplitude parameters for the hypothetical pair As-S. The structural parameters and respective standard deviations are shown in Table III.1. Arsenic adsorbs directly to sulfur atoms on the cysteine molecules, with the lost of three water molecules and no pH variation (Rey*, et al.*, 2004; Teixeira*, et al.*, 2005).Arsenic is adsorbed by the biomass as an inner-sphere complex. Structural parameters obtained experimentally in the present work - coordination number (CN) 2.5-2.7 and interatomic distance of approximately 2.25Å at neutral or acid pH - are in accordance with the results described in Chapter 2 for pH 5.0 and to the theoretical predictions described later in this chapter.

The adsorptive complexes obtained at acid or neutral pH are similar to those pyramidal As/S structures described for As interaction with biological material such as those bonds to the active sites of some enzymes responsible for arsenic resistance and detoxification (Kaur and Rosen, 1992; Bhattacharjee and Rosen, 1996; Farrer, et al., 2000; Bennett, et al., 2001; Messens, et al., 2002); phytochelatins (Pickering, et al., 2000; Schmoger, et al., 2000) or cysteine and gluthathione molecules (Knowles and Benson, 1983; Farrer*, et al.*, 2000; Hughes, 2002; Mukhopadhyay, et al., 2002; Bhattacharjee*, et al.*, 2004). They are also in accordance with inorganic As/S complex obtained by Helz (Helz, et al., 1995), who proposes that in As (III) sulfide solutions arsenite forms oligomers, such as As_3S_6 rings.

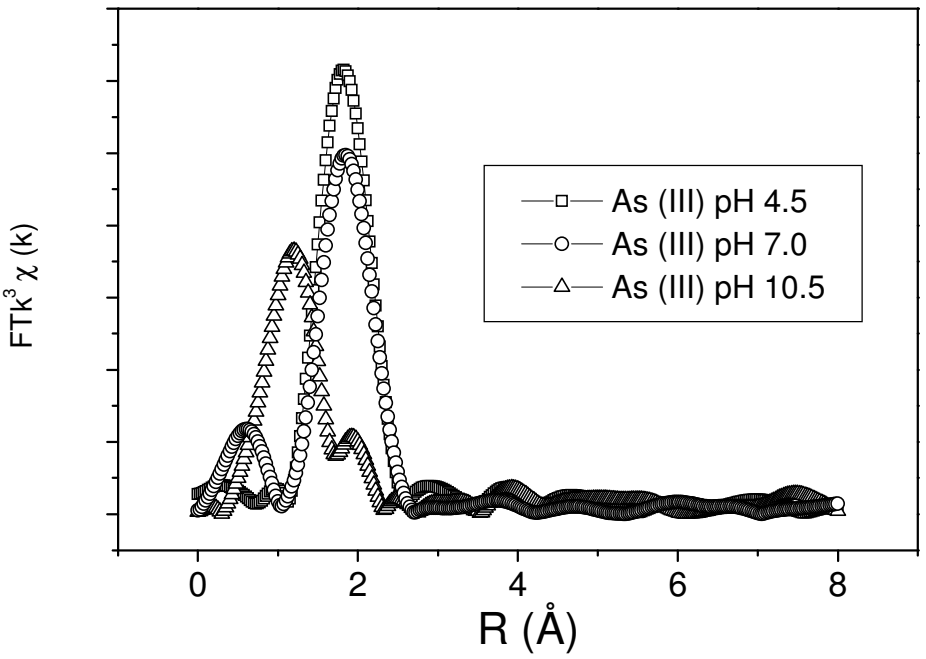

Figure 3.2. Fourier Transform amplitude (K=3). Radial distribution functions for As (III) adsorbed onto biomass at pH 4.5, 7.0 and 10.5. Uncorrected for phase shift.

In fact, each one of those rings consists of three AsS_3 pyramids, joined by two S corners to the other two pyramids. In these oligomers, the experimentally determined As-S and As-As distances are 2.21-2.23 and 3.4-3.5Å. Adsorption of arsenite on PbS and ZnS (Bostick*, et al.*, 2003) produced As-S distances of 2.23-2.52Å. By comparing the As-S distance in realgar, 2.15-2.18Å (Helz*, et al.*, 1995) with the As-S distances shown in Table III.1 it is possible to rule out the precipitation of that sulfide. The As-S interatomic distances in the mineral structure (Helz*, et al.*, 1995; Bostick*, et al.*, 2003) are significantly shorter than the values obtained here assuming adsorption.

Figure 3.2 shows also the FT spectrum produced by the adsorption of arsenite at pH 10.5. By comparing the three spectra, the differences between the results obtained in alkaline with those obtained at neutral and acid pH become evident. The differences are not restricted to the intensity of the peak, that may be explained by the relatively low adsorption observed at basic pH, but also by the occurrence of two "shoulders", one at R value lower than 2.0 Å and a very small one close to R=2.0 Å. This feature is an indication of the co-existence of two different elements in the arsenic first coordination shell when arsenite adsorption is carried out at pH 10.5. It is important to observe that the distance assigned to this second "shoulder" is not big enough to characterize a second coordination shell.

Figure 3.3 shows the EXAFS data fitting using phase and amplitude functions derived from FEFF 6.01 software. The approach simulated the occurrence of two distinct pairs As-S and As-O at the arsenic (arsenite) first coordination shell environment during adsorption at pH 10.5. Under those conditions the structural parameters experimentally obtained for the pairs As-S and As-O are respectively: interatomic distance (R) of 2.31 and 1.626 Å and coordination number (CN) of 0.9 and 2.1 for sulfur and oxygen atoms. The occurrence of only oxygen atoms in the arsenic first coordination shell was also simulated but the fitting was not satisfactory (E_0=12.81).

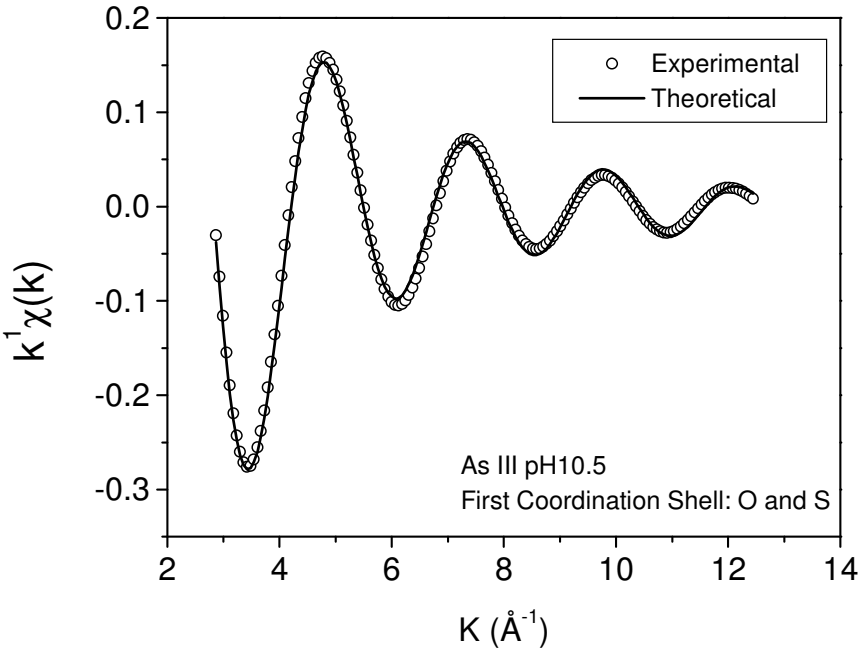

Figure 3.3. Second Fourier Transform (K-space), first coordination shell. Best fit of EXAFS data to As (III) adsorbed on biomass. Experimental data were fitted to hypothetical As-S and As-O pairs using FEFF 6.0. Scatter and line curves represent experimental and theoretical data, respectively. Structural parameters obtained are: R=2.31±0.02 Å, CN=0.92±0.02, E_0=-7±1 and σ^2=0.055±0.005 for As-S and R=1.63±0.0 Å, CN=2.08±0.0, E_0=1.4±0.1 and σ^2=0.00379±0.00015 for As-O.

Table III.1 summarizes the data obtained at various pH values. One may observe that as pH increases, the CN for the As-S pair decreases with the pH while the Debye-Waller factor (σ^2) increases. This parameter has not one absolute value; it offers rather an estimation of the bond length deviation compared to the data adopted for phase and amplitude calculations. As σ^2 is inversely related to the order of the system it is possible to conclude that as pH increases, the degree of order of the adsorptive complex decreases (once more compared to the hypothetical model). The σ^2 obtained at pH 10.5 is 40 times greater than that obtained at acid pH. Hence it means that at basic pH the presence of oxygen atom in the adsorptive complex causes a decrease in the order degree of the system. Farrer and coworkers (Farrer*, et al.*, 2000) stated that As (III) is always able to distort polypeptide structure in order to satisfy its desire to form trigonal-pyramidal thiolate coordination with a 1:3 As/S ratio, justifying in that way the mechanism of arsenic toxicity. However, in that study the authors only considered the physiological pH. Helz (1995) (Helz*, et al.*, 1995) analyzed the molecular structure of an amorphous orpiment ($AsS_{2.86}$) and concluded that its first shell geometry was affected by the sulfur deficiency, i.e. by the increase in the As/S molar ratio. The observed twisting in the orpiment molecular structure was attributed to the occasional replacement of As-S-As by As-As bonds or by As-O-As bridges, causing distortion in the structural sheets.

A similar approach may explain the results obtained at pH 10.5. The high disorder degree detected by σ^2 and the variation on As-S and As-O interatomic distances compared to the experiments done at acid or neutral pH may have been caused by a distortion on the trigonal pyramidal As/S complex structure. The As-S distance increased from 2.25 to 2.31 Å while the arsenic coordination number decreased from ~2.6 to 0.9. We propose that the complexation of arsenite at pH 10.5 will involve the replacement of only one oxygen atom from the negatively charged arsenic species ($H_2AsO_3^-$) by one sulfur atom from the biomass (Table III.1). The loose structure produced by the different interatomic distances of the pairs As-O^-, As-OH and As-S (see Table III.2) and also different bond angles, 92.7° for S-As-S (Bhattacharjee*, et al.*, 1996) and 109.33° for O-As-O bonds (Ferraris and Chiari, 1970), justifies the

occurrence of a twisted less ordered structure, in which two oxygen atoms together with one sulfur atom fulfills the structure of the pyramid.

Table III.1 indicates an As-O interatomic distance of 1.63 Å for the experiments at pH10.5. The As-O distances within the arsenic first coordination shell are typically of 1.8Å for As (III) and 1.68 Å for As (V). According to the literature (Table III.2), these values may vary between 1.67-1.85 Å for arsenite and from 1.62 to 1.88 Å for arsenate. Compared to the typical As (III)-O distances, a shorter distance reported here may be partially explained by the presence of As(V) at pH 10.5, as indicated by XANES measurements. As the EXAFS analyses do not distinguish between the different possible As-O bonds, the obtained result would be an average of the different distances corresponding to the arsenite and arsenate species but, the main responsible for the decrease in the As-O distance is proposed to be the depronation of the hydroxyl groups.

Table III.1 – EXAFS structural parameters obtained for arsenite adsorption onto cysteine rich biomass at different pH values.

		As-S	
	pH 4.5	**pH 7.0**	**pH 10.5**
CN	2.669±0.003	2.516±0.003	0.92±0.02
R	2.2460±0.0001	2.251±0.001	2.31±0.02
σ^2	0.00126±0.00002	0.00276±0.00002	0.055±0.005
E_0	7.016±0.006	7.498±0.007	-7±1
		As-O	
CN	-	-	2.08±0.0
R	-	-	1.6264±0.0007
σ^2	-	-	0.003793±0.00015
E0	-	-	1.4±0.1

Coordination Number (CN) typical error is approximately 30%, while interatomic distance (R) varies within 0.02 Å. Debye Waller (σ^2) represents the variance in R and is correlated with the disorder of the system.

Table III.2 – Interatomic distances between Arsenic and Sulfur or Oxygen atoms. Theoretical and experimental data.

Molecule	Bond Distance (Å)	Bond Angle (degrees)	Observation
	As-S		
$As(SH)_3$	2.236[a]; 2.23[b]	97.3	Calc.
$AsS(OH)(SH)^-$	2.11-2.26[b]		Calc.
$As(OH)(SH)_2$	2.25 [b]		Calc.
$AsS(SH)_2^-$	1x2.119; 2x2.314 2.249(average)		Calc.[a]
$AsS(SH)_2^-$	2.08-2.32		Exp.[a]
$AsS_2(SH)^{2-}$	2x2.176; 1x2.532 2.295(average)		Calc.[a]
AsS_3^{3-}	2.289[a]	107.3	Calc.
AsS_3^{3-}	2.27[a]		Exp.
$As_3S_6^{3-}$ (ring)	2.21-2.314 (As-S) int 2.153-2.159 (As-S)ext	95.8-98.6 ($As\text{-}S_{int}\text{-}As$) 99.6-100.1 ($As\text{-}S_{ext}\text{-}As$)	Exp.[a]
AsIII on PbS	2.48		Exp.[b]
$As(Cys)_3$	2.23[c] 2.24[d,e] 3.2 (S-S)[c]	92.7 (S-As-S)[c]	Biological system Exp.[c,d,e]
	As-O		
As (V)	1.68-1.69[f] 1.661-1.742[g]	109.33 (O-As-O, average) [g]	
	1.62-1.66 [h] 1.75-1.88 (As-OH) [h]		In metal complexes Calc.
As (III)	1.70[b]; 1.83[d]; 1.78[f] 1.67[d] (As=O)		Exp.
$AsS(OH)(SH)^-$	1.81[b]		Calc.
$As(OH)(SH)_2$	1.82[b]		Calc.

[a] (Helz, *et al.*, 1995); [b] (Bostick, *et al.*, 2003); [c](Bhattacharjee, *et al.*, 1996); [d] (Bennett, *et al.*, 2001); [e] (Farrer, *et al.*, 2000); [f] (Arai, et al., 2001); [g] (Ferraris, *et al.*, 1970); [h] (Myneni, et al., 1998).

The data listed in Table III.2, corroborated by the detailed work of Myneni (1998) show clearly that the As-O distance may varies significantly with arsenic speciation, and therefore with pH. Different As-O distances are found for solvated, protonated or metal complexed arsenate molecules (Myneni*, et al.*, 1998).Those experimental and theoretical As-O and As-OH distances point to the fact that regardless of the As oxidation state, As-O distances are always shorter than As-OH distances. Therefore, the As-O distance of 1.63 Å would represent an average of the contributions of the As (III)-O distance on the adsorptive complex $[As(Cys)(OH)O]^-$ and the As (V)-O distance in adsorption complexes, such as $[As(Cys)(OH)O_2]^-$ or $[As(Cys)O_3]^{2-}$. In the latter, arsenic is bound to oxygen by single or double bonds. According to the optimized DFT calculations the As-O distance for the deprotoned species were 1.688 Å for As (III) ($H_2AsO_3^-$) and 1.679 Å for As (V) ($H_2AsO_4^-$). Therefore, both species showed As-O bond distances of the same order magnitude of the EXAFS measurements.

3.3.2 Density Functional Calculations

The interaction of cysteine with As (III) has been studied using Density Functional (DFT) calculations. Cysteine is the amino acid residue available to adsorb As (III) in the treated biomass. However, due to the lack of detailed structural information, it was considered the interaction of the free, gas phase cysteine molecule with As (III) as a model for the adsorption process. Different possible structures for the 1:3, 1:2 and 1:1 As/cysteine complexes have been fully optimized and vibrational analysis performed. All frequencies are real values assuring that a minimum in the potential energy surface has been achieved. Calculated geometrical properties of the most stable structures are shown in Table III.3.

The optimized 1:3 ($As(HL)_3$), 1:2 ($AsOH(HL)_2$) and 1:1 ($As(OH)_2HL$) metal/ligand species are shown in Figure 3.4. Rey *et al.* (2004) had studied the coordination of As (III) by cysteine and estimated the respective stability constants. However, the formation of 1:2 metal/ligand species was not observed in the pH range studied. According to these authors, the species 1:1 is an anion. Considering the pKa's of the

$As(OH)_3$ it is expected that the oxo group from the $As(OH)_2HL$ complex will deprotonate, thus forming the $As(OH)OHL^-$ species in pH above 9.0. In the present work this species was also calculated, since the deprotonation can lead to significant geometry changes. The As-S bond distances increase with the number of cysteine molecules and it is estimated to be about 2.28 Å. The As-OH distance in the H_3AsO_3 is estimated to be about 1.801 Å, and this increases to 1.830 Å in the $As(OH)(HL)_2$. However, the deprotonation of the $As(OH)_2(HL)$, leads to a decrease of the As-O and an increase of the As-S bond distances. The As-O distance is estimated to be 1.688 Å and the As-S distance of 2.450 Å for the deprotonated species. The As-O bond becomes stronger, which increases the charge density on the As center and, in turn, decreases the strength of the As-S bond. A detailed analysis of the bonding mechanism in this species is presently being undertaken in our laboratory.

Table III.3: Geometrical properties of the As/cysteine species. DFT and experimental bond distances in the As(III)/cysteine species.

Species	As-O (Å)	As-S (Å)
H_3AsO_3	1.801	—
$As(OH)OHL^-$	1.688/1.852	2.450
$As(OH)_2(HL)^-$	1.812	2.276
$As(OH)(HL)_2^-$	1.830	2.283
$As(HL)_3$	—	2.287
$As(HL)_3$ experimental[a]	—	2.25

[a] Ref.(Teixeira, *et al.*, 2005).

The coordination ability of the cysteine residues may not be affected by the protein structure surrounding it, in that sense; one could argue that the system might behavior similarly to the interaction of cysteine molecules with As (III) in aqueous solution. Based on this assumption, at pH < 8 the predominant species is expected to be $As(HL)_3$ (Rey *et al.*, 2004). In fact, the EXAFS data at pH 4.5 and 7 do not present the As-O bond. According to our results, the As-S bond distance is approximately 2.287 Å, i.e. 0.041 and 0.036 Å larger than the experimental values obtained at the pH 4.5 and 7.0. The DFT results are in very good agreement with the EXAFS experiments and support

the model in which the sulfydryl groups at the cysteine solid residues are available to coordinate metals, similarly to the reactions in solution. The increase of pH increases the hydroxyl concentration in solution, leading to a competition that favors the 1:1 species. This was discussed by Rey (2002) for complexation in aqueous phase. The presence of an As-O distance in the EXAFS data for the system at pH 10.5 is a strong evidence that the As/biomass behaves similarly. An EXAFS distance of 1.63Å for As-O is typical for the oxo groups, i.e., the deprotonated species. Since that pH is about 10.5 (pKa_1 = 9.2 for the arsenous acid) it is expected that in fact the species will be at least partially deprotonated. DFT calculations for the $As(OH)O(HL)^-$ species estimates the As-O and As-OH bond distances of 1.688 and 1.852 Å A, respectively. The first value is in good agreement with the experimental value of 1.63A. The presence of a As-OH bond distance of 1.852 Å, would cause a broadening in the EXAFS spectra, as observed by the larger value of σ^2. On the other hand, the estimated As-S bond distance of 2.450 Å is about 0.15 Å larger than the expected EXAFS value. This is much larger than the usually error bars of theoretical estimates at the level of theory used. We do not have an explanation for this discrepancy at this moment. However, it is important to observe that the calculation was done for the gas phase and considering the adsorption sites as cysteine molecules while in the biomass, the cysteine residues are immobilized. In addition, pH variation can modify the chemical adsorption sites and their rigidity significantly, thus preventing that the As (III) and sulfydryl groups find their best geometrical arrange.

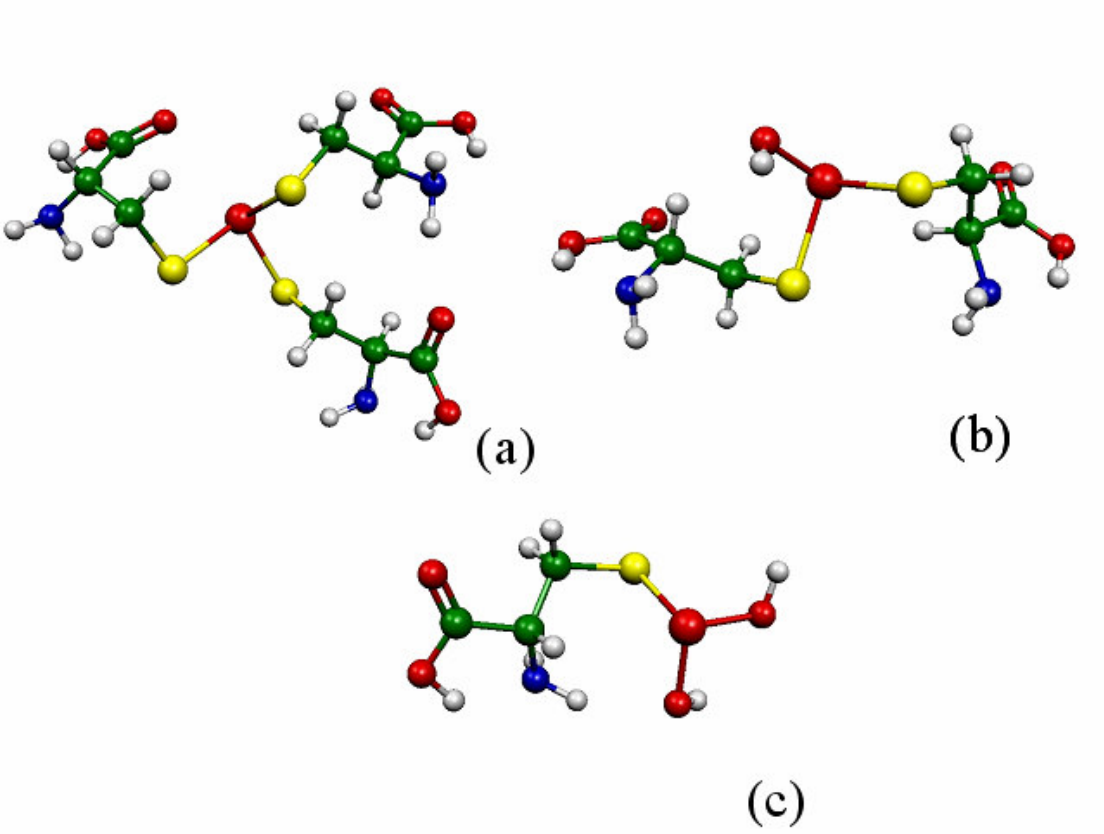

Figure 3.4. DFT optimized structures of the cystein/As (III) system.(a) 1:3 ($As(HL)_3$), (b) 1:2 ($AsOH(HL)_2$) and (c) 1:1 ($As(OH)_2HL$) metal/ligand species.

Colors legend: white, H; green, C; blue, N; red (small) O; yellow, S and red (big), As.

3.4 CONCLUSIONS

The adsorptive complexes formed during arsenite adsorption on protein rich biomass, at different pH, have been determined by a combination of macroscopic measurements with the analysis of structural data provided by X-Ray Absorption Spectroscopy (XANES and EXAFS) and with the theoretical predictions provided by Density Functional Calculations. Under acid or neutral conditions, arsenic atoms are directly bound to sulfur atoms; as pH increases, the sulfur groups may be replaced by the oxo-hydroxyl groups. This mechanism is consistent with the highest As (III) uptake observed under neutral and acid conditions. XAS analyses indicated that the stoichiometry of the As/Cys complex will depend on pH and, in turn, on the arsenous acid speciation. At acid or neutral pH, each arsenic atom is bound directly to three sulphur atoms at the reduced cysteine aminoacids, with the release of three water molecules. The As-S interatomic distance was found to be approximately 2.25 Å. At pH 10.5 a partial oxidation of arsenite to arsenate is observed. In addition, arsenic species become deprotonated. EXAFS and DFT data point to the existence of oxygen and sulfur atoms within the As first coordination shell. At pH 10.5, the As-S and As-O interatomic distances are respectively, 2.3 and 1.63 Å, for the experimental data, and 2.45 and 1.69 Å, for the calculated data. The presence of oxygen causes a distortion in the original trigonal-pyramidal structure of the arsenite adsorption complex, which is corroborated by the increase of the Debye Waller factor.

3.5. REFERENCES

Arai, Y.;Elzinga, E. J. and Sparks, D. (2001). X-ray absorption spectroscopy investigation of arsenite and arsenate adsorption at the aluminum oxide-water interface. *Journal of Colloid and Interface Science*, 235, p. 80-88.

Becke, A. D. (1987). A multicenter numerical integration scheme for polyatomic molecules. *J. Chem. Phys*, 88, p. 2547-2553.

Becke, A. D. (1988). Density-functional exchange-energy approximation with correct asymptotic-behavior. *Phys. Rev. A*, 38, p. 3098-3100.

Bennett, M. S.;Guan, Z.;Laurberg, M. and Su, X.-D. (2001). *Bacillus subtilis* arsenate reductasse is structurally and functionally similar to low molecular weight protein tyrosine phosphatases. *PNAS*, 98, p. 13577-13582.

Bhattacharjee, H.;Carbrey, J.;Rosen, B. P. and Mukhopadhyay, R. (2004). Drug uptake and pharmacological modulation of drug sensitivity

in leukemia by AQP9. *Biochemical and Biophysical Research Communications*, 322, p. 836–841.

Bhattacharjee, H. and Rosen, B. (1996). Spatial Proximity of Cys 113, Cys172, and Cys 422 in the Metalloactivation Domain of the ArsA ATPase. *The Journal of Biological Chemistry*, 271, p. 24465-24470.

Bostick, B. C. and Fendorf, S. (2003). Arsenite sorption on troilite (FeS) and pyrite (FeS_2). *Geochimica et Chosmochimica Acta*, 67, p. 909-921.

Ciminelli, V. S. T.;Ladeira, A. C. Q.;Duarte, H. A. and Oliveira, A. F. (2004). As(III) adsorbed on gibsite: structural model of surface complex based on EXAFS and DFT calculations. *submitted to Geochimica Chosmochimica Acta.*

Dambies, L.;Vincent, T. and Guibal, E. (2002). Treatment of Arsenic-Containing Solutions using Chitosan Derivatives: Uptake Mechanism and Sorption Performances. *Water Research*, 36, p. 3699-3710.

Dixit, S. and Hering, J. g. (2003). Comparision of Arsenic(V) and Arsenic(III) Sorption onto Iron Oxide Minerals: Implications for Arsenic Mobility. *Environmental Science and Technology*, 37, p. 4182-4189.

Farrer, B. T.;McClure, C. P.;Penner-Hahn, J. E. and Pecoraro, V. L. (2000). Arsenic (III)-Cysteine Interactions Stabilize Three-Helix Bundles in Aqueous Solution. *Inorganic Chemistry*, 39, p. 5422-5423.

Ferraris, G. and Chiari, G. (1970). The crystal structure of $Na_2HAsO_4.7H_2O$. *Acta Cryst.*, B26, p. 1574-1583.

Ghimire, K. N.;Inoue, K.;Yamagushi, H.;Makino, K. and Miyajima, T. (2003). Adsorptive separation of arsenate and arsenite anions from aqueous medium by using orange waste. *Water Research*, 37, p. 4945-4953.

Godbout, N.;Salahub, D. R.;Andzelm, J. and Wimmer, E. (1992). Optimization of gaussian-type basis-sets for local spin-density functional calculations 1. Boron through neon, optimization technique and validation. *Can.J. Chem.*, 70, p. 560-571.

Goldberg, S. and Johnston, C. T. (2001). Mechanisms of arsenic adsorption on amorphous oxides evaluated using macroscopic measurements, vibrational spectroscopy and surface complexation modeling. *Journal of Colloid and Interface Science*, 234, p. 204-216.

Helz, G. R.;Tossel, J. A.;Charnock, J. M.;Pattrick, R. A. D.;Vaughan, D. J. and Garner, C. D. (1995). Oligomerization in As(III) sulfide solutions: Theoretical constraints and spectroscopy evidence. *Geochimica et Cosmochimica Acta*, 59, p. 4591-4604.

Hughes, M. F. (2002). Arsenic Toxicity and Potential Mechanisms of Action. *Toxicology Letters*, 133, p. 1-16.

Johnson, J. M. and Voegtlin, C. (1930). Arsenic derivatives of cysteine. *Journal of Biological Chemistry*, 89, p. 27.

Kaur, P. and Rosen, B. P. (1992). Plasmid-Encoded Resistance to Arsenic and Antimony. *Plasmid*, 27, p. 29-40.

Knowles, F. C. and Benson, A. A. (1983). The biochemistry of arsenic. *TIBS*, 8, p. 178-179.

Koester, A. M.;Calaminici, P.;Gómez, Z. and Reveles, U. (2002). Density Functional Theory Calculation of Transition Metal Clusters. In: Sen, K. *"Reviews of Modern Quantum Chemistry, A Celebration of the Contribution of Robert G. Parr"*. World Scientific Publishing Co: p.

Loukidou, M. X.;Matis, K. A.;Zouboulis, A. I. and Liakopoulou-Kyriakidou, M. (2003). Removal of As(V) from wastewaters by chemically modified fungal biomass. *Water Research*, 37, p. 4544-4552.

Mandal, B. K. and Suzuki, K. T. (2002). Arsenic Round the World: a Review. *Talanta*, 58, p. 201-235.

Manju, G. N.;Raji, C. and Anirudhan, T. S. (1998). Evaluation of coconut husk carbon for the removal of arsenic from water. *Water Research*, 32, p. 3062-3070.

Messens, J.;Martins, J. C.;Belle, K. V.;Brossens, E.;Desmyter, A.;Gieter, M. D.;Wieruszeski, J.-M.;Willem, R.;Wyns, L. and Zegers, I. (2002). All intermediates of the arsenate reductase mechanism, including an intramolecular dynamic disulfide cascade. *PNAS*, 99, p. 8506-8511.

Mukhopadhyay, R.;Rosen, B. P.;Phung, L. T. and Silver, S. (2002). Microbial Arsenic: from Geocycles to Genes and Enzymes. *FEMS Microbiology*, 26, p. 311-325.

Myneni, S. C. B.;Traina, S. J.;Waychunas, G. A. and Logan, T. J. (1998). Experimental and theoretical vibrational spectroscopic evaluation of arsenate coordination in aqueous solutions, solids and at mineral-water interfaces. *Geochimica et Cosmochimica Acta*, 62, p. 3285-3300.

Perdew, J. P. (1986). Density-functional approximation for the correlation-energy of the inhomogeneous electron-gas. *Phys. Rev. B*, 33, p. 8822-8824.

Pickering, I. J.;Price, R. C.;George, M. J.;Smith, R. D.;George, G. N. and Salt, D. E. (2000). Reduction and Coordination of Arsenic in Indian Mustard. *Plant Physiology*, 122, p. 1171-1177.

Rey, N. A.;Howarth, O. W. and Maia, E. C. P. (2004). Equilibrium characterization of the As(III)-cysteine and the As(III)-glutathione systems in aqueous solution. *Journal of Inorganic Biochemistry*, 98, p. 1151-1159.

Schlegel, H. B. (1987). Optimization of equilibrium geometries and transition structures. In: Lawley, K. P. *Ab-Initio Methods in Quantum Chemistry-I*. Wiley & Sons: p. 249-286.

Schmoger, M. E. V.;Oven, M. and Grill, E. (2000). Detoxification of Arsenic by Phytochelatins in Plants. *Plant Physiology*, 122, p. 793-801.

Singh, T. S. and Pant, K. K. (2004). Equilibrium, kinetics and thermodynamic studies for adsorption of As(III) on activated alumina. *Separation Purification Technology*, 36, p. 139-1478.

Teixeira, M. C. and Ciminelli, V. S. T. (2005). Development of a Biosorbent for Arsenite: Structural Modelling Based on X-Ray Spectroscopy (XAS). *Environmental Science and Technology*, 39, p. 895-900.

Weerasooriya, R.;Tobschall, H. J.;Wijesekara, H. K. D. K.;Arachchige, E. K. I. A. U. K. and Pathirathne, K. A. S. (2003). On the mechanistic modeling of As(III) adsorption on gibbsite. *Chemosphere*, 51, p. 1001-1013.

Capítulo 4

Raman Spectroscopy Analyses and Theoretical Studies of Arsenite Complexes with Avian Keratin and Cysteine

Aceito para publicação no Journal of Colloid and Interface Science

Autores: *Mônica C. Teixeira, Virgínia S.T. Ciminelli, Maria Sylvia S. Dantas, Sirlaine F. Diniz e Hélio A. Duarte*

Raman Spectroscopy and DFT calculations of As (III) Complexation with a Cysteine-rich biomaterial

Mônica C. Teixeira[1], Virgínia S.T. Ciminelli[2a], Maria Sylvia Silva Dantas[2]; Sirlaine F. Diniz[3], Hélio A. Duarte[3].

[1] Permanent Address: Department of Pharmacy – Federal University of Ouro Preto (UFOP), 35400-000 – Ouro Preto, MG, Brazil. teixeira@ef.ufop.br
[2] Department of Metallurgical and Materials Engineering – Federal University of Minas Gerais (UFMG). 30 030 160 – Belo Horizonte – MG, Brazil. ciminelli@demet.ufmg.br
[3] Chemistry Department – Federal University of Minas Gerais (UFMG), 31270-901 – Belo Horizonte – MG, Brazil. duarteh@ufmg.br

[a] Corresponding Author

Abstract

Arsenite adsorption onto a protein-rich biomass and, more specifically, the chemical groups involved in the uptake were investigated using Raman Spectroscopy and DFT calculations. The study was based on spectroscopic analyses of raw and arsenic loaded biomass as well as standard samples of amino acids and arsenic salts. The predominant secondary structure of the protein was identified as the β-sheet type, with some contribution from α-helix structures. The participation of sulfidryl groups from cystine/cysteine molecules during the adsorption of arsenite was demonstrated. Only the *gauche-gauche-gauche* (g-g-g) conformation type of the disulfide bonds was involved in arsenic complexation. The formation of a pyramidal trigonal As $(HCys)_3$ complex was modeled according to the Density Functional Theory - DFT. The agreement of the DFT harmonic frequencies with the RAMAN spectra of the As $(HCys)_3$ complex demonstrated the relevant features of the cysteine-rich biomaterial regarding arsenic uptake as well as of the mechanism involved in the As (III)/biomass interaction at a molecular level. The results also illustrate that Raman spectroscopy can be successfully applied to investigate the mechanism of metal adsorption onto amorphous biomaterials.

Keywords: Arsenite sorption, arsenite complexes, cysteine, Raman Spectroscopy, sulphidryl, DFT calculations.

4.1 INTRODUCTION

Arsenic is a ubiquitous toxic metalloid. A worldwide concern about human contamination with arsenic from superficial and ground waters has resulted in a vast number of reports covering the various aspects related to this issue. The significance of this contamination, as well as the efficiency of the remediation techniques, is very much dependent on arsenic speciation. The predominant water-soluble species are the inorganic As (III) and As (V) derivatives of the arsenous (H_3AsO_3) and arsenic (H_3AsO_4) acids, respectively. Under conditions of moderate or high redox potential, such as those found in well-oxygenated surface waters, As (V) (arsenate) species predominate. Under reducing conditions, as usually observed in ground waters, As (III) (arsenite) species prevail. (Gupta and Chen, 1978; Case and Robinson, 1983; Knowles and Benson, 1983; Kaur and Rosen, 1992; Chiu, et al., 1994; Ramaswami, et al., 2001).

Arsenite species are considered 10 times more toxic than arsenate species and 70 times more toxic than organic species - dimethylarsinate ($(CH_3)_2AsOH$ and $(CH_3)_2OAsOH$) and monomethylarsonate ($CH_3AsO_2H_2$, and $CH_3AsO_3H_2$) (Kumaresan and Riyazuddin, 2001). The toxicity of As (III) species can mostly be explained by its irreversible complexation with sulphydril groups present in active biomolecules, such as enzymes. (Kumaresan*, et al.*, 2001). Sulphydril groups are usually found in the structure of some aminoacids, mainly cysteine. Therefore, enzymes whose activity sites depend on the sulphydril groups may have their metabolic activities totally or partially impaired by complexation with As (III). As (III) reacts when in contact with sulphur and sulphydryl groups such as cysteine, organic dithiols, proteins and enzymes, but it does not react when in contact with amine groups or organics with reduced nitrogen constituents. On the other hand, As (V) reacts when in contact with reduced nitrogen groups such as amines, but not when in contact with sulphydryl groups. The toxicity of arsenate species is mainly related to its competition with phosphate groups. Pentavalent arsenic can disrupt the oxidative phosphorylation - the process by which ATP is formed - by the production of an arsenate ester of ADP. This process is known as arsenolysis (Kumaresan*, et al.*, 2001; Mandal and Suzuki, 2002).

In addition to its toxicity, arsenite is the most mobile species in the environment due to its weaker, reversible adsorption on soil constituents, such as iron and aluminum oxyhydroxides (Ladeira and Ciminelli, 2004). This reversible, weaker adsorption of As (III) on soil constituents, and apparently inconsistent formation of inner-sphere adsorption complexes, was discussed by before (Oliveira, et al., 2006). Based on density functional methods and cluster models, it was shown that in contrast to the As (V) species, As (III) is not adsorbed via an acid/base, but rather by a non-dissociative mechanism in which O–H bonds are not broken. The complexation of As (III and V) in natural environments by dissolved organic matter, thus preventing sorption and co-precipitation, may also increase arsenic mobility (Kumaresan*, et al.*, 2001)

Various potential applications can be envisaged for materials capable of a direct As (III) removal and immobilization. Arsenic speciation in natural waters and effluents is increasingly important for the assessment of toxicity and bioavailability of arsenic species in an aqueous environment. Therefore, the possibility of an efficient separation of As (III) and As (V) species in the field, during sampling, minimizes the errors resulting from sample alteration prior to the analyses. In another context – treatment of water and aqueous effluents - a direct removal of As (III) would eliminate the need of previous oxidation of arsenite to arsenate by solid-phase or liquid-phase oxidants. The oxidation of As (III) is an obligatory and expensive stage of the usual schemes for water and effluent treatment by co-precipitation or adsorption on iron oxy-hydroxides (Deschamps, et al., 2005)

The understanding of the interaction mechanism of arsenite with biological molecules, and more specifically the biochemical fundamentals that explain arsenic toxicity, was applied to the development of a biomaterial capable to selectively remove As (III) from aqueous environments (Teixeira and Ciminelli, 2005). The results of this original approach for the treatment of arsenic-containing solutions demonstrated that a cysteine-rich biomass – a residue from the poultry industry - was highly selective for arsenic removal in its trivalent form, without important effects of the studied competitor ions on the solid's adsorption capacity. X-Ray Absorption Analysis (XAS) indicated that each arsenic atom is bound directly to three sulphur atoms from the reduced cysteine

aminoacids present in biomass. Arsenic is adsorbed as As (III) thus avoiding the need for previous arsenite oxidation.

In a further development of this project, the aim was to obtain detailed structural information about the protein-rich biomaterial as well as the changes taking place during arsenite complexation. The present work shows the results obtained by Raman Vibrational Spectroscopy of the raw and arsenic loaded biomass, as well as of selected amino acids and standard As (III) salts. Density functional calculations were also performed and the results were compared with the Raman frequencies observed experimentally. The obtained results provide a better understanding of the relevant features of the cysteine-rich biomaterial regarding arsenic uptake as well as of the mechanism involved in the As (III)/biomass interaction at a molecular level. It was demonstrated that only the *gauche-gauche-gauche* (g-g-g) conformation type of the disulfide bonds is involved in arsenic complexation.

4.2 MATERIALS AND METHODS

4.2.1 Materials

Residues from the poultry industry - white chicken feathers - were rinsed thoroughly with warm tap water and dried at 45 ±5°C for 24 hours. The dried material was ground and sieved to obtain a size range below 0.037 mm (400 Mesh Tyler). Biomass activation was accomplished by adding 10 ml of a 7.8 % (w/w) basic ammonium thioglycolate solution. The treatment did not imply any loss of mass. Following this activation step, the powdered biomaterial was filtered and washed with 100 mL of Milli-Q water. The adsorption experiments were carried out according to the previously described protocol (Teixeira*, et al.*, 2005). Arsenic uptake at pH 5 was 20 mg As (III)/g of biomass.

An As (III)-cysteine precipitate was prepared by the reaction created upon mixing As (III) (13.4 mmol.L^{-1}) with Cysteine (3.0 mmol.L^{-1}) at pH 5.0. The reaction was

carried out in an aqueous solution, degassed with N_2 at pH 5.0, with an excess of sodium meta-arsenite. Cystine and cysteine amino acids (Merck, 99.0%), sodium arsenite and arsenate aqueous solutions (13.4 mmol.L^{-1}, pH 4.5 and 10.5), and an $AsNaO_2$ salt (Fluka, 99.0%) were also used in the present investigation.

4.2.2 Raman Spectroscopy

Raman spectra were obtained through a Labran HR 800 (Jobin Yvon/Horiba). A He-Ne laser with a 632.8 nm wavelength and a 20 mW power output measured at the laser head was used as the excitation source. The Raman signal was collected by Olympus microscope objectives (50 X 0.75 and 100 X 0.90) in back scattering configuration. The entrance slits to the spectrograph were 100 µm with a correspondent resolution of 2.0 cm^{-1}. The utilized holographic grating was of 600 or 1800 g/mm for inorganic or biological material. Liquid nitrogen cooled CCD was used as a detector.

Depending on the sample background fluorescence, the acquisition time ranged from 10 to 120s. To reduce the signal/noise ratio, spectra were acquired 100-300 times after a photobleaching of 5-30 minutes. Collected Raman spectra were analyzed and optimized with Labspec 1.1 and Origin 5.0. Spectra collected were averaged, the background was corrected and, if necessary, normalized, and the peak was deconvoluted.

4.2.3 Computational aspects

The interactions of $As(OH)_3$ with Cysteine (HCys) leading to different metal/ligand proportion complexes have been studied using the LCGTO-KS-DF (Linear Combination of Gaussian Type Orbital-Kohn Sham-Density Functional) method implemented in deMon-2002 program (Koester, et al., 2002b). The generalized exchange correlation (XC) functional has been used with the Becke expression (Becke, 1988) for exchange and with that of Perdew (Perdew, 1986a; Perdew, 1986b) for correlation (GGA-BP). The one-electron orbitals are expanded in triple-zeta orbital basis sets explicitly optimized by Godbout (Godbout, et al., 1992). Auxiliary basis sets (A2) have been used for fitting the density charge. Adaptive grid (Krack and Koster, 1998; Koster, et al., 2004) with a tolerance of 10^{-6} for the numerical integration of the

exchange-correlation energy and potential was used. The numerical integration is based on Becke's partition scheme (Becke, 1987) in an adaptive grid. The calculation of the expansion coefficients of the approximated density is described in detail elsewhere (Koester, et al., 2002a). All structures have been fully optimized using the BFGS (Schlegel, 1987) method. Vibrational analysis was performed for the most stable species using the harmonic approximation. The Hessian matrix was evaluated numerically from the analytical gradients of the potential energy surface. Positive frequencies assure that true minima on the potential energy surface have been found.

4.3 Results and Discussion

4.3.1 Raman Spectroscopy

Over the past two decades, Raman spectroscopy has been successfully applied to the area of biopolymer research. It has also helped to elucidate the structure of amorphous, biological materials, such as proteins, enzyme lipids, or nucleic acids (Fabian and Anzenbacher, 1993), which show short range ordering for distances up to three or four bond lengths (Brodsky, 1983). Therefore, despite the amorphous nature of the sorbent, Raman spectroscopy can provide information about the intrinsic structure of the avian biomass prepared for As (III) uptake in addition to the molecular level modification following the reaction.

Figure 4.1 shows the Raman vibrational spectrum obtained with the raw biomass sample. The main band observed at 510 cm^{-1} is assigned to the (S-S) symmetric stretching vibrational mode (Yu, et al., 1985; Akhtar, et al., 1997b). It is also possible to observe two weak bands at 622 and 644 cm^{-1} attributed to the stretching of the gauche C-S bonds, much like those described by previously (Akhtar and Edwards, 1997a) at 621 and 643 cm^{-1}. The intensity of C-S band is usually related to the sulfur content in amino acids, such as methionine, cysteine, and cystine. The methionine contribution to the C-S vibrational modes is expected to be negligible since its content in avian keratin

is lower than 0.4% as compared to 7.8% from cysteine (Akhtar*, et al.*, 1997a; Akhtar*, et al.*, 1997b).

Other relatively intense bands are observed at 827, 855 (highlighted) and 1205 cm^{-1} (not shown) and may be attributed to the vibrational modes of the C-OH stretching of the phenolic OH groups from the amino acids tyrosine and phenylalanine. The first two bands are exclusive from tyrosine (Fabian*, et al.*, 1993). A relatively low intensity 1603 cm^{-1} band may also be attributed to the vibrational mode ν(C=C) of olefinic carbon bonds (Akhtar*, et al.*, 1997a).

At the region near 1000-1100 cm^{-1}, the observed bands were correlated with the C-C stretching vibrational modes (Fabian*, et al.*, 1993; Akhtar*, et al.*, 1997a; Akhtar*, et al.*, 1997b). The sharp band observed at 1003 cm^{-1} is attributed to the C-C stretching vibration mode of aromatic carbon rings in the phenylalanine side chain (Akhtar*, et al.*, 1997a). This assigning is consistent with the fact that phenylalanine is the major aromatic side chain amino acid detected in the composition of avian keratin (3.1%) Some other less intense bands (not highlighted in Figure 4.1) were observed at 1031, 1088, 1124, 1156, and 1171 cm^{-1}. The bands located at 1031 and 1124 cm^{-1} are assigned to the *cis* and *trans* (C-C) stretching, respectively, while the band at 1088 is characteristic of a randomic (C-C) skeletal conformation.

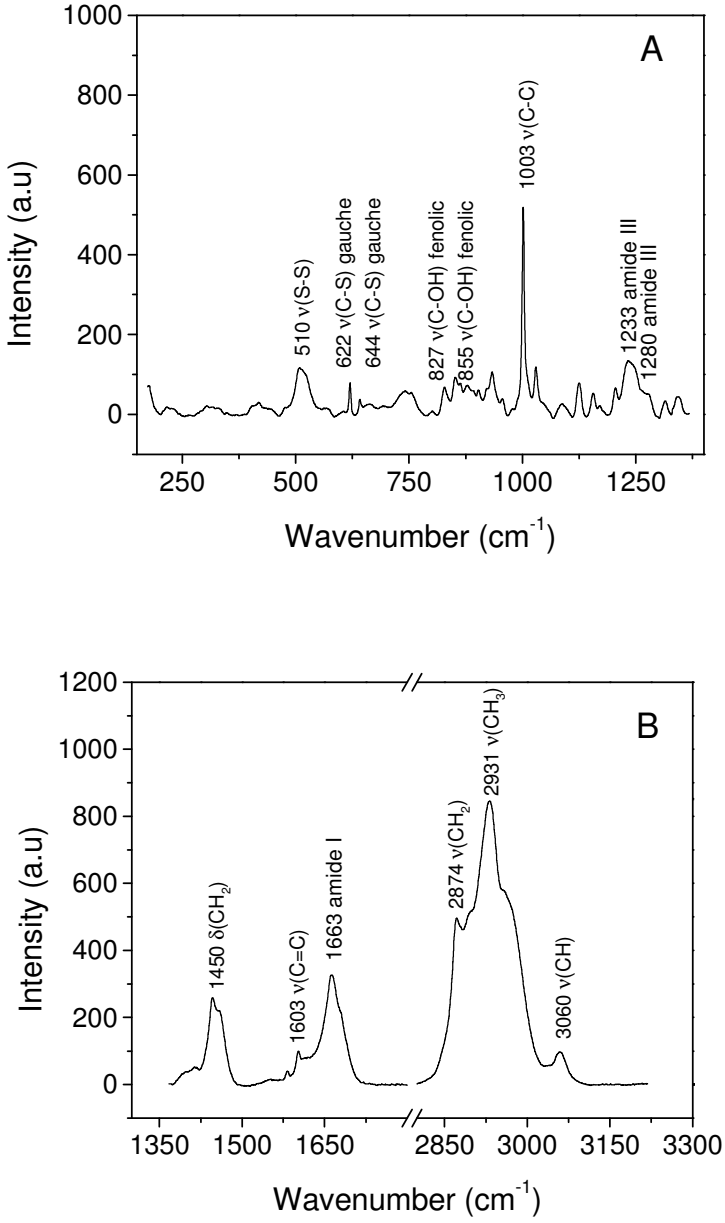

Figure 4.1 Raman spectroscopy of natural biomass (Baseline corrected for fluorescence)

Raman spectra of proteins contain the contributions from the vibrational groups of peptide backbones and those related to the amino acids themselves. There are some characteristic bands frequently detected in Raman spectra of all proteins. These include the amide I vibrational modes, with the contribution of C=O stretching, and the amide III band, resulting of C-N stretching coupled with N-H bending. Depending on the secondary structure (which include the bidimensional structures stabilized by hydrogen bonds) of the protein, the hydrogen atom from the amino group will be bound to the nitrogen in a different manner (in or out of the plane) and amide I and III vibrational modes will show different absorption wavenumbers. At 1233 cm^{-1} (Figure 4.1) one may observe a relatively intense and broad band, which, together with a small band at 1280 cm^{-1}, is related to the amide III vibrational modes. At 1663 cm^{-1}, another intense broad band with other contributions at 1680 cm^{-1} attributed to amide I vibrational mode, was observed. For β-sheet proteins, like avian keratins, the amide I and III bands are detected between 1665 and 1680 and between 1230 and 1240 cm^{-1}, while for α-helix proteins the expected wavenumbers were between 1645 and 1657 and between 1260 and 1300 cm^{-1} (Akhtar*, et al.*, 1997a; Akhtar*, et al.*, 1997b; Edwards, et al., 1998). The presence of a broad amide III band, resulting from the overlapping of bands located at 1233 and 1280 cm^{-1}, is suggestive of the existence of a less ordered protein secondary structure comprised mainly of β-sheet, with a possible minor contribution of α-helix structures.

The vibrational modes of CH_3, CH_2, and CH groups were also detected but only the most intense bands were highlighted in Figure 4.1. The CH_3 deformation modes were observed at 932 and 956 cm^{-1}, which is characteristic of $\rho(CH_3)$ and at 1415 cm^{-1} for $\delta(CH_3)$. The $\nu(CH_3)$ symmetric stretching produced a band with the wavenumber of 2931 cm^{-1}. Two bands located at 744 and 754 cm^{-1} may be attributed to the deformation ρCH_2) in phase. The vibrational modes of the deformation (δ) and the stretching (ν_3) of CH_2 were observed at 1317 and 2874 cm^{-1}. Another two bands located near 1450 cm^{-1} (1447 and 1460) may also be assigned to methylene (CH_2) scissoring deformation, which is a characteristic band of keratins. For the CH group, the observed vibrational modes were one relative to the C-H bending at 1345 cm^{-1} and

other two at 2721 and 3060 cm^{-1} related to the stretching of the aliphatic and olefinic ν(CH) vibrational modes, respectively (Fabian*, et al.*, 1993; Akhtar*, et al.*, 1997b). The sum of the contribution of CH, CH_2, and CH_3 stretching vibrational modes results in a broad intense band observed at the region between 2800 and 3100 cm^{-1}.

In this section, the features of the biomass prior to and after adsorption of As (III) will be discussed. Prior to adsorption, the predominant arsenic species in the aqueous phase at pH 5 is the neutral H_3AsO_3. XAS measurements indicated that As (III) adsorption involves an inner sphere complexation with the sulphydril groups available in the biomass upon the release of three water molecules. Figure 4.2 illustrates the normalized spectra of the natural powdered biomass and arsenite-loaded powdered biomass. The spectra are similar in the regions between 600 and 3200 cm^{-1}. It is important to emphasize that the reduction with thioglycolate caused no detected modification in the characteristic spectra of the natural sample (data not shown).

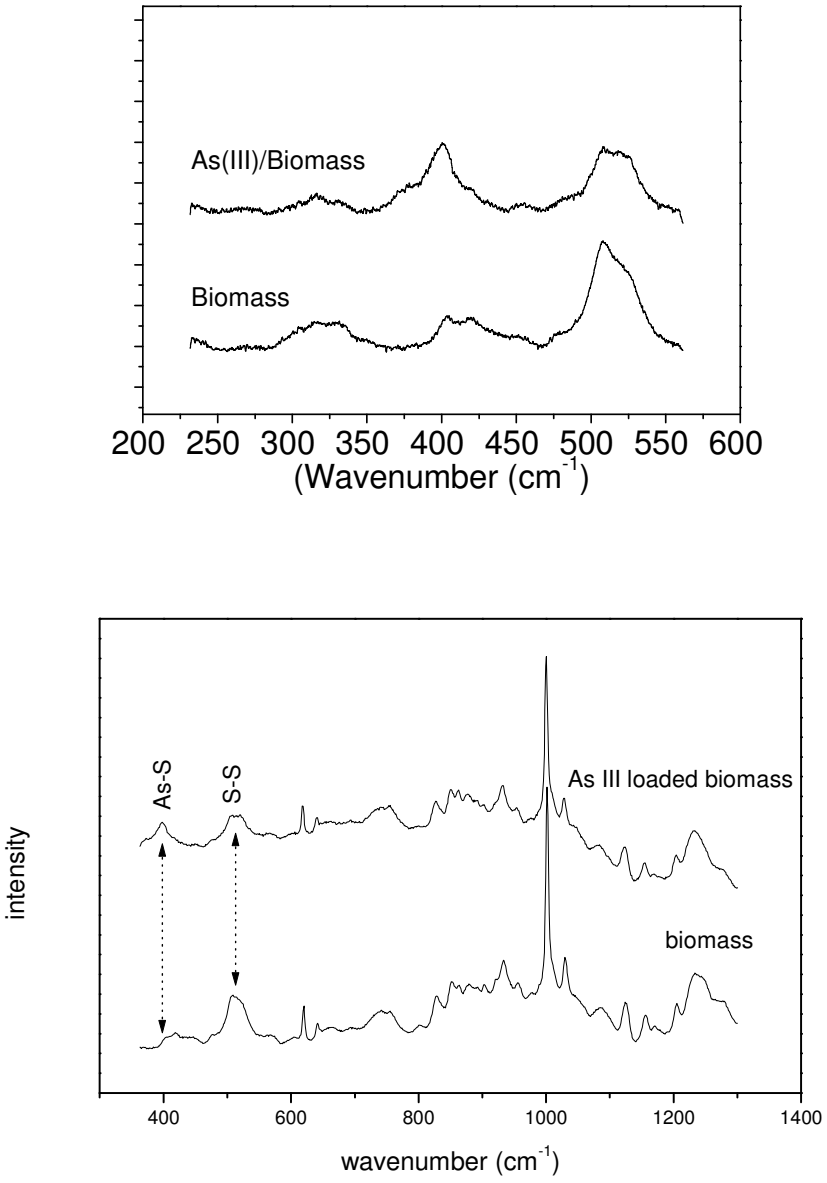

Figure 4.2 Raman spectra for natural powdered biomass and arsenite-loaded powdered biomass at pH 5.0. Detailed spectra (top) were obtained with an 1800 g/mm holographic grating.

The major differences between the natural and the arsenite loaded biomass spectra were observed in the region below 600 cm^{-1}, which is highlighted in the upper part of Figure 4.2. The first represents the decrease in the intensity of the band located between 500 and 550 cm^{-1} following As (III) uptake. The second interesting aspect is the appearance of one broad band between 340 and 420 cm^{-1} after arsenic uptake. Both phenomena took place within the regions where the main expected features were the S-S symmetric stretching and the As-S symmetric stretching (for arsenite loaded biomass), respectively.

Figure 4.3 (a and b) explores the characteristic region of S-S stretching vibrational modes, which were fitted and deconvoluted using a Lorentz function. It was possible to observe that the broad band at 500-550 cm^{-1} is the result of the overlapping of two bands - one centered at 507 cm^{-1} and the second at 524 or 522 cm^{-1} for the biomass samples prior to and after arsenic adsorption, respectively. It was also possible to notice that while the intensity of the second band is maintained after adsorption, the first had its intensity diminished by more than 50%. The S-S symmetric stretching mode, frequently detected at frequencies around 510 cm^{-1} (Yu*, et al.*, 1985; Fabian*, et al.*, 1993; Akhtar*, et al.*, 1997b), is caused exclusively by cystine. Each cystine molecule is comprised of two cysteine residues that bind to each other by one disulfide bridge (S-S) in a strong chemical binding characteristic of keratins produced after the oxidation of two sulfydryl groups. All the analyzed samples provide broad bands centered at 507 cm^{-1}. It was also observed that the S-S vibrational mode amplitude was slightly diminished for the sample treated with thioglycolate (data not shown), confirming the reduction of the S-S bridge.

Figure 4.3c shows the spectrum produced after the subtraction of the spectra obtained prior to and after arsenic uptake. The resulting spectrum indicates that the amplitudes of the vibrational modes located at the region around 500 cm^{-1} have decreased (negative). The negative values observed at Figure 4.3c around 500 cm^{-1} indicate the utilization of sulfur containing groups during arsenite adsorption according Figure 4.4. Based on the results shown above, it is possible to conclude that only a special type of S-S bonds is involved in arsenite complexation. In fact, the atoms involved in the disulfide bonds (C-

C-S-S-C-C) of keratin structure may assume different spatial orientations, causing three different conformations for the chemical bonds: *trans-gauche-trans*, *gauche-gauche-trans* and *gauche-gauche-gauche.* The latter is the characteristic conformation of the avian β-keratin. For the *trans-gauche-trans* and *gauche-gauche-trans* conformations, the expected wavenumbers for the S-S stretching vibration are 540 and 525 cm^{-1} respectively, while for the *gauche-gauche-gauche* it is 510 cm^{-1} (Yu*, et al.*, 1985; Fabian*, et al.*, 1993; Akhtar*, et al.*, 1997b). The results shown in Figure 4.3 indicate that the *gauche-gauche-gauche* disulfide bridges prevail in the keratin-rich biomass utilized in the present work and was preferably consumed during arsenite adsorption. The involvement of the other type of disulfide bridge, *gauche-gauche-trans* and *trans-gauche-trans*, in arsenic complexation may be disregarded.

Figure 4.3c also depicted an evident alteration on the spectral features at 340 and 420 cm^{-1} after arsenite adsorption. The S-S bridges are disrupted by reduction, thus producing two SH groups, which are involved in arsenic adsorption. The region between 350 and 450 cm^{-1} is usually assigned to the vibrational modes of the As-S group (Brodsky, 1983; Bell, et al., 1997). For the arsenic containing pigments, the vibrational modes of the As-S stretching produced bands are 292, 309, 353, and 381 cm^{-1} for orpiment (As_2S_3), 330 and 360-376 cm^{-1} for realgar (As_4S_4), and a broad band composed of four different peaks centered in 330 cm^{-1} produced by pararealgar (As_4S_4) (Trentelman, et al., 1996). The As-S stretching vibrational mode frequencies calculated for synthetic arsenite sulfide solutions were found at 286 and 430 cm^{-1} depending on the oligomerization of arsenic complexes in the solution (Helz, et al., 1995).

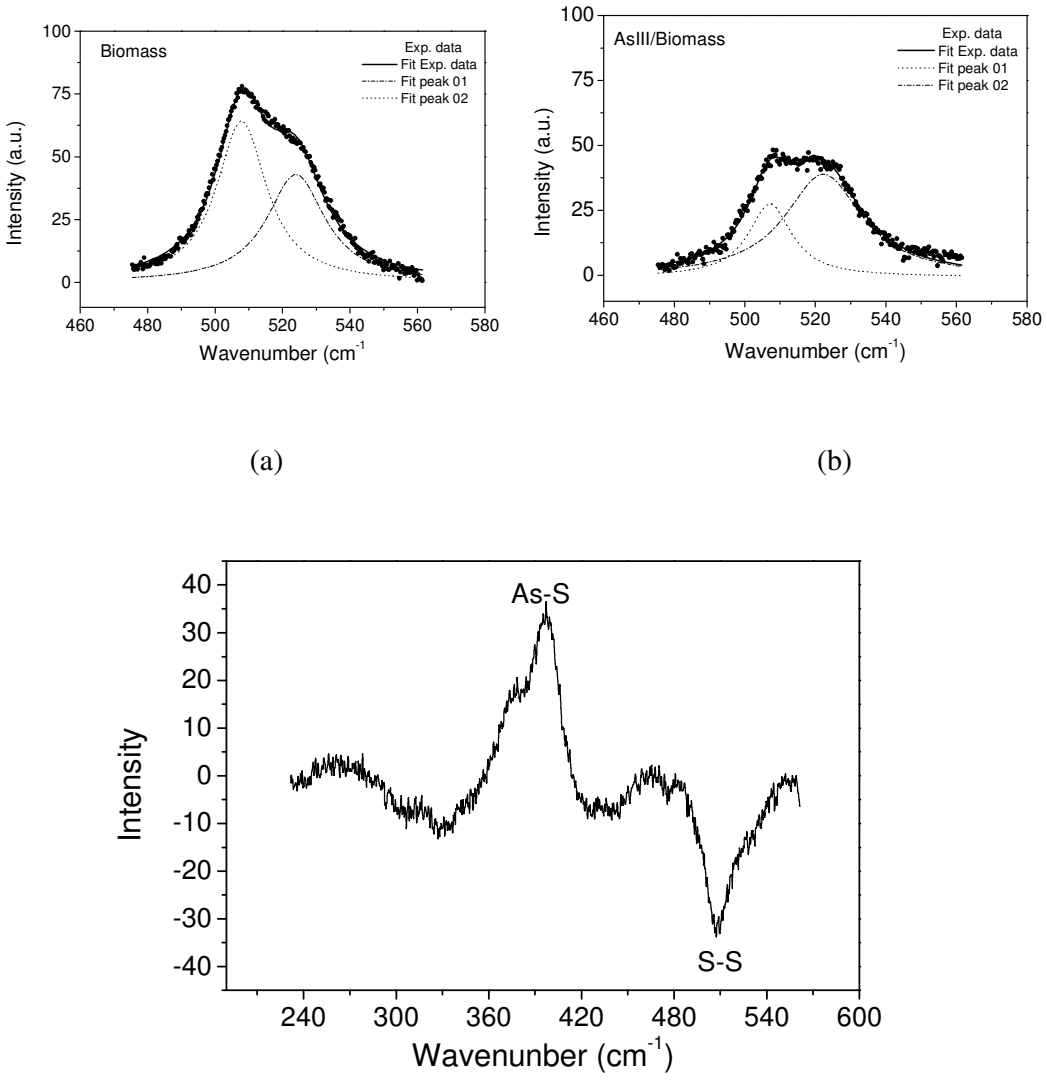

Figure 4.3 - Differences between natural and arsenite loaded biomass. Fitting of S-S stretching band for the (a) biomass, (b) As (III)/Biomass, and (c) Difference spectrum As (III)/Biomass-Natural Biomass (lower)

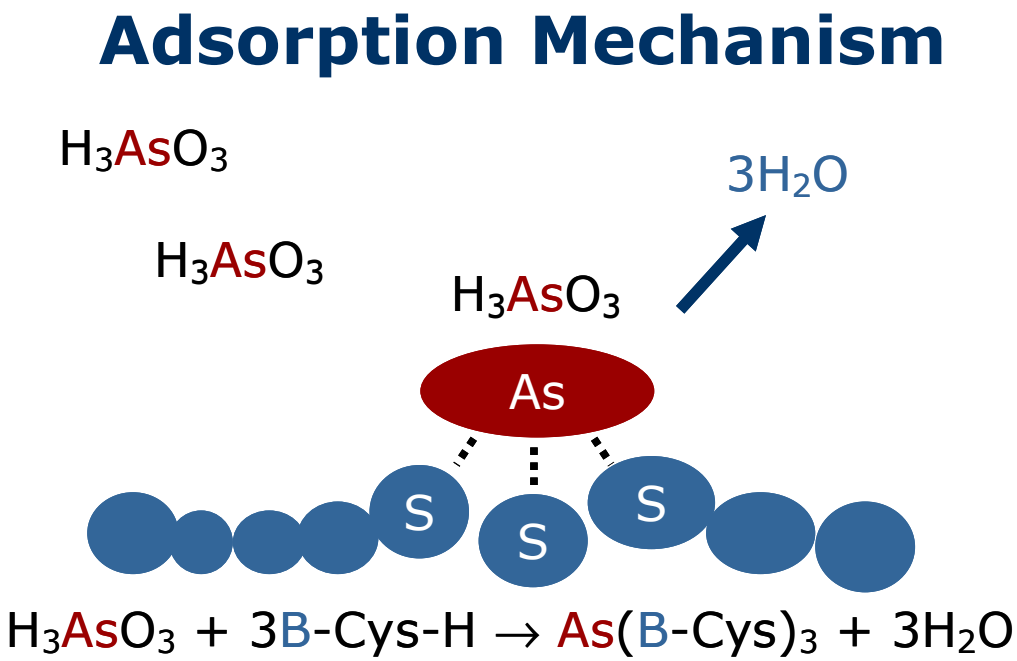

Figure 4.4 – Schematic picture of As (III) adsorption onto a protein-rich biomass. Each arsenic atom reacts with three sulfur atoms from cysteine aminoacids. Three water molecules are released and a pyramidal As-S complex is formed. Biomass structure is represented by B.

4.3.2 Cysteine/As (III) complexes

In order to maximize the signal amplitude of the As-S vibrational modes, the arsenic complexation with pure cysteine amino acid was investigated. The As (III)-cysteine precipitate was prepared by reacting pure cysteine with an excess of sodium meta-arsenite. Raman analyses of the precipitate produced a spectrum with well-defined bands, which is compared to the cysteine standard spectrum in Figure 4.5.

Figure 4.5 clearly demonstrates that the sharp band at 2556 cm^{-1} (ν(S-H) vibrational mode) shown in the cysteine spectrum disappears after reaction with arsenite. In the precipitate spectrum, one may notice the appearance of four intense bands near to 400 cm^{-1} (358.5; 384, 401.5, and 427.8 cm -1). These frequency values coincide with the frequency range of the broad band described earlier in Figure 4.3. The vibrational frequency calculated for the As-S symmetrical stretching was 390-403 cm^{-1} for the internal or the externally located As-S bonds, respectively, in the $As_3S_3(SH)_6$ complex (Helz*, et al.*, 1995). The intense band observed at 401.5 cm^{-1} (Figure 4.5) indicates the formation of an As-S band (symmetric stretching) after cysteine reaction with sodium arsenite.

It can also be observed that the intense and sharp band at 684 cm^{-1}assigned to the C-S stretching (Susi, et al., 1983) in the cysteine spectrum is preserved as a broad band after reaction with arsenite. The C-H symmetric stretching vibrational mode, observed for the cysteine molecule at 2996 cm^{-1} and the NH_3^+ stretching mode at 3000 cm^{-1}, seems to have been shifted to the lower frequencies of 2924 and 2960 cm^{-1}, respectively, in the precipitate sample. There is also an apparent splitting in the precipitate in the NH_3^+ band. Due to the complexity of the keratin structure, or perhaps because of the low arsenite content, the signal was not strong to indicate the participation of C-H and NH_3^+ groups during arsenic adsorption

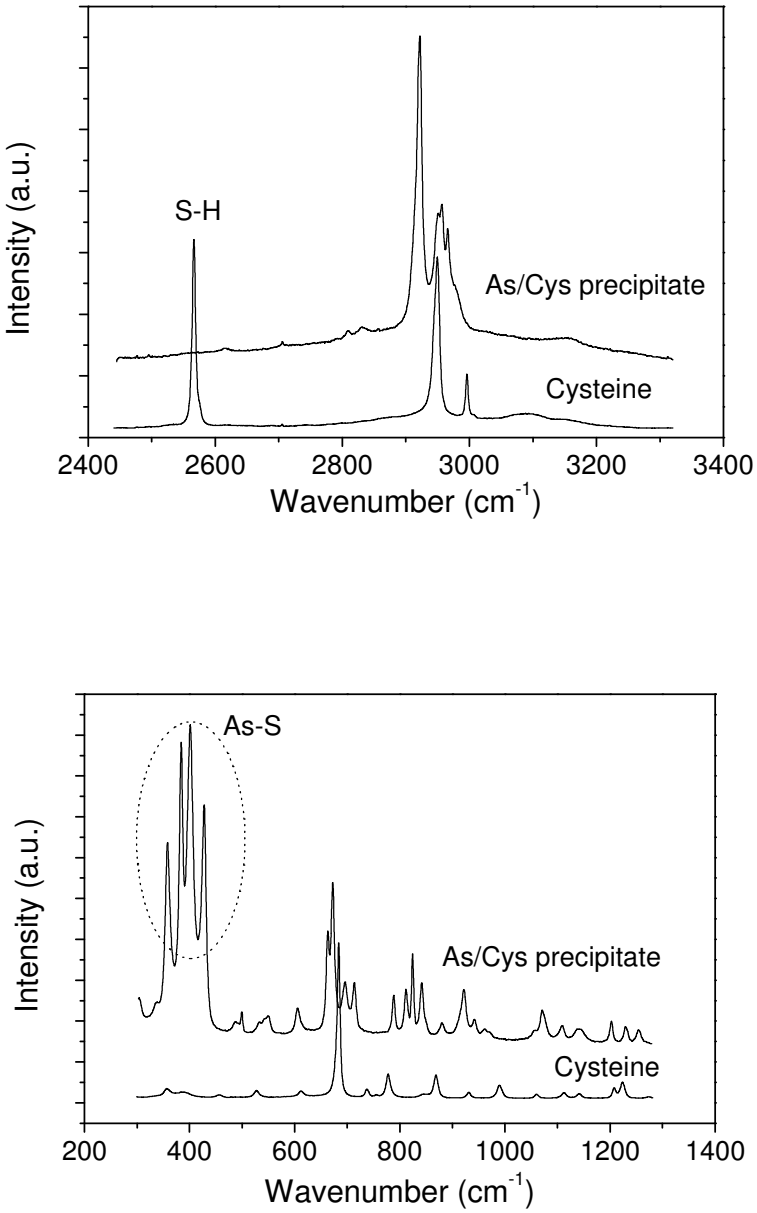

Figure 4.5 - Raman spectra of Cysteine and As/Cysteine complex (centered at 800 and 2900 cm $^{-1}$)

4.3.3 DFT calculations

Recent XANES and EXAFS studies of the As (III) with the cysteine rich biomass showed that As (III) is adsorbed in its trivalent form (Teixeira*, et al.*, 2005). Therefore, the theoretical model for the adsorption was based on the 1:3 As:HCys complex, shown in Figure 4.6. The optimized structure presents the As center with a pyramid trigonal as expected and the As-S bond distance at approximately 2.287Å. This value may be compared to the EXAFS value of 2.26 Å. Table IV. 1 shows the DFT harmonic frequencies for different complexes with respect to the As-O, As-S, and S-C strengths. At the level of theory used, the calculated frequencies are commonly overestimated and the error bars are normally up to 50 cm^{-1} (Frisch, et al., 1998). The calculated C-S frequencies are about 657-685 cm^{-1}, in reasonable agreement with the experimental range of around 622-644 cm^{-1}. The C-S frequency for the cysteine is predicted to be 684 cm^{-1}, slightly shifted for larger wavenumbers. The As-O frequency for the $As(OH)_3$ is in the range of 600-634 cm^{-1}, approximately 60 cm^{-1} smaller than the respective experimental value. The As-S frequency is the most important feature of the Raman spectra, since this bond strength is not present in the original biomass. However, it lies in the range of low frequencies and its precise peak is difficult to be determined experimentally. The $As(SH)_3$ complex has been calculated for comparison. The As-S frequency is about 372-382 cm^{-1}, in the same range as the predicted values for the As/cysteine complexes. Vibrational frequencies reflect the nature of the bond and, therefore, provide information about the adsorption site. However, it is reasonable to observe that the As-S frequency is probably modified due to the extended solid (biomass) that can perturb the As-S strength through the steric hindrance of the system or through an inductive chemical mechanism. To answer those questions, more detailed calculations with larger models that can take into account part of the molecular structure of the β-keratin would be required. The DFT results show that the $As(HCys)_3$ is a satisfactory model to describe the interaction of the As (III) with the cysteine rich biomass with a pyramid trigonal geometry.

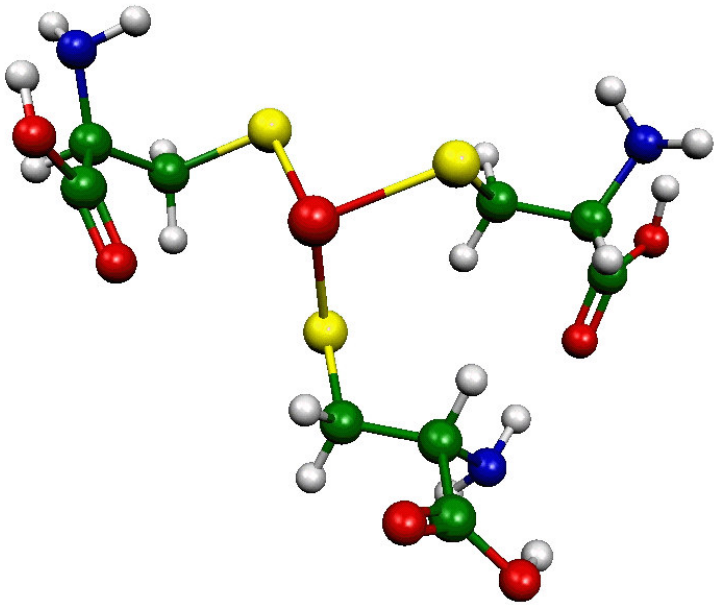

Figure 4.6 - Optimized structure of As $(HCys)_3$. Arsenic atoms are represented by the central sphere in red surrounded by three yellow spheres representing sulfur atoms from three different cysteine molecules.

Table IV. 1 - DFT harmonic frequencies (in cm^{-1}) for As-O, As-S and C-S bond strength.

Complexes	**As-O**	**As-S**	**C-S**
As $(HCys)_3$		368.7 372.2 401.1	657.8 681.7 684.5
H_2Cys			684
As $(OH)_3$	600.1(669)[a] 609.6(709)[a] 633.2		
As $(SH)_3$		372.5 372.5 381.2	
Raman[b]		350-460	622/644 (684)[c]

[a] Value in parentheses are from Refs. (Tossel, 1997; Goldberg and Johnston, 2001).
[b]Values in parentheses are for cysteine/As (III) system at pH 5.0.
[c] Value in parentheses for the cysteine.

4.4 Conclusions

The secondary structure of the proteins contained in the biomass utilized during this work was investigated by Raman spectroscopy. The predominant secondary structure of the protein was shown to be the β-sheet, as expected for avian keratins, with minor contribution from the α-helix structures. The adsorption of arsenite on the sulfidryl groups from cystine/cysteine molecules present in the biomass was investigated. The disulfide bond in the biomass protein structure is spatially ordered, predominantly in a *gauche-gauche-gauche* (g-g-g) conformation. Part of the disulfide bonds assumes the *gauche-gauche-trans* (g-g-t) conformation. The results showed that only the g-g-g type disulfide bonds are involved in arsenic adsorption. The adsorption site is correctly modeled by the interaction of cysteine molecules with the As (III) forming a pyramid trigonal As $(HCys)_3$ complex as was evidenced by the RAMAN and DFT calculations.

4.5 References

Akhtar, W. and Edwards, H. G. M. (1997a). Fourier-transform Raman spectroscopy of mammalian and avian keratotic biopolymers. *Spectrochimica Acta Part A*, 53, p. 81-90.

Akhtar, W.;Edwards, H. G. M.;Farwell, D. W. and M.Nutbrown (1997b). Fourier-transform Raman spectroscopic study of human hair. *Spectrochimica Acta Part A*, 53, p. 1021-1031.

Becke, A. D. (1987). A multicenter numerical integration scheme for polyatomic molecules. *J. Chem. Phys*, 88, p. 2547-2553.

Becke, A. D. (1988). Density-functional exchange-energy approximation with correct asymptotic-behavior. *Phys. Rev. A*, 38, p. 3098-3100.

Bell, I. M.;Clark, R. J. H. and Gibbs, P. J. (1997). Raman spectroscopy library of natural and synthetic pigments (pre 1850 AD). *Spectrochimica Acta Part A*, 53, p. 2159-2179.

Brodsky, M. H. (1983). Raman scattering in amorphous semiconductors. In: Cardona, M. *Light Scattering in solids I*. Second. Berlin, Heidelberg, New York, Springer-Verlag. 8: p. 205-251.

Case, C. and Robinson, M. F. (1983). Some Aspects in Nutritional Trace Elements. In: Siegel, H. *Methods Involving Metal Ions and Complexes in Clinical Chemistry*. New York, Marcel Dekker, Inc. 16: p. 1-26.

Chiu, K.-H.;Chen, S.-L.;Dzeng, S. R.;Shieh, G.-M.;Yang, M.-H. and Wal, C. M. (1994). Arsenic Species in Groundwaters of the Blackfoot Disease Area, Taiwan. *Environ. Sci. Technol.*, 28, p. 877-881.

Deschamps, E.;Ciminelli, V. S. T. and Holl, W. H. (2005). Removal of As(III) and As(V) from water using a natural Fe and Mn enriched sample. *Water Research*, 39, p. 5212-5220.

Edwards, H. G. M.;Hunt, D. E. and Sibley, M. G. (1998). FT-Raman spectroscopic study of keratotic materials: horn, hoof and tortoiseshell. *Spectrochimica Acta Part A*, 54, p. 745-757.

Fabian, H. and Anzenbacher, P. (1993). New developments in Raman spectroscopy of biological systems. *Vibrational Spectroscopy*, 4, p. 125-148.

Frisch, M. J.;Trucks, G. W.;Schlegel, H. B.;Scuseria, G. E.;Robb, M. A.;Cheeseman, J. R.;Zakrzewski, V. G.;J. A. Montgomery, J.;Stratmann, R. E.;Burant, J. C.;Dapprich, S.;Millam, J. M.;Daniels, A. D.;Kudin, K. N.;Strain, M. C.;Farkas, O.;Tomasi, J.;Barone, V.;Cossi, M.;Cammi, R.;Mennucci, B.;Pomelli, C.;Adamo, C.;Clifford, S.;Ochterski, J.;Petersson, G. A.;Ayala, P. Y.;Q. Cui;Morokuma, K.;Malick, D. K.;Rabuck, A. D.;Raghavachari, K.;Foresman, J. B.;Cioslowski, J.;Ortiz, J. V.;A. G. Baboul;Stefanov, B. B.;Liu, G.;Liashenko, A.;Piskorz, P.;Komaromi, I.;Gomperts, R.;Martin, R. L.;Fox, D. J.;Keith, T.;Al-Laham, M. A.;Peng, C. Y.;Nanayakkara, A.;Gonzalez, C.;Challacombe, M.;Gill, P. M. W.;Johnson, B.;Chen, W.;Wong, M. W.;Andres, J. L.;Gonzalez, C.;Head-Gordon, M.;Replogle, E. S. and Pople, J. A. (1998). Gaussian 98-Revision A.7. Pittsburgh PA, Gaussian, Inc.

Godbout, N.;Salahub, D. R.;Andzelm, J. and Wimmer, E. (1992). Optimization of gaussian-type basis-sets for local spin-density functional calculations 1. Boron through neon, optimization technique and validation. *Can.J. Chem.*, 70, p. 560-571.

Goldberg, S. and Johnston, C. T. (2001). Mechanisms of arsenic adsorption on amorphous oxides evaluated using macroscopic measurements, vibrational spectroscopy and surface complexation modeling. *Journal of Colloid and Interface Science*, 234, p. 204-216.

Gupta, S. K. and Chen, K. C. (1978). Arsenic removal by adsorption. *Journal of Water Pollution Control Federation*, 50, p. 493-506.

Helz, G. R.;Tossel, J. A.;Charnock, J. M.;Pattrick, R. A. D.;Vaughan, D. J. and Garner, C. D. (1995). Oligomerization in As(III) sulfide solutions: Theoretical constraints and spectroscopy evidence. *Geochimica et Cosmochimica Acta*, 59, p. 4591-4604.

Kaur, P. and Rosen, B. P. (1992). Plasmid-Encoded Resistance to Arsenic and Antimony. *Plasmid*, 27, p. 29-40.

Knowles, F. C. and Benson, A. A. (1983). The biochemistry of arsenic. *TIBS*, 8, p. 178-179.

Koester, A. M.;Calaminici, P.;Gómez, Z. and Reveles, U. (2002a). Density Functional Theory Calculation of Transition Metal Clusters. In: Sen, K. *"Reviews of Modern Quantum Chemistry, A Celebration of the Contribution of Robert G. Parr"*. World Scientific Publishing Co: p.

Koester, A. M.;Flores, R.;Geudtner, G.;Goursot, A.;Heine, T.;Patchkovskii, S.;Reveles, U.;Vela, A. and Salahub, D. (2002b). deMon Software.

Koster, A. M.;Reveles, J. U. and del Campo, J. M. (2004). Calculation of exchange-correlation potentials with auxiliary function densities. *Journal of Chemical Physics*, 121, p. 3417-3424.

Krack, M. and Koster, A. M. (1998). An adaptive numerical integrator for molecular integrals. *Journal of Chemical Physics*, 108, p. 3226-3234.

Kumaresan, M. and Riyazuddin, P. (2001). Overview of speciation chemistry of arsenic. *Current Science*, 80, p. 837-846.

Ladeira, A. C. Q. and Ciminelli, V. S. T. (2004). Adsorption and desorption of arsenic on an oxisol and its constituents. *Water Research*, 38, p. 2087-2094.

Mandal, B. K. and Suzuki, K. T. (2002). Arsenic Round the World: a Review. *Talanta*, 58, p. 201-235.

Oliveira, A. F.;Ladeira, A. C. Q.;Ciminelli, V. S. T.;Heine, T. and Duarte, H. A. (2006). Structural model of arsenic(III) adsorbed on gibbsite based on DFT calculations. *Journal of Molecular Structure-Theochem*, 762, p. 17-23.

Perdew, J. P. (1986a). Density-functional approximation for the correlation-energy of the inhomogeneous electron-gas. *Phys. Rev. B*, 33, p. 8822-8824.

Perdew, J. P. (1986b). Erratum: Density-functional approximation for the correlation-energy of the inhomogeneous electron-gas. *Phys. Rev. B*, 34, p. 7404E.

Ramaswami, A.;Tawachsupa, S. and Isleyen, M. (2001). Batch-Mixed Iron Treatment of High Arsenic Waters. *Wat. Res.*, 35, p. 4474-4479.

Schlegel, H. B. (1987). Optimization of equilibrium geometries and transition structures. In: Lawley, K. P. *Ab-Initio Methods in Quantum Chemistry-I*. Wiley & Sons: p. 249-286.

Susi, H.;Byler, D. M. and Gerasimowiscz, W. V. (1983). Vibrational analisis of aminoacids: cysteine, serine, β-chloroalanine. *Journal of molecular structure*, 102, p. 63-79.

Teixeira, M. C. and Ciminelli, V. S. T. (2005). Development of a Biosorbent for Arsenite: Structural Modelling Based on X-Ray Spectroscopy (XAS). *Environmental Science and Technology*, 39, p. 895-900.

Tossel, J. A. (1997). Theoretical studies on arsenic oxide and hydroxide species in minerals and in aqueous solution. *Geochimica et Cosmochimica Acta*, 61, p. 1613-1623.

Trentelman, K.;Stodulski, L. and Pavlosky, M. (1996). Characterization of pararealgar and other light-induced transformation products from realgar by Raman microspectroscopy. *Analytical Chemistry*, 68, p. 1755-1761.

Yu, N. T.;DeNagel, D. C.;Pruett, P. L. and J.F. Kuck, J. (1985). Disulfide bond formation in the eye lens. *Proc. Natl. Acad. Sci USA Biochemistry*, 82, p. 7965-7968.

Capítulo 5

Considerações Finais

5.1 CONCLUSÕES

Foi demonstrado que biomassa obtida a partir da trituração de penas de galinha é eficiente e seletiva na remoção do arsênio em sua forma trivalente. A adsorção do As (III) ocorre de maneira quase imediata, sem alteração de pH, sendo necessários menos de 10 minutos para que o sistema atinja o equilíbrio.

A capacidade de adsorção da biomassa é inversamente proporcional ao pH da solução. A biomassa adsorve mais eficientemente as espécies neutras do arsenito, corroborando a hipótese de que o mecanismo de adsorção de arsênio por biomassa rica em proteínas fibrosas não pode ser creditado à ocorrência de interações eletrostáticas entre as espécies arsenicais e a superfície da biomassa.

Ainda no capítulo 2, os resultados da Espectroscopia de Absorção de Raios X (XANES e EXAFS) do complexo de adsorção obtido em pH 5,0 confirmaram que o As é adsorvido em seu estado trivalente e que são necessários aproximadamente três átomos de enxofre para promover a adsorção de cada átomo de arsênio trivalente. Foi observado ainda que a distância interatômica As-S é de aproximadamente 2,26 Å para os complexos de adsorção obtidos em pH ácido.

Foi observado que a estrutura molecular do complexo de adsorção As (III)/Biomassa varia em função do pH. Em pH ácido ou neutro o As (III) complexa diretamente com os átomos de enxofre da biomassa. A primeira camada de coordenação do As sofre uma alteração estrutural confirmada pelos valores de distância interatômica observados experimentalmente. Os grupamentos hidroxila da estrutura do arsenito são substituídos pelos átomos de enxofre da biomassa, com a liberação simultânea de três moléculas de água. Em pH básico, a espécie de As (III) negativamente carregada conserva parcialmente a estrutura da sua primeira esfera de coordenação e é adsorvida como um oxi-ânion. A estrutura molecular do complexo de adsorção formado em pH 10,5 é completamente diferente e apresenta-se desordenada. Na primeira esfera de coordenação do As tem-se a substituição de um único átomo de O. A proporção As (III)/S é de 1:1, e a distância entre eles é aumentada, passando a aproximadamente 2,3 Å. Além disso, parte do arsênio presente no sistema sofre oxidação. O fato de que em pH 10,5 as espécies arsenicais apresentam-se negativamente carregadas e

parcialmente oxidadas explica a diminuição na eficiência da adsorção observada anteriormente para valores de pH elevados.

Os cálculos baseados na Teoria DFT confirmaram os dados experimentais discutidos nos Capítulos 2 e 3. Os valores calculados para as distâncias interatômicas As (III)/S nos complexos de adsorção obtidos simulando-se diferentes condições de pH são bastante próximos daqueles obtidos experimentalmente. As diferenças são creditadas às limitações do modelo teórico.

Os dados de Espectroscopia Vibracional Raman e das predições teóricas baseadas em DFT, obtidos até o momento, possibilitaram a caracterização estrutural tanto da biomassa quanto dos complexos de adsorção obtidos em pH ácido. Os grupos vibracionais característicos das proteínas estruturais foram identificados nas amostras analisadas. Além disso, foi possível também observar os modos de vibração dos grupamentos químicos característicos das estruturas das queratinas e em particular, das β-queratinas das aves.

As pontes dissulfeto (S-S) presentes na estrutura da biomassa em seu estado natural assumem duas conformações estruturais distintas, *gauche-gauche-trans (g-g-t-)* e *gauche-gauche-gauche* (*g-g-g*), sendo esta segunda, a conformação predominante. Após os processos de pré-tratamento da biomassa e adsorção de arsênio, observou-se um consumo das pontes dissulfeto, evidenciado pela diminuição da intensidade do sinal correspondente ao modo vibracional da ligação S-S do tipo *g-g-g*. Considerando-se esse dado e os resultados das análises de EXAFS discutidas anteriormente pode-se concluir que os átomos de enxofre presentes na estrutura da biomassa rica em queratina participam ativamente da reação de complexação do arsênio trivalente. Além disso, pode-se perceber também que apenas um tipo específico de ponte dissulfeto (*g-g-g*) é consumido durante o processo. Simultaneamente à diminuição da intensidade do sinal das bandas Raman referentes aos modos vibracionais de estiramento da ligação S-S observou-se o surgimento de outras bandas cujas freqüências estavam localizadas na região onde são observados os modos vibracionais do estiramento das ligações entre o arsênio e o enxofre. Os cálculos de predição teórica DFT foram empregados no sentido de validar os dados experimentais obtidos e os resultados foram coincidentes.

O mecanismo de adsorção de arsenito em biomassa animal rica em queratina em pH neutro ou ácido pode ser resumido da seguinte maneira: a molécula neutra do arsenito interage com três átomos de enxofre de três resíduos de cisteína, após a redução das pontes dissulfeto do tipo *g-g-g* presentes na estrutura da queratina. Durante a interação os três grupamentos hidroxila da molécula do oxi-ânion arsenito são substituídos por três átomos de enxofre. Simultaneamente, os três prótons H^+ liberados dos grupamentos sulfidrila da biomassa reagem com as três hidroxilas liberadas do oxi-ânion, formando três moléculas de água, evitando alterações de pH do sistema. Os três átomos de enxofre se organizam em torno do átomo de arsênio formando uma estrutura trigonal piramidal regular, na qual a distância entre os átomos de As e S é de aproximadamente 2,3 Å.

5.2 CONTRIBUIÇÕES ESPECÍFICAS DESTE TRABALHO

Este trabalho de Tese apresenta a particularidade de ter sido embasado nos conhecimentos clássicos de Bioquímica, Química, Física e Metalurgia bem como em dados recentemente publicados sobre a toxicologia dos compostos arsenicais e a remediação de problemas ambientais causados por este elemento. Durante a realização desta Tese a adsorção de arsenito na biomassa selecionada foi avaliada experimentalmente tanto do ponto de vista macro quanto microscópico. Aos resultados experimentais somaram-se os resultados dos cálculos de predição teórica das estruturas dos complexos de adsorção. A estrutura molecular dos complexos As/S foi elucidada com o emprego de técnicas espectroscópicas clássicas e modernas, bastante sensíveis e precisas. Como contribuições específicas deste trabalho podem ser consideradas:

- O uso de material biológico de origem animal como suporte para a adsorção dos ânions arsenicais. Geralmente os materiais utilizados como biossorventes têm origem vegetal ou microbiana.

- O desenvolvimento de um biossorvente específico para os íons de arsênio trivalente capaz de removê-los mais eficientemente em pH neutro ou ácido. Esse fato é interessante, visto que o pH natural dos efluentes contaminados com arsênio é, em geral, ácido.

- Até onde se tem conhecimento, essa é a primeira vez que se propõe o emprego de um biossorvente efetivo na remoção do As (III) que ao mesmo tempo rejeita os ânions arsenato e os tradicionais íons competidores, como o fosfato. Além disso, o processo de adsorção de arsênio aqui proposto dispensa a etapa de oxidação do arsenito a arsenato usualmente necessária para garantir a eficiência de sua remoção.

- A elucidação da estrutura molecular do complexo formado entre o As e o S, por meio do emprego das técnicas de Espectroscopia de Absorção de Raios-X e de Espectroscopia Vibracional, nos permitiu identificar os grupamentos ativos do adsorvente e propor um mecanismo de adsorção de arsênio muito particular, no qual o arsenito é adsorvido como o íon As^{3+} e não como o oxi-ânion $As(OH)_3$.

5.3 PERSPECTIVAS DE TRABALHOS FUTUROS

- Avançar na utilização dos conhecimentos adquiridos para a produção de um biossorvente ou biosensor.

- Avaliar mais detalhadamente a adsorção de arsenito em meio básico e a sua complexação com cisteína por intermédio de Espectroscopia de Absorção de Raios-X (XAS) e Espectroscopia Raman.

- Avaliar a capacidade de adsorção de arsênio de outros materiais biológicos ricos em queratina e compará-las aos dados aqui obtidos.

- Comparar a toxicidade e a bioacumulação dos sais de arsênio trivalente e dos complexos de As (III)/cysteína através de estudos biológicos *in vivo*. Avaliar a distribuição dos compostos resultantes das reações de detoxificação do arsênio nos diferentes órgãos e tecidos corporais por meio de XAS e espectroscopia Raman.

- Avaliar a possibilidade de emprego dos sais de arsênio trivalente e dos complexos de As (III)/cysteína no tratamento da Tripanossomíase e da Leishmaniose experimentais usando como modelo o cão.

5.4 PRODUÇÃO CIENTÍFICA GERADA A PARTIR DO PRESENTE TRABALHO DE TESE

Trabalhos publicados em periódicos internacionais:

Teixeira, M.C. and Ciminelli, V.S.T. Development of a Biosorbent for Arsenite: Structural Modeling Based on X-Ray Spectroscopy (XAS). Environ. Sci. Technol. 2005, 39, 895-900

Teixeira, M.C.; Ciminelli, V.S.T.; Dantas, M.S.S.; Diniz, S. F.; Duarte, H. A. Raman Spectroscopy and DFT calculations of As (III) Complexation with a Cysteine-rich biomaterial. Aceito para publicação: Journal of Colloid Interface Science em junho de 2007.

Trabalhos publicados em periódicos nacionais:

TEIXEIRA, Mônica Cristina; DUARTE, Graziele; CIMINELLI, Virgínia Sampaio Teixeira. Arsenic Biosorption Mechanism - A X-Ray Spectroscopy Study. Activity Report 2002 Brazillian Synchrotron Light Laboratory, Campinas - SP, p. 115-116, 2003.

Trabalhos apresentados em eventos internacionais

TEIXEIRA, Mônica Cristina; DUARTE, Graziele; CIMINELLI, Virgínia Sampaio Teixeira. Structural modelling of arsenic biosorption using X-ray spectroscopy (XAS). In: 15TH INTERNATIONAL BIOHYDROMETALLURGY SYMPOSIUM, 2003, Atenas. 15th International Biohydrometallurgy Symposium - Symposium Proceedings. 2003.

Trabalhos apresentados em eventos nacionais

TEIXEIRA, Mônica Cristina; DUARTE, Graziele; CIMINELLI, Virgínia Sampaio Teixeira. Uso de biomassa animal rica em proteínas fibrosas como biossorvente para remoção de arsênio trivalente. In: ENCONTRO NACIONAL DE TRATAMENTO DE MINÉRIOS E METALURGIA EXTRATIVA XX ENTMME, 2004, Florianópolis. Encontro Nacional de Tratamento de Minérios e Metalurgia Extrativa XX ENTMME. 2004. p. 451-458.

TEIXEIRA, Mônica Cristina; DUARTE, Graziele; CIMINELLI, Virgínia Sampaio Teixeira. Arsenic sorption onto proteic biomass - a X-Ray approach. In: XIV REUNIÃO ANUAL DE USUÁRIOS DO LNLS, 2004, Campinas. XIV Reunião Anual de Usuários do LNLS. 2004. v. 1, p. 93-93.

ANEXOS

ANEXO 1

Balanço de massa do íon metálico no sistema SAM (Pagnaneli *et al*., 2000).

$$v_1 C_0 + q_{i-1} X_{i-1} (V_{i-1} - u) + (V_{i-1} - u) C_{i-1} = C_i V_i + q_i X_i V_i$$

(*i*) e (*i-1*) – referentes à etapa de adição do metal

(C_0) – concentração da solução de metal adicionada

(*v*) – volume de solução de metal adicionada

(*V*) – volume total da suspensão

(*u*) – Volume de alíquota retirada para análise

(*X*) – concentração de biomassa

(*q*) – carregamento específico para o metal

ANEXO 2

Ajuste dos dados da Figura 4.4 – Modelo Lorentz, Programa Origin 5.0

Pena Natural		Pico 1	Pico 2
	Centro	507.8±0.1	524.0±0.2
	Largura	18.0±0.3	21.0±0.4
	Intensidade	1821±42	1419±44
χ^2	3.13177		
Pena + As (III)		Pico 1	Pico2
	Centro	507.1±0.2	522±0.4
	Largura	14.9±0.7	27±1
	Intensidade	658±54	1648±89
χ^2	3.66355		

ANEXO 3

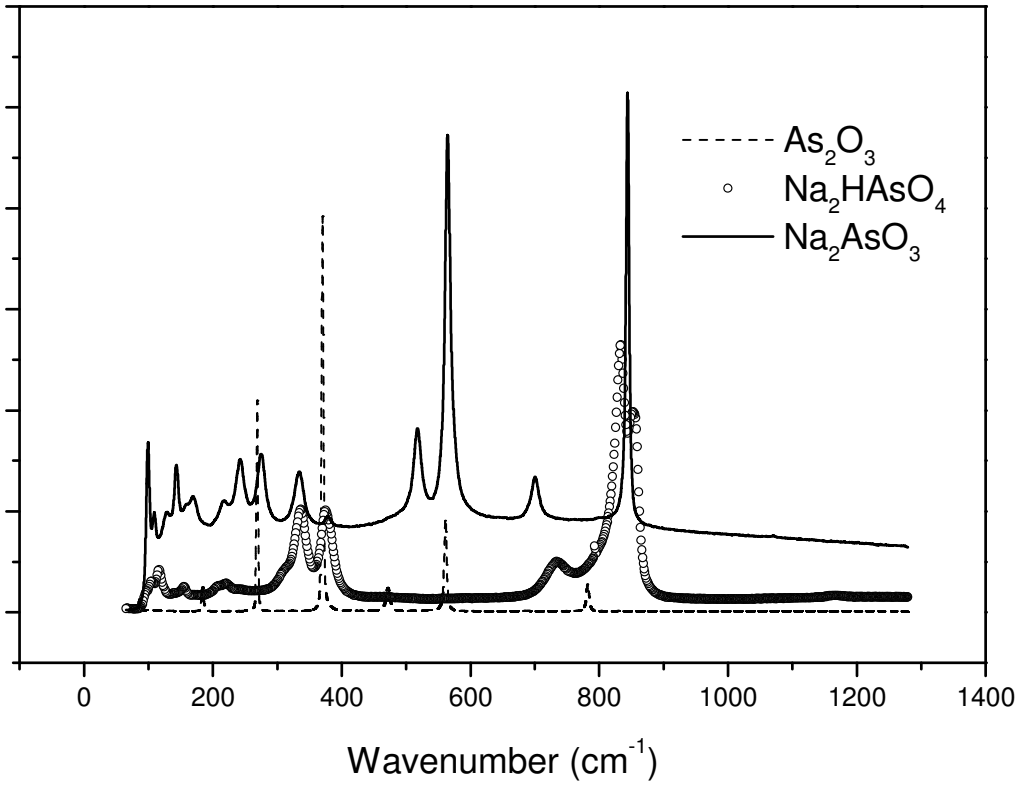

Espectros Raman dos padrões de Arsênio